GEORGIA INSTITUTE OF TECHNOLOGY
OFFICE OF CONTRACT ADMINISTRATION
SPONSORED PROJECT INITIATION

Date: 9/5/80

Project Title: Electromagnetic Detection of Agricultural Products in Travelers' Baggage

Project No: A-2673

Project Director: R.L. Seaman

Sponsor: U.S. Department of Agriculture
Science and Education Administration

Agreement Period: From May 30, 1980 Until ~~May 31, 1981~~ 12/31/81

Type Agreement: Research Contract Agreement No. 53-7B30-0-247

Amount: $80,075

Reports Required: Quarterly; Final

Sponsor Contact Person (s):

Technical Matters

Dr. S.O. Nelson
USDA-SEA-AR
Richard B. Russell Agricultural
Research Center
P.O. Box 5677
Athens, GA 30604

Contractual Matters
(thru OCA)

Henry R. Vogt, III
Research Contracts & Grants Officer
USDA-SEA-AR
Southern Region
701 Loyola Avenue
P.O. Box 53326
New Orleans, LA 70153

Defense Priority Rating: N/A

Assigned to: ETL/BRG (~~School~~/Laboratory)

COPIES TO:

Project Director
Division Chief (EES)
School/Laboratory Director
Dean/Director–EES
Accounting Office
Procurement Office
Security Coordinator (OCA)
Reports Coordinator (OCA)

Library, Technical Reports Section
~~Office of Computing Services~~ EES R+P
~~Director, Physical Plant~~
EES Information Office
Project File (OCA)
Project Code (GTRI)
Other F.L. Cain

-3 (3/76)

GEORGIA INSTITUTE OF TECHNOLOGY OFFICE OF CONTRACT ADMINISTRATION

SPONSORED PROJECT TERMINATION SHEET

Date 4-14-82

Project Title: Electromagnetic Detection of Agricultural Products in Traveler's Baggage

Project No: A-2673

Project Director: R. L. Seaman

Sponsor: USDA, Science & Ed. Adm.

Effective Termination Date: 12/31/81

Clearance of Accounting Charges: 12/31/81

Grant/Contract Closeout Actions Remaining:

- [x] Final Invoice and Closing Documents
- [ ] Final Fiscal Report
- [x] Final Report of Inventions
- [x] Govt. Property Inventory & Related Certificate
- [ ] Classified Material Certificate
- [ ] Other _____

Assigned to: ECSL/BRD (~~School~~/Laboratory)

COPIES TO:

Administrative Coordinator	Research Security Services	EES Public Relations (2)
Research Property Management	Reports Coordinator (OCA)	Computer Input
Accounting	Legal Services (OCA)	Project File
Procurement/EES Supply Services	Library	Other _____

FORM OCA 10:781

ENGINEERING EXPERIMENT STATION
GEORGIA INSTITUTE OF TECHNOLOGY • ATLANTA, GEORGIA 30332

2 September 1980

Dr. S. O. Nelson
USDA-SEA-AR
Richard B. Russell Agric. Res. Cntr.
P. O. Box 5677
Athens, GA 30604

Reference: Contract No. 53-7B30-0-247,
"Electromagnetic Detection of Agricultural
Products in Travelers' Baggage"

Contractor: Georgia Tech Research Institute

Subject: First Quarterly Report
Georgia Tech Project A-2673

Project
Director: Dr. Ronald L. Seaman, (404) 894-3963

Dear Dr. Nelson:

The overall objective of this project is to develop an electromagnetic device to detect fruit, vegetables, and meat in baggage. Detection is necessary so that agricultural products can be intercepted and prevented from entering the country. This exclusion reduces the amounts of foreign organisms, such as plant diseases and insect larvae, available to infect or infest native crops. An electromagnetic detection method offers the potential of inspection without opening the baggage. This procedure has the dual advantages of speeding up the inspection process and increasing the intercept rate. This project deals specifically with assessing different electromagnetic approaches to this detection problem.

During the first three months of this project, data on moisture (water) content and dielectric properties of agricultural products have been accumulated. Moisture content of fruits and vegetables is high, typically 73 to 95%. Moisture content of meats is somewhat lower, depending on the type of meat. Because the moisture content is greater than 55% in all cases, this variable may form the basis by which an electromagnetic device can detect these agricultural products. Although there is quite a volume of literature on

the dielectric properties of agricultural products, data directly applicable to the fruits, vegetables, and meats of interest here are limited in the number of products and the frequency ranges considered. However, because of the similar high moisture content of most of the products, the dielectric properties may also be similar.

In addition, discussions have been held with USDA personnel to define further the requirements for detection. From these discussions, it was determined that the high moisture content of agricultural products may indeed be a valid parameter to differentiate the products from other baggage contents electromagnetically. Other items with high moisture content which may interfere with reliable detection are wet towels and bathing suits and containers of alcoholic beverages, after shave lotions, and perfume. It was also learned that dried fruits (low moisture content) need not be detected since they are poor hosts for the organisms to be excluded.

During the next three months, the moisture content and dielectric data will be used in the study of different electromagnetic schemes for detecting agricultural products. Attention will be directed to specifying 1) frequencies of the electromagnetic energy, 2) instrumentation interface with baggage, and 3) signal processing in order to optimize detection of only agricultural products. It is also planned to visit Atlanta's International Airport to observe current baggage inspection procedures.

Respectfully submitted,

Ronald L. Seaman
Project Director

Approved:

James C. Toler
Manager,
Biomedical Research Branch

QUARTERLY TECHNICAL REPORT NO. 2
PROJECT A–2673

ELECTROMAGNETIC DETECTION OF AGRICULTURAL PRODUCTS IN TRAVELERS' BAGGAGE

By

R. L. Seaman, J. Seals and A. R. Moser

Prepared for

U.S. DEPARTMENT OF AGRICULTURE
SCIENCE AND EDUCATION ADMINISTRATION
AGRICULTURAL RESEARCH – SOUTHERN REGION
701 LOYOLA AVENUE
NEW ORLEANS, LOUISIANA 70153

Under

Research Agreement No. 53-7B30-0-247

DECEMBER 1980

GEORGIA INSTITUTE OF TECHNOLOGY

Engineering Experiment Station
Atlanta, Georgia 30332

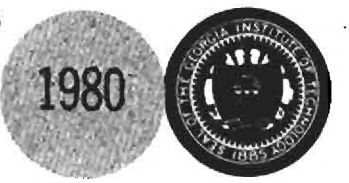

ELECTROMAGNETIC DETECTION OF AGRICULTURAL PRODUCTS IN TRAVELERS' BAGGAGE

Quarterly Technical Report No. 2

Project A-2673

December 1980

Under

Research Agreement No. 53-7B30-0-247

By

R. L. Seaman, J. Seals
and A. R. Moser

Prepared for

U.S. Department of Agriculture
Science and Education Administration
Agricultural Research - Southern Region
701 Loyola Avenue
New Orleans, Louisiana 70153

BIOMEDICAL RESEARCH DIVISION
Electronics and Computer Systems Laboratory
Engineering Experiment Station
Georgia Institute of Technology
Atlanta, Georgia 30332

FOREWORD

Research during the second three months of this one-year project was performed by personnel of the Biomedical Research Division of the Electronics and Computer Systems Laboratory of the Engineering Experiment Station at the Georgia Institute of Technology, Atlanta, Georgia. This project is sponsored by the Science and Education Administration of the U.S. Department of Agriculture, New Orleans, Louisiana, under Research Agreement 53-7B30-0-247. It has been assigned Georgia Tech Project No. A-2673. This report summarizes efforts carried out from 1 September 1980 through 30 November 1980.

Dr. R. L. Seaman served as Project Director. Mr. J. Seals performed the analyses and experiments on the capacitor plate approach. Dr. A. R. Moser performed the analyses and experiments on the signal transmission/reflection approach.

Respectfully submitted,

Ronald L. Seaman,
Project Director

Approved:

J. C. Toler, Manager
Biomedical Research Division

TABLE OF CONTENTS

LIST OF FIGURES

LIST OF FIGURES

LIST OF TABLES

I. INTRODUCTION

The Animal and Plant Health Inspection Service (APHIS) of the United States Department of Agriculture (USDA) is charged with regulating the entry of plants and animals into the country. Entry of plant and animal (agricultural) products is also controlled. Restrictions are necessary to prevent ingress of disease organisms and pests which could adversely affect native plants and animals.

Agricultural products cannot be brought into the country by international travelers. Fruits, vegetables, plants, and meats carried by these travelers are to be intercepted by APHIS. Travelers are questioned about agricultural products they are bringing into the country and, in some cases, their baggage is searched. All discovered agricultural products are confiscated. Although these rules and procedures are well known, travelers still attempt to bring illicit agricultural products through ports of entry. It has been estimated that 2% of international travelers attempt to bring contraband fruits, vegetables, and meats into the country. This comes to nearly one-half million illicit items carried by air passengers alone and amounts to a significant influx

Visual inspection of the contents of travelers' baggage offers the most reliable method for revealing agricultural products. However, this procedure is time consuming and often creates delays for travelers. A method of detecting the products without opening baggage would eliminate much of the inspection delay. It would also produce the additional benefit of an increased intercept rate.

The objective of this project is to study the feasibility of an electromagnetic device to detect fruits, vegetables, and meats in closed baggage. Electromagnetic detection methods are based on the differences between dielectric properties of agricultural products and those of other baggage contents. The following four approaches were proposed for investigation:

- capacitor plates,
- signal transmission/reflection,
- short pulse radar, and
- resonant cavity.

During the second three months of this project, significant progress was made in investigating the first three of these approaches. Efforts on the capacitor plate, signal transmission/reflection, and short pulse radar approaches are reported in Sections III, IV, and V, respectively. In addition, compilations of moisture and dielectric property data for agricultural products are presented in Section II. Plans for the next three months of this project are outlined in Section VI.

II. MOISTURE AND DIELECTRIC DATA

Agricultural products considered here were initially presumed to have high water, or moisture, content which would strongly influence their dielectric properties. The term "agricultural products" is used to mean fruits, vegetables, and meats in fresh or near-fresh condition. These products are the most likely ones to harbor disease organisms and insect larvae. Their detection is thus more desirable than detection of dried fruits and meats which are less likely to be infested.

A survey of the literature was carried out to evaluate the moisture content of fruits, vegetables, and meats [1-5]. Data collected for fruits and vegetables are listed in Table I; for meats and selected meat products, in Table II. Values are given without regard to method of determination. Since most were taken from recent compilations which do not reference original sources, it is possible that identical values given here from different references have come from the same original source. In all cases, the moisture content of fruits and vegetables is greater than 65% and in most greater than 80%. Moisture content of meats is generally lower than this with most values falling between 40 and 60%. Thus, moisture content, as expected, is high in the agricultural products which are to be detected in baggage.

Because of the high moisture content of agricultural products, their dielectric properties are determined to a large extent by the dielectric properties of water, particularly above about 100 MHz. A survey of the literature revealed values for agricultural products over a wide frequency range [5-12]. Data were gathered as the real and imaginary parts of the relative complex permittivity, ε_r' and ε_r'', where the relative complex permittivity $\varepsilon_r^* = \varepsilon_r' - j\varepsilon_r''$. The relative dielectric constant ε_r' is a measure of the electromagnetic energy storage capability of a material. The relative loss tangent ε_r'' is a measure of the capability of a material to dissipate electromagnetic energy as heat. These parameters are both functions of frequency and temperature.

TABLE I

MOISTURE CONTENT

FRUITS AND VEGETABLES

Fruits & Vegetables	Mohsenin 1970	McGraw-Hill 1977	Ockerman 1978			Nelson 1979	Hart & Fisher 1971
Apple	85	84.1	84.1	85	84	86	
Apricot	89	85.4		85	85.3		
Artichoke		83.7					
Avocado		65.4		74	75		
Banana		74.8	74.8	76	73.5		
Breadfruit					76.2		
Cantaloupe		94	94	91	92.6	90	
Carrots			88.2		88	86	
Cherimoya					73.3		
Cucumber	95.8	96.1			96		
Eggplant		92.7					
Grape		81.9	82		81.5		
Grapefruit: White	88	88.8	88.8	89	89		
Pink or Red	88	88.8	88.8	89	89		
Guava		80.6			80.6		
Honeydew Melon		90.5					

-continued-

TABLE I

MOISTURE CONTENT

FRUITS AND VEGETABLES

Fruits & Vegetables	Mohsenin 1970	McGraw-Hill 1977	Ockerman 1978			Nelson 1979	Hart & Fisher 1971
Lemon (edible)	80	89.3		90	88.7		90.08
(peel)							81.62
Lime	85	86			86.8		
Mangoes					81.7		
Onions: mature, raw	85.3	87.5		89			
Orange (edible)	86.1	87.2	87.2	86	87.1		85.23
(peel)							72.52
Papaya		88.3		89	88.6		
Passion fruit					80.0		
Peach		86.9	86.9	89	86.6	89-91	
Pear	82	82.7		83	83.2		
Pineapple				85	86.7		
Plum	76.6	85.7		87	82.0		
Pomegranate					81.3		
Potato			77.8		75	80	
Pumpkin		90.5		90			

-continued-

TABLE I

MOISTURE CONTENT

FRUITS AND VEGETABLES

-concluded-

Fruits & Vegetables	Mohsenin 1970	McGraw-Hill 1977	Ockerman 1978		Nelson 1979	Hart & Fisher 1971
Quince				83.2		
Soursop				80.2		
Squash: Summer		95		96		
Winter	88.3	88.6				
Tangerine		87.3	87			
Tomato	93.0	94.1	94.1	94		
Sweet Potato					74-84	

TABLE II

MOISTURE CONTENT

MEAT AND MEAT PRODUCTS

Meat and Meat Products	Mohsenin 1970	McGraw-Hill 1977	Ockerman 1978	Hart & Fisher 1971		
Beef: Calf Liver	75	70.8		55-69	71	
Chopped		47.7	54			
Roasting		60	67			
Veal		60	70	68-70		
Bologna		62.4				62
Braunschweiger						56
Pork: Ham	41.9	53	42	53		
Loin Chops			58	58		
Sausage		41.9			42	
Salami					31	
Summer Sausage					34	

Data were collected for temperatures from 20 to 25 ^{o}C so that values could be validly compared across frequency. This range includes common room temperatures and temperatures expected in baggage inspection areas. Dielectric data are presented in graph form in Figures 1-4. Figures 1 and 2 present data for frequencies from 1 kHz to 100 MHz; Figures 3 and 4, from 100 MHz to 10 GHz. Data have been taken from studies using several different methods and represent work done over a 30-year span.

There is some scatter in the dielectric values. The scatter is probably due to various factors. One factor is the use of different techniques by different investigators. Another is the difference in moisture content among different fruits, vegetables, and meats by species and variety. Other possible factors include duration of storage and stage of maturity. Despite the scatter, there are trends evident in the data.

The dielectric data summarized in Figures 1-4 have been useful in evaluating the different approaches to detecting agricultural products. Values of dielectric constants and loss tangents could be estimated from these data for all frequencies being considered.

For frequencies from about 3 GHz to 10 GHz, the relative dielectric constant and loss tangent were described by analytic functions. These functions were derived by adopting previous forms [16] to the agricultural product data by using appropriate constants. The procedure resulted in the following expressions:

$$\varepsilon_r' = 40 + 10/f \qquad (1)$$

and

$$\varepsilon_r'' = \frac{20}{f} + \frac{f}{1 + (f/25)^2} \quad , \qquad (2)$$

where f is the frequency in GHz. These relationships were particularly useful in studying the frequency effects in the signal transmission/reflection approach in Section IV.

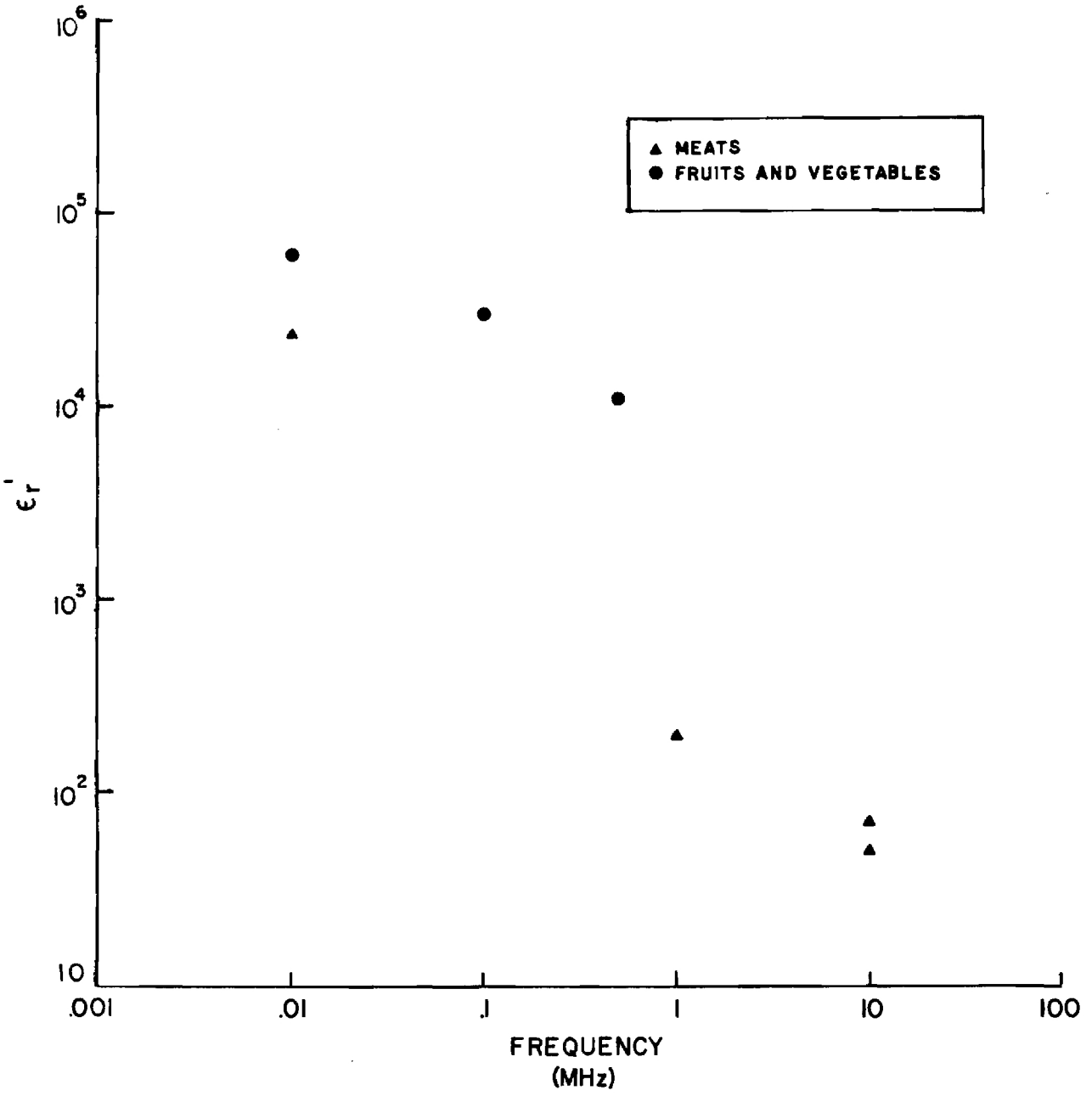

Figure 1. Relative dielectric constant of agricultural products versus frequency, 1 kHz to 100 MHz, 20 to 25°C.

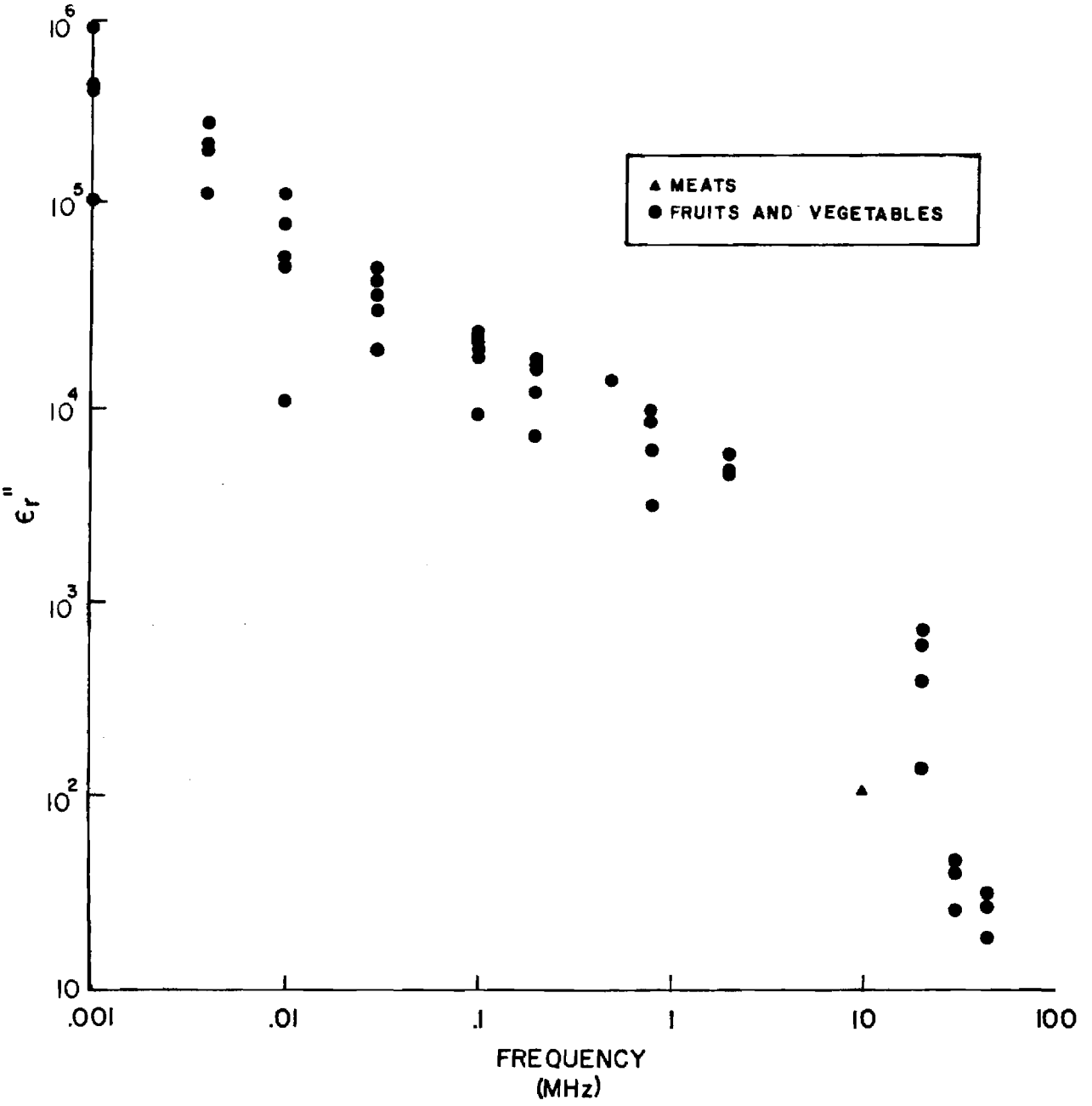

Figure 2. Relative loss tangent of agricultural products versus frequency, 1 kHz to 100 MHz, 20 to 25°C.

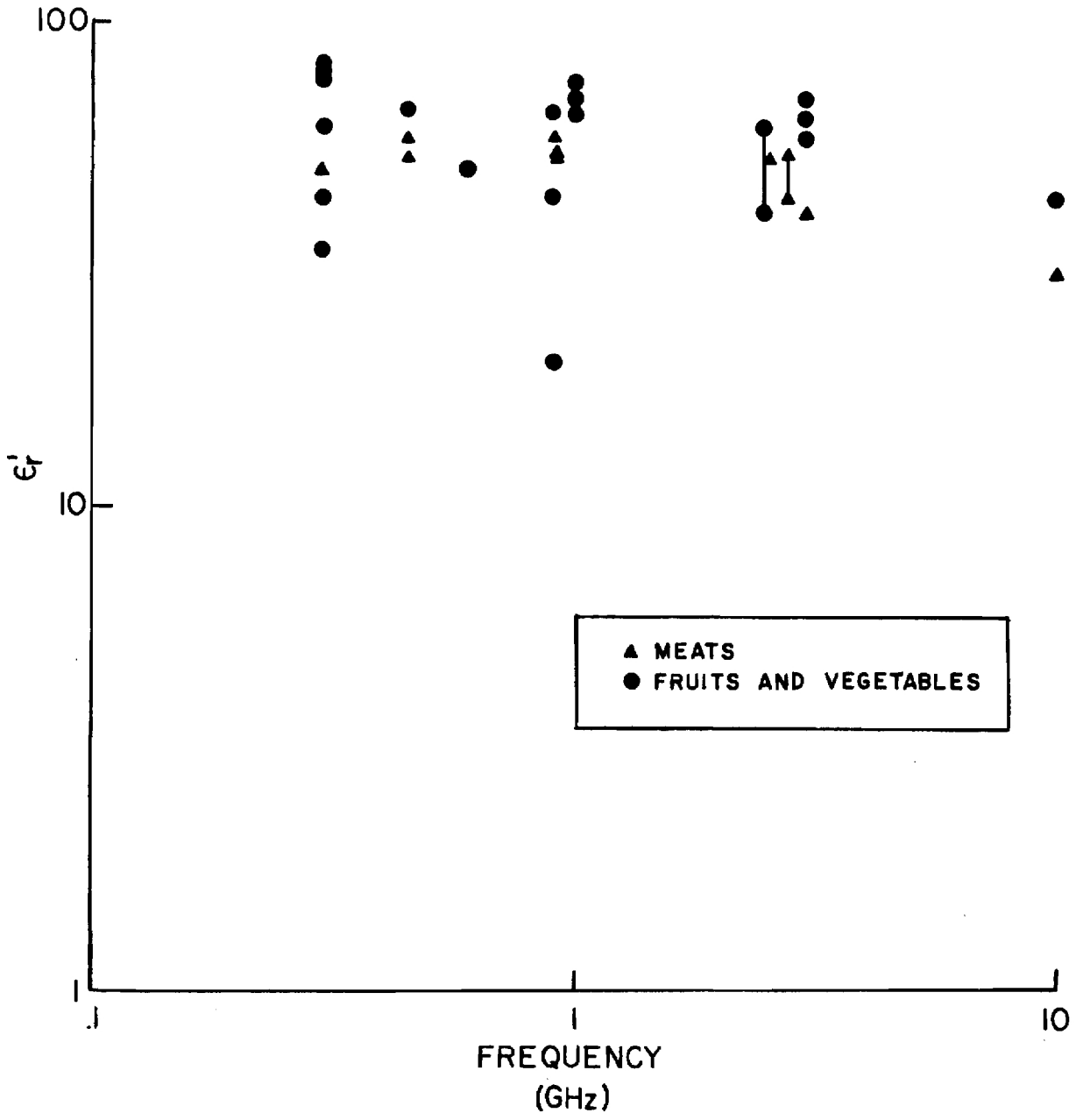

Figure 3. Relative dielectric constant of agricultural products versus frequency, 0.1 to 10 GHz, 20 to 25°C.

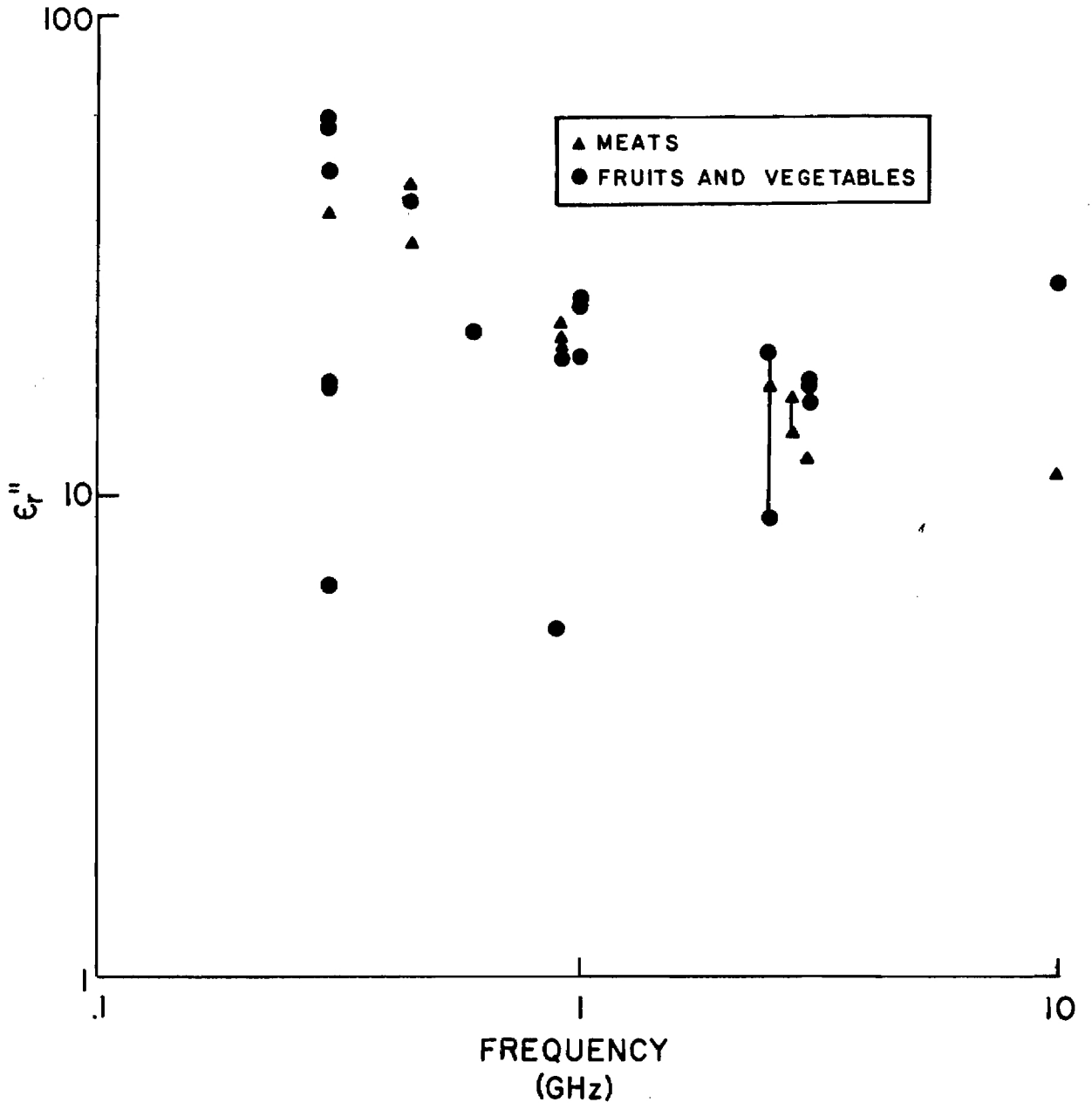

Figure 4. Relative loss tangent of agricultural products versus frequency, 0.1 to 10 GHz, 20 to 25°C.

The following conclusions were drawn from the compilations of moisture and dielectric data for agricultural products:

- Moisture content is high for all products of interest.
- Dielectric properties of these products are similar.
- Because of these similarities, a device which successfully detects one product will detect others.
- Results of experiments with one kind of fruit can be generalized to other fruits, to vegetables, and possibly to meats.

III. CAPACITOR PLATE APPROACH

Introduction of an agricultural product into a capacitor will change the electric field between the capacitor's plates. The change will be related to the product's permittivity which differs from that of the low-loss, low-dielectric constant material which usually fills interplate space. During this reporting period, effects of agricultural products on capacitance, and, consequently, capacitor impedance, have been investigated. Both theoretical analyses and experimental measurements were performed.

A. Analyses

A capacitor is formed by any two conductors separated by a dielectric medium. Voltage applied across the capacitor's conductors (usually plates) will result in (a) a build-up of electrical charge on each conductor and (b) an electric field between the conductors.

Capacitance is equal to the ratio of the magnitude of charge Q on each conductor to voltage V between conductors:

$$C = Q/V. \tag{3}$$

In general,capacitance is determined by (a) the size and separation of the plates forming the capacitor and (b) the dielectric properties of the intervening material between the plates. Because of this latter factor, measurement of capacitance can be used to detect objects placed between a capacitor's conductors.

An empty capacitor is one in which the electric field is established in a vacuum. The capacitance of an empty capacitor is denoted by C_o, the vacuum capacitance, which represents the effect of capacitor geometry on capacitance. It is extremely useful in analyzing the effect of an object inserted between the capacitor's conductors. For example, if the region between the conductors is completely filled by a material having a real relative permittivity ε_r, capacitance is given by [13]:

$$C = C_o \varepsilon_r. \tag{4}$$

Capacitance can be experimentally determined by measuring a capacitor's electrical impedance Z which is related to capacitance:

$$Z = 1/j\omega C = -j/\omega C \qquad (5)$$

where ω = angular frequency = $2\pi f$ and $j = \sqrt{-1}$. The simple relationships given by equations (4) and (5) are useful in evaluating the parallel-plate capacitor.

A capacitor consisting of a set of parallel metal plates was considered because of several features that make it extremely well-suited for detection applications. These features include the following:

- Restricted electric field to minimize potential problems such as electromagnetic interference and hazards that could result from unconfined, radiated fields;
- Uniform electric field, perturbations of which would be relatively insensitive to object location; and
- Conveniently modeled electrical response.

In an ideal parallel-plate capacitor, vacuum capacitance C_o can be accurately described as

$$C_o = \varepsilon_o A/d, \qquad (6)$$

where ε_o = permittivity of free space,
A = area of each plate, and
d = distance between plates.

This relation makes it possible to study the electrical response of an ideal parallel-plate capacitor. Since C_o of most capacitors is extremely small, equation (5) indicates that the impedance of an empty parallel-plate capacitor is a very large negative reactance.

The electric field of a parallel-plate capacitor can be assumed to be completely contained within the volume directly between its plates. This means that if the volume between the plates is filled by a material with a relative permittivity ε_r^*, equation (4) holds and, from equation (5), impedance of the filled capacitor is

$$Z = -j/\omega\varepsilon_r^* C_o. \tag{7}$$

The magnitude and phase of Z depend on the relative permittivity of the material placed between the capacitor plates. In fact, knowledge of C_o from equation (6) and ε_r^* (from measurement or from the literature) makes it possible to predict accurately the electrical response of the capacitor. Materials such as plastics, fabrics, air, or other non-conductors that are normally found in baggage typically have a real relative permittivity that is between 1 and 5. When these materials are placed between the plates of a parallel plate capacitor, equation (7) shows that the impedance will be a large negative reactance comparable in magnitude to that of the empty capacitor.

Conversely, agricultural products with high moisture content have complex relative permittivities as discussed in Section II. When these materials are placed between the plates of a parallel-plate capacitor, the impedance will no longer be purely reactive. Instead, it will take the form

$$Z = [j\omega C_o \varepsilon_r^*]^{-1} \tag{8}$$

$$= [\omega C_o \varepsilon_r'' + j(\omega C_o \varepsilon_r')]^{-1}.$$

That is, the impedance will have both resistive and reactive components and can be modeled as a parallel resistor and capacitor.

The data presented earlier in Figures 1-4 show large values of ε_r' and ε_r'' for agricultural products with high-moisture content. At frequencies between 1 and 10 MHz, the values range between approximately a hundred and several thousand. This means that, in addition to being a complex quantity, the impedance magnitude is significantly smaller than the impedance when only non-conducting, low-dielectric constant materials are present between the plates. In fact, for comparative purposes, the complex impedance of equation (8) can be approximated as a short-circuit.

In implementing a capacitor plate detection system, the capacitor plates would be positioned so that baggage can pass between the plates. If the baggage contained only non-conducting, low-dielectric constant materials, the capacitor impedance could be adequately described using the simple model for a solid dielectric developed in the preceding paragraphs. However, if the baggage contained an agricultural product, the previously developed simple model is no longer adequate since there is now a conductive object imbedded in a non-conducting, low-dielectric-constant medium. These situations are depicted in Figure 5.

The equivalent impedance of the more complex configuration can be determined by extending the simple model. This is achieved by assuming that infinitely thin sheets of metal foil are located at positions corresponding to the top and bottom of the conducting object. The foil sheets are the same size as the capacitor plates and parallel to them. Since the electric field between the plates of a parallel plate capacitor is perpendicular to the plates (and hence the foil sheets), the infinitely thin foil sheets will not disturb the electric field and the impedance of the capacitor plate will not be affected [14]. With the foil positioned this way, each set of adjacent conductors (i.e., metal plates and metal foil sheets) will comprise a capacitor. The capacitor models depicted in Figure 5 can be remodeled as three capacitors in series as shown in Figure 6 to which results from the simple model can be applied. If this is done for the case in Figure 6a where no agricultural product is present, the total impedance (which is the sum of the three series impedances) is identical to the impedance previously obtained in Figure 5a. Examination of Figure 6b shows that, when an agricultural product is present, the total impedance can be expressed as

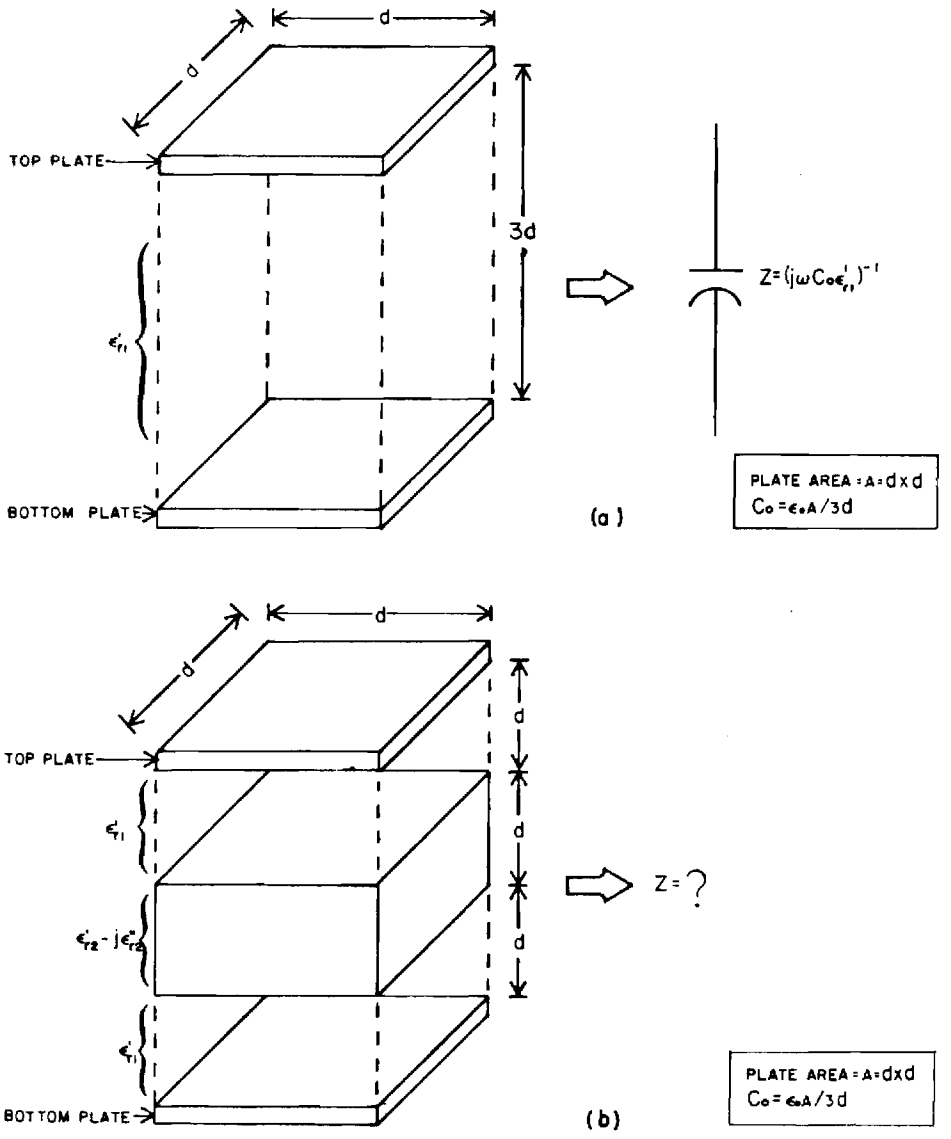

Figure 5. Parallel-plate capacitor. In Figure 5a, the volume between the plates is filled with material that has a real relative permittivity (ε'_{r1}) that is small in magntiude. In Figure 5b, material with a complex relative permittivity ($\varepsilon'_{r2} - j\varepsilon''_{r2}$) that is large in magnitude partially fills the volume between the capacitor plates.

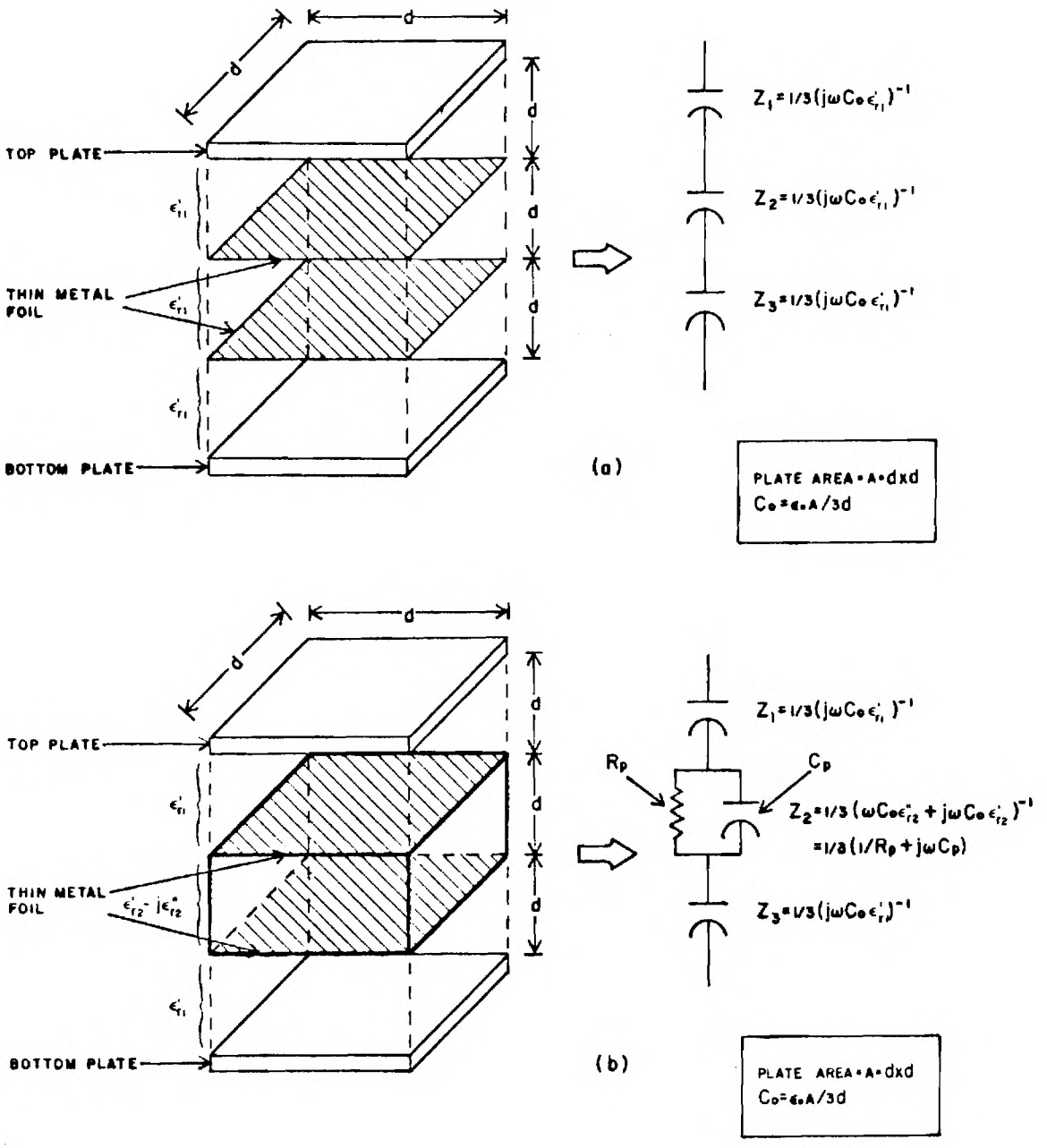

Figure 6. Parallel-plate capacitor with thin metal sheets inserted. In Figure 6a, the volume between the plates is filled with materials that have a real relative permittivity (ε'_{r1}) that is small in magnitude. In Figure 6b, the volume between the two metal sheets is filled by material with a complex relative permittivity ($\varepsilon'_{r2} - j\varepsilon''_{r2}$) that is large in magnitude.

$$Z_{total} = Z_1 + Z_2 + Z_3 \qquad (9)$$

$$= \frac{2}{3} \left(j\omega C_o \varepsilon_{r1}'\right)^{-1} + \frac{1}{3} \left[\omega C_o \varepsilon_{r2}'' + j(\omega C_o \varepsilon_{r2}')\right]^{-1}$$

It has already been noted that the impedance magnitude of a capacitor filled with an agricultural product would be extremely small in comparison to the impedance magnitude of the same capacitor filled with a non-conducting, low-dielectric constant material. If this fact is now applied to the impedance described by equation (9), it can be seen that the total impedance of the capacitor configuration in Figure 6b is approximately two-thirds of the impedance when no agricultural product is present. That is, the presence of the agricultural product effectively short-circuits its volume fraction of the impedance. Therefore, plate size as it affects capacitor volume is an important design factor. Since the impedance in equation (9) is a complex quantity, it seems that either its amplitude or phase (or both) could serve as useful measurement parameters. However, because an object with a large relative complex permittivity essentially acts as a "short-circuit," the net impedance remains almost purely reactive even when an object is present. Therefore, the impedance phase is not a very useful parameter for detection purposes.

Impedance magnitude is potentially useful if the capacitor plates are of appropriate size in relation to the object being detected. The effect of capacitor plate size is shown in Figure 7. The object in this example is a cube of saline d x d x d in size between plates separated by 3d. Figure 7 shows that the maximum change in impedance occurs when the size of the capacitor plates is equal to or smaller than the cross-sectional area of the target cube. Therefore, for maximum sensitivity, the size of the capacitor plates should be comparable to the dimensions of the agricultural products to be detected.

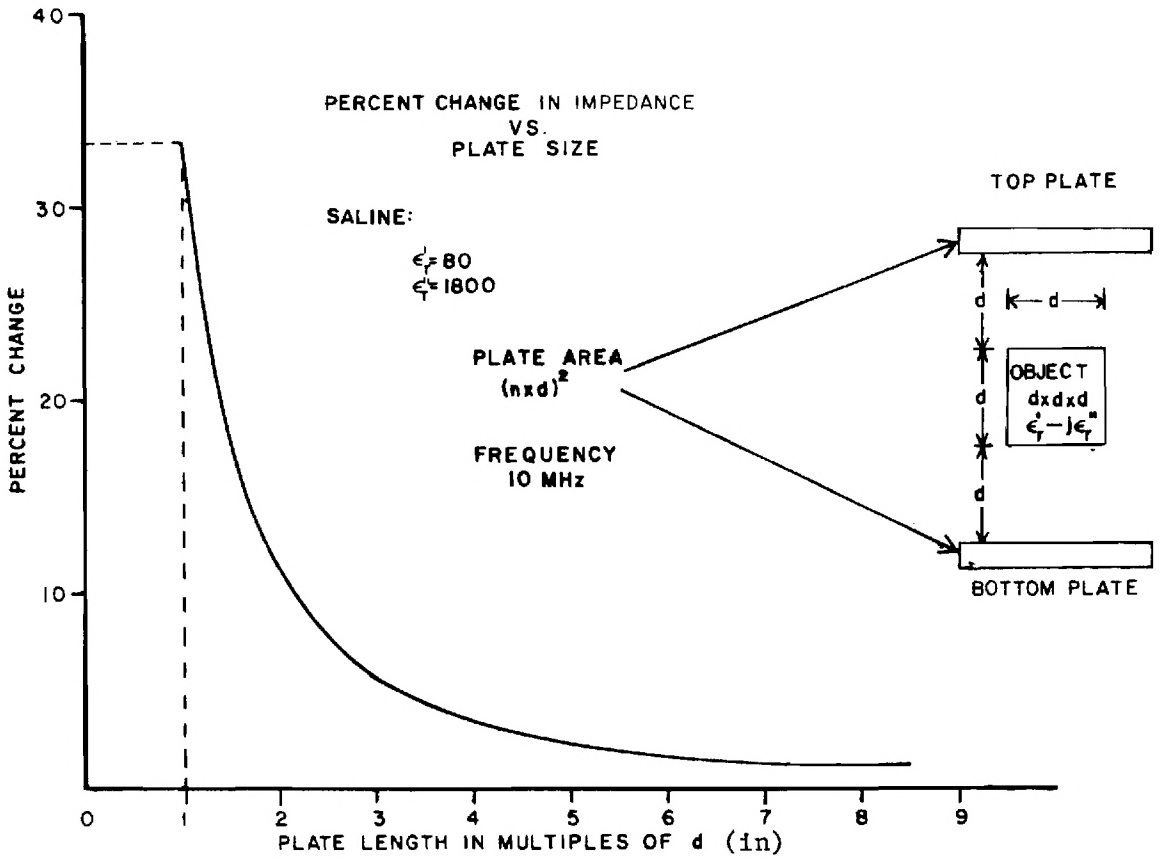

Figure 7. Percent change in impedance of capacitive plate detector as a function of plate size. The target object is modeled as a dxdxd cube centered between the air filled ($\epsilon_r' = 1$) plates. Percent impedance change is determined from the difference in impedance of the plate capacitor when empty and with the target present. Plate size (square) is specified by the length of one side in integral multiples of d.

B. Measurements

Results of the theoretical analysis indicated the potential feasibility of the capacitor plate detection concept. However, since this theoretical analysis was based on idealized models, a series of laboratory tests were performed to provide further evaluation of this approach.

Laboratory tests involved measuring the complex impedance of a set of prototype capacitor plates under a variety of conditions. Several practical problems were encountered in implementing a capacitor detection system. One was determination of a method for measuring the large reactive impedances associated with capacitor plates with size and geometry suitable for detecting agricultural products in baggage. This problem was greatly reduced by using relatively high frequencies since the capacitor impedance was inversely proportional to frequency. An RF range of 1 to 10 MHz was finally selected because of the availability of a network analyzer system which operated over this range.

A second major problem was development of a suitable method for feeding RF energy to the capacitor plates. Initially, a feed system comprised of a twisted pair of thin diameter insulted wires was employed. However, the wires were found to radiate significantly. A satisfactory feed system was subsequently implemented by soldering the exposed center conductor of a flexible coaxial cable to one plate. The second plate of the capacitor plate configuration was electrically grounded at a point near the feed point of the first plate (Figure 8). It was experimentally determined that if a shielded wire (shield not grounded) was used in grounding the second plate, coupling between RF-fed plate and this grounding wire could be minimized.

A diagram of the apparatus used in these tests is shown in Figure 8. A Hewlett Packard (HP) 8601 Sweeper/Generator provided the 1-10 MHz RF signal. An HP 8407 Network Analyzer mainframe with an HP 8412 Phase-Magnitude Display was used to compute the complex ratio of the two sampled test signals (V_v/V_i). Since V_v and V_i were directly proportional to the capacitor voltage V and current I, respectively, their ratio was directly related to the capacitor impedance ($Z = V/I$). The magnitude of the ratio was displayed in dB units (i.e., 20 log V_v/V_i) while the phase was

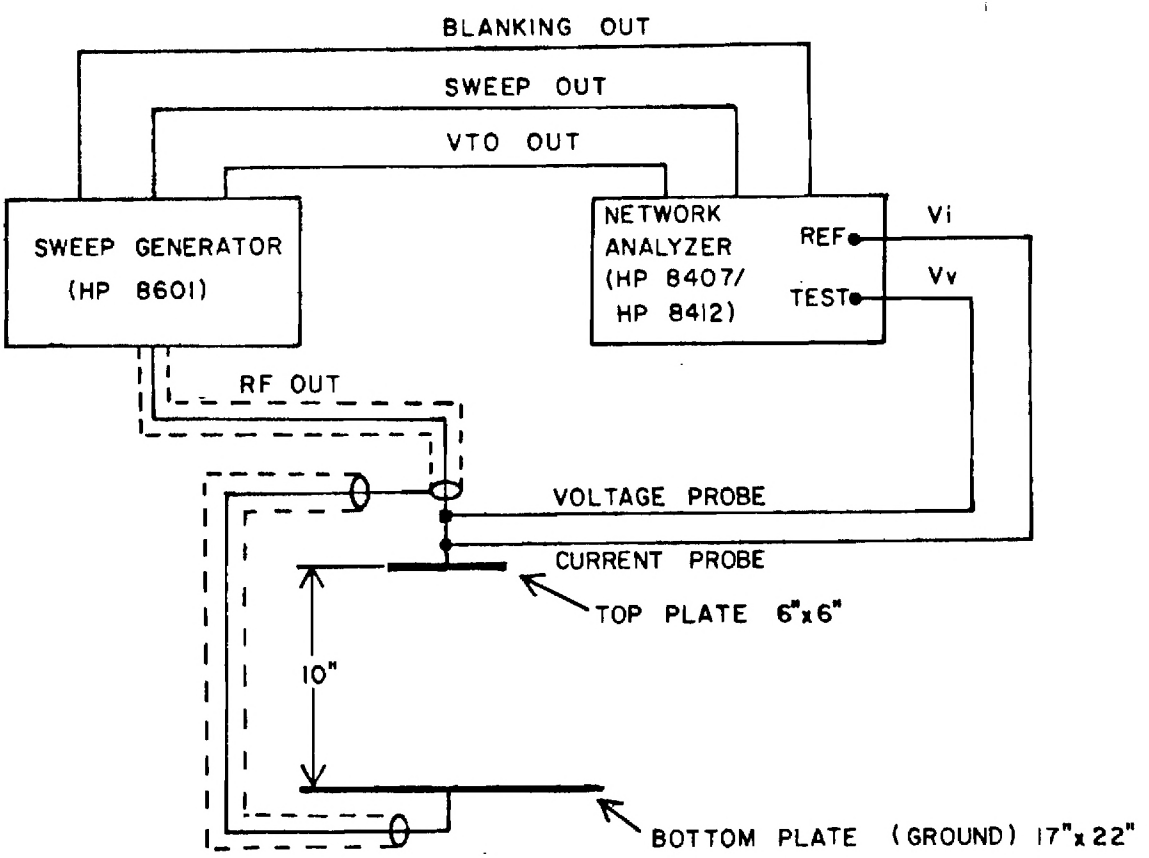

Figure 8. Apparatus used in testing capacitor-plate detection concept. The voltages V_v and V_i sampled by the network analyzer are respectively proportional to the voltage and displacement current across the capacitor formed by the two plates.

displayed in degrees. Only the impedance magnitude has been evaluated so far. The capacitor plates selected for the initial tests consisted of one small plate (6 by 6 inches) and one large plate (22 by 17 inches). Plate separation distance was 10 inches. The smaller plate was fed RF energy while the larger plate served as the ground plate as described above.

Measurements performed to date consist of swept-frequency measurements of the capacitor plate impedance when the volume between the plates (a) was empty and (b) contained 750 ml of a saturated sodium chloride solution in a 1000 ml glass beaker. Since the capacitor impedance is inversely proportional to frequency, it was anticipated that, in both cases, the impedance magnitude should decrease by 20 dB as the frequency was increased from 1 to 10 MHz. Further, a constant 2-3 dB decrease in impedance magnitude was expected over the frequency range when the beaker of saline was placed between the plates (based on saline volume). An example of the actual measurement results obtained are in Figure 9. As predicted, the impedance magnitude decreased in each case by approximately 20 dB as the frequency increased from 1 to 10 MHz. Presence of the beaker of saline resulted in an almost constant decrease of 2 dB over the entire 1 to 10 MHz range. Both results are in excellent agreement with the analytical predictions and indicate the validity of the derived equivalent circuit models.

C. Future Investigations

Results of theoretical analyses and laboratory measurements have indicated the potential feasibility of the capacitor plate approach. Future investigations will concentrate on determining optimal performance that can be practically expected employing this detection concept. It is anticipated that future investigations will continue to employ both theoretical analysis and laboratory testing. Performance characteristics that will be considered in these future investigations include the following:

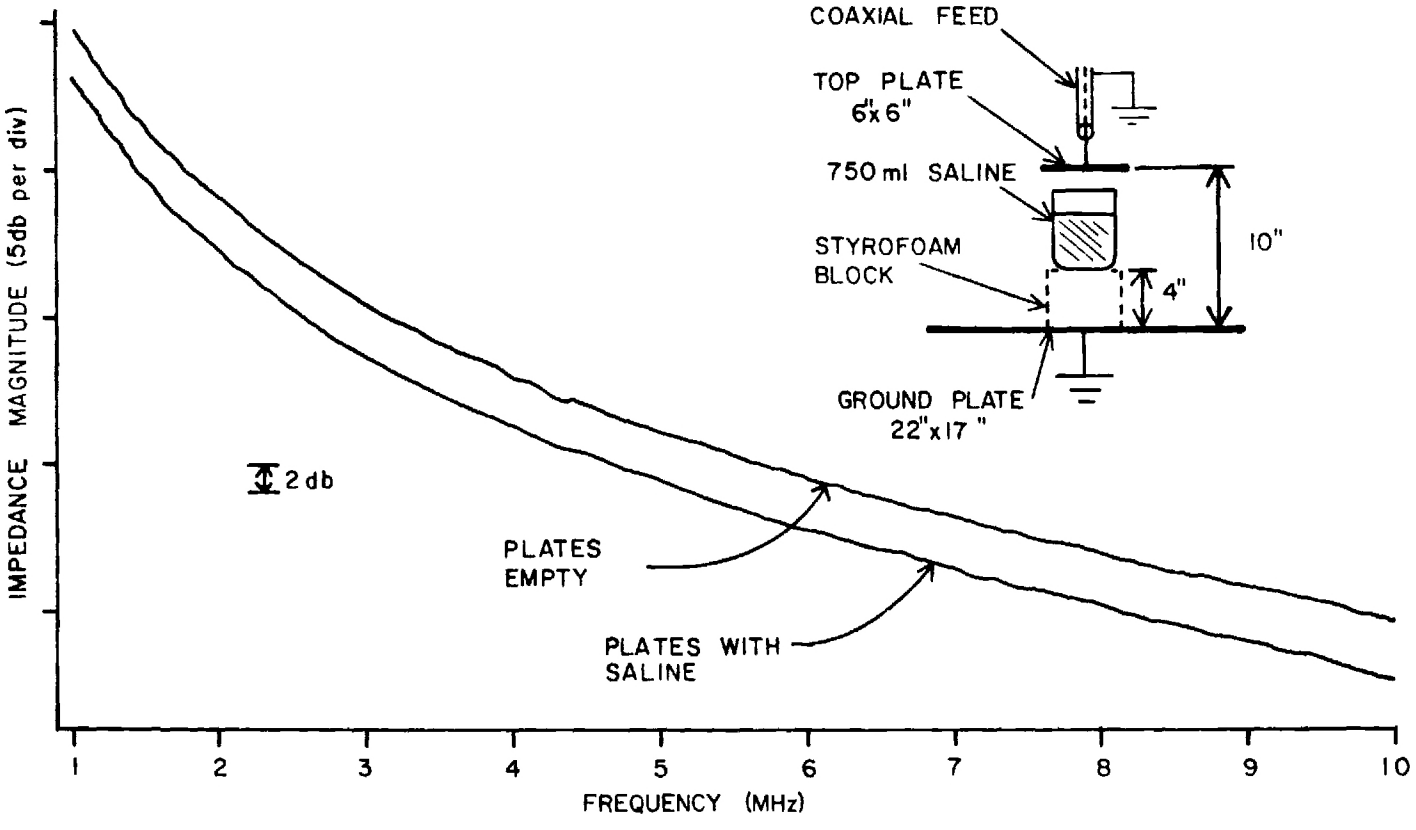

Figure 9. Experimental results obtained from tests of capacitor plate detection concept.

- Accuracy (ability to detect consistently an agricultural product),
- Resolution (ability to yield an estimate of the size and position of any detected agricultural product), and
- Speed (ability to analyze quickly raw data and indicate whether an agricultural product is present).

The accuracy which can be achieved with the capacitor plate approach will be largely determined by the suitability of the capacitor configuration selected. In general, the optimal detection accuracy is obtained when the observed impedance change is as large as possible. The capacitor configuration used in the preliminary laboratory tests (see Figure 9) exhibited an easily observable 2 dB decrease in impedance magnitude when a relatively large beaker of saline was placed between the plates. However, when the tests were repeated using a smaller-sized orange as the target object, a smaller 1 dB decrease in impedance magnitude was observed. Therefore, it is likely that capacitor plates used in future investigations will be smaller to match the size of fruit more closely. With smaller capacitor plates, fringing effects may become more pronounced because of the reduced plate size-to-plate separation ratio. Laboratory tests, in which target objects will be positioned at various locations between the capacitor plates, will be performed to characterize the electrical behavior of the capacitor plates and determine the nature of any existing fringing effects. If these tests indicate that fringing effects are pronounced, it may be necessary to employ guard rings or to modify the basic rectangular parallel plate configuration.

The size of the capacitor plates will also significantly impact the attainable resolution. An advantage (in terms of resolution) of small plates is that it should be possible to detect small objects. A major disadvantage of small plates is that only a small part of the volume of an average suitcase could be interrogated. This will probably make it necessary to investigate an approach that either (a) employs multiple sets of capacitor plates, or (b) employs moving capacitor plates that can scan over an extended area.

IV. SIGNAL TRANSMISSION/REFLECTION APPROACH

The possibility of detecting the presence of agricultural products in baggage utilizing the transmission and reflection of electromagnetic waves depends upon the differences between the dielectric properties of these items and those of other common objects found in travelers' baggage. Because of the different properties, electromagnetic waves in air are more strongly reflected and more greatly attenuated in encounters with agricultural products than they are when striking materials such as cloth, leather, and plastic. For the transmitted signal, a phase shift results from the slower velocity of the wave through the material. Similarly, a phase shift in the reflected signal comes from the discontinuity at the dielectric interface. During this reporting period, these differences in transmitted and reflected signals have been investigated using theoretical analyses and experimental measurements.

A. Analyses

The simplest case involving the transmission and reflection of electromagnetic waves is that of a uniform plane wave passing through two dielectric materials occupying regions of semi-infinite extent. These regions adjoin at a single planar interface as illustrated in Figure 10. The reflected and transmitted electric fields, E_R and E_T, at the interface are given in terms of the incident field E_F, by:

$$\rho \equiv \frac{E_R}{E_F} = \frac{\eta_2 - \eta_1}{\eta_1 + \eta_2} \tag{10}$$

and

$$\tau \equiv \frac{E_T}{E_F} = \frac{2\eta_2}{\eta_1 + \eta_2} , \tag{11}$$

where η_1 and η_2 are the intrinsic impedances of materials 1 and 2, and ρ

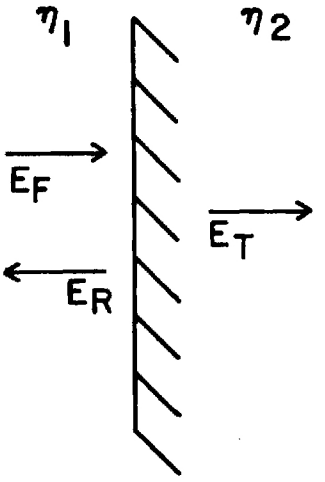

Figure 10. Forward, reflected, and transmitted signals at a planar interface between two dielectric media.

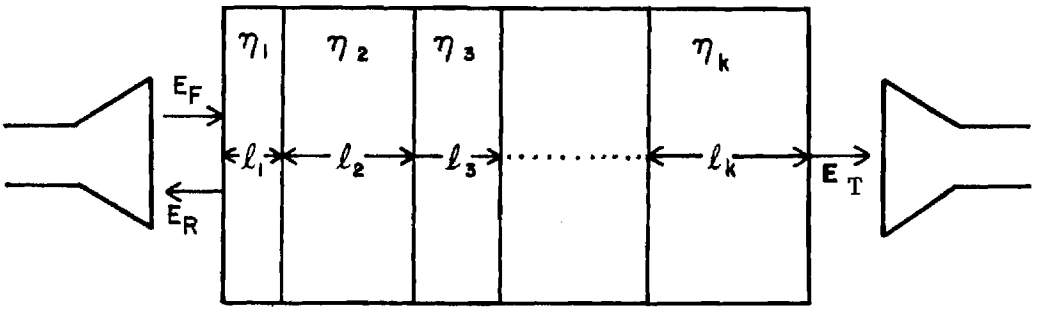

Figure 11. Forward, reflected, and transmitted signals for layers of dielectric materials.

and τ are defined as the voltage reflection and transmission coefficients, respectively. The intrinsic impedance is given by

$$\eta = \sqrt{\mu/\varepsilon^*} \tag{12}$$

where μ is the magnetic permeability of the material (assumed to be that of free space for all materials discussed in this report) and ε^* is the complex permittivity discussed in Section II. This example illustrates the basic phenomena, namely, that part of the wave is reflected while part is transmitted and that phase shifts occur because of the complex nature of the impedances. However, this case is much too simple to give an accurate indication of the signals which might be observed reflecting from or traveling through baggage containing many items. For the transmitted signal, one is interested in describing the wave after it has passed through the suitcase, possibly having met several interfaces, and arrived at the detector. Similarly, the reflected signal is influenced by the baggage thickness and its contents.

The first level of complexity approaching this situation is illustrated in Figure 11. This model consists of a plane wave impinging upon successive planar layers, or slabs, of material characterized by their intrinsic impedances and thicknesses. Although this is still a highly idealized geometry, it better represents a suitcase with inhomogeneous contents. It is adequate for an investigation of the behavior of reflected and transmitted signals as functions of the characteristics of a lossy layer. In addition, the frequency response can also be investigated.

Even with this simple geometry, a complex situation exists because reflections occur at each interface for both reflected and transmitted waves. This problem can be analyzed by utilizing the analogy of plane waves propagating through dielectrics to signals traveling through transmission lines. The powerful tools of network theory for cascaded two-port devices can then be employed. Each interface and section of dielectric is treated as a two-port device characterized by a transmission matrix T. Signals are represented by complex numbers a_1, a_2, b_1, and b_2 as shown in Figure 12. The signals are related to each other through the T-matrix by:

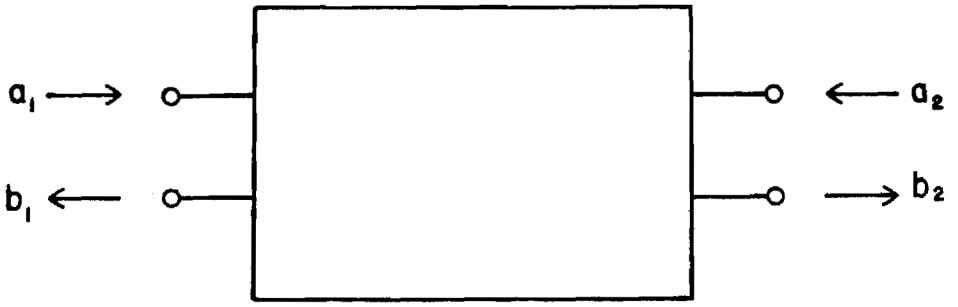

Figure 12. Two-port device with input signals a_1 and a_2 and output signals b_1 and b_2.

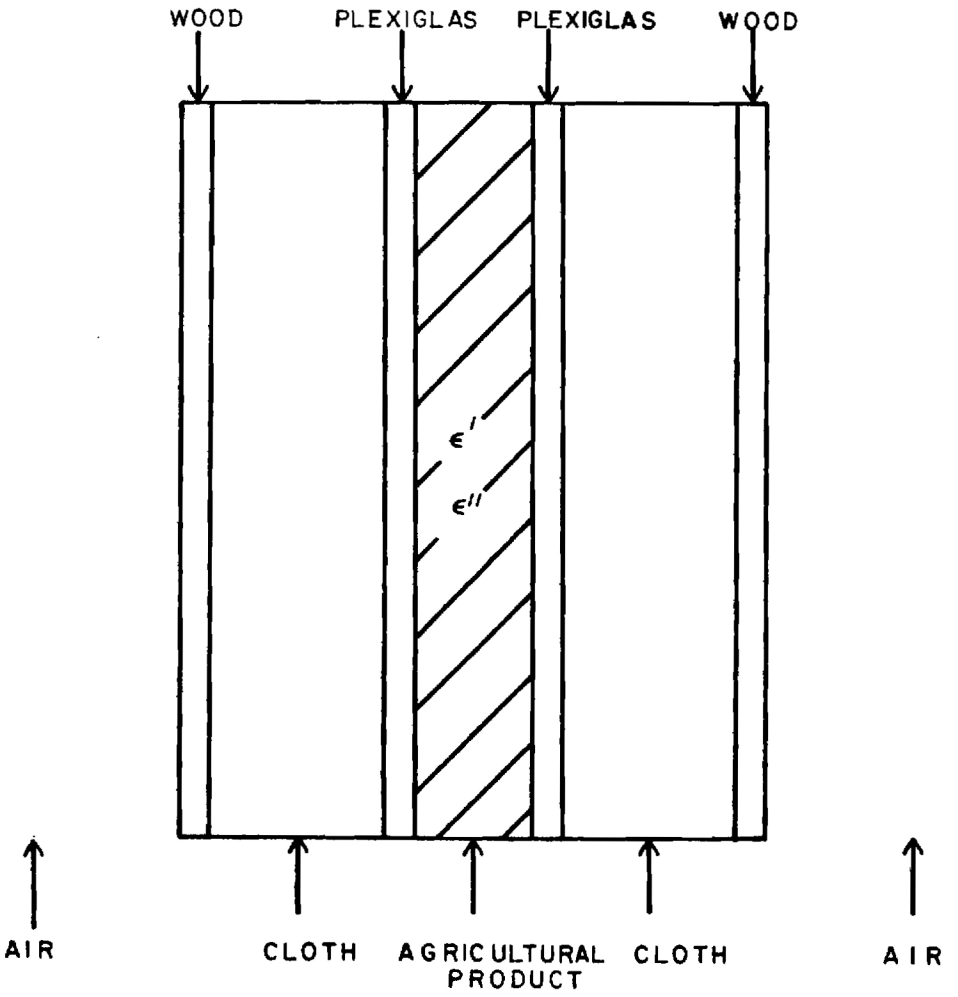

Figure 13. Layered model used in the analytic study.

$$\begin{pmatrix} b_2 \\ a_2 \end{pmatrix} = \begin{pmatrix} T_{11} & T_{12} \\ T_{21} & T_{22} \end{pmatrix} \begin{pmatrix} a_1 \\ b_1 \end{pmatrix} \tag{13}$$

The entire network consisting of the cascaded layers of material is represented by a sequence of two-ports representing layers and boundaries. The T-matrix for an interface "two-port" is

$$T = \begin{pmatrix} \dfrac{\eta_1 + \eta_2}{2\eta_1} & \dfrac{\eta_1 - \eta_2}{2\eta_1} \\ \dfrac{\eta_1 - \eta_2}{2\eta_1} & \dfrac{\eta_1 + \eta_2}{2\eta_1} \end{pmatrix} \tag{14}$$

for a uniform section of dielectric,

$$T = \begin{pmatrix} e^{-jk\ell} & 0 \\ 0 & e^{+jk\ell} \end{pmatrix} \tag{15}$$

where $k = \omega\sqrt{\mu\epsilon^*}$ (ω being the angular frequency) and ℓ is the layer thickness. If ϵ^* is complex, the waves are attenuated as well as phase shifted. Both attenuation and phase shift depend on frequency and layer thickness.

In order to obtain the total response of the cascaded sequence, the T-matrices for each successive "two-port" are multiplied. Finally, to obtain the reflection and transmission coefficients, the total T-matrix is transformed to the scattering or S-matrix whose components are directly related to these coefficients. The transformation is:

$$\begin{aligned} S_{11} &= -T_{21}/T_{22}, \\ S_{12} &= 1/T_{22}, \\ S_{21} &= (T_{11}\,T_{22} - T_{12}\,T_{21})/T_{22}, \text{ and} \\ S_{22} &= T_{12}/T_{22}\,. \end{aligned} \tag{16}$$

Outputs in terms of the inputs and the S-matrix are:

$$\begin{pmatrix} b_1 \\ b_2 \end{pmatrix} = \begin{pmatrix} S_{11} & S_{12} \\ S_{21} & S_{22} \end{pmatrix} \begin{pmatrix} a_1 \\ a_2 \end{pmatrix} . \qquad (17)$$

As can be seen from Figure 12 and the above relation, S_{11} is the voltage reflection coefficient and S_{21} is the voltage transmission coefficient for incident waves propagating from left to right.

The model used for computer computation is illustrated in Figure 13 and the properties of each layer are listed in Table III with wood and cloth dielectric data estimated from Reference 9. This situation was chosen to represent baggage containing a layer of fruit-like lossy material imbedded in clothing. It also represented an actual experimental model described below.

For this model, the dependence of the voltage reflection and transmission coefficients on ε', ε'', and ℓ were determined. In addition, the frequency response over the range of 1 to 5 GHz was determined for certain thickness and dielectric properties. The purpose of this simulation was to obtain an idea of signal changes one might expect to observe due to the lossy layer, and to determine trends with the variation of the parameters describing the layer. In order to evaluate changes with the insertion of the lossy layer, the ratios of ρ and τ values with the lossy layer (ρ_w and τ_w) were taken to those without the lossy layer (ρ_{wo} and τ_{wo}) when replaced by air to keep the overall length constant. Thus, the results were expressed as ρ_w/ρ_{wo} and τ_w/τ_{wo}. The magnitudes of these quantities when given in dB are then $20 \log \rho_w - 20 \log \rho_{wo}$ and $20 \log \tau_w - 20 \log \tau_{wo}$. The phase of the quantities are the phase shifts $\phi^{\rho}_{w} - \phi^{\rho}_{wo}$ and $\phi^{\tau}_{w} - \phi^{\tau}_{wo}$.

Figures 14 and 15 show the computer solutions for ρ_w/ρ_{wo} and τ_w/τ_{wo} for the frequency range of 1 to 5 GHz with the thickness of the lossy layer fixed at 3 inches. The frequency dependence of the lossy layer's permittivity was programmed as described in Section II.

TABLE III

CHARACTERISTICS OF MATERIALS USED IN LAYER MODEL

Layer	Material	Thickness (in)	ε_r'	ε_r''
1	air	---	1.0	0.0
2	wood	1/4	2.1	0.07
3	cloth	3-1/4	2.0	0.2
4	Plexiglas	1/4	2.5	0.001
5	"fruit"	variable	variable	variable
6	Plexiglas	1/4	2.5	0.001
7	cloth	3-1/4	2.0	0.2
8	wood	1/4	2.1	0.07
9	air	---	1.0	0.0

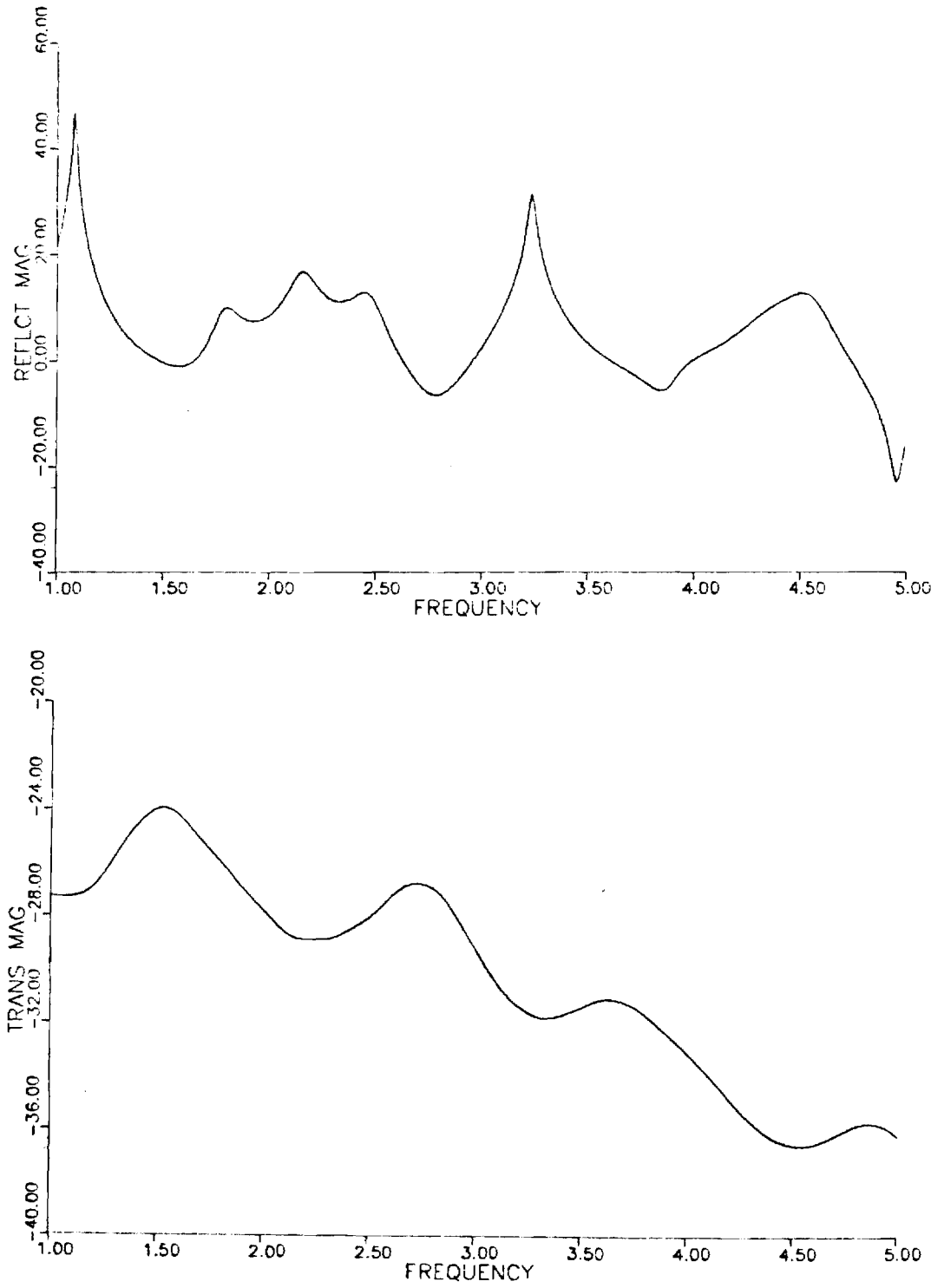

Figure 14. Magnitude ratios of voltage reflection (top) and transmission (bottom) coefficients for layered model as functions of frequency. Both are plotted in dB as functions of frequency in GHz.

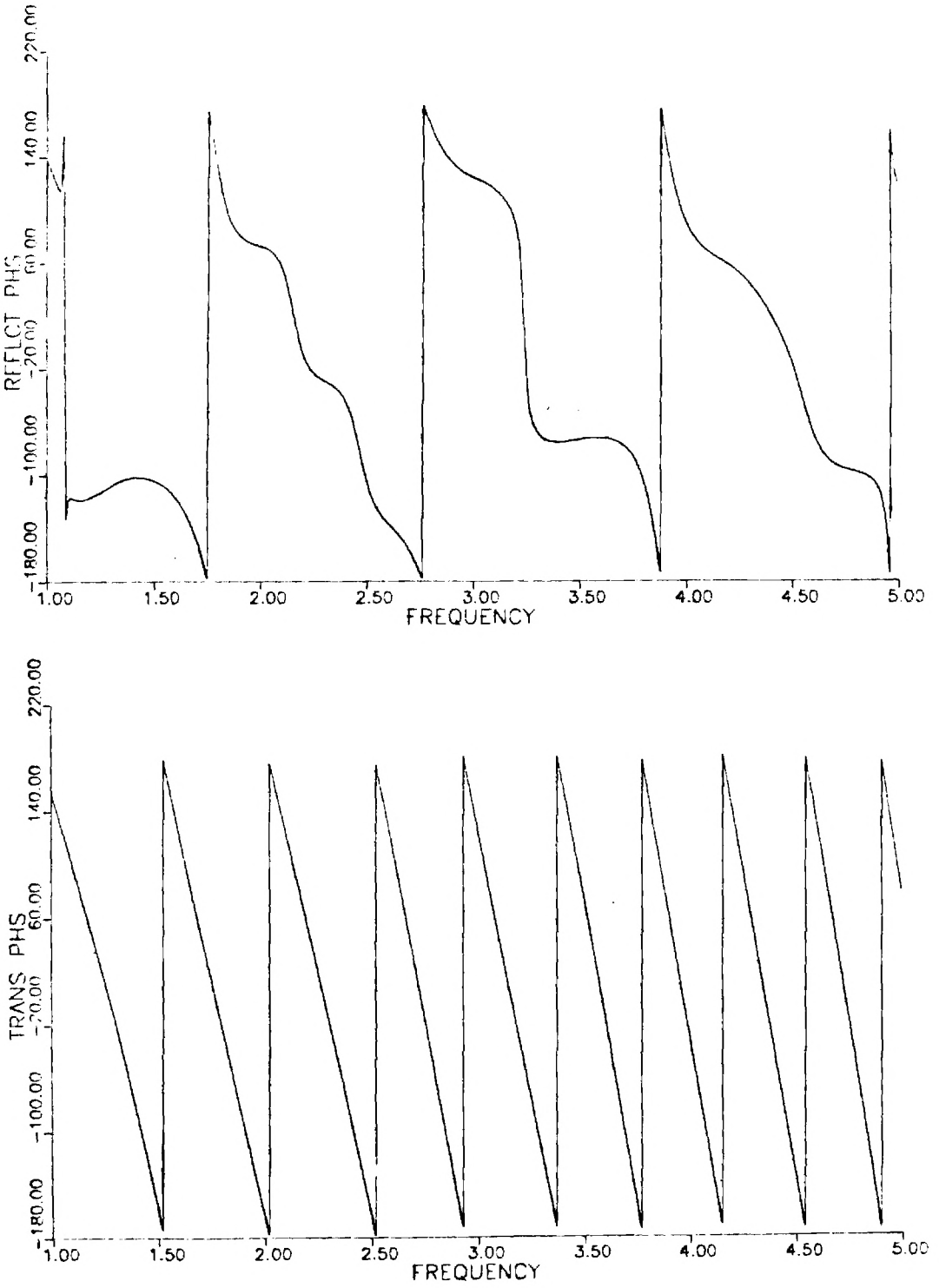

Figure 15. Phase differences of voltage reflection (top) and transmission (bottom) coefficients for layered model as functions of frequency. Both are plotted in degrees as functions of frequency in GHz.

Magnitude ratios in Figure 14 show the expected behaviors. The reflection is greater with the insertion of the high dielectric, lossy layer. In addition, there are sharp peaks which arise from a half-wavelength window effect. At certain frequencies, the air layer thickness (used in computing ρ_{wo}) is a half-wavelength multiple resulting in little reflection of the incident wave. With the insertion of the lossy dielectric layer, these dips are smoothed out and moved in the frequency domain, resulting in spikes in the difference, 20 log ρ_w - 20 log ρ_{wo}. Secondary structure is also evidently arising from similar effects in the other layers. The positions of these spikes depend on an interplay of the thicknesses of the layers and the dielectric properties. The transmitted wave is greatly attenuated by about 30 dB by the lossy layer. This attenuation generally increases with frequency. It should also be noted that there are small bumps and dips which correlate with changes in the reflected signal. These are smoothed out, however, due to the attenuation of the transmitted wave.

Phase shifts shown in Figure 15 generally increase with frequency. For the reflected signal, the detailed structure is roughly periodic with deviations corresponding to peaks in reflection magnitude. For the transmitted signal, the increase is quite regular and may be a good indicator of the nature of the intervening dielectric. The period of the phase shift as a function of frequency with the dielectric inserted is much shorter because of the longer electrical length (i.e., the wavelength is contracted by $\sqrt{\varepsilon}$). The beat between phase signals may be a sensitive indicator of the material inserted.

Figures 16 and 17 show the computed behavior of ρ_w/ρ_{wo} and τ_w/τ_{wo} as functions of the thickness of the inserted lossy layer. For this case, the total length of "layer 5" in Table III was kept fixed by replacing this section with three layers—air, "fruit", air—such that, as the fruit layer grew, the air layers shrank. The frequency was 2 GHz.

The reflected magnitude ratio shown in Figure 16 has some fine structure at small thicknesses which is caused by half-wavelength window phenomena in the air layers described previously. When the thickness

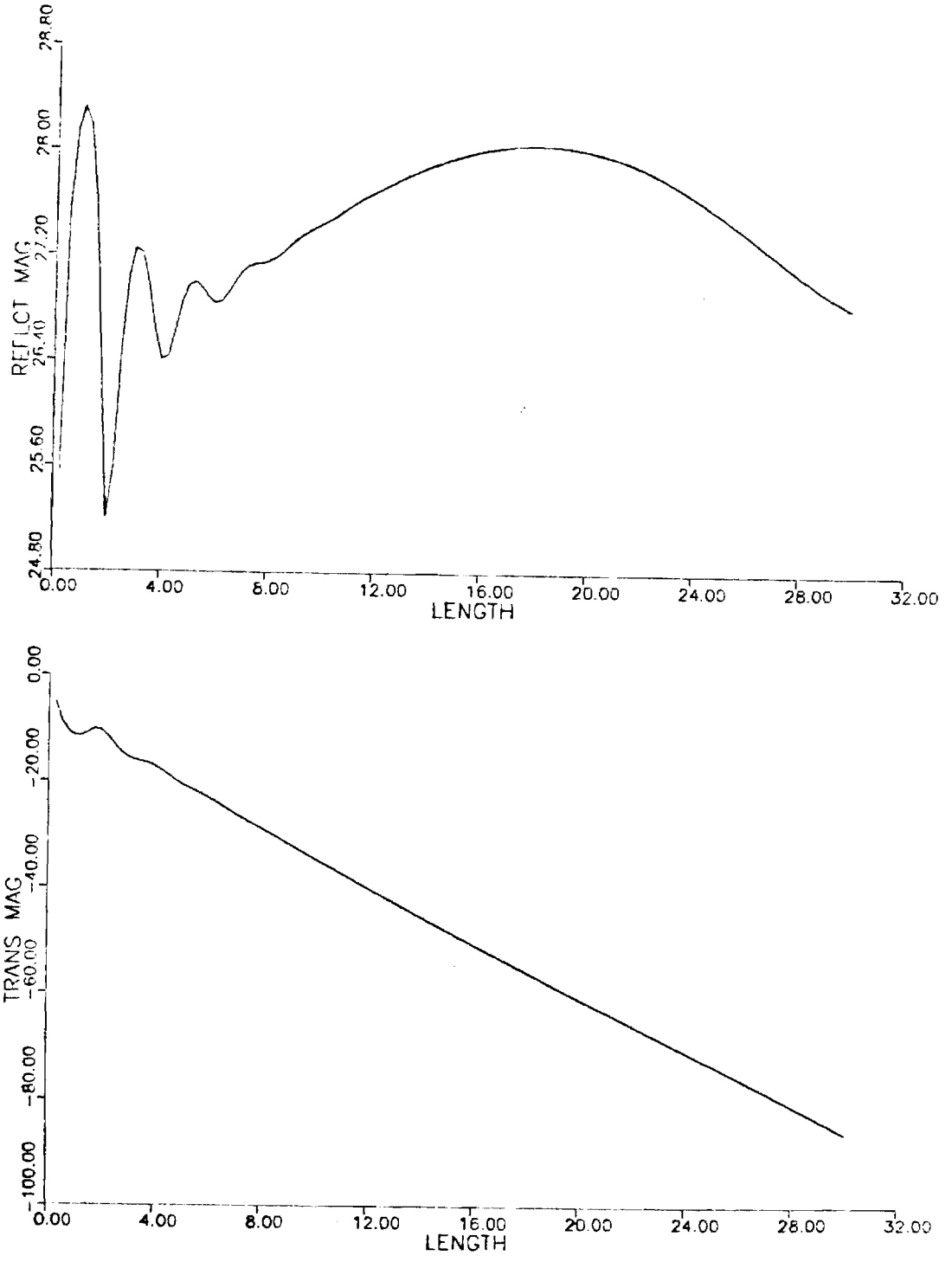

Figure 16. Magnitude ratios of voltage reflection (top) and transmission (bottom) coefficients for layered model as functions of lossy layer thickness. Both are plotted in dB as functions of lossy layer thickness in cm.

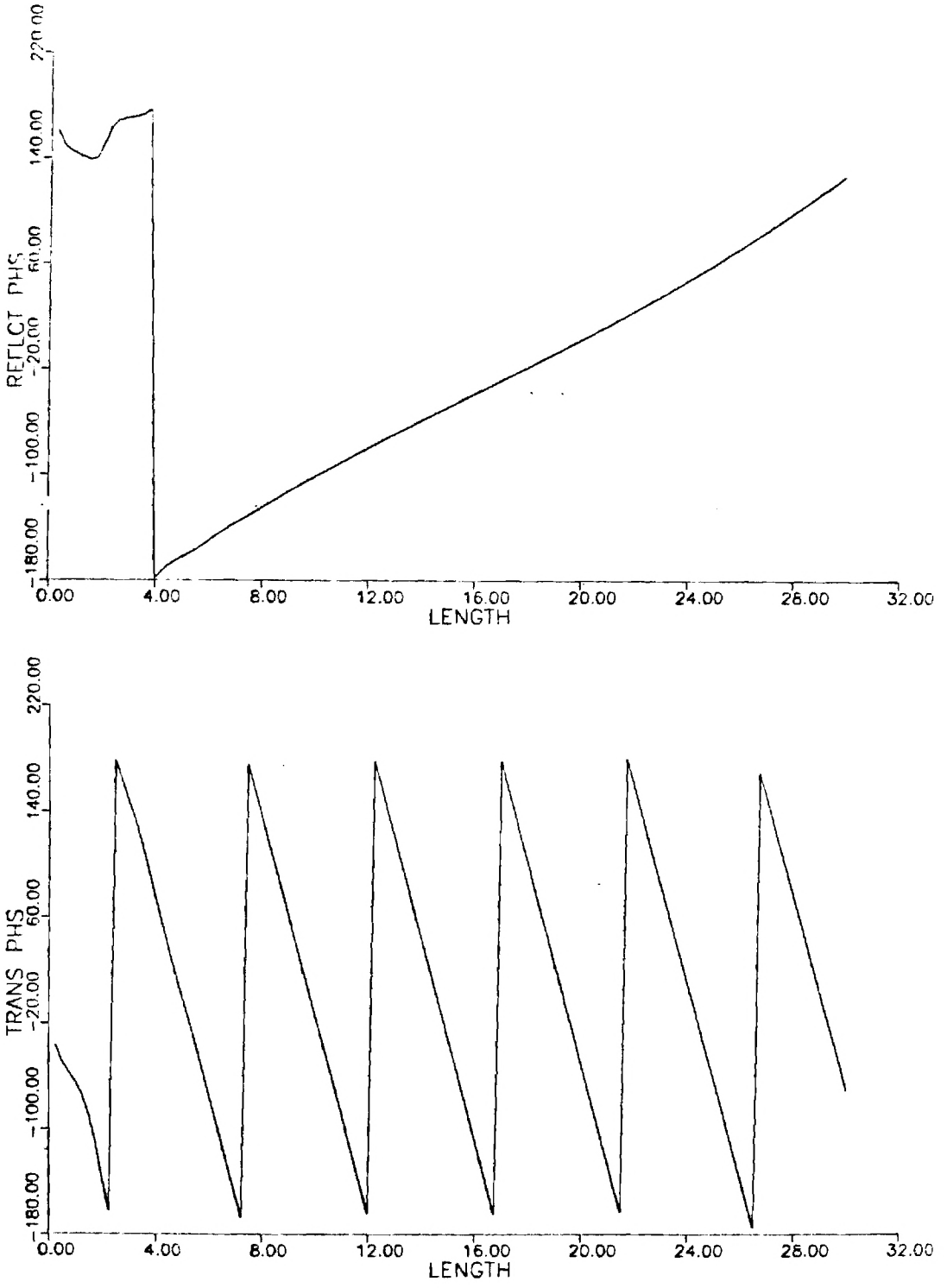

Figure 17. Phase differences of voltage reflection (top) and transmission (bottom) coefficients for layered model as functions of lossy layer thickness. Both are plotted in degrees as functions of lossy layer thickness in cm.

of the lossy layer is larger (and the air layers are thinner), the behavior is fairly smooth. As expected, the transmitted wave magnitude diminishes with thickness (Figure 16). For a thickness of 30 cm, the transmitted signal is about 90 dB below the signal without dielectric.

The reflected phase shift shown in Figure 17 has a gradual dependence on thickness. In contrast, the transmitted phase shift (also Figure 17) shows a rapid period which results from the increasing electrical length through which the wave propagates.

B. Measurements

Experiments were performed in order to determine the feasibility of observing changes in the reflected and transmitted signals when fruit-like material was placed in an RF field. The equipment employed included an HP 8410B network analyzer, an HP 8743A transmission/reflection unit, and an HP 8620C/86222A sweep oscillator. As a first step, a wooden box was constructed with the approximate dimensions of a suitcase, 10 x 18 x 30 inches, with a slot into which a plastic (Plexiglas) tray containing a liquid with fruit-like dielectric properties could be inserted. This test apparatus was designed to correspond, roughly, to the analytic case examined in the preceding section. A schematic of the apparatus is given in Figure 18.

Tests were made with the Plexiglas tray empty and with it filled with a 30% (w/w) mixture of glycerol and water. The properties of this solution [17] mimic those of food items like fruits and meats. For example, its relative dielectric constant of 48 and relative loss factor of 14 at 2.45 GHz [17] agree very well with literature values for fruit given in Figures 3 and 4. The thickness of this layer was 3 inches. The box was placed 2-1/2 feet from the LS-band transmitting horn antenna, outside the near field but not actually in the far field region. This horn also functioned as the receiving antenna for the reflected signal. The receiving horn for the transmitted signal was placed 2 feet from the opposite side of the box. The RF generator was swept from 1.8 to 2.4 GHz to correspond to the frequency range of the waveguide and horn antennas. The reflected signal showed a great deal of structure not related to the box or its contents but which was probably caused by the

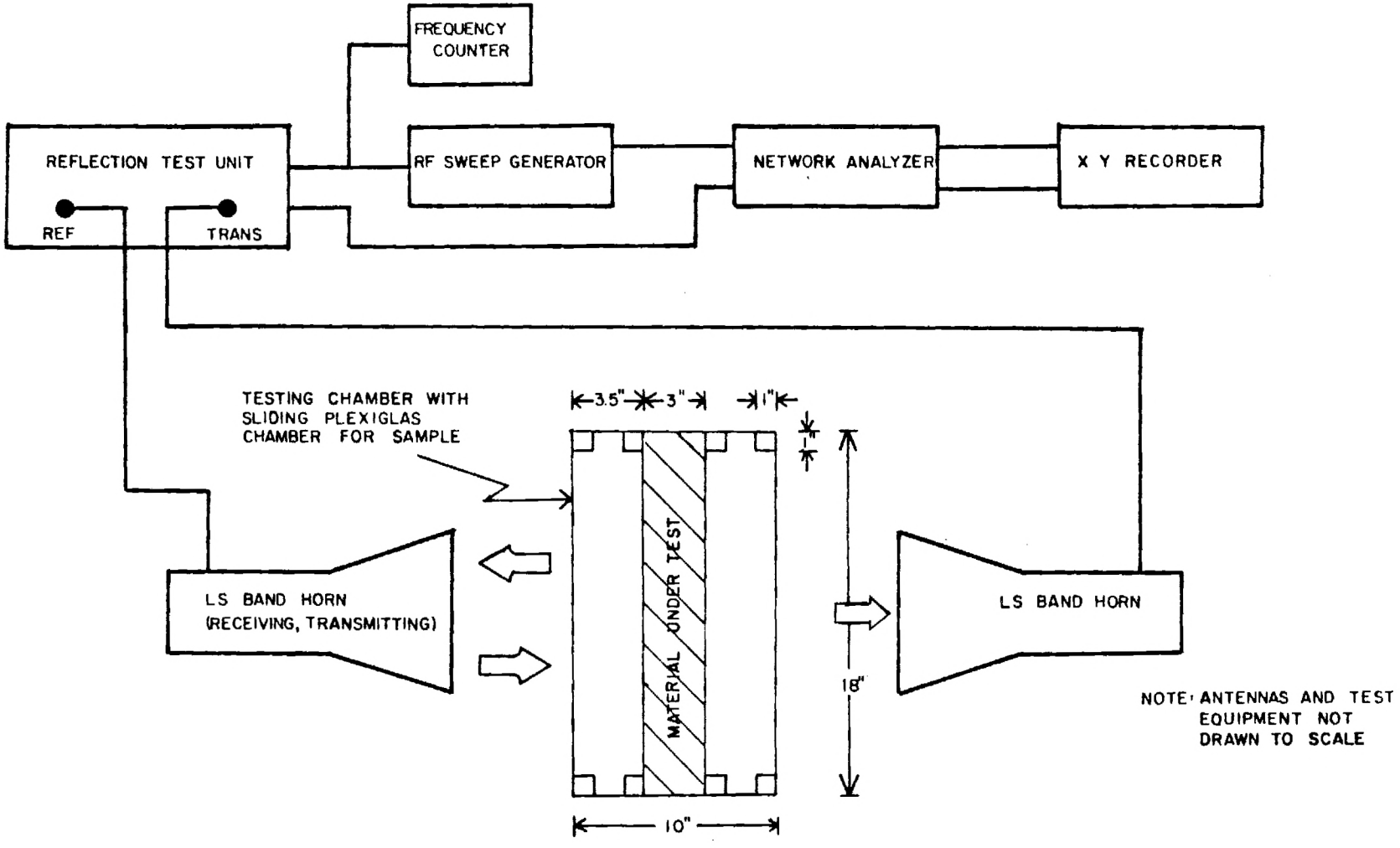

Figure 18. Experimental apparatus used for observing changes in transmission and reflection coefficients.

match of the transmitting system to air and signals reflected from other nearby objects. When the lossy layer was inserted, this structure did not change appreciably; however, the overall magnitude of the reflected signal increased by about 2 dB. The transmitted signal did not show as much structure as the reflected signal and thus could be displayed on a more sensitive scale. Measurements taken with and without the inserted layer showed a 14 dB reduction in transmission caused by the layer.

The next step in the experiment used the same setup except that oranges were placed at the center of the "suitcase." Figures 19 and 20 show the magnitudes of reflected and transmitted signals, respectively, with and without oranges present. Because of the large variation of the reflected signal with frequency due to factors unrelated to the "suitcase" and oranges, a sensitivity of 5 dB/division had to be used to display the entire frequency range. Changes on the order of 1 dB can be seen at some frequencies; however, it should be noted that the largest change, occuring at 1870 MHz, involved a -1 dB change for one orange and a +1 dB change for two oranges. The transmitted signal was more uniform with frequency and could be displayed with a greater sensitivity of 0.5 dB/division. It is seen that the transmitted signal was attenuated approximately 0.3 dB for one orange and 0.9 dB for two oranges. Thus, the changes in transmitted signal magnitude were more consistent over the frequency range and with the number of oranges than was reflected signal magnitude.

Rapid variations in phase precluded any attempt to see details of phase shift due to oranges over the entire frequency range. A narrow frequency band from 1799.5 MHz to 1800.5 MHz was examined to see the order of magnitude of the phase shift. For the reflected signal, the phase shift was about 4^{o} for one or two oranges; however, it was not constant within the narrow band and appeared to decrease with frequency. The transmitted phase shift was fairly constant around 5^{o} for one orange and 10^{o} for two oranges. Transmitted phase thus seems to be more sensitive than reflected phase to the number of oranges over this narrow frequency range.

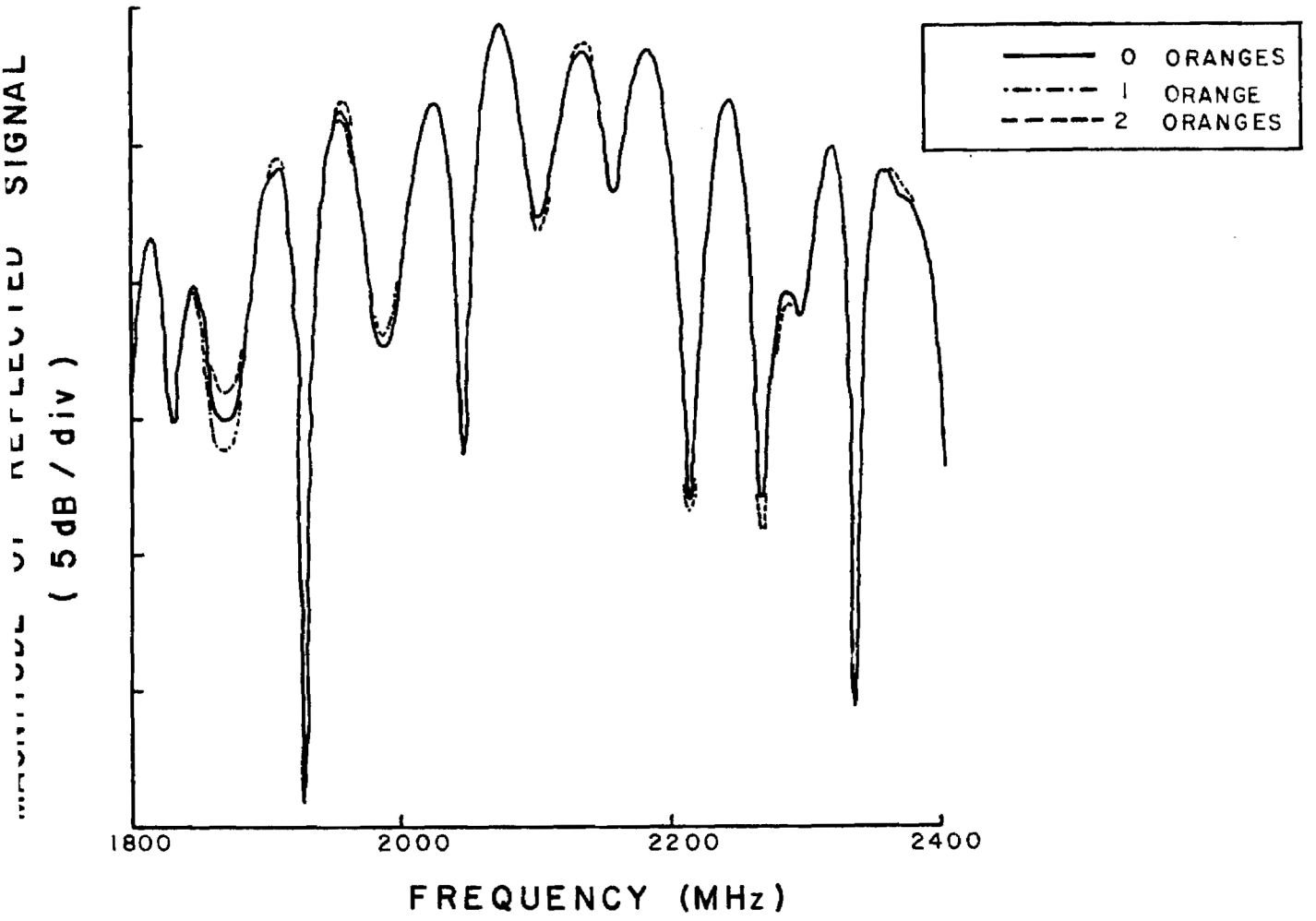

Figure 19. Magnitude of the reflected signal with and without oranges present.

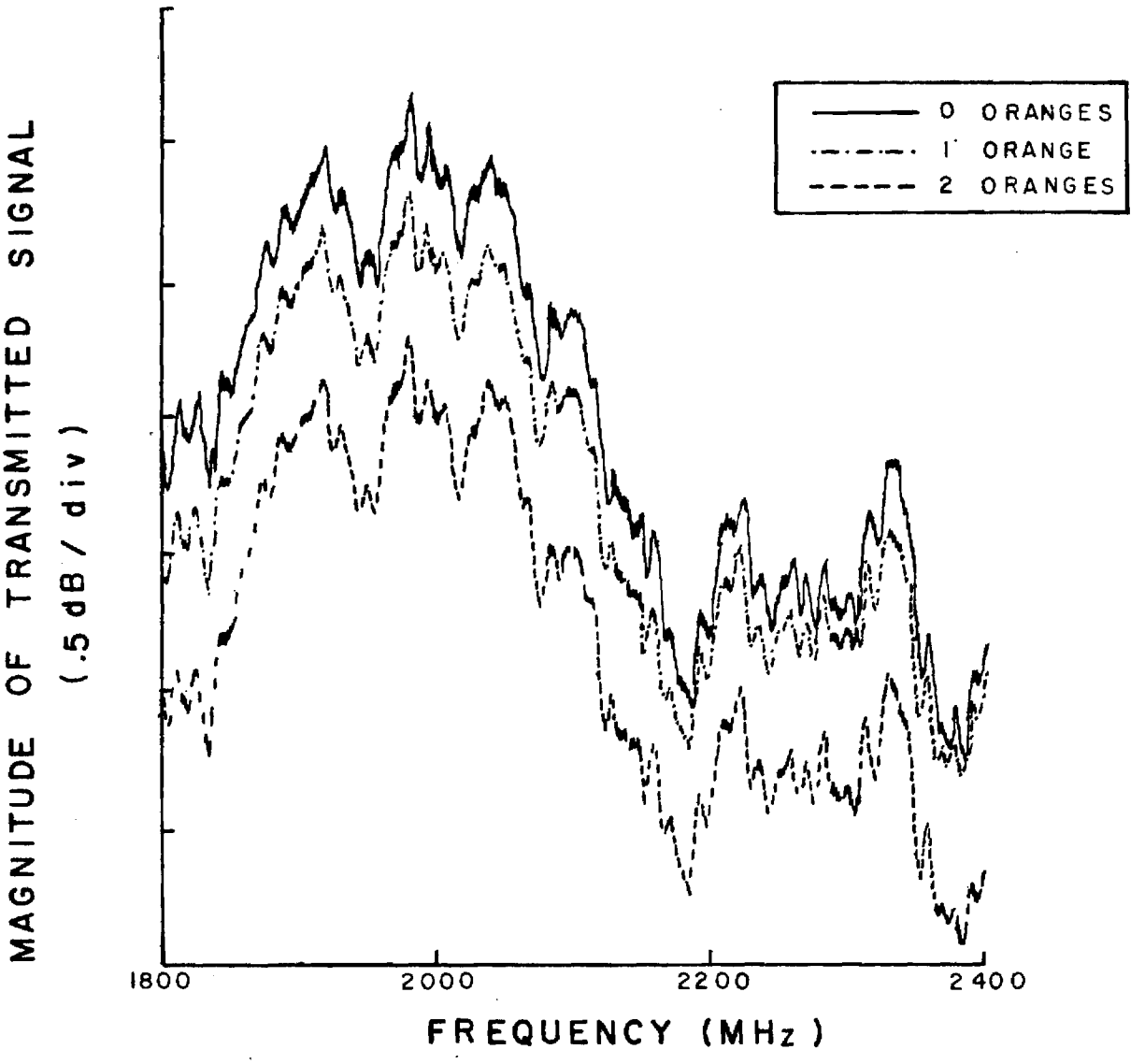

Figure 20. Magnitude of the transmitted signal with and without oranges present.

C. Future Investigations

Analysis of the layered model showed the transmitted signal as the most sensitive indicator of the presence of the fruit-like lossy dielectric layer. The predicted attenuation of the transmitted signal was borne out in the experimental tests. The phase shift of the transmitted signal compared to a signal not passing through the lossy dielectric displayed a regular pattern as a function of frequency (Figure 15). This offers a possibility for identification of materials in that this information contains the signal time delay caused by the slower velocity of the wave in the media. The phase shift for oranges measured at a single frequency also was quite stable.

Plans for the next quarter on the analytic approach will include further investigation of the transmission and reflection coefficients as functions of frequency for different sets of dielectric parameters and thicknesses. The effect of less idealized geometry may also be treated if it appears that such considerations are necessary.

Experimentally, the next step will be to implement computer control of the network analyzer for the reflection and transmission tests so that problems related to the sensitivity of the display units will be eliminated. Another priority will be the construction of antennas more applicable to the problem and capable of investigating other frequency ranges. Initially, antennas will be constructed to illuminate the entire cross section of the suitcase; however, in the future it may be necessary to design a directional array of antennas for segmented illumination in order to gain spatial resolution of the suitcase contents. Another experimental effort will be the formation of a reference signal which can be merged with the transmitted signal. This would eliminate the need for removing the fruit-like layer to form a reference signal.

V. SHORT PULSE RADAR APPROACH

Short Pulse Radars (SPRs), also known as "impulse" and "baseband" radars, use very brief, transient pulses in their operation. The narrow pulse, typically 1-to-10 ns width, provides a transmitted signal with broad frequency content. Typical pulse amplitude is on the order of 1000 V to provide sufficient energy across the frequency spectrum. The SPR works by emitting a pulse from an appropriate antenna and then receiving the energy reflected by objects in front of the antenna. Received signals (reflections, or returns) tend to be pulsatile but their shape is determined by the nature of the object causing the reflection, as well as the shape of the transmitted pulse. Distance to the object, or target, can be derived from the delay between transmitted and reflected pulses and is easily extracted from SPR returns when dielectric properties of the propagation medium are known. Additional information about the target can be gained from an analysis of reflected pulse shape. In this section, operation of SPR is further described and its application to detection of fruits and vegetables in baggage is considered.

The SPR has already been used successfully in several applications. Identification of underground objects such as utility pipes [18], tunnels and voids [19], metallic and dielectric explosive mines [20-21], and pieces of wood and plastic [21] is possible. Voids under concrete highways have also been detected [22]. In another type of application, SPR has been used to determine subsurface structure of icebergs [23] and geophysical strata [19,24]. All of these applications utilize returned pulse delays to determine distances. Returned pulse frequency content is required to identify and classify buried objects.

In the SPR approach, detection of a buried object is very similar to detection of fruit in a suitcase. In both cases, an object a few centimeters in size is surrounded by a larger volume with dielectric properties different from the object's. Also, in both cases, the larger volume's surface facing the antenna is flat. Thus, a description of SPR detection of buried objects is useful in considering SPR detection of fruit in baggage.

For the idealized situation of a single buried object, SPR operation can be simply explained. A pulse of electromagnetic energy is emitted from the SPR antenna and propagates in air to the ground surface. At this interface, part of the energy is reflected to the antenna now acting in a receive mode. The remainder of the energy propagates through the soil to the target where part of it is reflected through soil and air to the antenna. The part of the energy not reflected by the target proceeds on through the soil and is dissipated. This situation is shown in Figure 21 in which forward energy propagates to the right.

Shape and amplitude of the reflected pulse waveform depend on the difference in dielectric properties at the respective interfaces. A feel for the approximate shapes can be had from consideration of the voltage reflection coefficient ρ, which is the complex ratio of reflected to forward electric fields of the propagated waves as given by equation (10) in Section IV. The reflected electric field can be expressed as

$$E_R = \rho E_F. \tag{18}$$

The maximum magnitude of ρ is unity. Since all materials considered here have the magnetic permeability of free space, ρ is a function only of the complex permittivities involved. Using equations (10) and (12),

$$\rho = \frac{\sqrt{\varepsilon_1^*} - \sqrt{\varepsilon_2^*}}{\sqrt{\varepsilon_1^*} + \sqrt{\varepsilon_2^*}} \quad . \tag{19}$$

Forward energy propagates through region 1 into region 2. For $\varepsilon_2^* > \varepsilon_1^*$, as it is for the air/soil interface, $\rho < 0$ and $E_R < 0$ with $E_F > 0$ assumed. Thus, the pulse reflection will be mostly negative, as shown in the sample reflected waveform, Figure 21. The pulse return is an inversion of the transmitted pulse. By following a similar procedure for the buried target with $\varepsilon_{ob}^* < \varepsilon_2^*$, $\rho > 0$ at the soil/target interface. This effect is illustrated in Figure 21 as a mostly positive waveform.

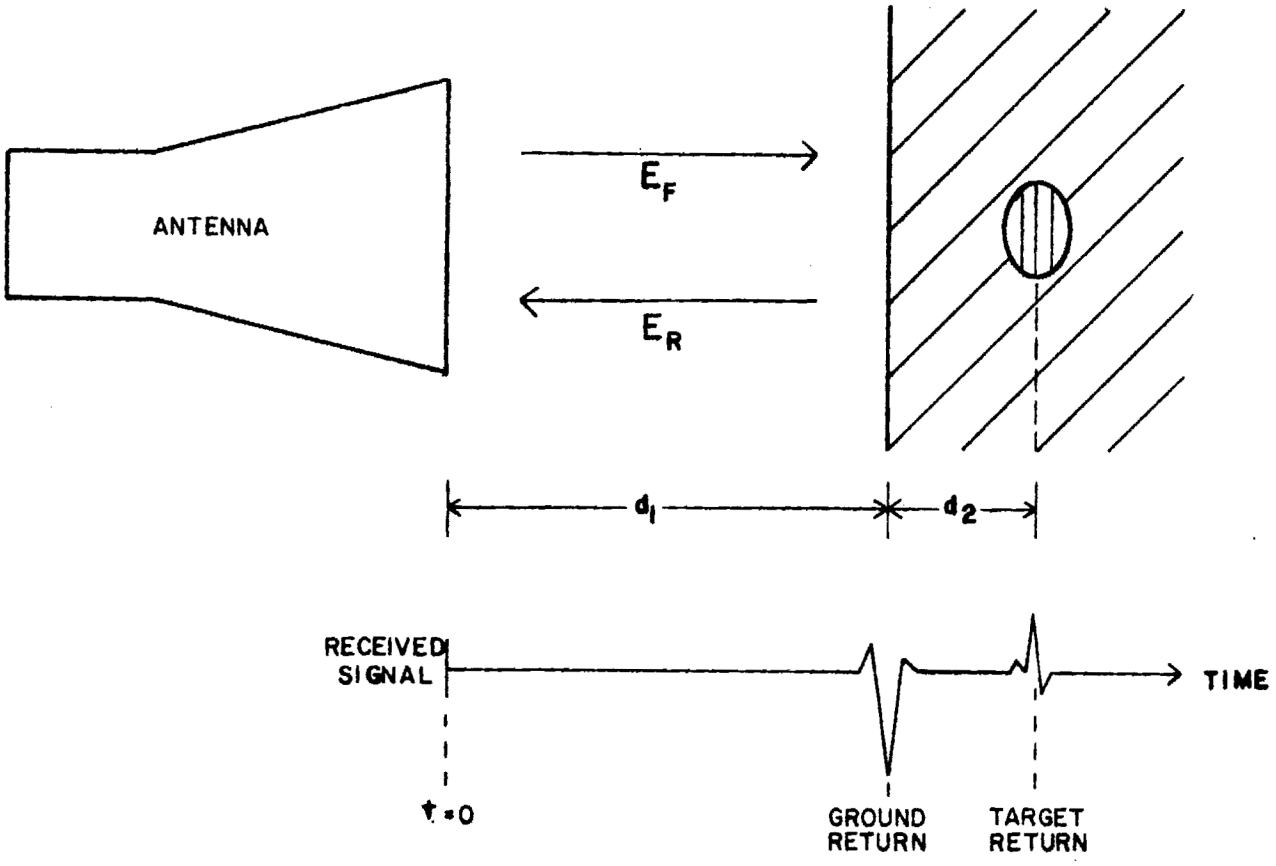

Figure 21. Diagram of typical SPR arrangement and response for subsurface targets.

Delay to the reflected pulse return from the air/soil interface is twice the product of propagation velocity in air and antenna distance above ground, d_1. Similarly, the additional delay to the target return is twice the product of propagation velocity in soil and burial depth, d_2. These delays are longer for larger distances.

Relative amplitudes of the returns can be estimated from equation (19). It is seen that a larger difference in permittivities causes a larger reflected pulse. Attenuation of propagating signals has not been considered in this example. However, dissipation of energy in soil would reduce the amplitude of the target return estimated from equation (19).

For baggage subjected to interrogation by SPR, a dielectric slab is taken to represent the suitcase and its contents. For simplicity, the slab extends infinitely in directions orthogonal to the propagation direction. A suitcase and its normal contents of clothing has a relative permittivity of approximately 2.5 and is essentially lossless (nondissipative). The target fruit has relative complex permittivity of approximately 50 - j 20, corresponding to frequencies in the gigahertz range, Figures 3 and 4. Propagation velocity in air is $30 \cdot 10^9$ cm/s ($11.8 \cdot 10^9$ in/s); in the suitcase, $19.9 \cdot 10^9$ cm/s ($7.5 \cdot 10^9$ in/s). Propagation delays in the two media are then 0.033 ns/cm (0.085 ns/in) in air and 0.053 ns/cm (0.134 ns/in) in the suitcase.

For the suitcase alone, there will be two returns: one from the front surface and one from the rear surface. Substituting the dielectric constants for air (free space) and slab into equation (19) gives $\rho = -0.225$ for the front surface and $\rho = 0.225$ for the rear surface. The first return will be similar to the ground return in Figure 21; the second, an inverted form of the ground return. The two returns will be separated by a delay of twice the product of propagation delay per unit length and suitcase thickness. For a thickness of 10 in, the delay is 2.68 ns; for 5 in, 1.34 ns. The range of 5-to-10 ins includes most baggage thicknesses. This very short delay between returns from the suitcase surfaces may very well limit the detection of fruit which would have a return occurring between these. Typical time courses for target

returns are 1-to-2 ns [19-21]. So for the suitcase alone, there would be two signals of this duration only 1.3-to-2.7 ns apart, onset to onset. In other words, the suitcase returns would be very close to one another and may even overlap.

For a suitcase with fruit inside, there will be three returns: two for the suitcase surfaces and one for the fruit. The fruit return will occur between the two surface returns discussed above. This fact alone may prevent its observation because it may be obscured by the surface returns which will be very close to one another. But, if the fruit return is much larger than the surface returns, it may be discernible. Based on equation (19), the reflection coefficient for the fruit return will be nearly -1 since the magnitude of the fruit's permittivity is larger than that of the suitcase. This reflection is 4 times that predicted for the suitcase surface. The return to the antenna will be approximately 3 times larger because only a fraction of the incident energy reaches the fruit. However, since the fruit will present a much smaller cross section to the propagating wave, its return may instead actually be smaller than the surface returns.

Various strategies may improve the detectability of fruit with SPR. The rear surface return could be effectively eliminated by placing an appropriate absorbing material next to this surface. There then would be very little difference in dielectric properties and consequently a very small return. Returns from the front surface and the fruit could then be better discriminated. However, fruit near the front surface would produce a return nearly simultaneous with the front-surface return. Detection of a fruit return would be reliable for all possible fruit locations only if the fruit return is larger than the surface return. Hence, the absorbing material would provide no real advantage since this was also the case with both surface returns.

Another strategy to improve the detection of fruit return lies in analyzing the composite signal consisting of all three returns. Some success has been achieved in other SPR systems by transforming the signal into the frequency domain. These techniques use a process such as a Fourier transform to determine the frequency content of the signal. If

the signal returned from fruit produces a characteristic frequency content, this may provide a basis for detection. Characteristic frequency contents have already been observed for underground targets [20,21]. One might expect that resonances in the fruit might strongly influence the composite return. If the fruit return magnitude is comparable to or larger than surface returns, this influence may be enough to allow detection on this basis.

Since baggage surface returns can be readily estimated from work in other areas, the only information necessary for a more complete analysis is the return from fruit. This information could be obtained experimentally using an SPR with the fruit suspended in air. The return would be slightly larger than with the fruit in the suitcase but would provide an accurate measure of the return whose estimation is otherwise difficult because of the fruit's size. Another way to obtain the fruit return would be to use an appropriate mathematical model. These two methods for determining fruit return will be further considered. However, unless the fruit return is similar in magnitude to the surface returns, SPR detection of fruit may not be feasible.

VI. PLANS FOR NEXT QUARTER

Research efforts planned for the next three months of this project are based on findings of the first six months and on proposed efforts. During the next three months, approaches to electromagnetic detection of agricultural products will be pursued further. Specific efforts to be undertaken are described below.

A. Capacitor Plate Approach

For the capacitor plate approach, emphasis will be placed on determining optimum plate size. Attention will also be directed to the use of an array of plates each of which will detect agricultural products by changes in impedance as described in Section III. In this way, it may be possible to obtain an impedance profile of baggage to be used in detecting the presence of agricultural products.

B. Transmission/Reflection Approach

For the transmission/reflection approach, computer controlled measurements will be implemented using available equipment. There will be greater resolution under computer control as well as the capability to compensate for errors which originate in the test equipment. Measurements done at 1.8 - 2.4 GHz this quarter will be repeated under computer control to obtain these improvements. Measurements will also be carried out in the range of 110 MHz to 2.0 GHz. In this frequency range, the higher loss tangent of agricultural products may produce larger changes in transmission/reflection parameters than for the higher frequencies. Work in this range will also bridge the frequencies up to 100 MHz used in the capacitor plate approach and those used to date in the transmission/reflection approach.

C. Short Pulse Radar Approach

The Short Pulse Radar (SPR) returns from fruit will be investigated in the next quarter. As discussed in Section V, the return from fruit will be the major factor in further evaluation of SPR detection of fruit in baggage. The first step will be to hold discussions with personnel of the Georgia Tech EES Radar and Instrumentation Laboratory who have experience with SPR. Based on these discussions, a decision will be

made whether the SPR approach merits further consideration. It is anticipated that further efforts would then take the form of experimental measurement of fruit return or mathematical modeling of the return. With this information in hand, it is felt that a definite conclusion can be reached on the feasibility of SPR detection of fruit in baggage.

D. Resonant Cavity Approach

A resonant rectangular cavity large enough to accommodate a large suitcase will be constructed. Changes in the resonant frequencies and Q-factors of the cavity due to the introduction of fruit will be measured. Fruit will be inserted with and without a suitcase present and swept frequency measurements will be made for each condition using available equipment.

VII. REFERENCES

1. N. N. Mohsenin, Physical Properties of Plant and Animal Materials Volume I, Gordon and Breach Science Publishers, New York, 1970, 734 pp.

2. F. L. Hart and H. J. Fisher, Modern Food Analysis, Springer-Verlag, New York, 1971, 519 pp.

3. McGraw-Hill, Encyclopedia of Food, Agriculture, and Nutrition, D. N. Lapedes, ed., McGraw-Hill, New York, 1977, 732 pp.

4. H. W. Ockerman, Source Book for Food Scientists, The AVI Publishing Company, Westport, Connecticut, 1978, 926 pp.

5. S. O. Nelson, Microwave Dielectric Properties of Fresh Fruits and Vegetables, American Society of Agricultural Engineers, Winter Meeting, Dec. 11-14, 1979, paper 79-3546.

6. T. M. Shaw and J. A. Galvin, High-Frequency-Heating Characteristics of Vegetable Tissues Determined from Electrical-Conductivity Measurements, Proc. IRE 37: 83-86, 1949.

7. W. E. Pace, W. B. Westphal, S. A. Goldblith, and D. Van Dyke, Dielectric Properties of Potatoes and Potato Chips, J. Food Sci. 33: 37-42, 1968.

8. N. E. Bengtsson and P. O. Risman, Dielectric Properties of Foods at 3 GHz as Determined by a Cavity Perturbation Technique. II. Measurement on Food Materials, J. Microwave Power 6: 107-123, 1971.

9. W. R. Tinga and S. O. Nelson, Dielectric Properties of Materials for Microwave Processing-Tabulated, J. Microwave Power 8: 23-65, 1973.

10. T. Ohlsson, N. E. Bengtsson, and P. O. Risman, The Frequency and Temperature Dependence of Dielectric Food Data as Determined by a Cavity Perturbation Technique, J. Microwave Power 9: 129-145, 1974.

11. E. C. To, R. E. Mudgett, D.I.C. Wang, S. A. Goldblith, and R. V. Decareau, Dielectric Properties for Food Materials, J. Microwave Power 9: 303-315, 1974.

12. S. O. Nelson, Electrical Properties of Agricultural Products - A Critical Review, in Quality Detection in Foods, J. J. Gaffney, ed., American Society of Agricultural Engineers, St. Joseph, Michigan, 1976, pp. 86-97, 101.

13. A. R. Von Hippel (Ed.), Dielectric Materials and Applications, The M.I.T. Press, 1954, p. 3.

14. J. D.Kraus and K. R. Carver, Electromagnetics, McGraw-Hill, New York,1973, pp. 71-73.

15. S. Ramo, J. R. Whinnery, and T. Van Duzer, Fields and Waves in Communication Electronics, John Wiley & Sons, New York, 1965, p. 603 ff.

16. K. R. Foster, J. L. Schepps, D. D. Stoy, and H. P. Schwan, Dielectric Properties of Brain Tissue Between 0.01 and 10 GHz, Phys. Med. Biol. 24: 1177-1187, 1979.

17. M. A. Stuchly, S. S. Stuchly, and G. Kantor, Diathermy Applicators with Circular Aperture and Corrugated Flange, IEEE Trans. Microwave Theory Tech. MTT-23: 267-271, 1980.

18. A. C. Eberle and J. D. Young, The Development and Field Testing of a New Locator for Buried Plastic and Metallic Utility Lines, Transportation Research Record 631: 47-52, 1977.

19. D. L. Moffatt and R. J. Puskar, A subsurface Electromagnetic Pulse Radar, Geophysics 41: 506-518, 1976.

20. J. D. Echard, J. A. Scheer, E. O. Rausch, W. H. Licata, J. R. Moore, and J. A. Nestor,"Radar Detection,Discrimination, and Classification of Buried Non-Metallic Mines," Final Technical Report for U.S. Army Mobility Equipment Research & Development, Contract No. DAAG54-76-C-0112, Georgia Tech Project A-1828, February 1978.

21. L. C. Chan, D. L. Moffatt, and L. Peters, Jr., A Characterization of Subsurface Radar Targets, Proc. IEEE 67: 991-1000, 1979.

22. J. R. Moore and J. D. Echard, "Radar Detection of Voids Under Concrete Highways," Final Technical Report, Georgia Department of Transportation, Georgia Tech Project A-2107, May 1978.

23. J. R. Rossiter and K. A. Gustajtis, Determination of Iceberg Underwater Shape with Impulse Radar, Disalination 29: 99-107, 1979.

24. A. P. Annan and J. L. Davis, Impulse Radar Sounding in Permafrost, Radio Sci. 11: 383-394, 1976.

QUARTERLY TECHNICAL REPORT NO. 3
PROJECT A–2673

ELECTROMAGNETIC DETECTION OF AGRICULTURAL PRODUCTS IN TRAVELERS' BAGGAGE

By

R. L. Seaman, M. L. Studwell, J. Seals and A. R. Moser

Prepared for

U.S. DEPARTMENT OF AGRICULTURE
SCIENCE AND EDUCATION ADMINISTRATION
AGRICULTURAL RESEARCH – SOUTHERN REGION
701 LOYOLA AVENUE
NEW ORLEANS, LOUISIANA 70153

Under

Research Agreement No. 53-7B30-0-247

MARCH 1981

GEORGIA INSTITUTE OF TECHNOLOGY

Engineering Experiment Station

Atlanta, Georgia 30332

ELECTROMAGNETIC DETECTION OF AGRICULTURAL PRODUCTS IN TRAVELERS' BAGGAGE

Quarterly Technical Report No. 3

Project A-2673

March 1981

Under

Research Agreement No. 53-7B30-0-247

By

R. L. Seaman, M. L. Studwell
J. Seals and A. R. Moser

Prepared for

U.S. Department of Agriculture
Science and Education Administration
Agricultural Research - Southern Region
701 Loyola Avenue
New Orleans, Louisiana 70153

By

BIOMEDICAL RESEARCH DIVISION
Electronics and Computer Systems Laboratory
Engineering Experiment Station
Georgia Institute of Technology
Atlanta, Georgia 30332

FOREWORD

Research during the third three months of this one-year project was performed by personnel of the Biomedical Research Division of the Electronics and Computer Systems Laboratory of the Engineering Experiment Station at the Georgia Institute of Technology, Atlanta, Georgia. This project is sponsored by the Science and Education Administration of the U.S. Department of Agriculture, New Orleans, Louisiana, under Research Agreement 53-7B30-0-247 and has been assigned Georgia Tech Project No. A-2673. This report summarizes efforts carried out from 1 December 1980 through 28 February 1981.

Dr. R. L. Seaman served as Project Director. Mr. J. Seals performed the experiments on the capacitor plate approach; Dr. A. R. Moser, on the signal transmission/reflection approach. Mr. M. L. Studwell performed the analyses and experiments on the resonant cavity approach. Mr. R. M. Kobert has assisted in several aspects of the technical efforts.

Respectfully submitted,

Ronald L. Seaman,
Project Director

Approved:

J. C. Toler, Manager
Biomedical Research Division

TABLE OF CONTENTS

LIST OF FIGURES

(cont'd)

LIST OF FIGURES

(continued

LIST OF TABLES

I. INTRODUCTION

The goal of this project is to identify an electromagnetic method for detecting agricultural products (fruits, vegetables, and meats) in closed baggage. Such a method of inspecting baggage would greatly assist the Animal and Plant Health Inspection Service (APHIS) in detecting agricultural products brought into this country by international travelers. A division of the Department of Agriculture (USDA), APHIS is charged with the interception of agricultural products which are diseased or carry insect pests. Intercepted products which are diseased or infested are destroyed to prevent adverse effects on native plants and animals. Of course, agricultural products must be detected before they are inspected. Since not all products are declared by travelers, a noninvasive method of detecting the products in baggage would greatly facilitate the inspection process.

During this reporting period, a visit was made to the International Concourse of Atlanta's Hartsfield International Airport to observe current APHIS inspection procedures. The visit was arranged through Atlanta APHIS personnel, who were very interested in this project. During the visit, passengers from several international flights were processed through customs, immigration, and APHIS. It was found that all APHIS inspections were referred by the customs officials, who had first contact with passengers. That is, the customs inspectors sent passengers who had declared agricultural products, or who had been discovered to have them, to the APHIS inspector on duty. This inspector then determined whether the product could be admitted or should be intercepted. The decision to intercept was based on several factors: product species, country of origin, and recent plant pathologies and pests in the country of origin.

About 2% of international travelers declare possession of agricultural products. However, it is estimated by inspectors that many more actually bring in agricultural products. During the airport visit, inspectors related experiences of examining all baggage from an international flight when it would not inconvenience passengers. During such a complete

search, more than half of the baggage is usually found to contain agricultural products. It is clear that noninvasive inspection of baggage could substantially increase the intercept rate of contraband products.

During the first two quarters of this project, significant progress was made toward identifying a means of electromagnetic detection of fruit inside baggage. Moisture-content and dielectric data were obtained from the literature for use in analyzing possible approaches. Analyses of three approaches -- capacitor plate, signal transmission/reflection, and short pulse radar -- were performed. Also, preliminary measurements of capacitor-plate and signal-transmission/reflection prototype systems were made. Information gained from these studies was used to guide subsequent studies in this reporting period.

During the third three months of this feasibility study, further progress was made on the various approaches to the electromagnetic detection of agricultural products in closed baggage. It was felt that detection of one type of product would be a sufficient test of a method, so fruit was taken as a representative agricultural product in this study. Values of dielectric properties of fruit were measured using a probe antenna technique (Section II). Measurements were made using capacitor plates to obtain spatial response to a fruit-like target (Section III). Initial analyses and measurements were performed for the resonant cavity approach (Section IV). Measurements were made on the signal transmission/reflection approach with improvements in accuracy obtained by using a computer (Section V). The short pulse radar approach was discussed with a Georgia Tech group familiar with the approach and found to have potential (Section VI). Plans for investigations during the fourth, and last, quarter of this project are presented in Section VII.

II. MEASUREMENTS OF FRUIT DIELECTRIC PROPERTIES

Since the electromagnetic detection of agricultural products depends strongly on the differences between the dielectric properties of the products and those of other baggage items, the dielectric properties of fruit have been further researched during this reporting period. Values for the dielectric properties of fruit, vegetables, and meat had been obtained from the literature and presented in graphs in the Second Quarterly Technical Report. Values for the relative dielectric constant and the relative loss factor were available for frequencies from 1 kHz to 10 GHz. Most of the dielectric data exhibited consistent patterns across frequency; however, the relative loss factor from 0.1 to 10 GHz showed considerable scatter and a pattern was difficult to discern.

Because three of the four proposed approaches for detecting agricultural products utilize frequencies between 0.1 and 10 GHz, more definitive dielectric data were desired in this frequency range. More exact values would be especially useful for the theoretical analyses of the approaches. After discussion with the USDA technical monitor for this project, it was decided that Georgia Tech's Biomedical Research Division would measure the dielectric properties of representative fruits by using methods already developed within the Division.

A. Measurements

The dielectric properties of fruit were measured during this reporting period using an in-vivo probe technique. This technique has been used successfully to measure the dielectric properties of liquids and animal tissues from 0.1 to 10 GHz [1,2]. As reported here, the technique also worked well for plant tissues.

The in-vivo probe technique for measuring dielectric properties is based on an antenna modeling theorem which relates the complex reflection coefficient of an antenna to the intrinsic impedance of the medium surrounding the antenna. A medium's intrinsic impedance is determined by its dielectric and magnetic properties. Since the magnetic properties of plant and animal tissues are that of free space, differences in the intrinsic

impedance of tissue are directly related to differences in dielectric properties. Consequently, changes in an antenna's complex reflection coefficient can also be related to the dielectric properties of the medium into which the antenna is submerged.

The complex reflection coefficient was measured using an HP Network Analyzer System. Results were obtained from 150 MHz (0.15 GHz) to 6.4 GHz using this system. To cover this broad frequency range, several instrument sub-unit substitutions were made. Accuracy and speed were maximized by having the system under the control of a computer which also calculated the dielectric properties from the reflection coefficient. The reflection coefficient with the antenna in air had been measured and stored in computer memory before measurements on tissue were made.

The probe antenna consisted of the cut end of a small section of 0.085-inch semi-rigid coaxial cable. The cable's copper center and outer conductors had been gold plated to resist corrosion so that antenna properties would remain constant with use. The center conductor was extended only slightly beyond the cut outer conductor and insulator so that a large majority of the coupling of electromagnetic fields to the plant tissue was by a capacitive, fringing electric field (and the magnetic field associated with it). This meant that the measurement was influenced by dielectric properties within a few hundred micrometers of the antenna. Thus, the results indicated rather localized values for dielectric properties. This regional nature was taken advantage of to measure values for both the skin and for the interior of each fruit.

The measurement procedure started with the initial calibration of the probe and the determination of correction factors for use in compensating for various sources of error in the transmission lines used. Correction factors were derived for each frequency range investigated. The properties of deionized water (assumed known) were determined to check for correct operation of the measurement setup. Fruit skin was then placed against the probe antenna by moving up intact fruit on a laboratory jack until good contact was made with the downward pointing antenna. For measurement on fruit interiors, a surface was exposed by slicing with a sharp scalpel blade. This surface was moved up to contact the antenna in the same manner as intact fruit was moved.

Dielectric properties were derived as relative dielectric constant ε_r', relative loss factor ε_r'', and conductivity. The relative dielectric constant is a measure of the electromagnetic energy storage capability of the tissue and is the real part of the relative complex permittivity. The relative loss factor is a measure of the tissue's capability to dissipate electromagnetic energy as heat and is the imaginary part of the relative complex permittivity. Conductivity is the ratio of induced current density (combined conduction and displacement) to the electric field and is also equal to the product of the relative loss factor and radial frequency. Relative dielectric constant and relative loss factor are dimensionless; conductivity is here given in millisiemens per centimeter (mS/cm). Temperature was measured by inserting a YSI probe and ranged from 19 to 23°C.

Dielectric properties have been determined for the skin and interior tissue of the following fruits:

1. Golden Delicious apples,
2. Red Delicious apples,
3. Ripe (yellow skin) bananas,
4. Over-ripe (black skin) bananas, and
5. Tangelos and oranges.

Results for the interiors of Golden Delicious apples, tangelos, and ripe bananas have been completely analyzed and are presented in this report. Analysis of the data for the other fruit is underway and the results will be given in the Final Technical Report. Due to technical problems, results for the 2 to 4 GHz range are incomplete at this time and gaps have been left in the plots to indicate this. Figures 1 through 9 show the properties for banana, apple, and tangelo. Values were plotted as the mean of 3 to 5 measurements at each frequency and bars were used to show the standard deviation around each mean. In some cases, the standard deviation was as small as or smaller than the dot used to indicate the mean and the bars were omitted.

The values for relative dielectric constant for the three fruits (Figures 1-3) were similar across the frequency range investigated with the values for tangelo being about 10 units greater than for apple and

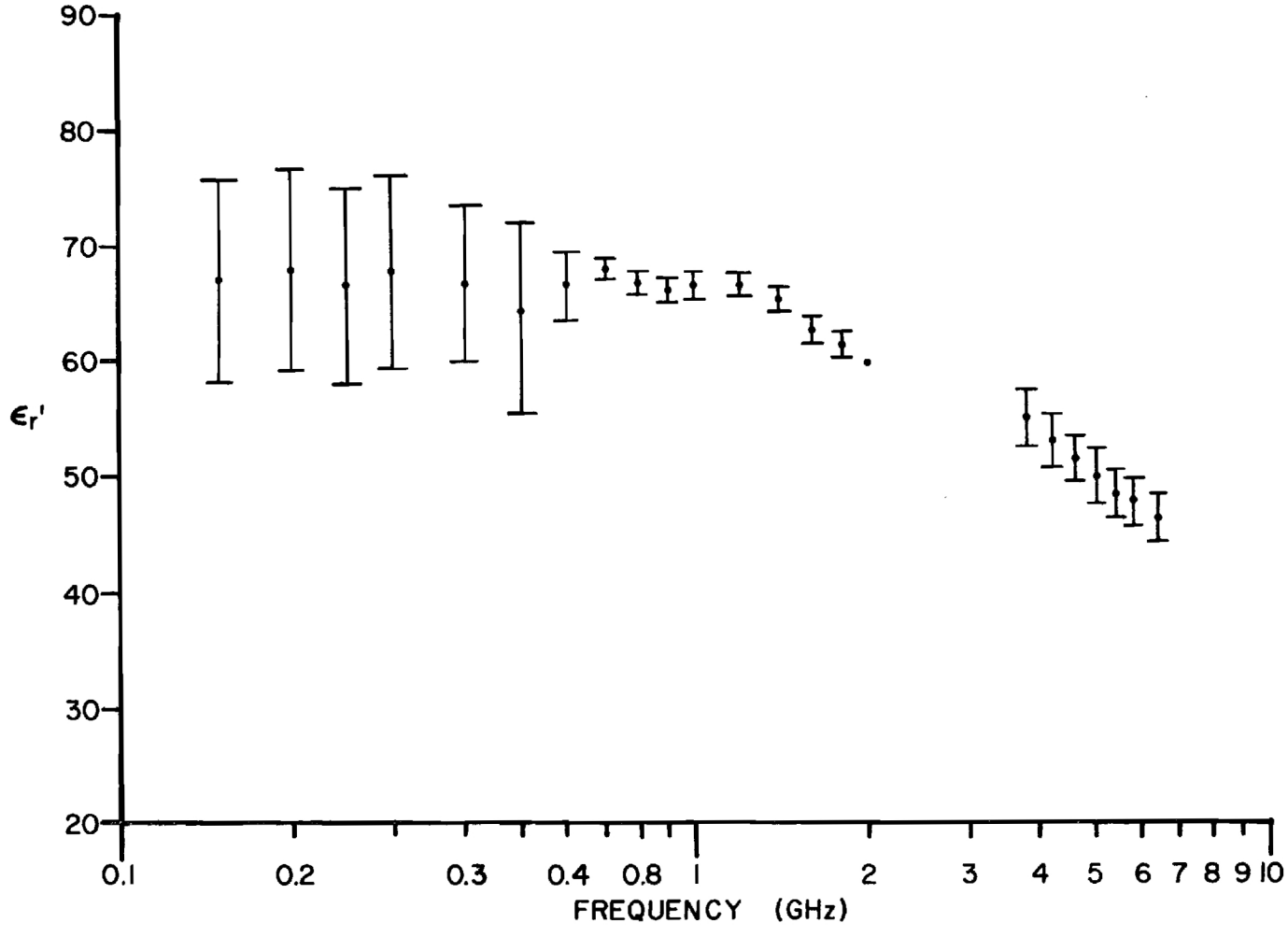

Figure 1. Relative dielectric constant of banana.

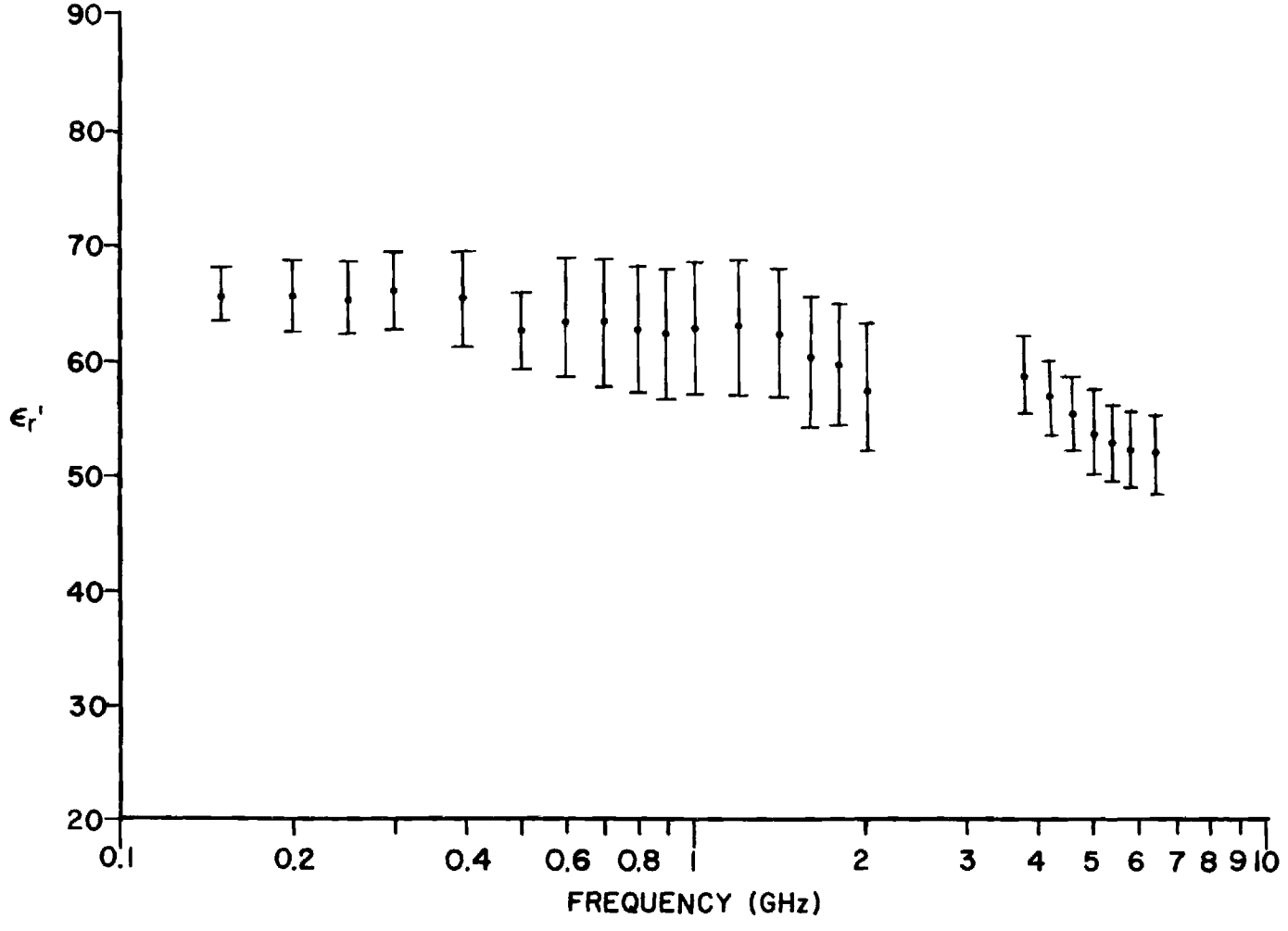

Figure 2. Relative dielectric constant of apple.

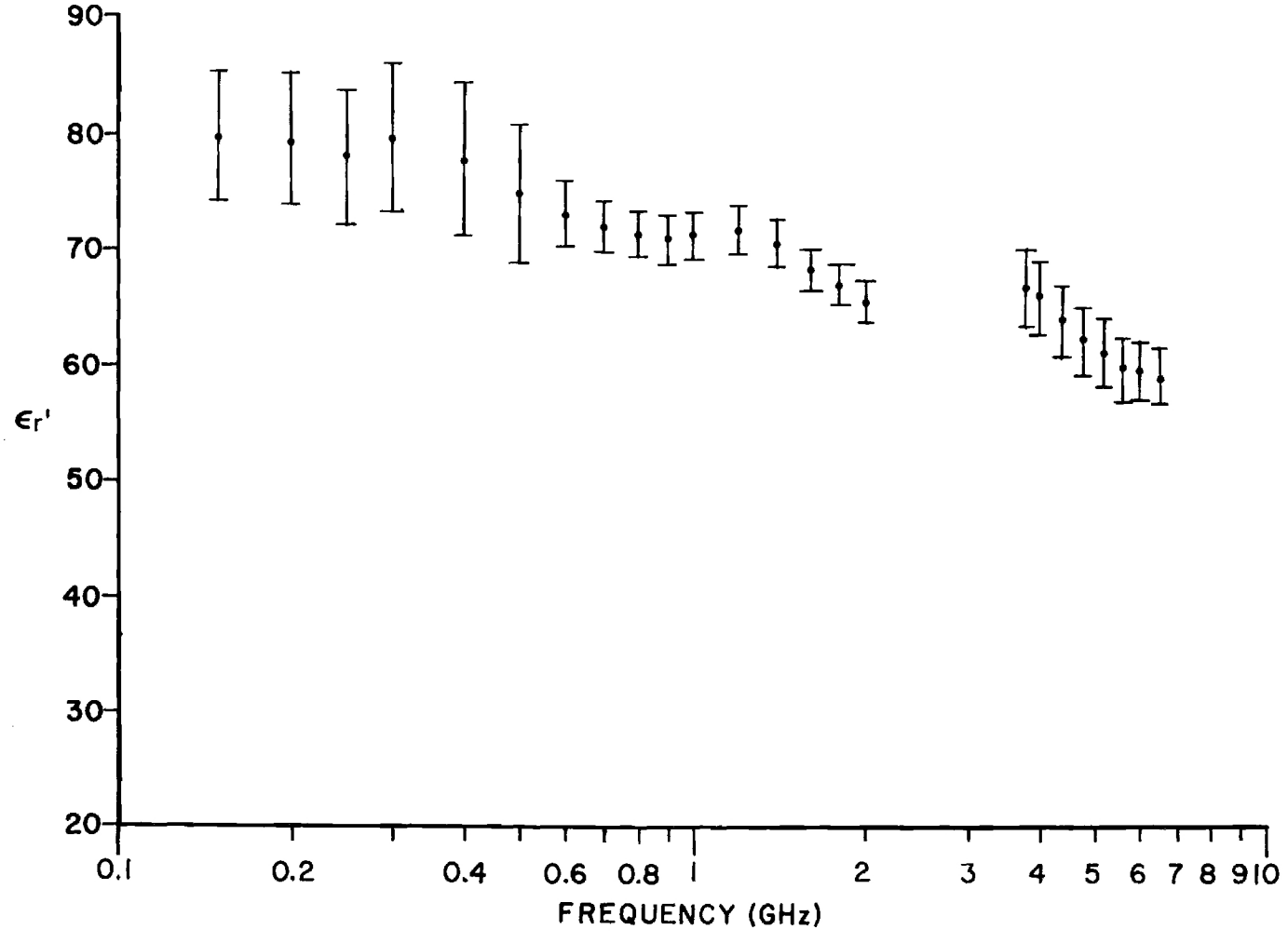

Figure 3. Relative dielectric constant of tangelo.

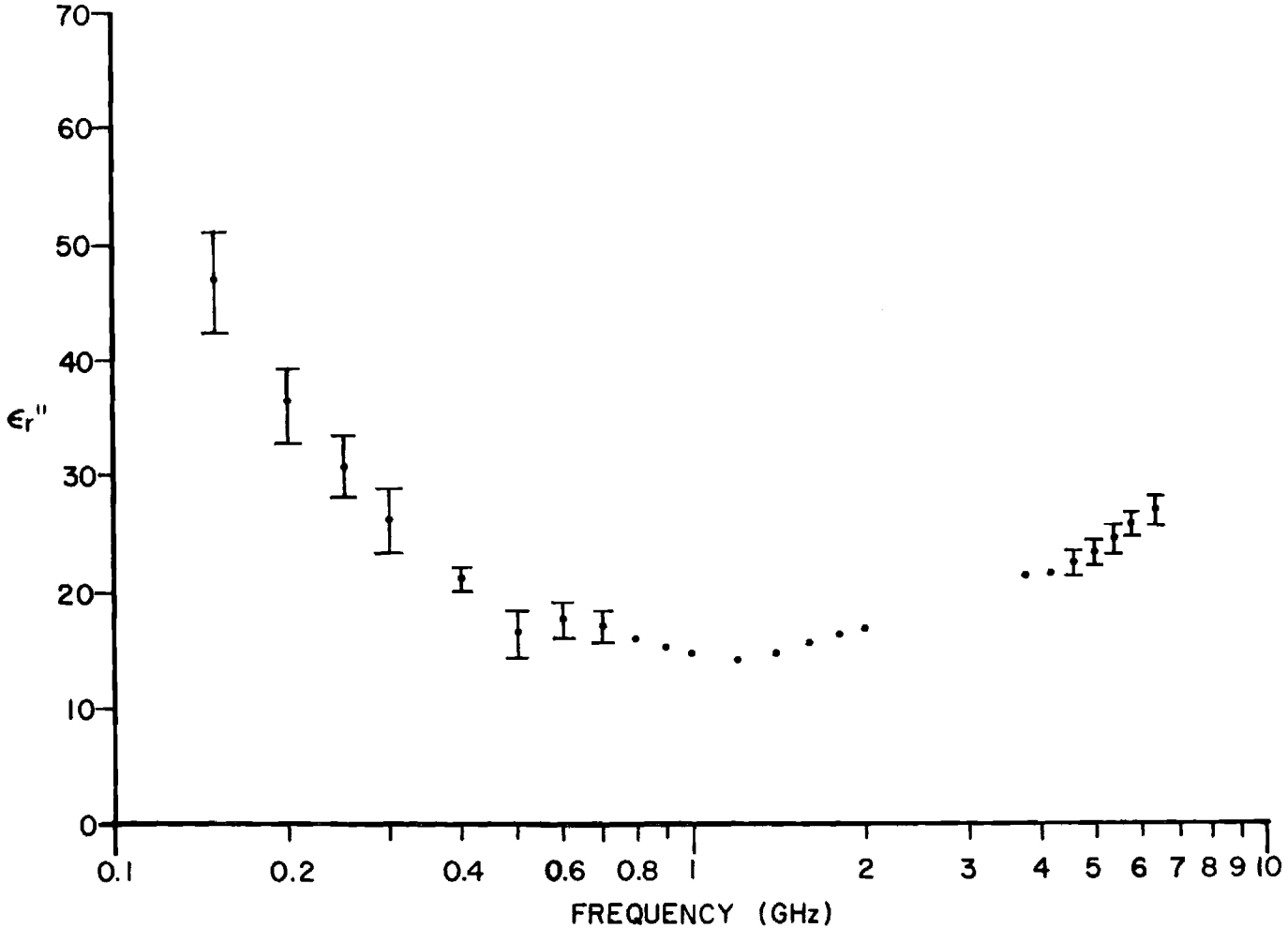

Figure 4. Relative loss factor of banana.

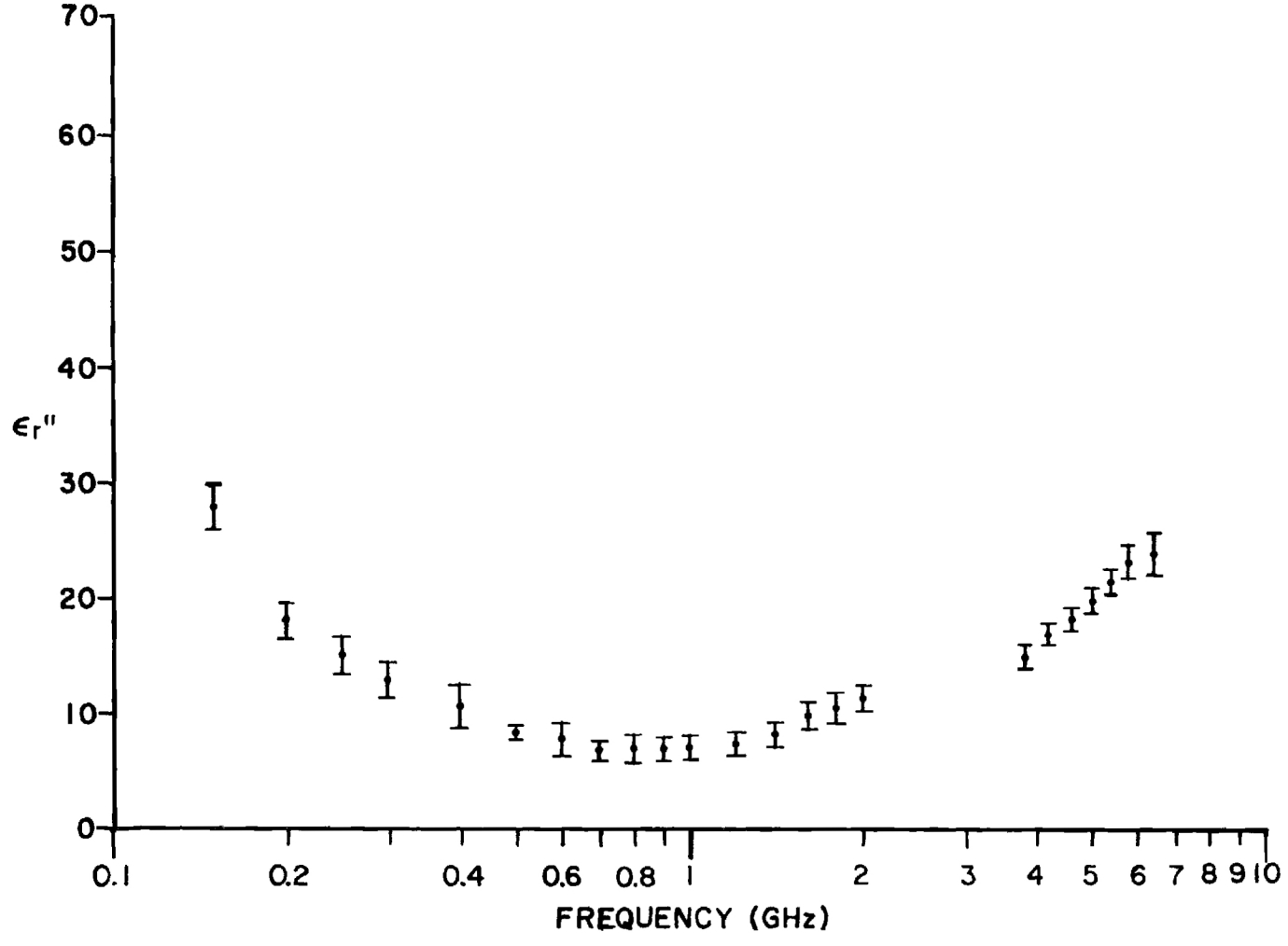

Figure 5. Relative loss factor of apple.

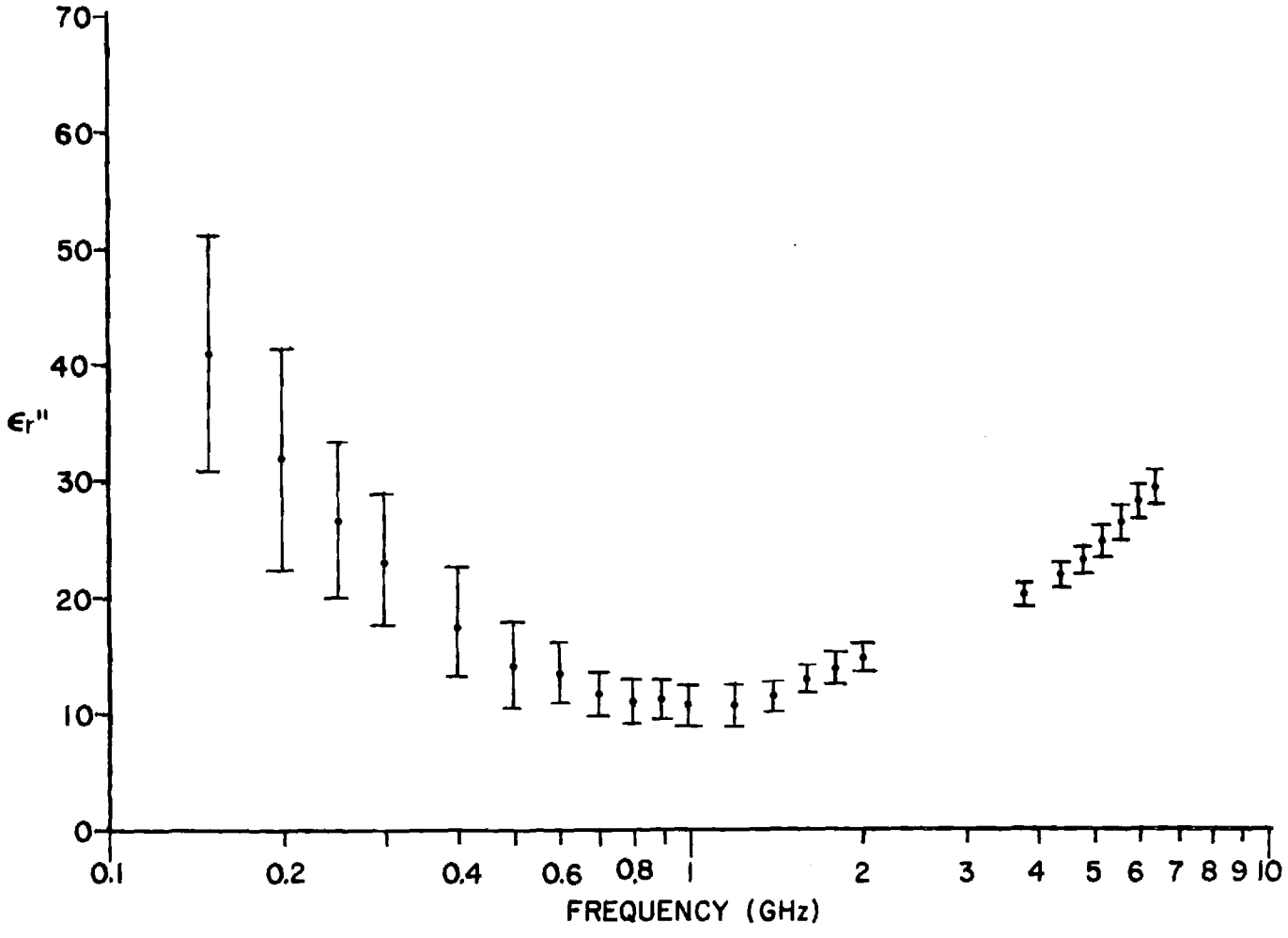

Figure 6. Relative loss factor of tangelo.

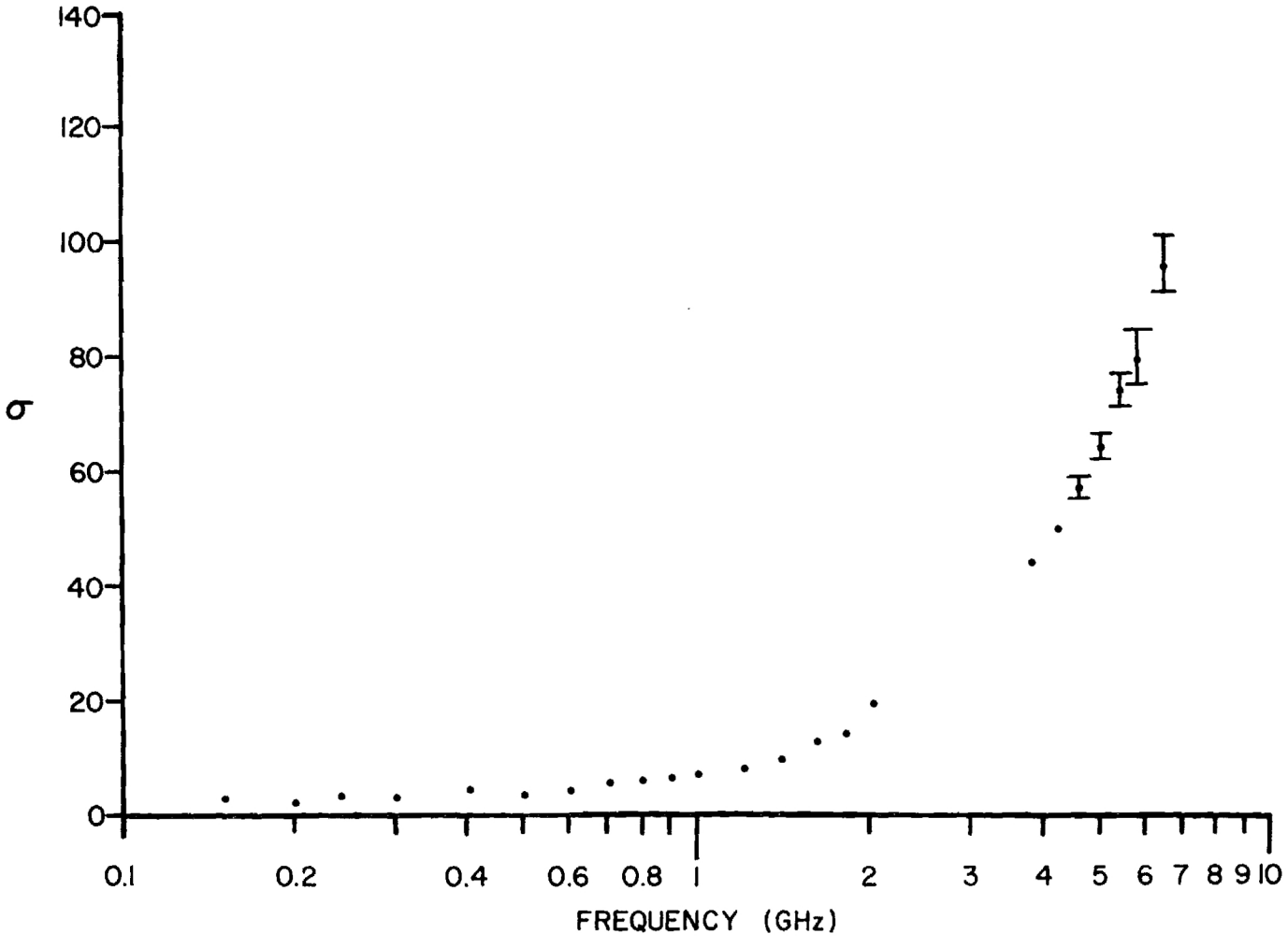

Figure 7. Conductivity (mS/cm) of banana.

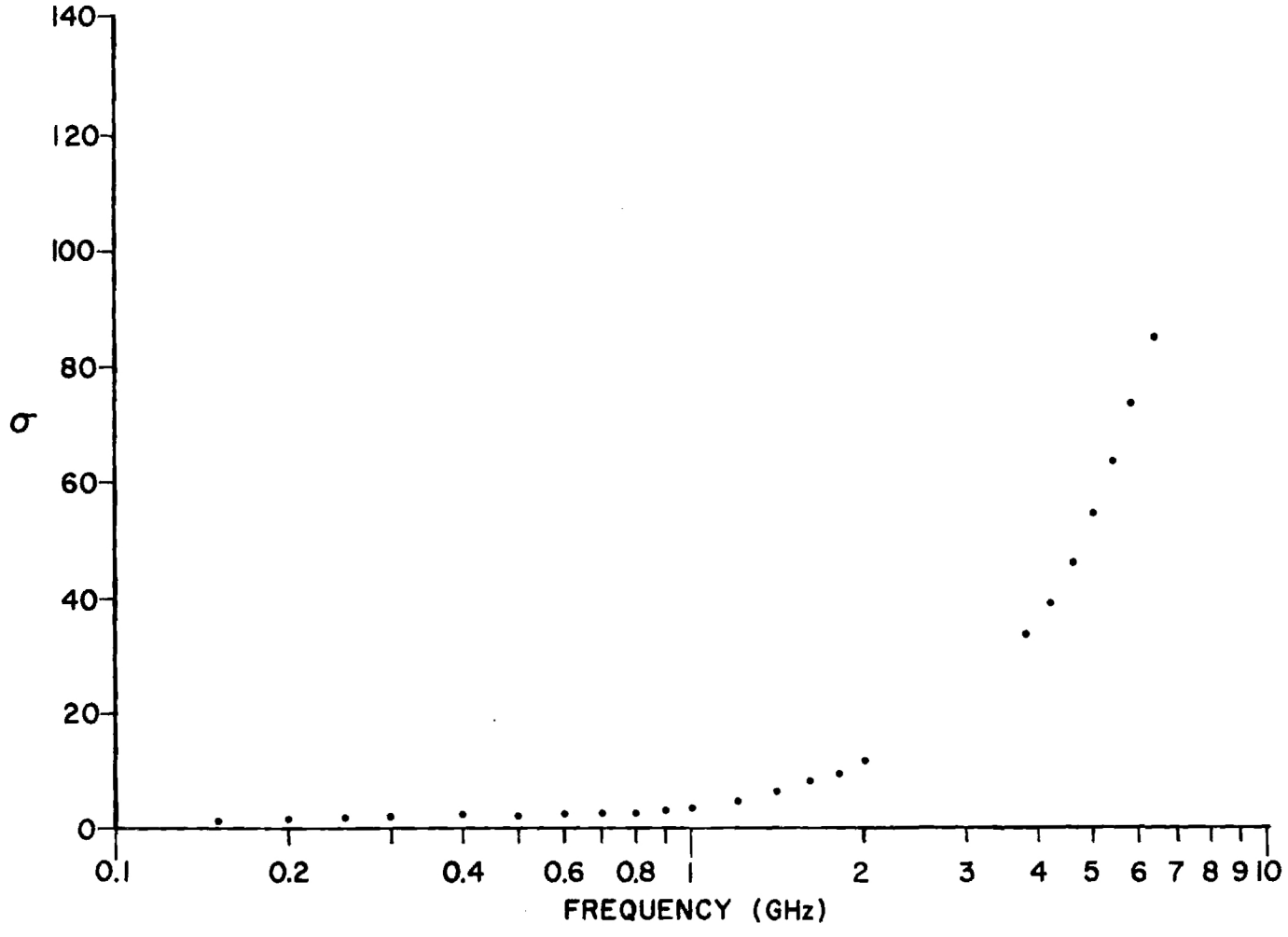

Figure 8. Conductivity (mS/cm) of apple.

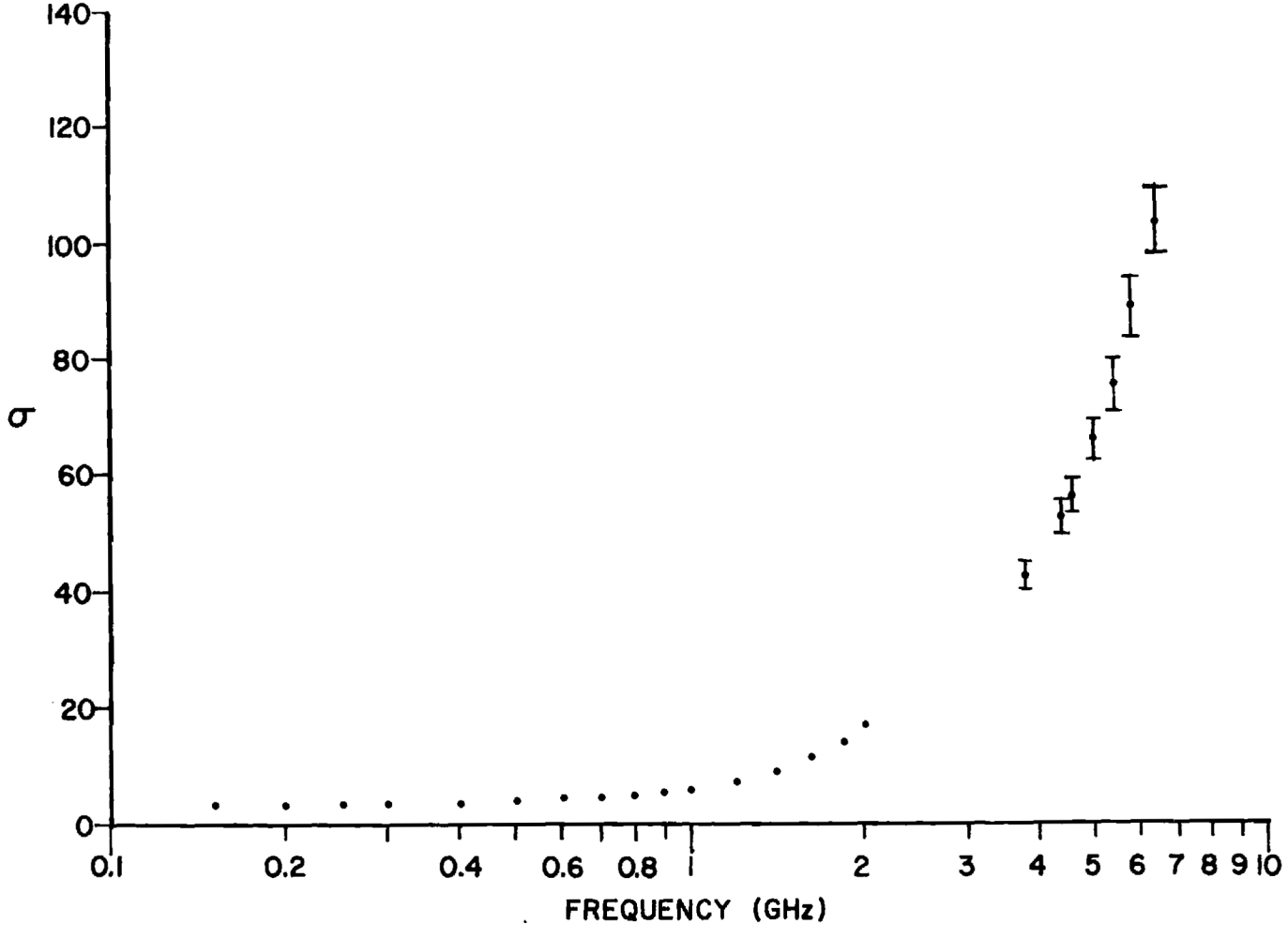

Figure 9. Conductivity (mS/cm) of tangelo.

banana. The values for relative loss factor (Figures 4-6) were also similar across the frequency range with banana and tangelo values overlapping. The relative loss factor of apple seems to be 5 to 20 units less than the values for bananna and tangelo, with the smaller differences occurring at higher frequencies. The values of conductivity (Figures 7-9) are very similar for all three fruits across this frequency range.

B. Comparison with Existing Data

The measured relative dielectric constant and relative loss factor values presented in Figures 1-6 can be readily compared with values from the literature (see Figures 3 and 4 in Second Quarterly Technical Report). The values of relative dielectric constant measured for the three fruits were generally higher than those previously reported and showed a decline for higher frequencies which was not obvious in the earlier data. For all three fruits, the measured values of relative loss factor showed a dip near 1 GHz which was not evident in reported data although the measured values fell among the scatter in values of those data. Thus, the measured values displayed definite patterns and were consistent with previous data in many respects. It should be kept in mind that the previous data were taken from several fruits and vegetables and that a better comparison can be had by comparing data by species. This will be done as completely as possible and reported in the Final Technical Report.

Since it was expected that the dielectric properties of all tissues of high water content would be similar above about 100 MHz, it was not surprising to see similar values for all three fruits. The values for fruit relative dielectric constant and relative loss factor were different from those of water which vary approximately from 80 to 70 and 1 to 25, respectively, over the frequency range being discussed [2]. This difference was expected because of the cell structure and dissolved substances in the plant tissues. The measured values of relative dielectric constant (Figures 1-3) and conductivity (Figures 7-9) were very similar to those reported for animal tissues of high water content [2-4]. These similarities were also predictable from the comparable water content and structure of plant and animal tissues.

Analysis of dielectric data from the other fruits is continuing and it is expected that these dielectric properties will be found to be similar to those reported here. If this is the case, then one fruit can be used to model the response of a prototype electromagnetic detector of fruit. Since water content strongly influences dielectric properties, especially at higher frequencies, values for some skins with low water content may be different from those for interiors. This difference will have to be taken into account for any electromagnetic detector of fruit.

III. CAPACITOR PLATE APPROACH

A. Introduction

The results of previous studies performed during this program (see Section III of Second Quarterly Technical Report) clearly demonstrated the feasibility of the capacitor-based detection concept. Studies are now being performed to assess the optimal performance that can be practically expected with this approach. The objective of the specific studies performed during this reporting period was the evaluation of the geometrical characteristics of the electrical response of a number of prototype capacitors. Fringing effects or any other deviations from ideal behavior exhibited by the prototype capacitors were of particular interest during these studies. This information will be extremely useful in the analysis and design of a promising multiple-plate capacitor configuration now being considered. The experimental results of the studies performed during this third quarter are discussed in the following paragraphs.

B. Measurements

The initial experiment performed during this reporting period involved measuring the electrical response (impedance magnitude) of a prototype parallel plate capacitor as a small dielectric target was moved through the volume between and adjacent to the capacitor plates. A partially filled beaker of water was used to provide a cylindrically shaped dielectric target that was approximately two inches in both height and diameter. The basic capacitor plate-network analyzer configuration described in Figure 8 of the Second Quarterly Technical Report was used in this experiment. However, measurements were performed at a fixed frequency instead of in the swept-frequency mode used in the previously reported studies. One of the capacitor plates (the RF-fed plate) was 6 x 6 inches and the second capacitor plate (the electrically grounded plate) was 22 x 17 inches. The two plates were mounted on the broad sides of an open-ended wooden box. This box was fabricated from one-quarter inch thick plywood and was approximately 30 inches long, 18 inches wide, and 10 inches high. Wooden runners mounted on opposite interior walls of this box

served as supports for a Plexiglas platform that could be positoned via a long Plexiglas handle. A diagram of this setup is depicted in Figure 10. It should be noted that the origin of the x-y-z coordinate system to which this setup is referenced is located at the center of the smaller, top plate.

The measurement procedure used during this experiment involved initially positioning the dielectric target at a selected x-position on the Plexiglas platform. Sighting crosshairs drawn on the bottom of the glass beaker were used to position precisely the target on graticules on the Plexiglas platform. The vertical (i.e., z-position) of the Plexiglas platform was selected so that the target was centered between the two capacitor plates. The handle of the Plexiglas platform was then used to vary the position of the target in the y-direction in one inch steps. A digital voltmeter was used to display the magnitude of the capacitor plate impedance after each one inch step. After the target had been stepped through the entire y-range of interest (minus eight to plus eight inches), the platform and target were returned to the starting position. The target was then shifted one inch in the x-direction. The y-position of the target was again varied in one-inch steps and new impedance data were recorded. This procedure was repeated for each position in the x-range of interest (minus six to plus six inches). In this manner, the magnitude of the capacitor impedance was measured for 221 different target locations. The measured impedance data was then used to produce a profile of the electrical behavior of the prototype capacitor as a function of x-y position. This profile is presented in Figure 11 in which the x- and y-coordinates correspond to the position of the target during the measurement procedure. The vertical displacement in this graph corresponds to the change in impedance magnitude (in decibels) that occurred due to the presence of the target.

A number of observations can be made from the graph in Figure 11 concerning the electrical response of the prototype capacitor. As expected, the electrical response is approximately Gaussian in distribution. Also, the changes in impedance magnitude when the target was positioned beneath the smaller capacitor plate are reasonably well-defined. However,

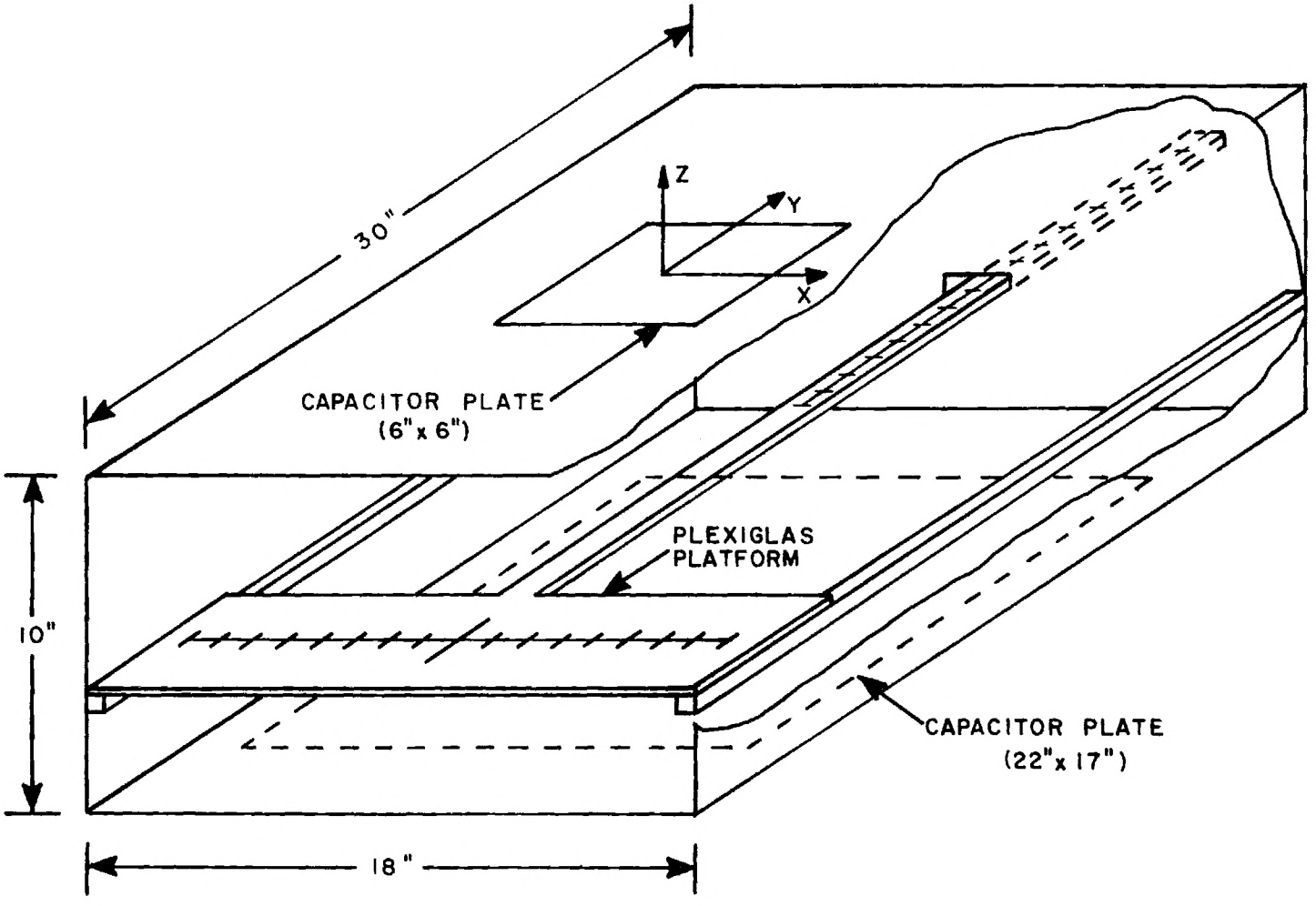

Figure 10. Diagram of setup used to evaluate the prototype capacitors.

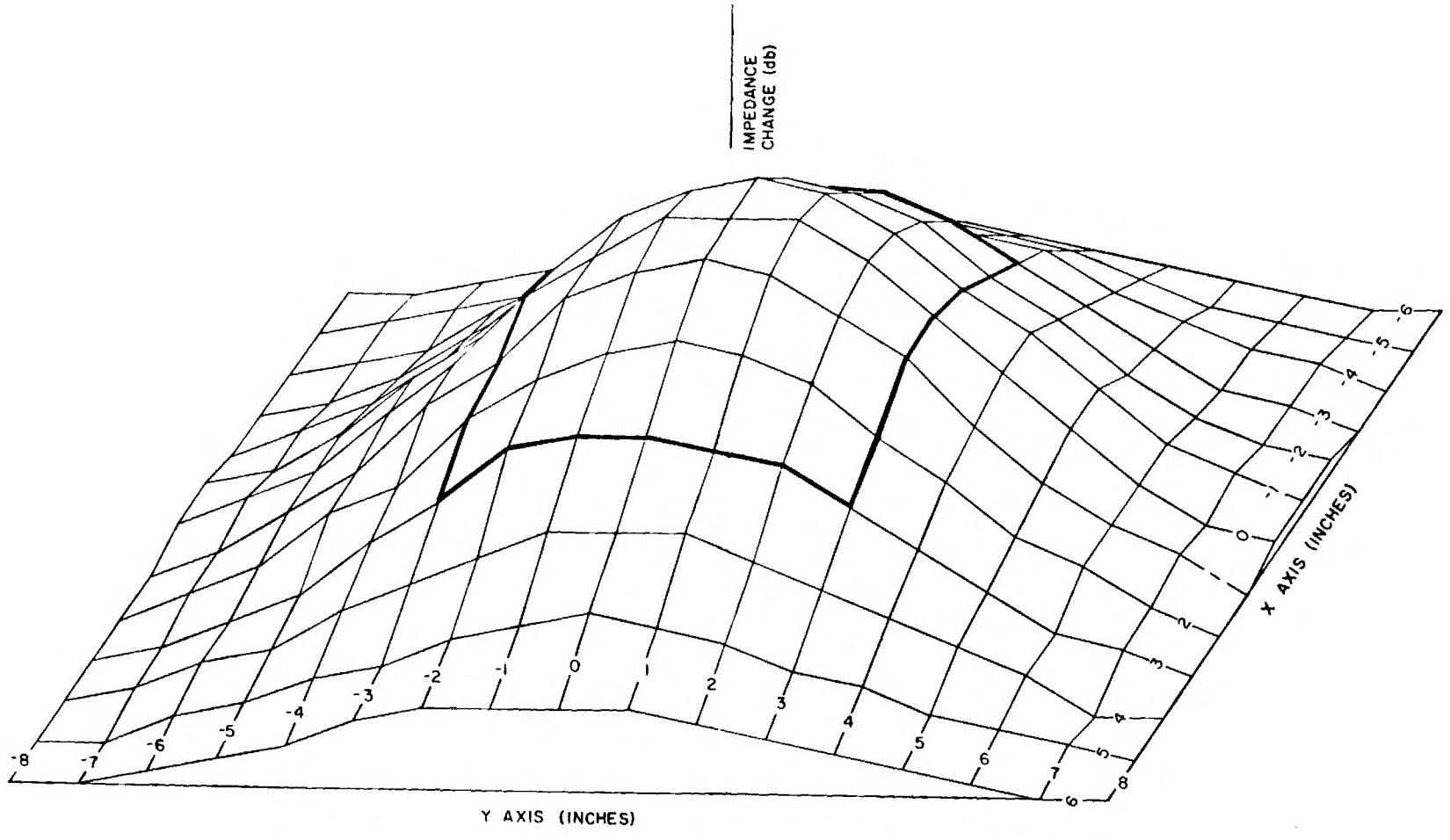

Figure 11. Profile of the electrical behavior of the prototype capacitor. Values taken at positions corresponding to the edges of the top 6 x 6 inch plate are indicated by heavy lines. Measurements performed at 10 MHz.

the impedance roll-off at positions beyond the edges of the smaller plate is not as sharp as would be expected for an ideal parallel plate capacitor. This non-ideal electrical response is partially due to the finite dimensions of the target. That is, when measurements were made at x-y positions near the edges of the smaller plate, the target was not completely clear of the smaller plate. This resulted in an impedance change even though the x-y position of the target center implied that it was clear of the smaller plate. The non-ideal electrical response of the prototype capacitor is also partially due to effects of the fringing electric fields. The existence of these fringing effects is most easily seen by noting the finite impedance changes measured near the extreme x- and y-positions where the target was completely clear of the smaller plate. Fortunately, these fringing effects do not appear to be severe enough to affect significantly the feasibility of the capacitor-based detection approach.

Following this experiment, a series of experiments was performed to evaluate the effects of a number of parameters on the electrical response of the prototype capacitor. In one experiment, the larger (22 x 17 inches) ground plate was replaced by a smaller (6 x 6 inches) ground plate to determine if the ground plate size would significantly affect the capacitor electrical response depicted in Figure 11. A comparison of impedance measurements obtained using the smaller ground plate and the results previously obtained with the larger ground plate is shown in Figure 12. Only the results for the cases where the x-position of the target was equal to zero are used in this comparison. The results shown in Figure 12 indicate that the ground plate size has little effect on the electrical response of the prototype capacitor. This fact may greatly benefit the multiple-plate capacitor configuration now being considered since it appears that it may be possible to use a single, large ground plate in conjunction with an array of smaller, RF-fed plates. However, a number of additional experiments are needed to further evaluate the effects of both the ground plate size and RF-fed plate size on the capacitor electrical response.

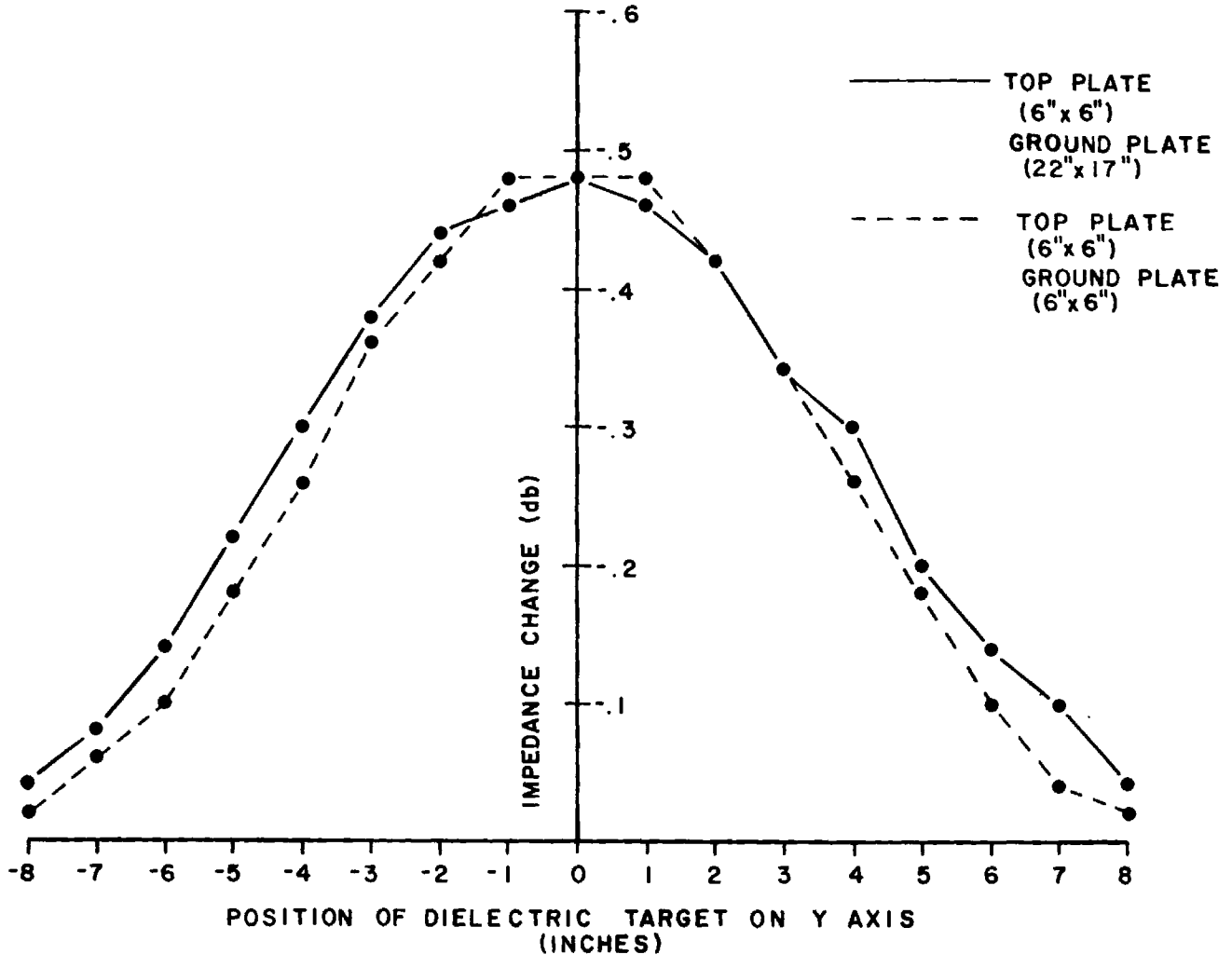

Figure 12. Effect of ground plate size on the electrical response of parallel plate capacitors. Measurements were performed at 10 MHz.

An additional experiment was performed to determine if the fringing effects evidenced by the data in Figure 11 exhibited any frequency dependence. Two frequencies, .1 MHz and 10 MHz, were used in this experiment. Both plates of the prototype capacitor used were 6 x 6 inches in size. The results of this experiment are depicted in Figure 13. The comparison is again made only for the case where the x-position of the target equals zero. The comparison in Figure 13 indicates that decreasing the test frequency by an order of magnitude had little impact on the previously observed fringing effects. This fact indicates that strict requirements concerning the operating frequency of future prototype capacitor-based detection systems are unlikely.

C. Future Investigations

A number of studies pertaining to the capacitor-based detection concept are planned for the fourth quarter of this program. One series of studies will be performed to evaluate the electrical response of a number of prototype capacitors. These studies will concentrate on capacitors built from smaller-sized plates (possibly 2 x 2 inches or 3 x 3 inches in size) since previous studies have indicated that a higher degree of detection accuracy and resolution should be attainable with smaller-sized plates (see Figure 7 of Second Quarterly Technical Report). If these studies show that the smaller capacitor plates exhibit excessive fringing effects, additional studies will be performed to determine if guard-rings can be used to produce a capacitor electrical response that more closely approximates the ideal case.

Preliminary studies performed during this reporting period indicated that guard-rings will reduce the fringing effects exhibited by a capacitor. However, guard-rings also resulted in a general decrease in the sensitivity of the prototype capacitor tested. Therefore, both the advantages due to reduced fringing and disadvantages due to decreased sensitivity will have to be evaluated carefully.

The results of these studies will then be employed to design and implement a prototype detection system that employs a multiple-plate capacitor configuration. It is anticipated that this capacitor configuration

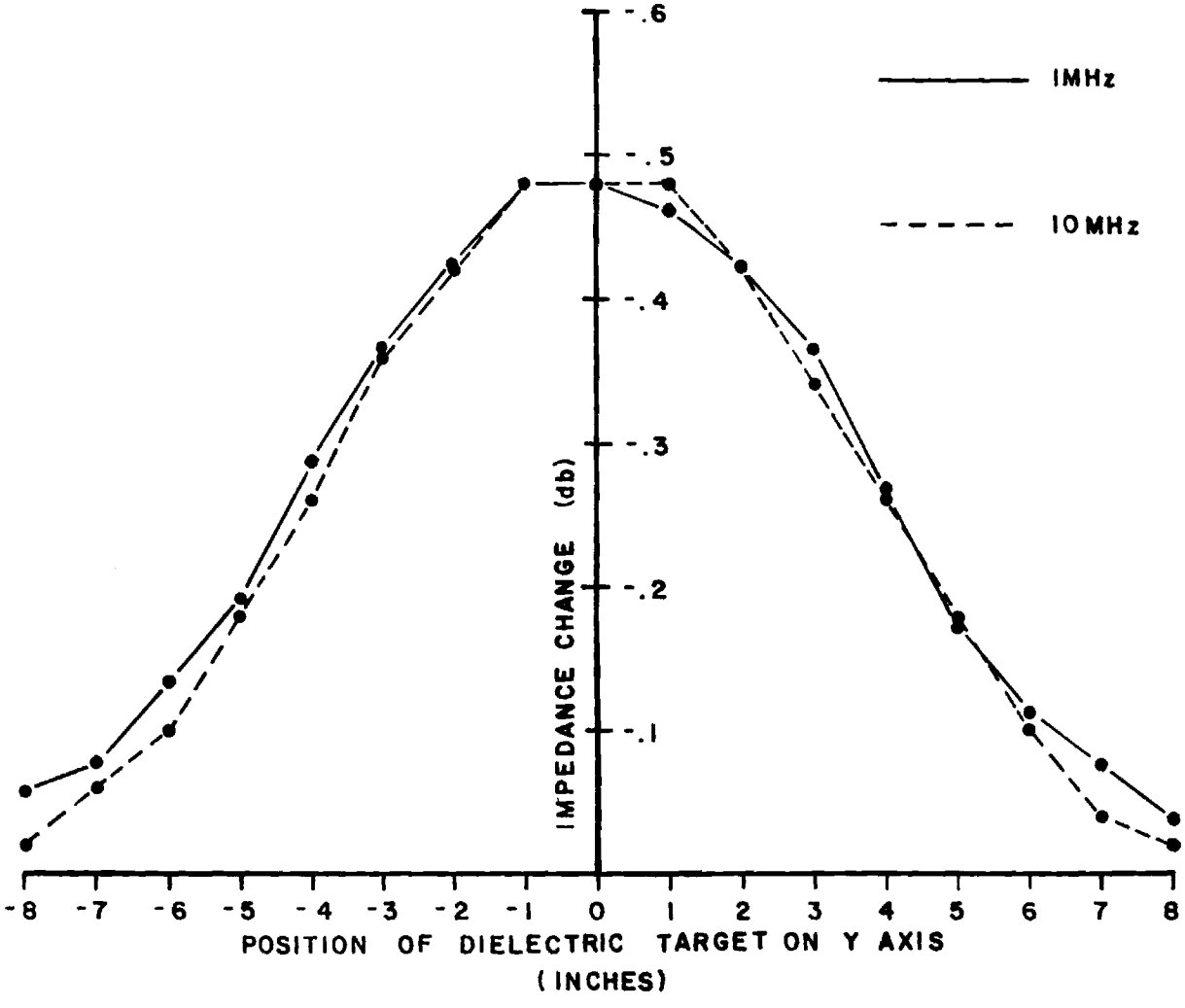

Figure 13. Effect of frequency on the electrical response of a parallel plate capacitor. Capacitor plates were both 6 x 6 inches in size.

will consist of a single, large ground plate (approximately 18 x 18 inches in size) and an array of three to six smaller, RF-fed plates. The size and separation of the plates in this array will be selected so that, in addition to being able to detect the presence of a hidden object, an estimate can be made of the location of the hidden object. A problem that may be encountered in implementing this prototype detection system is stray capacitivie coupling between the individual plates in the array of RF-fed plates. These interactions may result in a reduction of the sensitivity of the multiple-plate capacitor configuration and therefore reduce detection accuracy. A number of tests will be performed to determine a plate size and plate separation that will result in satisfactory performance in terms of accuracy, resolution, and overall sensitivity.

IV. RESONANT CAVITY APPROACH

A metal box exhibits cavity resonance characteristics when excited by an electromagnetic probe. At a resonant frequency, the maximum amount of energy is stored in the cavity's electric and magnetic fields. With the introduction of an agricultural product or other material into the cavity, it was anticipated that the resonant frequency would change and power losses within the cavity at resonance would increase. These changes would result from the agricultural product's complex permittivity which, in general, exhibits relatively high loss and high dielectric constant which are potentially capable of producing substantial changes in cavity loss and resonant frequency. Initial studies of this approach included analyses of the agricultural product's interaction with cavity fields. Also, measurements of resonant frequency shift and loss-related parameters were made using an experimental cavity.

A. Analysis

At resonant frequencies, electromagnetic standing waves may be excited within a cavity that satisfy the boundary conditions imposed by the walls. At these resonant frequencies, maximum energy storage in the fields inside the cavity is achieved and power is dissipated only by I^2R losses in the cavity walls or losses due to cavity perturbations. In general, the cavity boundary conditions do not require a unique solution and are satisfied by a theoretically infinite number of resonant frequencies above a fundamental frequency. This fundamental frequency is uniquely determined by cavity dimensions and contents. The field configuration corresponding to each resonant frequency is called a mode of the cavity. Modes of the higher resonant frequencies have a number of null points and repetitions of the standing wave pattern which could result in ambiguity in the interpretation of resonant frequency shifts caused by the introduction of agricultural products and so were not considered for this phase of the project. The TE_{101} and TM_{110} modes were used because they each have only one cycle of the standing wave pattern and have resonant

frequencies in the range where the complex permittivity of agricultural products is relatively high. Electric field configurations of these two modes are shown in Figures 14 and 15.

Electromagnetic waves traveling in a medium with a high complex permittivity, such as an agricultural product, travel slower and are more highly attenuated with distance than waves traveling in free space or air. When such a medium is introduced into a cavity, it effectively increases the electrical size of the cavity, lowering its resonant frequency, and attenuates the waves passing through it and so increases the power loss at resonance.

The relative amount of resonant frequency shift and power loss at resonance with insertion of a dielectric into the cavity will be related to the magnitude of the electric field within the dielectric sample compared to the average magnitude in the rest of the cavity [5]. Because the electric field magnitude varies with the cavity mode and position of the sample within the cavity, the resonant frequency shift and loss at resonance will vary with sample position.

The Q (quality) factor of a resonant circuit is defined as 2π times the energy stored in the reactive components of the circuit divided by the energy dissipated per cycle. Q is therefore an indication of the energy dissipated within a cavity and one of the quantities normally used to describe a resonant cavity electrically. The power dissipated within a lossy sample inserted into the cavity also depends on the magnitude of the electric field in the sample and therefore the cavity Q will change not only with the relative amount of agricultural product but also with the product's position within the cavity.

Q is often approximated by a formula obtained from a lumped circuit cavity model:

$$Q = \frac{f_r}{f_2 - f_1},$$

where f_r is the resonant frequency and f_2 and f_1 are frequencies at

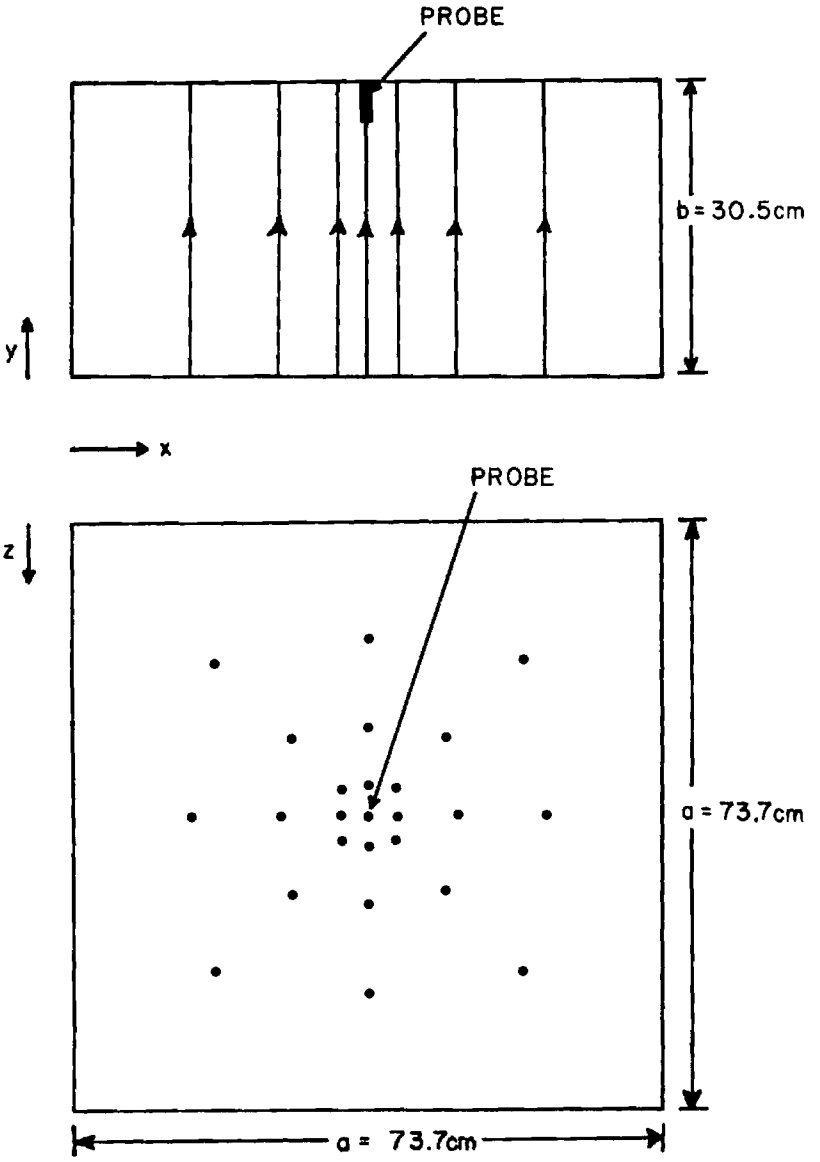

Figure 14. TE_{101} mode electric field configuration. Unperturbed field intensity is highest at x=a/2, z=a/2; no variation of intensity with respect to y-axis.

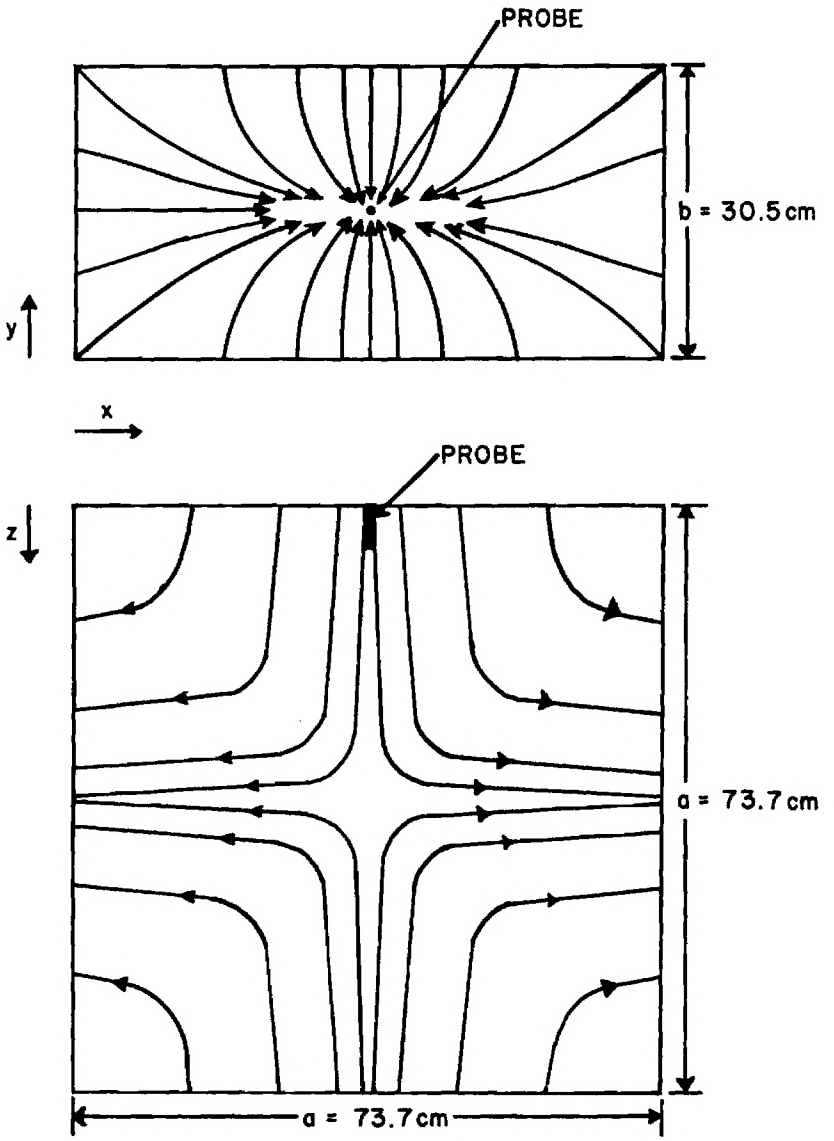

Figure 15. TM_{110} mode electric field configuration. Unperturbed field intensity along the periphery is higher than in the TE_{101} mode and varies with respect to y.

which the magnitude of the cavity reactance is equal to the cavity resistance. This formula becomes less accurate with low Q and large amounts of high loss dielectrics, but it was believed that it would show significant changes with the introduction of agricultural products and serve as a relative index of power loss within the cavity.

It was anticipated that the effective impedance at resonance would change with insertion of agricultural products by changing cavity impedance itself along with probe coupling efficiency. The cavity impedance at resonance is indicative of real power losses inside the cavity which would be increased by the loss factor of the agricultural product. The impedance of the cavity/probe system is also dependent upon the coupling coefficient between the probe and cavity. The coupling coefficient, which is analogous to a transformer turns ratio, depends on the electrical length of the probe and its position with respect to the cavity's field configuration. The electrical length of the probe varies with frequency and thus will vary as resonant frequency changes with introduction of an agricultural product. The agricultural product will alter the field configuration to some extent and will therefore alter the probe's relative position with respect to the field pattern. Because impedance at resonance would provide another measureable quantity related to the presence of an agricultural product, it was selected to be examined by measurement. It was anticipated that the impedance at resonance would therefore show significant changes with the insertion of the agricultural product.

B. Measurements

Because the effort involved in complete quantitative prediction of the cavity's behavior with insertion of an agricultural product would be prohibitive due to the complexity of the cavity field equations and need to recalculate for each sample position and volume, a cavity system was designed along general guidelines to measure the behavior. Considerations for cavity design included the following:

- o Cavity Size. A cavity approximating baggage size was needed to enable measurements to be made at the lower frequencies projected for final use. A smaller cavity and size scaling could have been used except that agricultural product dielectric parameters would have been different at the higher resonant frequencies of the smaller cavity.
- o Low Order Mode Excitation. Low order modes, TE_{101} and TM_{110} were selected because it was felt that changes in measured parameters would be less ambiguous and more predictable than those made using higher order modes with multiple null points within the cavity. In addition, these two modes were selected because their minima and maxima occur in different locations within the cavity. It was thought that this would enhance detection ability in addition to providing possible localization information.
- o Coupling Probes. Electric field probes were selected for ease of construction and efficiency in size needed for impedance matching as opposed to loops coupling to the magnetic fields.
- o Closed Cavity. A closed cavity design was selected rather than an open ended configuration because of anticipated higher immunity from external interference and increased sensitivity due to the tendency for open ended resonators to radiate. It was also anticipated that results could be interpreted in a more straight-forward fashion.

Measurements were made to examine the response of the system to agricultural products as a function of their positions in the cavity. Initial measurements were made of cavity response to the product alone to avoid problems in interpreting data because of field complexities which would be introduced by simulated baggage contents.

A closed rectangular cavity 29 x 29 x 12 inches was fabricated from 25 gauge tin-plated sheet steel. The dimensions were determined by available material size and a medium suitcase size of 25 x 20 x 8 inches. The cavity's seams were all soldered with the exception of those along one removable side which was sealed by a compliant metal braid tube. The sides were reinforced by 3/8" plywood for mechanical stability and durability.

Electric field probes consisting of a length of wire soldered to the center contact of a "type N" panel mount connector were fabricated. The probes were adjusted for critical coupling (match of the cavity/coupling system at resonance to transmission line impedance) by trimming the wire for minimum reflected power at the empty cavity resonant frequency.

Impedance measurements were made using an HP Network Analyzer System with swept frequency source set up for reflection coefficient display as a function of frequency on a Smith Chart overlay. These measurements were used to determine resonant frequency f_r, impedance at resonance, and the frequencies at which cavity/probe reactance magnitude equalled cavity/probe resistance. The cavity resonant frequency was determined by noting the frequency at which the impedance was purely real. The cavity "Q" with the sample introduced, Q_s, was determined by dividing f_r by the difference (Δf) in the frequencies at which reactance magnitude equalled resistance.

Measurements of resonant frequency and Q were first made for the empty cavity. The measured resonant frequencies, 286.13 MHz for the TE_{101} mode and 569.01 MHz for the TM_{110} mode were close to calculated values of 288.00 MHz and 570.20 MHz. The frequency differences were attributed to slight cavity dimension variations from the nominal design values. The unloaded Q of the cavity was measured to be 3577 for the TE_{101} mode, and 4064 for the TM_{110} mode.

A 6.4 cm diameter Red Delicious apple was introduced into the cavity and measurements made of f_r, Q_s and impedance at f_r as a function of cavity position. These positions are illustrated in Figure 16. The frequency was swept from approximately 283 to 287 MHz in the TE_{101} mode and 560 to 570 MHz in the TM_{110} mode. Measurements were made in one quadrant of the cavity only, due to symmetry of the unperturbed fields about the planes $x = a/2$, $y = b/2$, $z = a/2$. Tables I and II list results of these measurements and Figures 17 and 18 illustrate some of these changes in f_r and Q_s with changes in sample position.

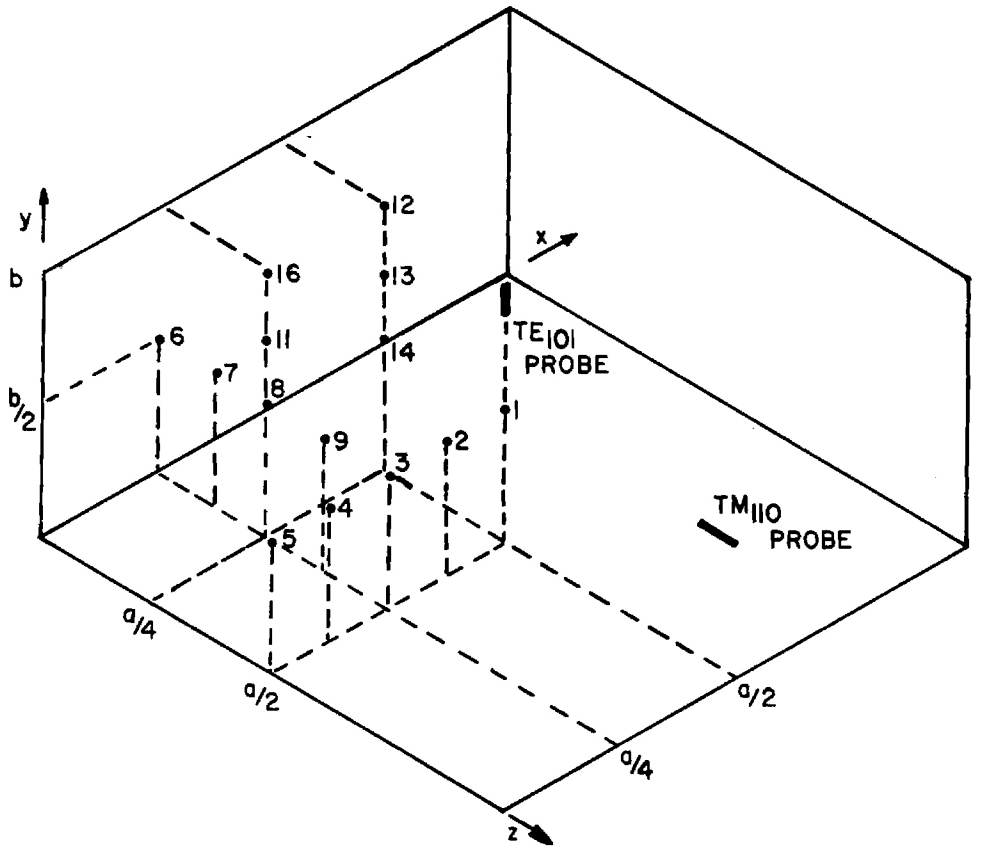

Figure 16. Apple positions for resonant cavity measurements. Positions in one quadrant were selected because of the unperturbed field symmetry about the planes x=a/2, y=b/2, z=a/2 (a=73.7 cm, b=30.5 cm).

TABLE Ia

MEASURED CAVITY PARAMETERS

TE_{101} mode: probe length 6.0 cm (undercoupled)
6.4 cm diameter Red Delicious Apple

Position	Impedance at resonance (ohms)	f_R(MHz)	$Q_s = \frac{f_R}{\Delta f}$
Empty	47	286.08	3177
1	65	284.16	861
2	70	284.46	917
3	65	285.089	950
4	65	285.55	921
5	65	285.83	986
6	60	285.92	1787
7	60	285.7	714
8	65	285.43	891
9	70	284.85	566
11	65	285.40	951
12	85	284.75	837
13	75	284.98	950
16	70	285.31	865

Table Ia. Measured parameters as a function of apple position in the TE_{101} mode (undercoupled probe). Largest effect on measured parameters was found at position 1 where unperturbed electric fields were strongest.

TABLE Ib

MEASURED CAVITY PARAMETERS

probe length 7.2 cm (critical coupling)

6.4 cm diameter Red Delicious Apple

Position	Impedance at resonance (ohms)	f_R(MHz)	$Q_s = \frac{f_R}{\Delta f}$
Empty	50	286.13	3577
1	60	284.23	2584
3	65	285.19	2377
5	65	285.99	2383
6	55	286.02	2600
8	60	285.63	2597
12	78	284.89	2035
16	65	285.53	2379

Table 1b. Measured parameters as a function of apple position in the TE_{101} mode (critically coupled probe). Largest effect on measured parameters was found at positions 1 and 16, similar to results in Table Ia.

TABLE II

MEASURED CAVITY PARAMETERS

TM_{110} mode: probe length 4.6 cm (critical coupling)

6.4 cm diameter Red Delicious Apple

Position	Impedance at resonance (ohms)	f_R(MHz)	$Q_s = \frac{f_R}{\Delta f}$
Empty	50	569.01	4064
1	50	568.83	4063
2	55	568.80	4062
3	60	569.00	3556
4	55	568.95	3793
5	55	568.95	4377
6	235	563.81	854
7	200	565.95	993
8	150	567.01	1289
9	80	568.67	3159
11	350	567.03	616
12	~1000	566.02	227
13	500	566.17	370
14	75	566.12	2573
16*	~5000	565.79	484
16*	~5000	568.25	455

* Two resonances very close together were observed at position 16; it was not possible to determine which was a parasitic resonance.

Table II. Measured parameters as a function of apple position in the TM_{110} mode (critically coupled probe). Largest changes in parameters were observed at positions 12 and 16.

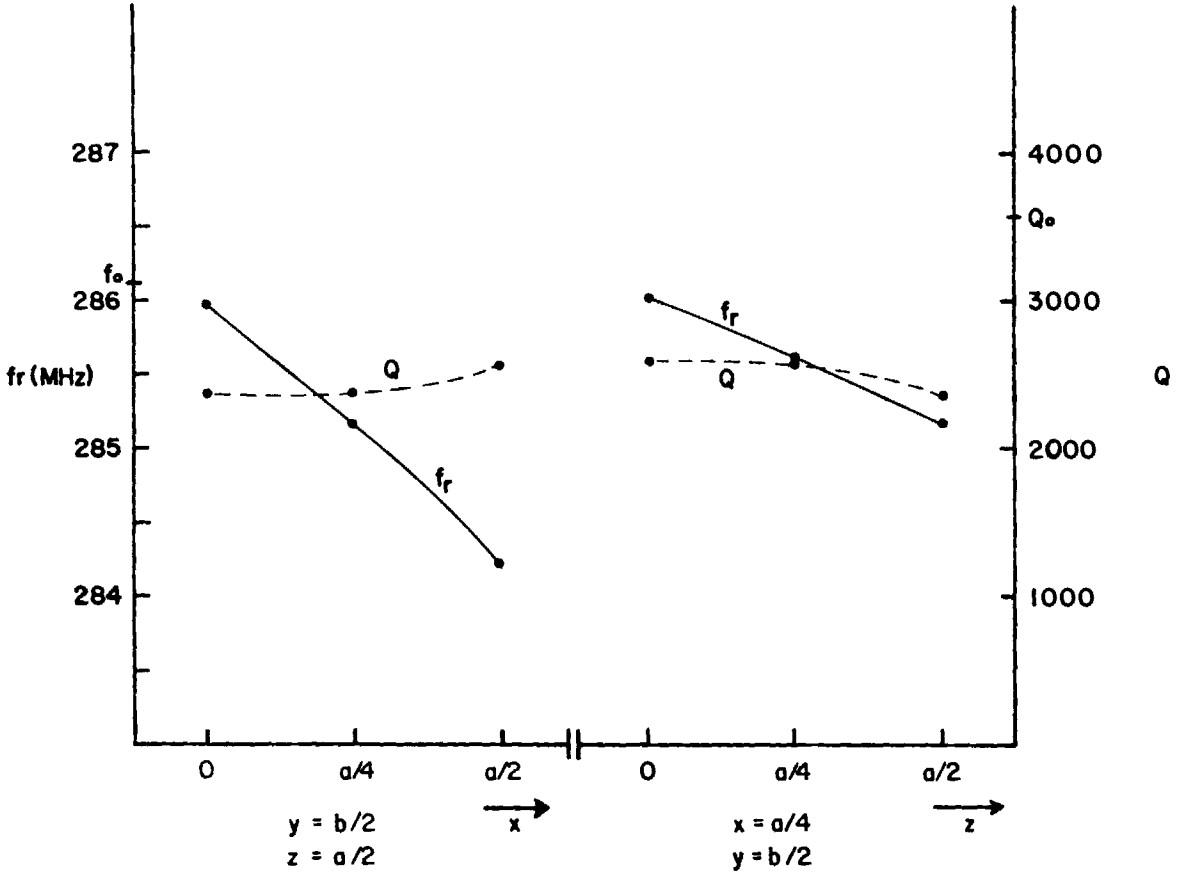

TE_{101} RESONANT FREQUENCY AND Q AS A FUNCTION OF APPLE POSITION

Figure 17. Q and f_r as functions of apple position in the TE_{101} mode. From left to right, the values are for positions 5, 3, 1, 6, 8, and 3 in Figure 14. Q_o and f_o were empty cavity Q and resonant frequency. Q demonstrated little change; f_r showed maximum change in the cavity center ($x=a/2$).

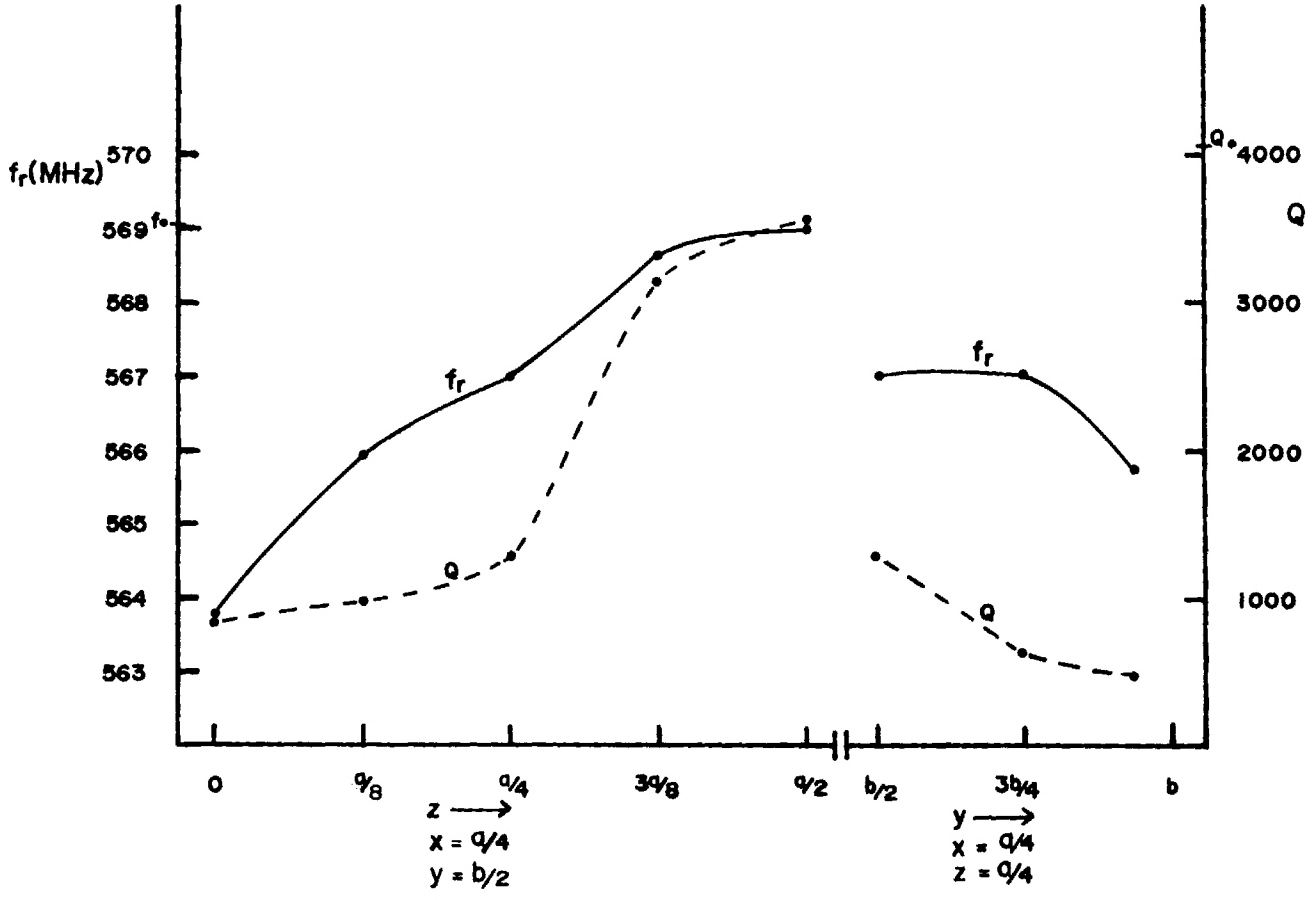

TM_{110} CAVITY RESONANT FREQUENCY AND Q AS A FUNCTION OF APPLE POSITION

Figure 18. Q and f_r as functions of apple position in the TM_{110} mode. From left to right, the values were for positions 6,7,8,9,3,8,11, and 16 in Figure 14. Q_o and f_o were empty cavity Q and resonant frequency. Largest changes occurred for positions around the periphery of the cavity (z=0, y=b); minimal changes, near the center (z=a/2, y=b/2).

Comparison of Figures 17 and 18 with the field configurations in Figures 14 and 15 shows that the largest changes in f_r and Q_s from the empty cavity resonant frequency, f_o, and empty cavity Q, Q_o, tended to occur at sample positions where the unperturbed electric field is most intense. Some exceptions to this occurred at z = a/2 in the TM_{110} mode and these were attributed to substantial changes in the field distribution by the apple. In general, these comparisons indicated that it may be possible to detect an agricultural product throughout much of the cavity volume by measuring changes in both modes.

C. Future Investigations

Having seen that changes in cavity response can indicate the presence of a moderate amount of agricultural product, it is necessary to evaluate the cavity's ability to show the presence of an agricultural product in the presence of luggage frames and non-agricultural contents. The effects of sample volume must also be assessed. During the final quarter of this project, measurements of resonant frequency, cavity Q, and impedance at resonance will be examined for an agricultural sample at different positions within a suitcase and surrounded by articles of varying electrical properties. A second probe will be installed to act as a receiving probe so that transmission through the cavity may be examined. Measurements of transmission coefficient data will be done to determine whether or not transmission measurements have more advantages than reflection coefficient measurements.

Data will be examined for the possibility of discrimination between responses due to agricultural products and responses caused by luggage framework or non-agricultural contents. It is anticipated that differences would occur not only in relative magnitudes of change but also in response differences observed between the two modes being examined.

V. SIGNAL TRANSMISSION/REFLECTION APPROACH

The signal transmission/reflection approach as a means of noninvasively detecting the presence of agricultural products in baggage is based upon the differences in dielectric properties between agricultural products and other baggage contents. This difference arises primarily from the relatively high moisture content of fresh fruits, vegetables, and meats as compared to materials such as leather and cloth. For a given object, the factors affecting the transmitted and reflected signals are its position, shape, size, permittivity, and loss factor. The transmitted and reflected signals, being complex, are completely described by four parameters: two magnitudes and two phases.

In the Second Quarterly Report, an analysis of the transmitted and reflected signals in terms of a planar multi-layered model was described and preliminary experimental results obtained with the use of a network analyzer operated in a manual mode were presented. This report includes further experimental results using the network analyzer under computer control. In this mode, phase and magnitude changes resulting from the insertion and removal of a sample were obtained. In addition, the dependence of the signals upon the position of the sample was explored. Two frequency ranges were covered: 1.8 - 2.6 GHz (LS-band) and 2.6 - 3.9 GHz (S-band).

A. Experimental Arrangement

The HP Network Analyzer System used to measure reflection and transmission coefficients was essentially the same as previously reported except for the addition of a computer and related hardware. The use of a computer to control the network analyzer had two major advantages over manual use. First, a calibration procedure using known terminations and loads could be used to make error corrections to parameters obtained in the course of an experiment. This calibration also allowed losses and phase shifts occurring in the connecting cables to be taken into account. The second advantage was that measurements could be reproducibly made for a set of frequencies. This capability allowed changes in transmission

and reflection parameters with the insertion of the sample to be determined. In all experiments, the "device under test" consisted of the transmitting and receiving antenna pair (along with their coaxial to waveguide adaptors) and the sample placed between the antennas.

Two different sets of antennas were required to cover the two frequency ranges. For the LS-band measurements, the transmitting horn had an aperture of 27.3 cm by 37.5 cm; the receiving horn, 11.4 cm by 11.4 cm. The dimensions of the transmitting horn were such that the near field extended to about 38 cm and the transition field to about 188 cm. The apertures of both S-band horns were 7.5 cm by 7.5 cm. In this case, the near field extended to about 3 cm and the transition field to about 15 cm. For both frequency ranges, the horns were placed 50 cm apart. This separation was chosen to be compatible with the spacing required for the insertion of a suitcase. The bottom edge of the transmitting horns were placed 15 cm above the surface of the support upon which the sample was placed and each receiving horn was aligned so that its aperture was centered with respect to the transmitting horn.

The sample consisted of a plastic bottle containing glycerol solution (30% by weight) having dielectric properties described in the Second Quarterly Technical Report to be $\varepsilon_r' = 48$ and $\varepsilon_r'' = 14$ at 2.45 GHz, which are comparable to previous data for agricultural products. These values are also similar to those measured during this quarter, except that measured values of relative dielectric constant were somewhat larger. However, these differences should have little net effect on the transmission and reflection coefficients measured here. The bottle was filled to the neck and thus, ignoring the thin plastic shell, the sampled could be considered as a cylinder of glycerol solution of diameter 6 cm and height 9.5 cm. This type of sample was chosen in lieu of a piece of fruit to allow reproducible results to be obtained over a period of several days.

The sample was placed on a 50 x 40 cm grid so that its position relative to the horn antennas could be determined. Figure 19 shows a top view of the horns and grid with the different sample positons ennumerated. The complete assembly of horn antennas and sample was surrounded by anechoic material to reduce the influence of extraneous reflections and noise upon the measurements.

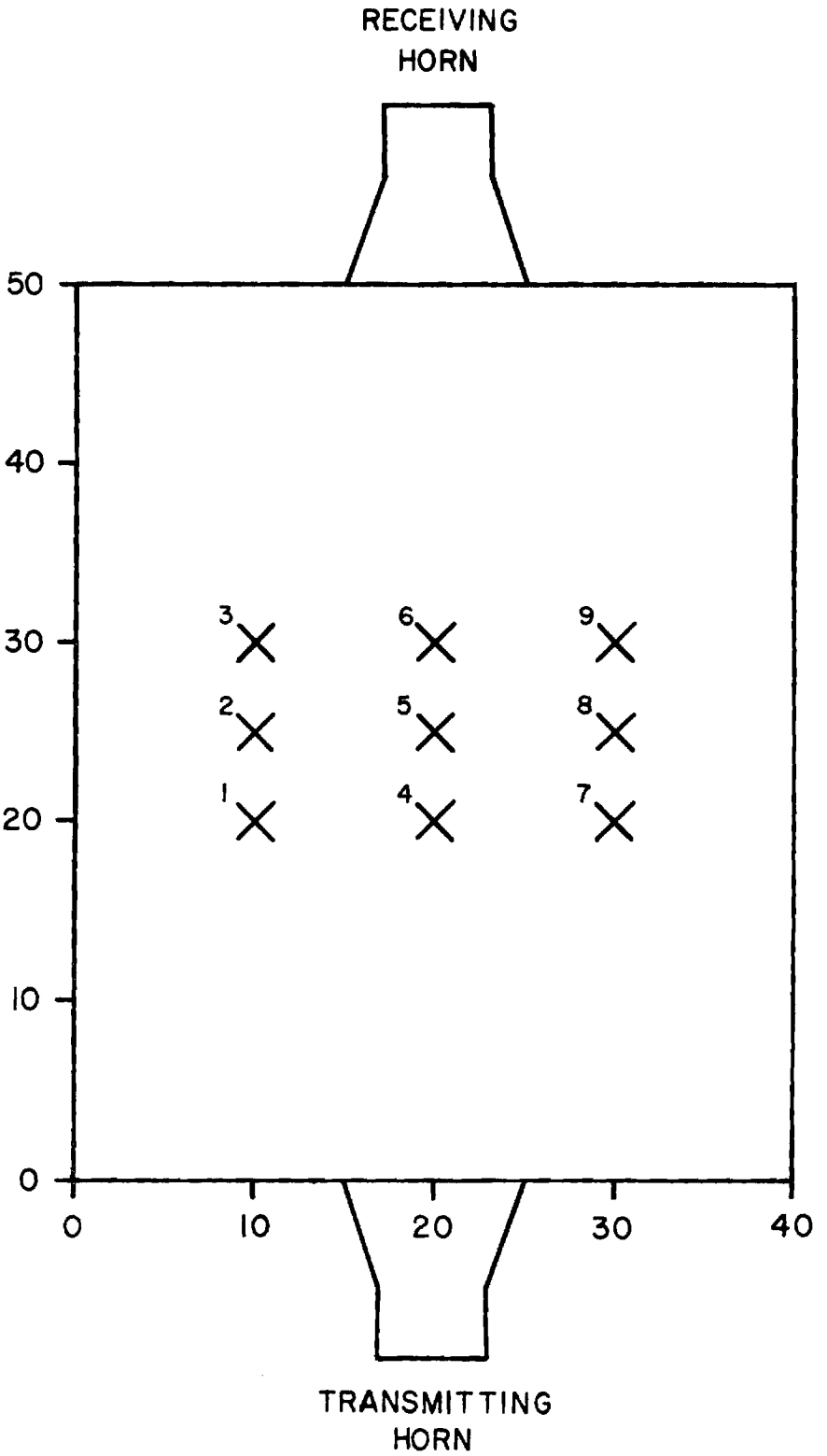

Figure 19. Top view of the horn antenna and sample positions (X) 1 through 9 used in transmission/reflection measurements. The axes show distances from the lower left-hand corner of the grid in centimeters.

During an experiment, the transmission and reflection coefficients were first determined with no sample present at preassigned frequencies in 0.1 GHz increments for both bands. The sample was then placed at each positon shown in Figure 19 and transmission and reflection measurements were taken for each frequency. After measurements at all positions were completed, the "no sample" measurements were repeated to check for any drift in the system. In both frequency bands covered, the drift for "no sample" conditions was less than 1% in all parameters except for measurements at 2.1 GHz. At this one frequency, the phase shift for the transmitted signal was near 180^{o} and thus with little variation in frequency could change quadrants making the measurement somewhat unstable. Accordingly, some data obtained at this frequency were represented by gaps in Figures 20-25 which are discussed below. The normally small instability in the measurements was most likely due to the accuracy with which the frequency could be controlled and slight movements of the horn antennas.

The results were put in the form of changes in the reflection and transmission coefficients with insertion of the sample. These were obtained by subtracting the numbers obtained from the "no sample" runs from those of the "sample present" runs. Because changes rather than absolute transmission and reflection coefficients were examined, effects arising from the imperfect shielding of the apparatus were minimized. These parameter changes are thus indicative of the effect one can hope to observe if agricultural products (of similar size, shape, and position) are present as compared to when they are not present.

B. Results

Results from the LS-band measurements (1.8 - 2.6 GHz) are displayed in Figures 20 through 25. Each figure contains data from three positions of the sample. Groupings were made for positions along axes parallel to the axis connecting the centers of the two horns -- positions (1,2,3), (4,5,6), and (7,8,9) shown in Figure 19. In these figures, the broken line corresponds to the positions nearest the transmitting horn, (1,4, or 7); the solid line to the center positions, (2,5, or 8); and the

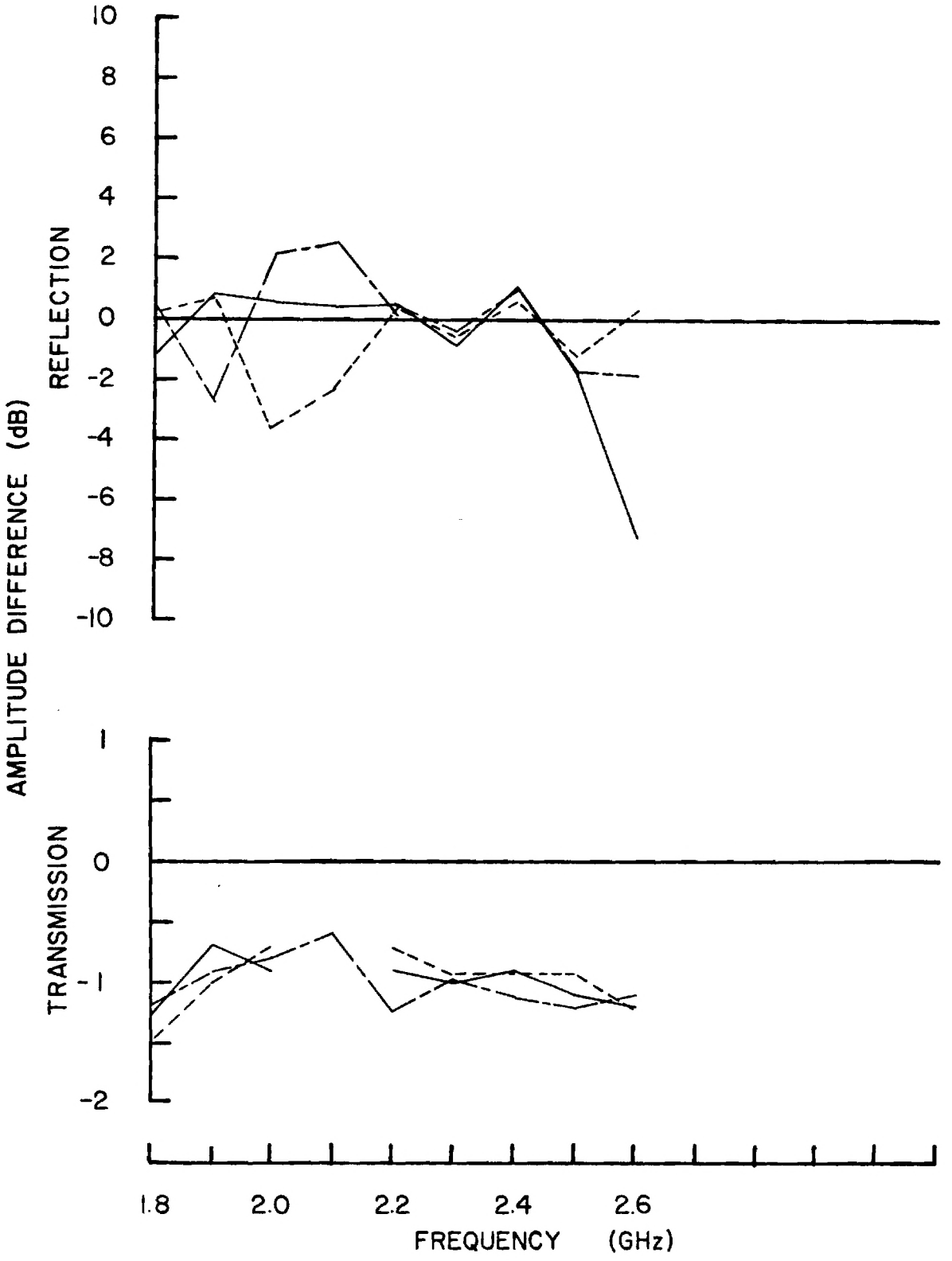

Figure 20. Magnitude (amplitude) change of reflection (upper) and transmission (lower) coefficients with insertion of the sample for the frequency range 1.8 to 2.6 GHz. The broken lines are for position 1; the solid lines, position 2; and the dashed lines, position 3.

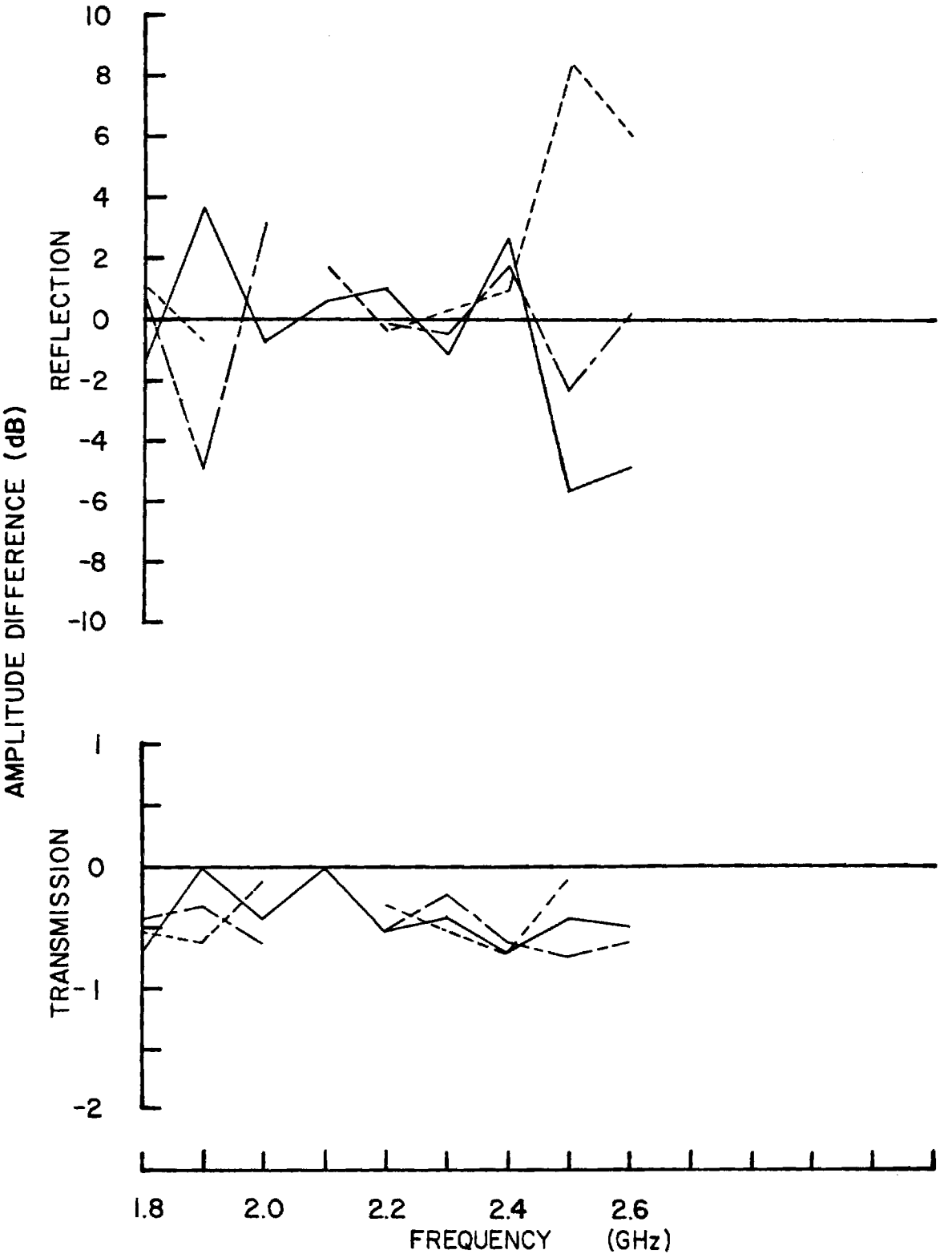

Figure 21. Magnitude (amplitude) change of reflection (upper) and transmission (lower) coefficients with insertion of the sample for the frequency range 1.8 to 2.6 GHz. The broken lines are for position 4; the solid lines, position 5; and the dashed lines, position 6.

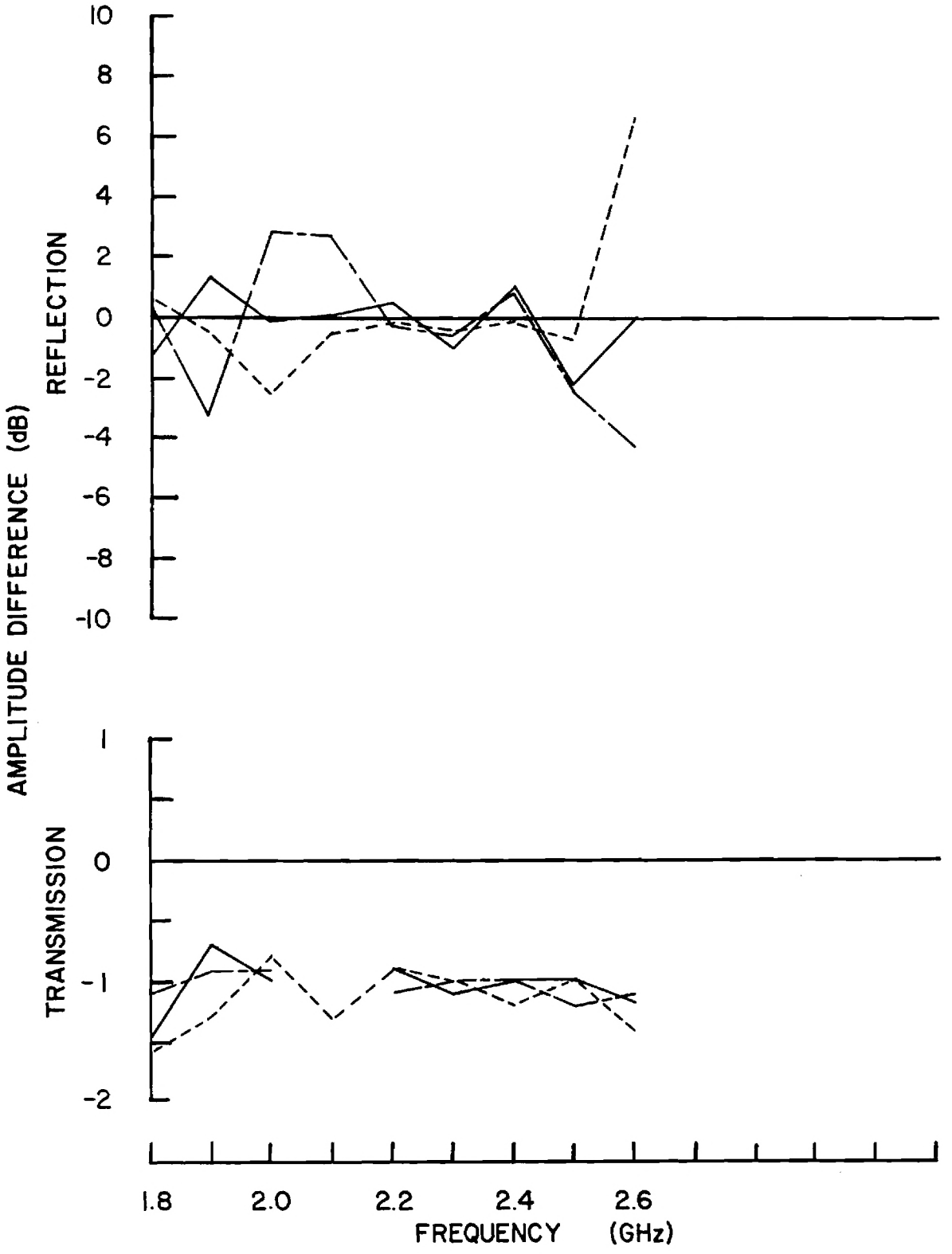

Figure 22. Magnitude (amplitude) change of reflection (upper) and transmission (lower) coefficients with insertion of the sample for the frequency range 1.8 to 2.6 GHz. The broken lines are for position 7; the solid lines, position 8; and the dashed lines, position 9.

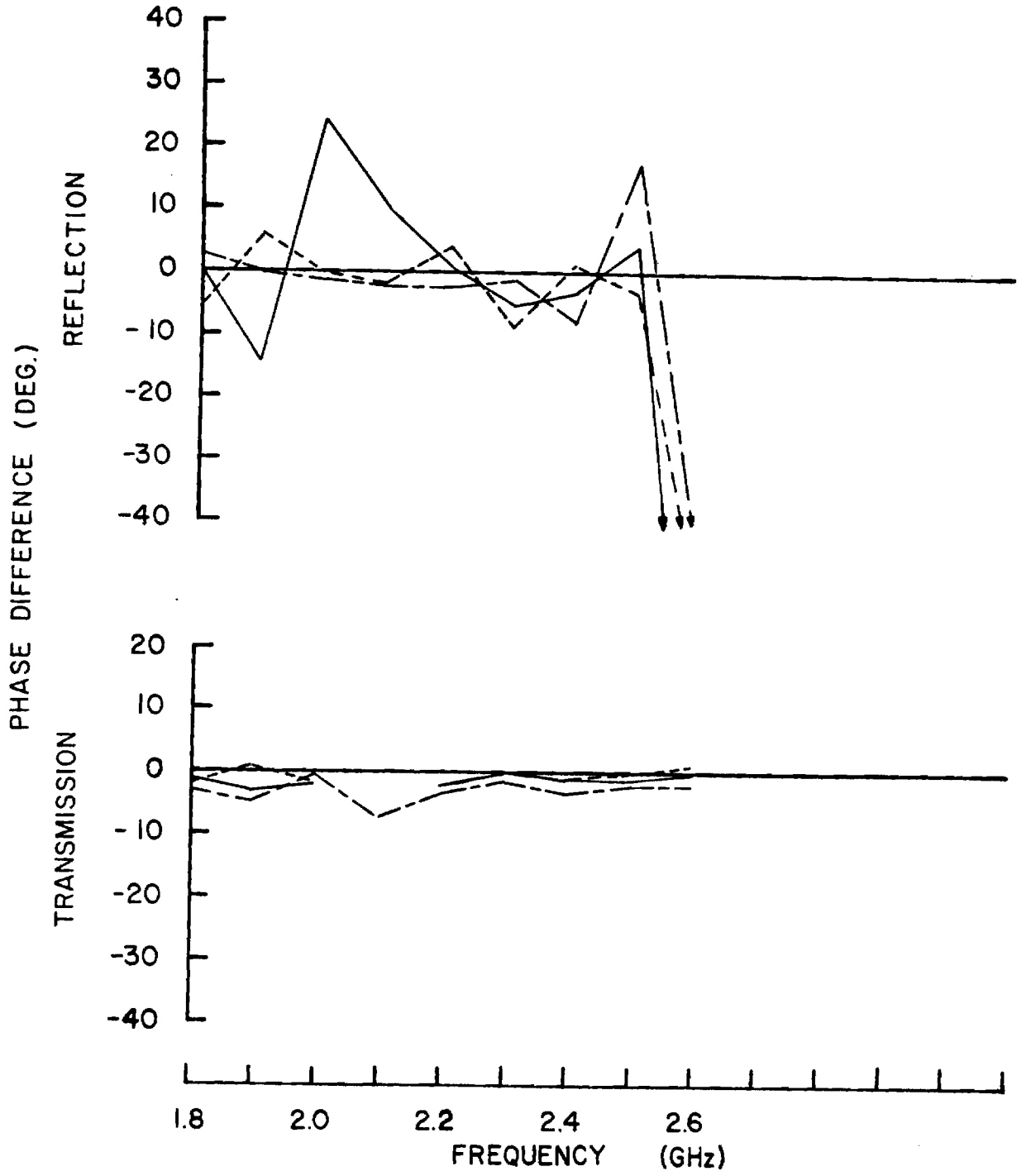

Figure 23. Phase shift of reflection (upper) and transmission (lower) coefficients with insertion of the sample for the frequency range 1.8 to 2.6 GHz. The broken lines are for position 1; the solid lines, position 2; and the dashed lines, position 3.

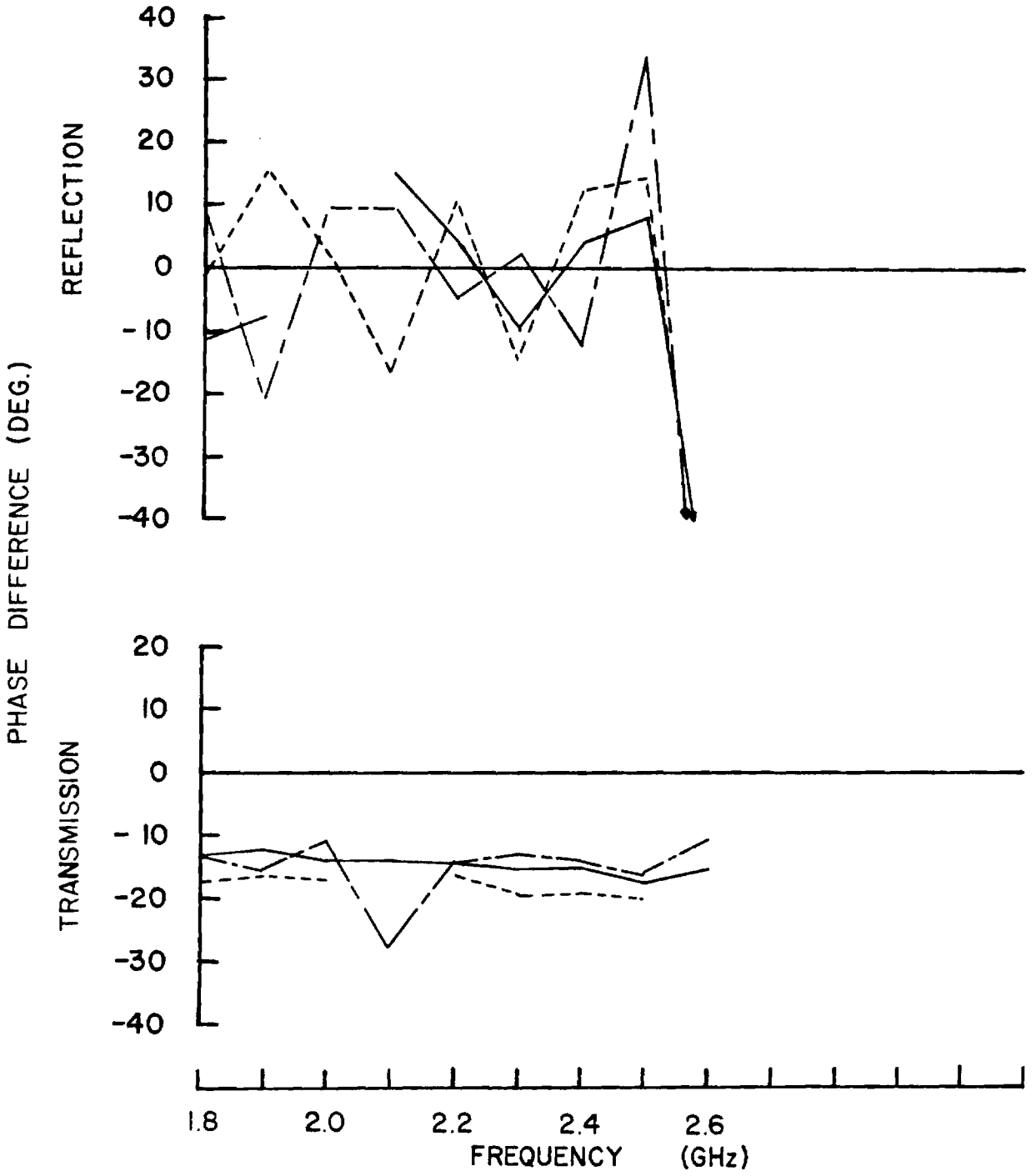

Figure 24. Phase shift of reflection (upper) and transmission (lower) coefficients with insertion of the sample for the frequency range 1.8 to 2.6 GHz. The broken lines are for position 4; the solid lines, position 5; and the dashed lines, position 6.

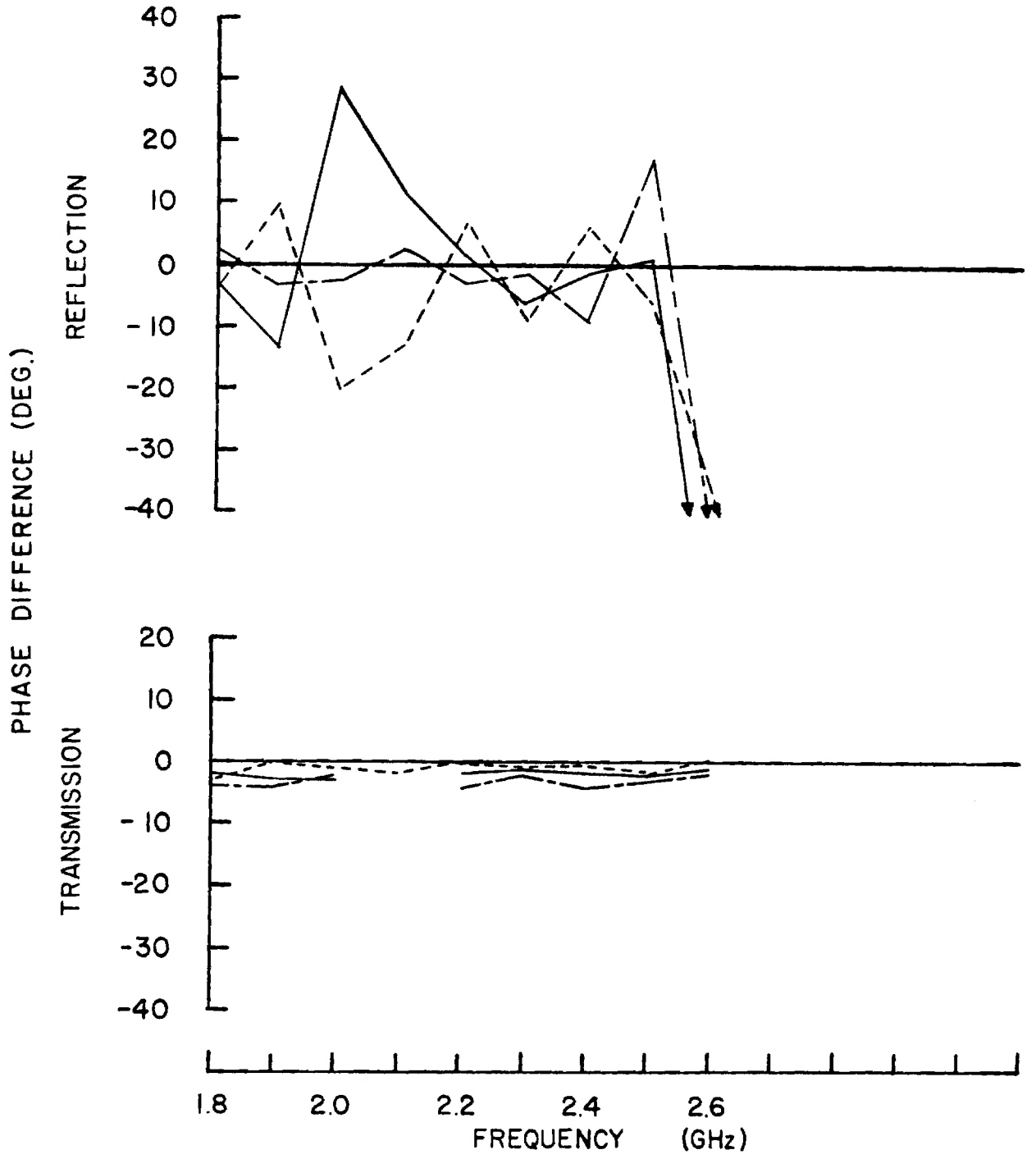

Figure 25. Phase shift of reflection (upper) and transmission (lower) coefficients with insertion of the sample for the frequency range 1.8 to 2.6 GHz. The broken lines are for position 7; the solid lines, position 8; and the dashed lines, position 9.

dashed line to the positions nearest the receiving horn, (3,6, or 9). Magnitudes for the transmission coefficient changes shown in Figures 20 through 22 were consistently negative, ranging from 0 to -1.5 dB. They were fairly uniform within the groupings shown and exhibited little variation with frequency. There was also a similarity between signals seen in the (1,2,3) and (7,8,9) groupings (left of center and right of center). The reflection coefficient magnitude changes were more erratic as seen in Figures 20 through 22, showing fluctuations on the order of $\pm$ 4 dB about zero. Phase shifts for the LS-band are shown in Figures 23 through 25. For the transmission phase shift, the largest values occurred for the central positions (4,5,6) directly between the antennas. As with magnitudes, there was left-right symmetry with almost no phase difference between side positions (1,2,3) and (7,8,9). The average phase shift for the central positions was about -15^{o} and was roughly independent of frequency. Phase shifts for the reflected signals also shown in Figure 23 through 25 displayed irregular behavior with fluctuations up to 30^{o}. The last point showing a very large phase shift was most likely an artifact due to the extremely low absolute reflection coefficient of magnitude -40 dB.

Figures 26 through 31 show results for the S-band (2.6 to 3.9 GHz) measurements. All figures show similar structure within the three position groupings (1,2,3), (4,5,6), and (7,8,9), demonstrating translation invariance along the direction connecting the two antennas. There was also a strong left-right symmetry about the center line as evidenced by the similarity of the data in groups (1,2,3) and (7,8,9). The magnitudes of the transmission coefficient change exhibited in Figures 26 through 28 had a marked frequency dependence. Additionally, the slope of this frequency dependence was different for the center positions as compared to the side positions. These magnitude changes ranged from -2 dB to + 0.3 dB. Reflection coefficient magnitude changes are also shown in Figures 26 through 28. Again, less uniform behavior as a function of frequency was evident with changes ranging from -4.5 dB to -3.5 dB. Phase shifts for the transmitted signal are shown in Figures 29 through 31. These were fairly independent of frequency, with the average value

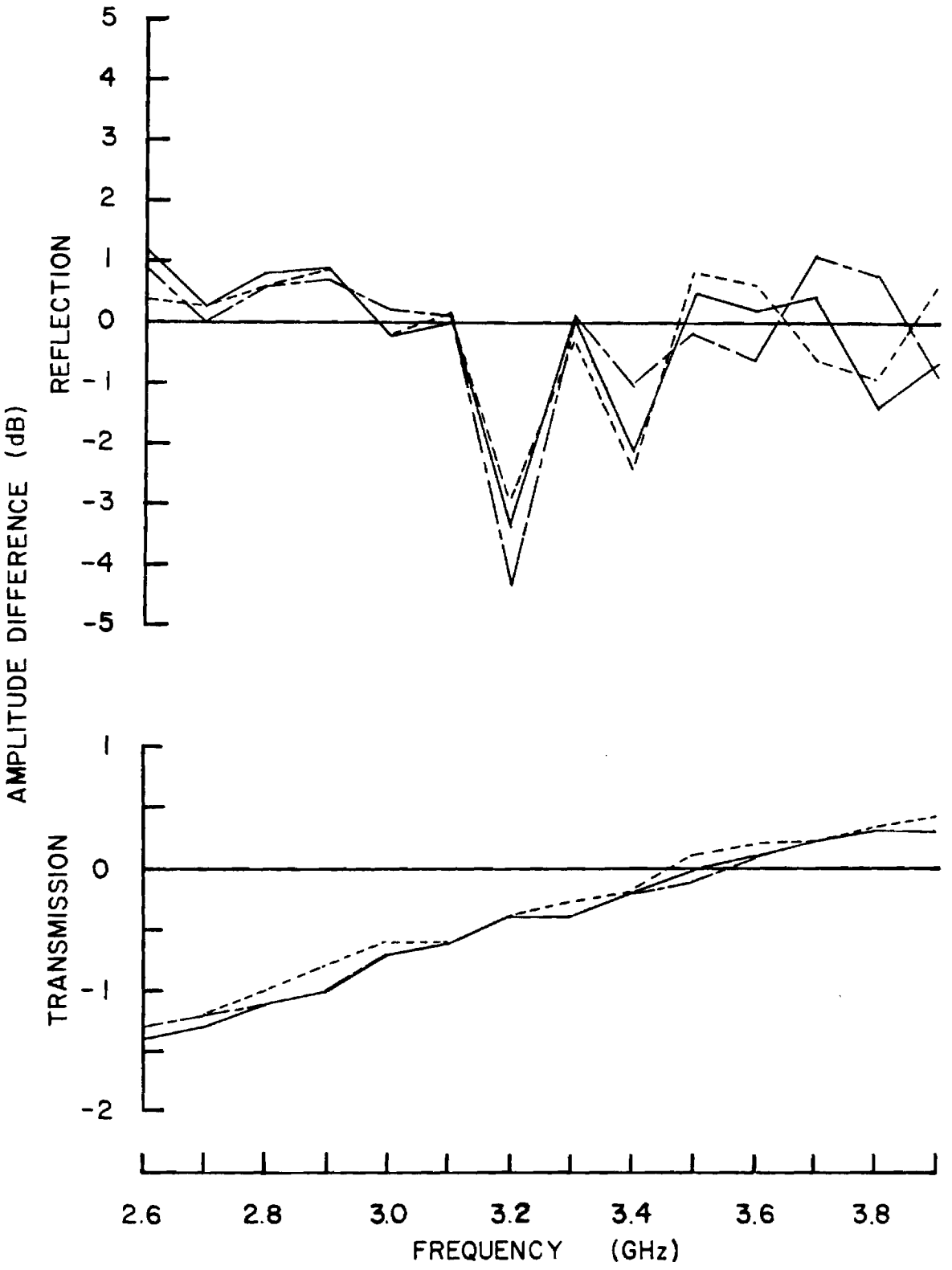

Figure 26. Magnitude (amplitude) change of reflection (upper) and transmission (lower) coefficients with insertion of the sample for the frequency range 2.6 to 3.9 GHz. The broken lines are for position 1; the solid lines, position 2; and the dashed lines, position 3.

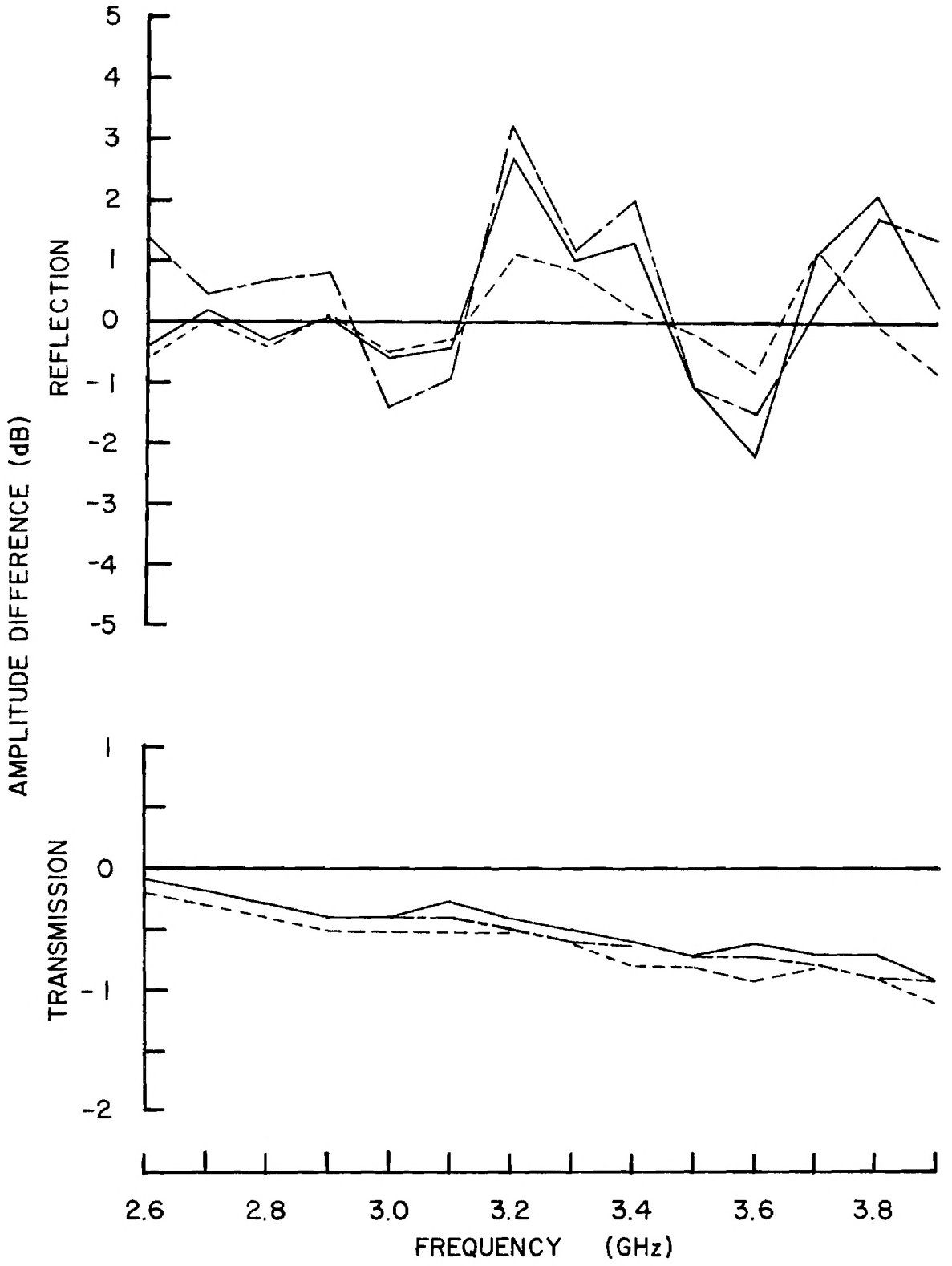

Figure 27. Magnitude (amplitude) change of reflection (upper) and transmission (lower) coefficients with insertion of the sample for the frequency range 2.6 to 3.9 GHz. The broken lines are for position 4; the solid lines, position 5; and the dashed lines, position 6.

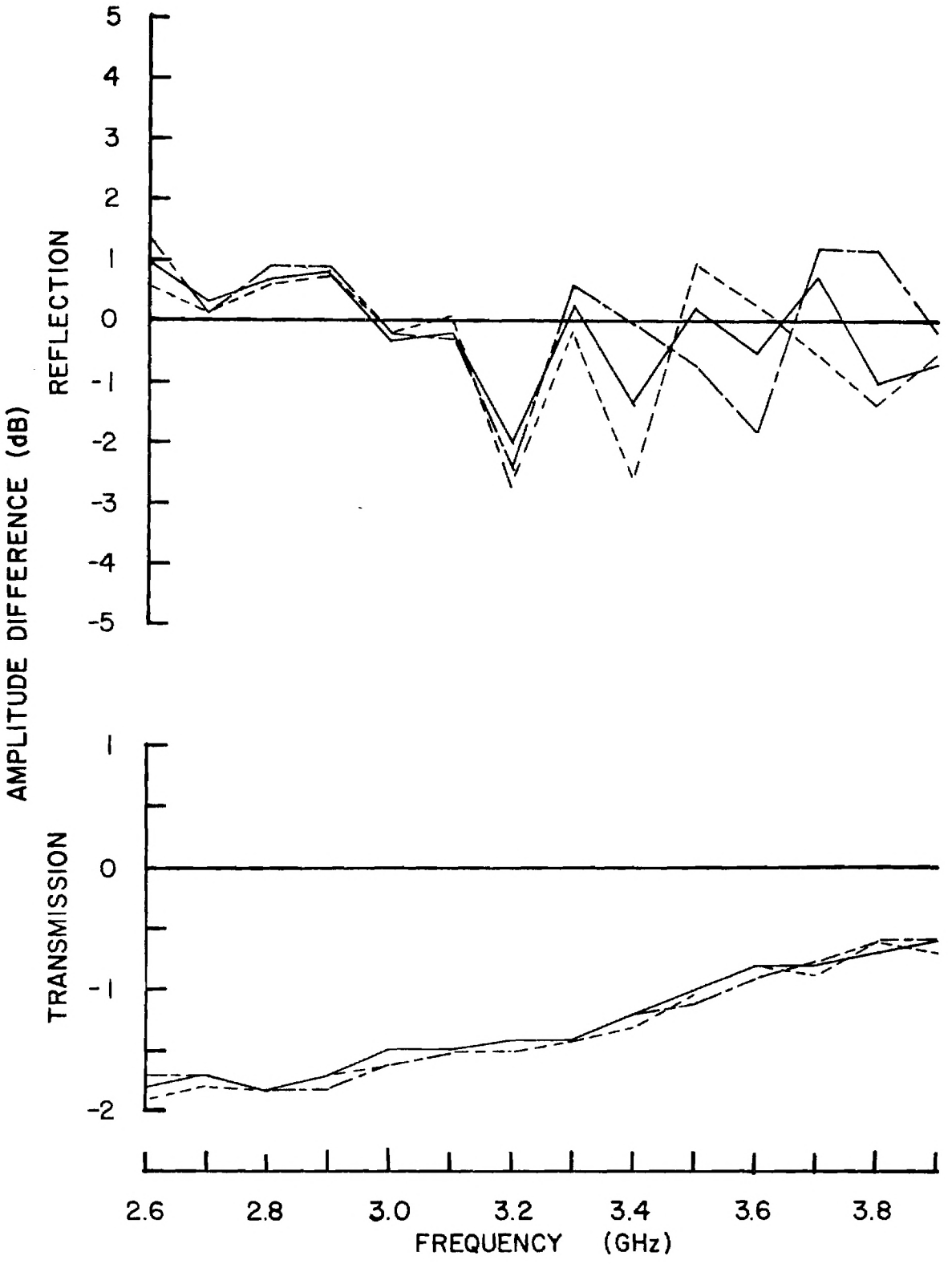

Figure 28. Magnitude (amplitude) change of reflection (upper) and transmission (lower) coefficients with insertion of the sample for the frequency range 2.6 to 3.9 GHz. The broken lines are for position 7; the solid lines, position 8; and the dashed lines, position 9.

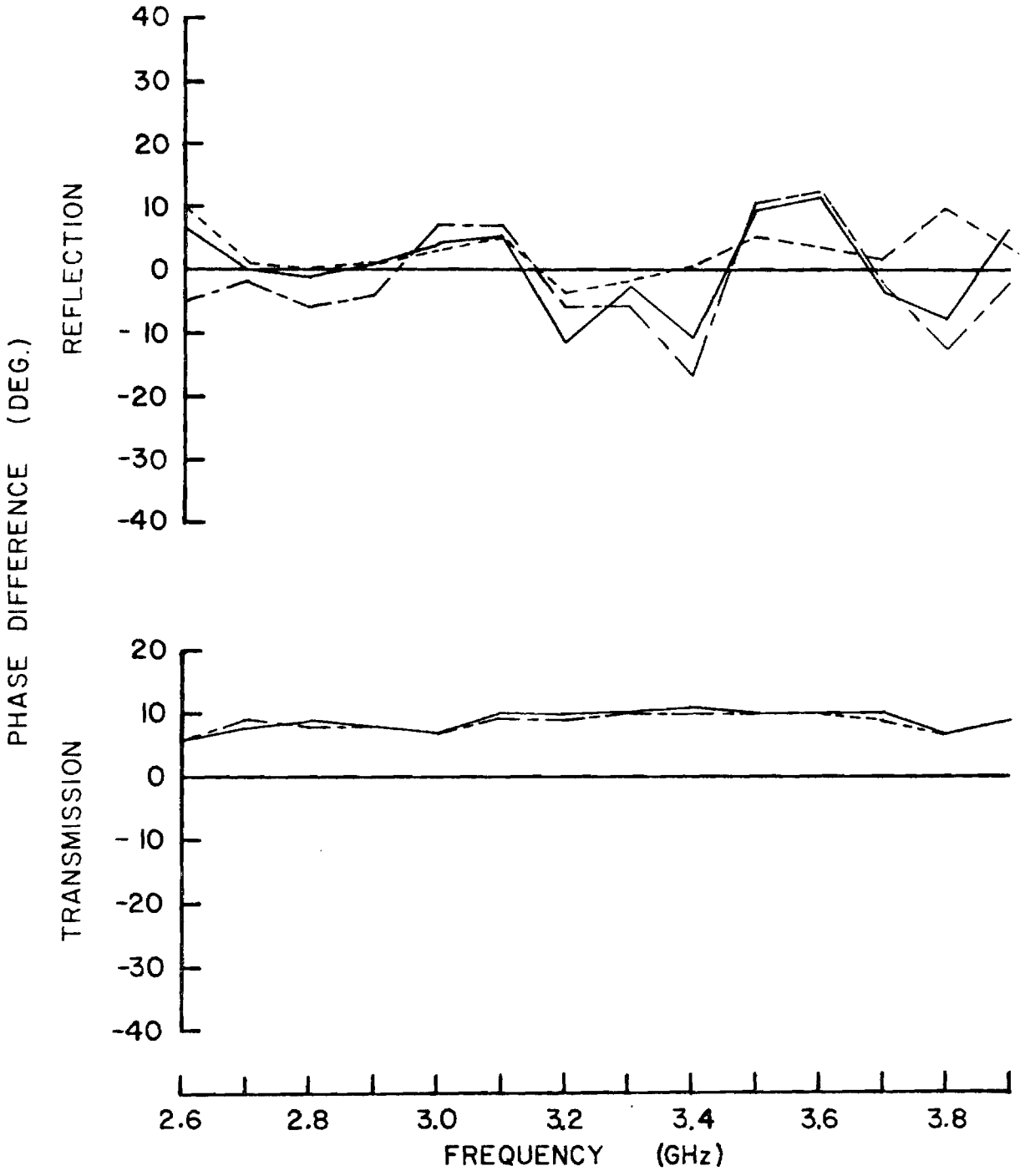

Figure 29. Phase shift of reflection (upper) and transmission (lower) coefficients with insertion of the sample for the frequency range 2.6 to 3.9 GHz. The broken lines are for position 1; the solid lines, position 2; and the dashed lines, position 3.

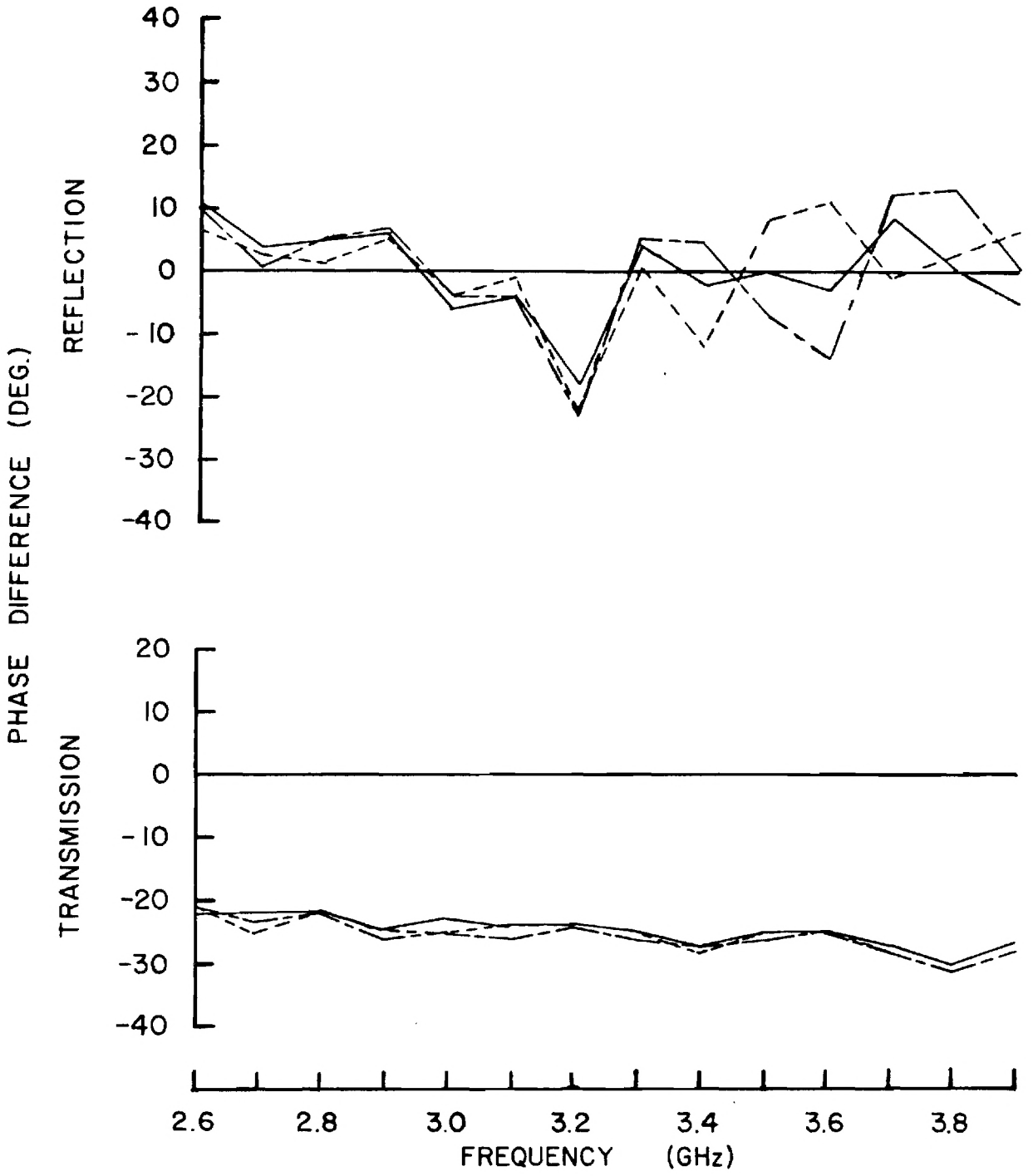

Figure 30. Phase shift of reflection (upper) and transmission (lower) coefficients with insertion of the sample for the frequency range 2.6 to 3.9 GHz. The broken lines are for position 4; the solid lines, position 5; and the dashed lines, position 6.

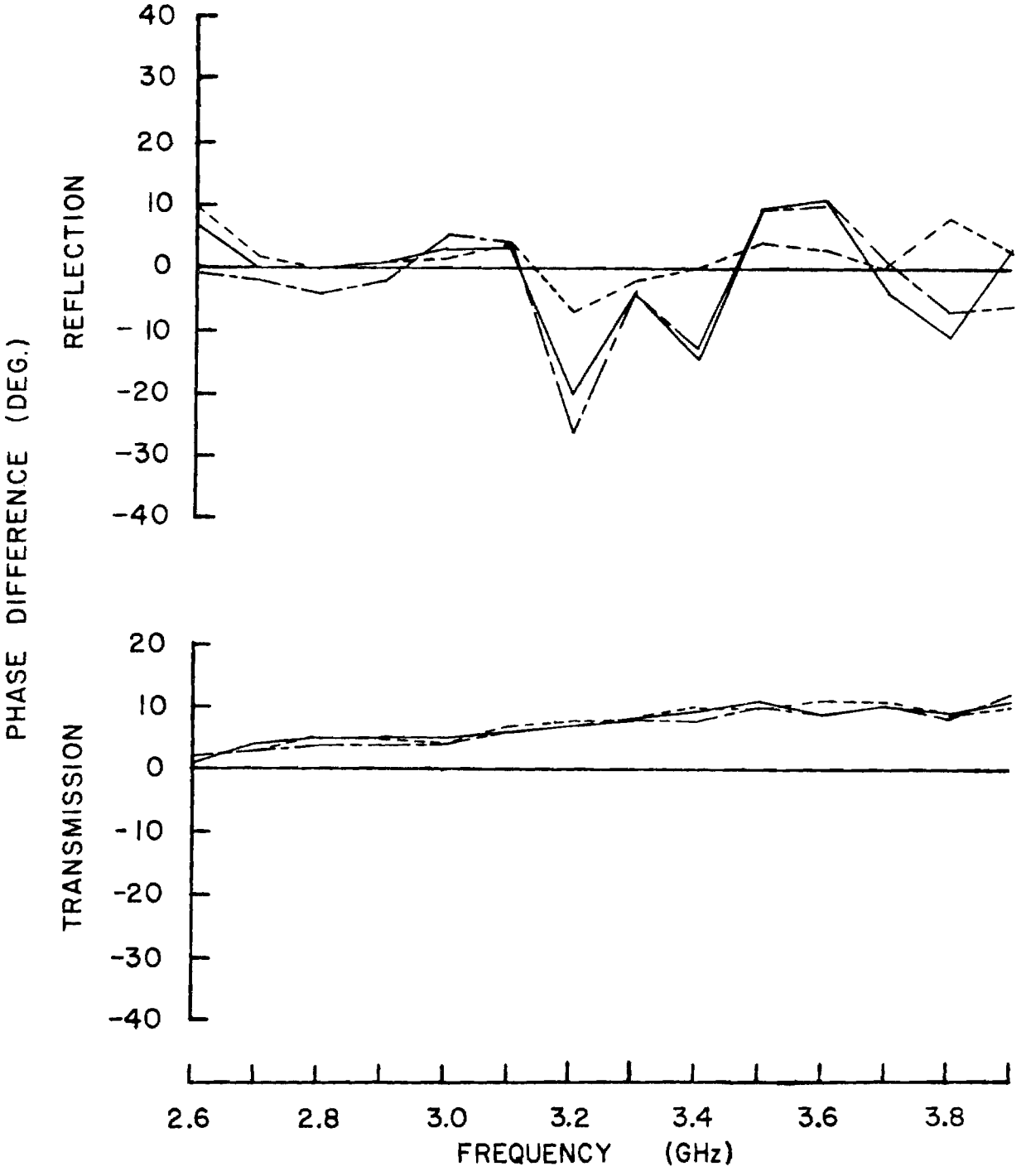

Figure 31. Phase shift of reflection (upper) and transmission (lower) coefficients with insertion of the sample for the frequency range 2.6 to 3.9 GHz. The broken lines are for position 7; the solid lines, position 8; and the dashed lines, position 9.

for the side positions being $+6^{o}$ and the value for the central positions being -25^{o}. Phase shifts for the reflected signals also shown in Figures 29 through 31 were less uniform showing fluctuations of -20^{o} to $+10^{o}$.

C. Conclusion

A comparison of the signals showed that a more uniform behavior was displayed by transmitted signals. This can be qualitatively explained by noting that reflections from interfaces are capable of setting up complex standing wave patterns which give sharp changes in reflection coefficients as a function of position and frequency whereas propagation through the sample has an integrating effect on transmission coefficients. This behavior is also displayed in the multi-layered model calculations presented in the Second Quarterly Technical Report.

Comparison of results from the two frequency ranges showed the higher band to produce more uniform behavior. This was most likely due to the sample being more deeply into the near field for the lower range such that position had a sharper influence upon signals.

One surprising aspect of the data was the almost flat frequency response for the transmission phase shift in a given frequency band. This was in contrast to the multi-layered model which had a periodic frequency response. This difference in behavior may be explained by the smaller relative cross section of the scattering object causing only a minor perturbation in the received signal. The difference in the two ranges, -15^{o} for 1.8 - 2.6 GHz and -25^{o} for 2.6 - 3.9 GHz, indicated that antenna geometry may have influenced this signal.

Another facet of the data was the dependence of the transmitted signal upon the lateral position of the scatterer. This indicated that there may be some ability to scan the contents of a suitcase in order to detect the location of agricultural products.

D. Future Investigations

From the above conclusions, this approach might best be pursued by coarsely imaging the suitcase contents utilizing transmitted signal information. A detailed imaging approach is already under development

[6] for biomedical applications in which the sample is immersed in water to reduce the wavelength in order to enhance resolution and to avoid large reflections from an air-tissue interface. Because of high attenuation in the water and sample, that study has been limited to frequencies of about 3.5 GHz. For the case of fruit in a suitcase, however, reflections at the suitcase-air interface should not be too large and attenuation not as much of a problem because of the small thickness of typical scattering objects. Since detailed resolution is not a necessity (5 cm should be sufficient), a frequency of 6 to 10 GHz would seem appropriate for this kind of imaging. It is anticipated that the range of about 6 to 10 GHz will be explored in the next quarter.

VI. SHORT PULSE RADAR APPROACH

As outlined in the Second Quarterly Technical Report, a Short Pulse Radar (SPR) may be useful in detecting fruit within baggage. This type of radar emits a very brief pulse of electromagnetic energy which is directed toward the material to be interrogated. The received signals, or returns, resulting from reflections at material interfaces are displayed as voltage versus time. Delays between the transmitted and received signals are typically on the order of a few nanoseconds and can be translated into distance by using the propagation velocity in the materials interrogated.

The SPR has previously been used to obtain profiles of underground strata and locate buried objects, as reviewed in the Second Quarterly Technical Report. This situation is similar to that of objects "buried" in a suitcase. To explore more fully the potential of SPR to detect fruit in baggage, discussions were held with personnel of the Radar Applications Division. This division of the Radar and Instrumentation Laboratory of Georgia Tech's Engineering Experiment Station had used SPR to detect buried objects and subsurface voids [7,8]. From these discussions, it was concluded that SPR had enough promise as a detector of agricultural products to warrant some actual measurements to check the feasibility of this approach.

The SPR measurements were begun during this reporting period and preliminary results have shown that SPR may be a useful detector of fruit. The experimental measurements involved burying tangerines, oranges, or grapefruit in sand and recording the SPR return for each condition. This situation was adopted to conform with the operation of existing SPR equipment. It was electromagnetically similar to a citrus fruit located in a filled suitcase since the relative dielectric constant of the sand was approximately 3.6, not much greater than the value of 2 to 3 expected for clothing and plastics in a suitcase.

In the preliminary measurements, there were indications of SPR returns being modified by the presence of fruit. As was evident in those measurements, SPR could detect fruit buried 9 inches deep in the sand and had

the additional advantage of providing range (depth) information. These measurements are continuing and the results will be reported fully in the Final Technical Report.

VII. PLANS FOR NEXT QUARTER

Research planned for the next three months of this project is based on findings of the first nine months' efforts. During the next quarter, approaches to the electromagnetic detection of agricultural products in travelers' baggage will be pursued further. Efforts to be undertaken for each approach are described below.

A. Capacitor Plate Approach

For the capacitor plate approach, attention will be directed to using smaller plates. This should increase the spatial resolution capability for this approach and allow a practical array of plates to be designed. The use of an array of plates will be investigated and the possible application of guard rings to minimize the interaction of the fields between adjacent pairs of plates will be included. All configurations will be tested with only fruit between the plates and with a suitcase containing fruit between the plates.

B. Resonant Cavity Approach

For the resonant cavity approach, changes in cavity resonant frequency and Q factor will be further investigated. Of primary interest is the effect of a suitcase and normal suitcase contents on these parameters since detection of fruit in baggage is the critical test of an approach. Preliminary observations with simulated suitcase contents in the cavity indicate a large reduction in sensitivity. These results will be further checked; however, if suitcase contents do cause a large enough reduction, this approach will not be feasible.

C. Signal Transmission/Reflection Approach

For the signal transmission/reflection approach, more data will be obtained for the magnitude and phase changes in the signals reflected from and transmitted through fruit. Emphasis will be placed on higher frequencies than have so far been employed. Results will be obtained for fruit alone and for fruit inside a suitcase.

D. Short Pulse Radar Approach

For the short pulse radar approach, the data obtained for fruit buried in sand will be completely analyzed. Because of the potential of this approach to provide accurate fruit presence and location information, it is anticipated that measurements will be made for fruit inside a suitcase otherwise filled with clothing. These various results will indicate the feasibility of the short pulse radar approach.

VIII. REFERENCES

1. E. C. Burdette, F. L. Cain, and J. Seals, In-Vivo Determination of Energy Absorption in Biological Tissue, Final Technical Report, Project A-1755, U.S. Army Research Office, Grant No. DAAG29-75-G-0182, January, 1979.

2. E. C. Burdette, F. L. Cain, and J. Seals, In-Vivo Probe Measurement Technique for Determining Dielectric Properties at VHF Through Microwave Frequencies, IEEE Trans. Microwave Theory Tech. 28: 414-427, 1980.

3. K. R. Foster, J. L. Schepps, R. D. Stoy, and H. P. Schwan, Dielectric Properties of Brain Tissue between 0.01 and 10 GHz, Phys. Med. Biol. 24: 1177-1187, 1979.

4. A. W. J. Dawkins, C. Gabriel,R. J. Sheppard, and E. H. Grant, Electrical Properties of Lens Material at Microwave Frequencies,Phys. Med. Biol. 26: 1-9, 1981.

5. C. G. Montgomery, R. H. Dicke, and E. M. Purcell, Principles of Microwave Circuits, Dover Publications, New York, 1965, pp. 387, 391.

6. J. H. Jacobi and L. E. Larsen, Microwave Time Delay Spectroscopic Imagery of Isolated Canine Kidney. Med. Phys. 7: 1-7, 1980.

7. J. D. Echard, J. A. Scheer, E. O. Rausch, W. H. Licata, J. R. Moore, and J. A. Nestor, Radar Detection, Discrimination, and Classification of Buried Non-Metallic Mines , Final Technical Report for U.S. Army Mobility Equipment Research & Development, Contract No. DAAG54-76-C-0112, Georgia Tech Project A-1828, February 1978.

8. J. R. Moore and J. D. Echard, Radar Detection of Voids Under Concrete Highways, Final Technical Report, Georgia Department of Transportation, Georgia Tech Project A-2107, May 1978.

INTERIM TECHNICAL REPORT
PROJECT A-2673

ELECTROMAGNETIC DETECTION OF AGRICULTURAL PRODUCTS IN TRAVELERS' BAGGAGE

By
R. L. Seaman and M. L. Studwell

Prepared for
U.S. DEPARTMENT OF AGRICULTURE
SCIENCE AND EDUCATION ADMINISTRATION
AGRICULTURAL RESEARCH - SOUTHERN REGION
701 LOYOLA AVENUE
NEW ORLEANS, LOUISIANA 70153

Under
Research Agreement No. 53-7B30-0-247

AUGUST 1981

GEORGIA INSTITUTE OF TECHNOLOGY
A Unit of the University System of Georgia
Engineering Experiment Station
Atlanta, Georgia 30332

1981

ELECTROMAGNETIC DETECTION OF AGRICULTURAL PRODUCTS IN TRAVELERS' BAGGAGE

Interim Technical Report

Project A-2673

August 1981

Under
Research Agreement No. 53-7B30-0-247

By
R. L. Seaman and M. L. Studwell

Prepared for

U.S. Department of Agriculture
Science and Education Administration
Agricultural Research - Southern Region
701 Loyola Avenue
New Orleans, Louisiana 70153

By

BIOMEDICAL RESEARCH DIVISION
Electronics and Computer Systems Laboratory
Engineering Experiment Station
Georgia Institute of Technology
Atlanta, Georgia 30332

FOREWORD

Research during this reporting period was performed by personnel of the Biomedical Research Division of the Electronics and Computer Systems Laboratory of the Engineering Experiment Station at the Georgia Institute of Technology, Atlanta, Georgia. This project is sponsored by the Science and Education Administration of the U.S. Department of Agriculture, New Orleans, Louisiana, under Research Agreement 53-7B30-0-247 and has been assigned Georgia Tech Project No. A-2673. This report summarizes efforts carried out from 1 March 1981 through 31 July 1981.

Dr. R. L. Seaman served as Project Director. Mr. M. L. Studwell performed the experiments on the resonant cavity approach and on the capacitor plate approach. Dr. A. R. Moser performed the experiments on the signal transmission/reflection approach. Mr. R. M. Kobert assisted in several aspects of the technical efforts.

Respectfully submitted,

Ronald L. Seaman,
Project Director

Approved:

J. C. Toler, Manager
Biomedical Research Division

TABLE OF CONTENTS

LIST OF FIGURES

LIST OF FIGURES

Continued

LIST OF TABLES

I. INTRODUCTION

The goal of this project is to identify an electromagnetic method for detecting agricultural products (fruits, vegetables, and meats) in closed baggage. Such a method of inspecting baggage would greatly assist the Animal and Plant Health Inspection Service (APHIS) in detecting agricultural products brought into this country by international travelers. A division of the Department of Agriculture (USDA), APHIS is charged with the interception of prohibited agricultural products and products which are diseased or carry insect pests. Intercepted products which are diseased or infested are destroyed to prevent infestation of native plants and animals. Of course, agricultural products must be detected before they are inspected and possibly intercepted. Since not all products are declared by travelers, a noninvasive method of detecting the products in baggage would greatly facilitate the inspection process.

International travelers are questioned about agricultural products they are bringing into the country and, in some cases, their baggage is searched. Although these rules and procedures are well publicized[1] and are well known, travelers still attempt to bring illicit agricultural products through ports of entry. About 2% of international travelers declare possession of agricultural products. However, it is estimated by inspectors that many more actually bring in agricultural products. During occasional extensive searches, more than half of the baggage from an international flight is usually found to contain agricultural products. It is clear that noninvasive inspection of baggage would substantially increase the intercept rate of contraband products.

The objective of this research program is to study the feasibility of an electromagnetic device to detect fruits, vegetables, and meats in closed baggage. Electromagnetic detection methods are based on the differences between dielectric properties of agricultural products and those of other baggage contents. The following four approaches have been investigated:

- capacitor plate,
- resonant cavity,
- signal transmission/reflection, and
- short pulse radar.

Results of previous investigations on this program have been presented in Quarterly Technical Reports Nos. 2 and 3. During this reporting period, significant progress has been made on each approach. Measurements on a capacitor plate array are presented in Section II. Measurements obtained from the resonant cavity and signal transmission/reflection approaches are presented in Sections III and IV, respectively. Results from the short pulse radar approach are given in Section V. Conclusions based on the results to date and recommendations for further research are made in Section VI.

II. CAPACITOR PLATE APPROACH

Work on this approach performed during the first three quarters of this program focused on the response characteristics of a single pair of plates. Studies performed during the current reporting period were directed toward designing a prototype multiple-plate array and measuring the array's response to a suitcase with and without fruit present. In addition, the response characteristics of two sizes of array elements were examined, as well as the effectiveness of a guard ring.

A. Array Design

The design of a multiple-plate array required that array size, element size and spacing, and guard ring dimensions be specified. Each element of an array consisted of a pair of parallel metal plates forming a capacitor. In some cases, one plate was large enough to act as a second plate for several array elements. Initial studies on guard rings were made using two plates and a guard ring with the set up described in Quarterly Technical Report No. 3. Measurements of plate impedance with a beaker of saline inserted as a target showed that although a guard ring would help produce a more uniform field in the area under the array elements, the electric field lines were distorted by the target so that the impedance change versus target displacement still showed a "fringing" response. Figure 1 illustrates the electric field line configurations for empty plates and for plates with a spherical fruit-like object between them. The object tends to "pull in" the field lines and when the plate is small enough or the object is close to a plate edge, field lines from an adjacent pair of plates are affected. This resulted in an effective fringing for the adjacent array element and was measured as a change in impedance. This effect produced the bell shape curves of impedance change versus target displacement presented in Quarterly Technical Report No. 3.

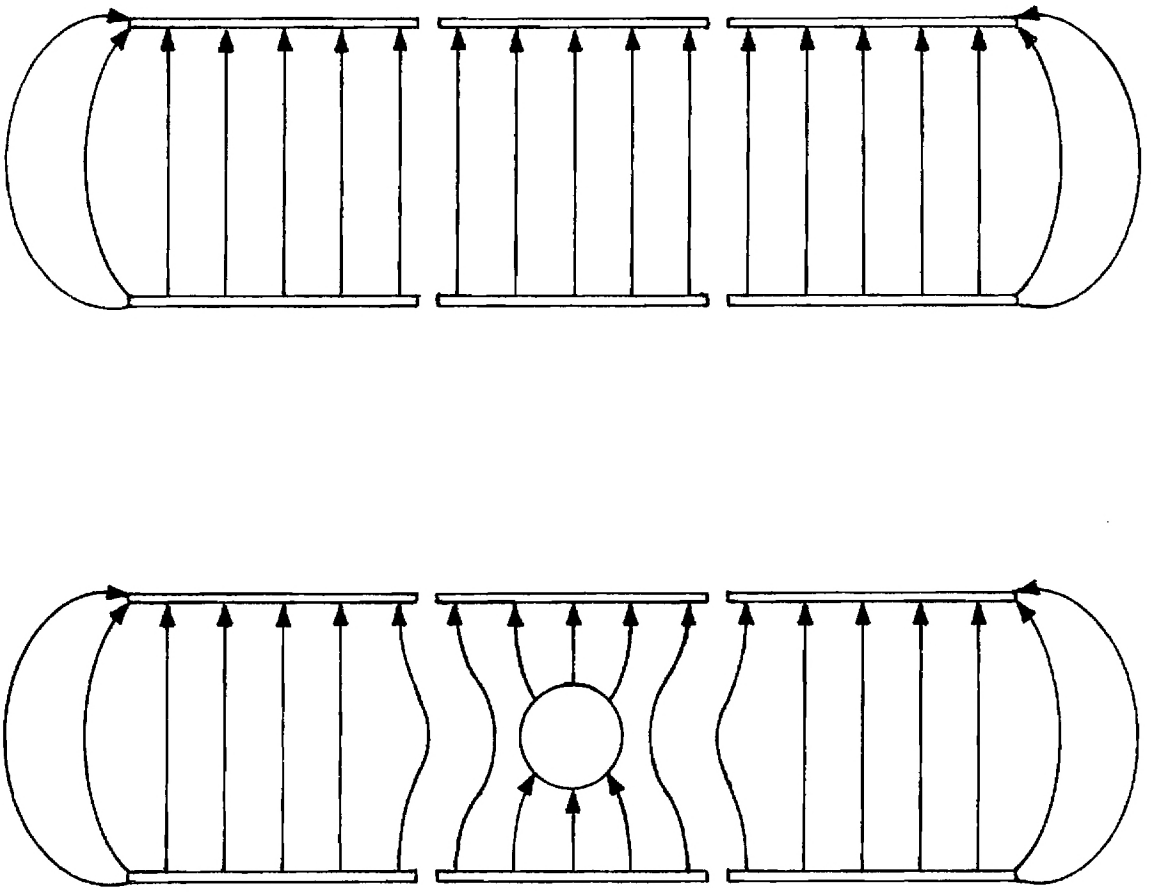

Figure 1. Electric field lines between capacitor plates with and without fruit present. Shows effective "fringing" in adjacent pairs of plates due to fruit.

Calculations based on field equations describing the fields surrounding a solid dielectric sphere and a metal sphere in a uniform electric field showed that the distortion by the target was small beyond two radial distances from the center of the sphere. In addition, it was found that dielectric spheres introduced very nearly the same field distortions as metal spheres when the relative dielectric constant was greater than 5. Even dielectric constants of 2 and greater exhibited substantial field distortion. However, it was noted that, although the spatial distribution varies little with small dielectric constant, the relative impedance change will vary substantially with dielectric constant. Metal objects would cause impedance changes similar to those caused by objects with a high dielectric constant.

Measurements had shown that an array element which was similar in size to a target's cross sectional area would exhibit a larger relative change in impedance than a larger element. However, array element impedance increased proportionally as element area decreased creating measurement difficulties. A trade-off between sensitivity and measurement capability resulted in prototype array elements of 6 inches by 6 inches, corresponding to roughly twice the diameter of apples which were selected as trial targets. This size also provided an element large enough to support nearly all electric field lines passing through a centered apple.

As reported in the analysis in Quarterly Technical Report No. 2, air gaps between the plates and target decreased sensitivity by effectively inserting large impedances in series with the small impedance of the target. Therefore, the prototype was designed so that the plate separation could be adjusted to allow positioning of the plates close to the sides of the baggage.

As stated before, the target distorted the field between an element's plates and produced an equivalent "fringing" in adjacent elements. A guard ring can be used to avoid fringing distortion of the field at the edges of the measurement volume. A guard ring configuration was installed on the prototype to help make element

responses uniform with respect to their distance from the array border. The guard ring was not expected to change the "fringing" phenomenon caused by the target's distortion of the electric field lines. It was decided to maintain initial field uniformity by driving all array elements and the guard ring at the same voltage. With the elements at the same voltage, stray coupling between elements was minimized by the reduction in plate-to-plate current flow.

As described in Quarterly Technical Report No. 2, element (capacitor) impedance was inversely proportional to frequency. Frequencies in the range of 1 to 5 MHz were chosen to drive the array so that element impedances would be low enough to be conveniently measured. Resonance in the cables to the array was not a factor at these frequencies.

The array was designed and constructed as shown in Figure 2. An array of 24 6-inch by 6-inch metal plates and surrounding 6-inch guard plates were supported on a sheet of 1/2-inch plywood. These plates formed the top of a 6 by 4 element array of capacitors. Each plate was insulated from adjacent plates so that each element's current could be measured individually. A single 36-inch by 48-inch plate was fastened to another 1/2-inch sheet of plywood to which four Plexiglas support rods were attached to serve as the bottom of the prototype array. The support rods had a series of holes so that pins could be inserted to hold the top array at plate separations from 4-1/2 to 14-1/2 inches in 1-inch increments. The top plates were each connected by a separate length of wire to a common tie point to which the guard ring plates were also connected. The connection at each top array plate was made by a tip plug so that a current probe could easily be inserted in series with each array element. The array and guard ring plates were connected to the signal generator ground and the large bottom plate was connected to the high side of the generator. The array was grounded to minimize current measurement errors due to stray reactive coupling to shields on the current probe leads. The electrical configuration of the array is pictured in Figure 3.

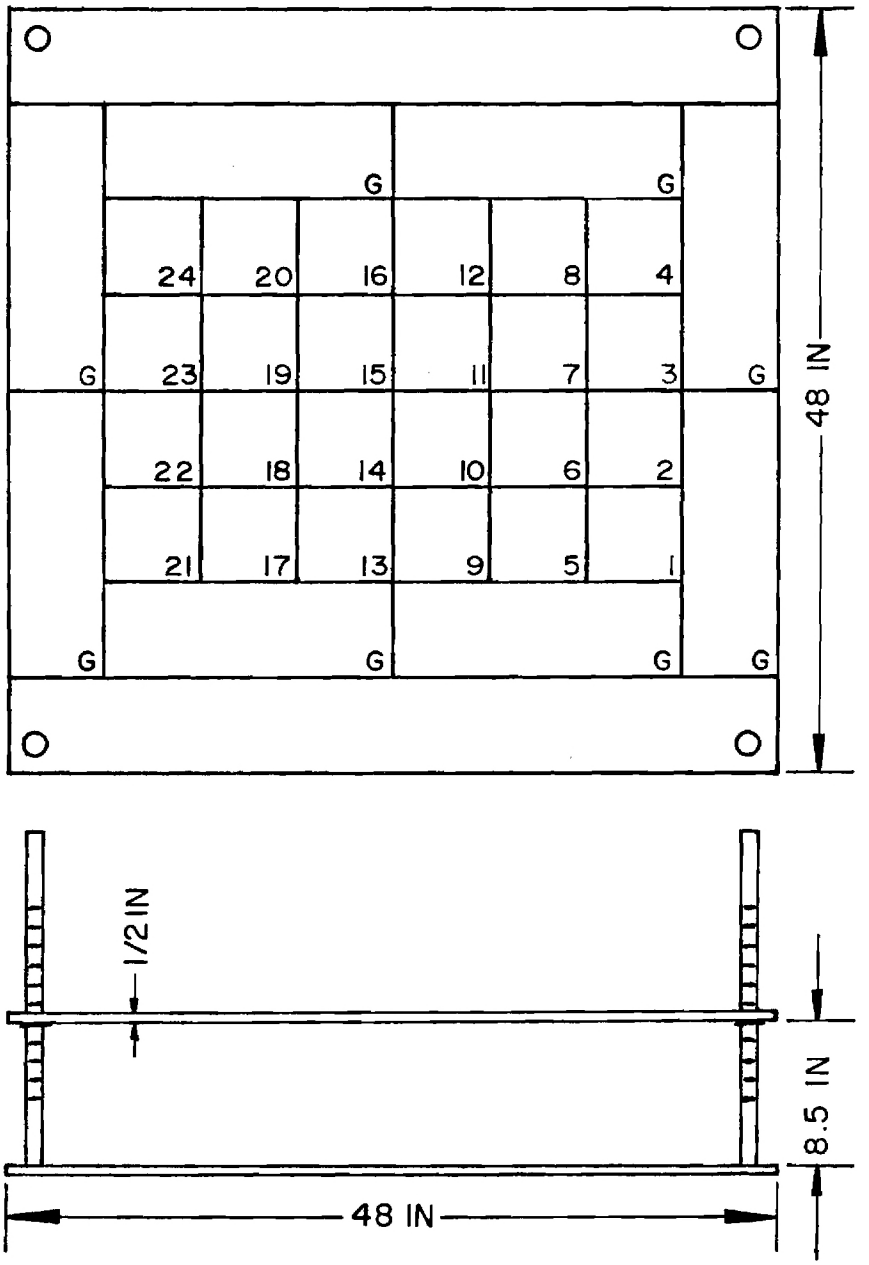

Figure 2. Top and side views of the capacitor plate array. Shows layout of capacitor plates (with numbers) and guard ring plates (G).

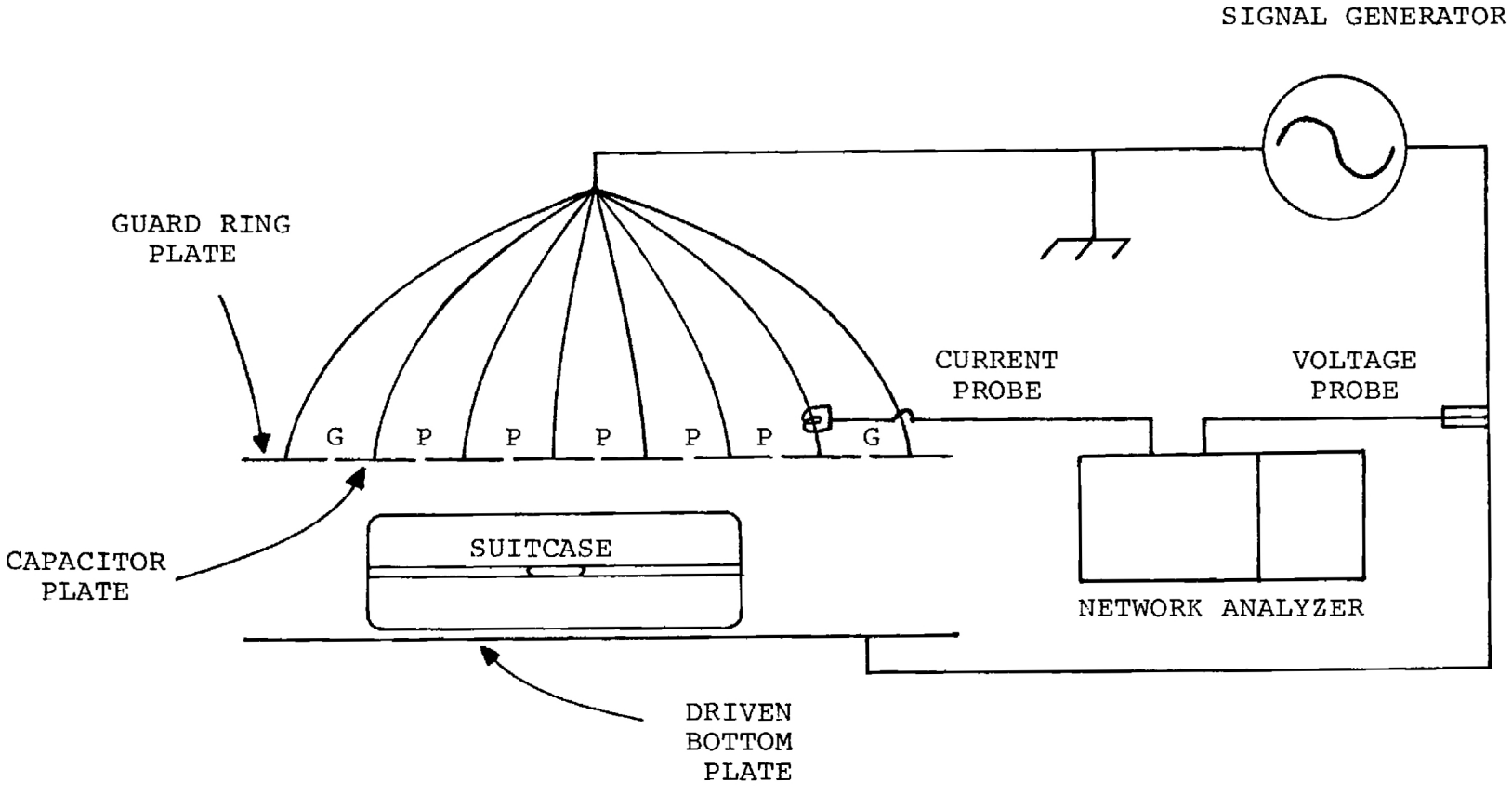

Figure 3. Electrical connections for capacitor plate array.

Features of this prototype design were as follows:

- The plate separation was made variable to permit optimum sensitivity for a given baggage size.
- The plate size allowed maximum sensitivity for measurable impedances.
- A guard ring was employed to help maintain a uniform field configuration.
- All array elements were operated with the same potential between top and bottom plates.

B. Measurements

Measurements were first performed using a configuration similar to that in Figure 10 of Quarterly Technical Report No. 3 with the addition of another 6-inch by 6-inch capacitor plate and 6-inch guard ring plates on the top of the plywood box. Measurements taken with this configuration confirmed that the guard ring, although helping eliminate non-uniform field effects at the sensing plate edges, would not significantly reduce the sensing of the target beyond the plate edges caused by field distortion by the target. Figure 4 shows typical results which, like all results in this section, are expressed as changes in impedance relative to empty plates.

Measurements were then made on a pair of 3-inch by 3-inch plates with a 6-inch guard ring in the same setup as above to give the results shown in Figure 5. The frequency was increased to 10 MHz to provide a lower, more conveniently measured impedance. The relative impedance changes were on the order of twenty times greater with the 3-inch plates than those measured with the 6-inch plates. Ten megahertz was approximately the highest frequency which could be used without resonance problems due to the cabling and measurement configuration.

After design and construction of the prototype capacitor array, measurements were performed on a typical hardsided suitcase packed with clothes and with different numbers of apples. Some of the results of these measurements are depicted in Figures 6, 7 and 8. The measurements showed that the suitcase with clothes caused a substantial

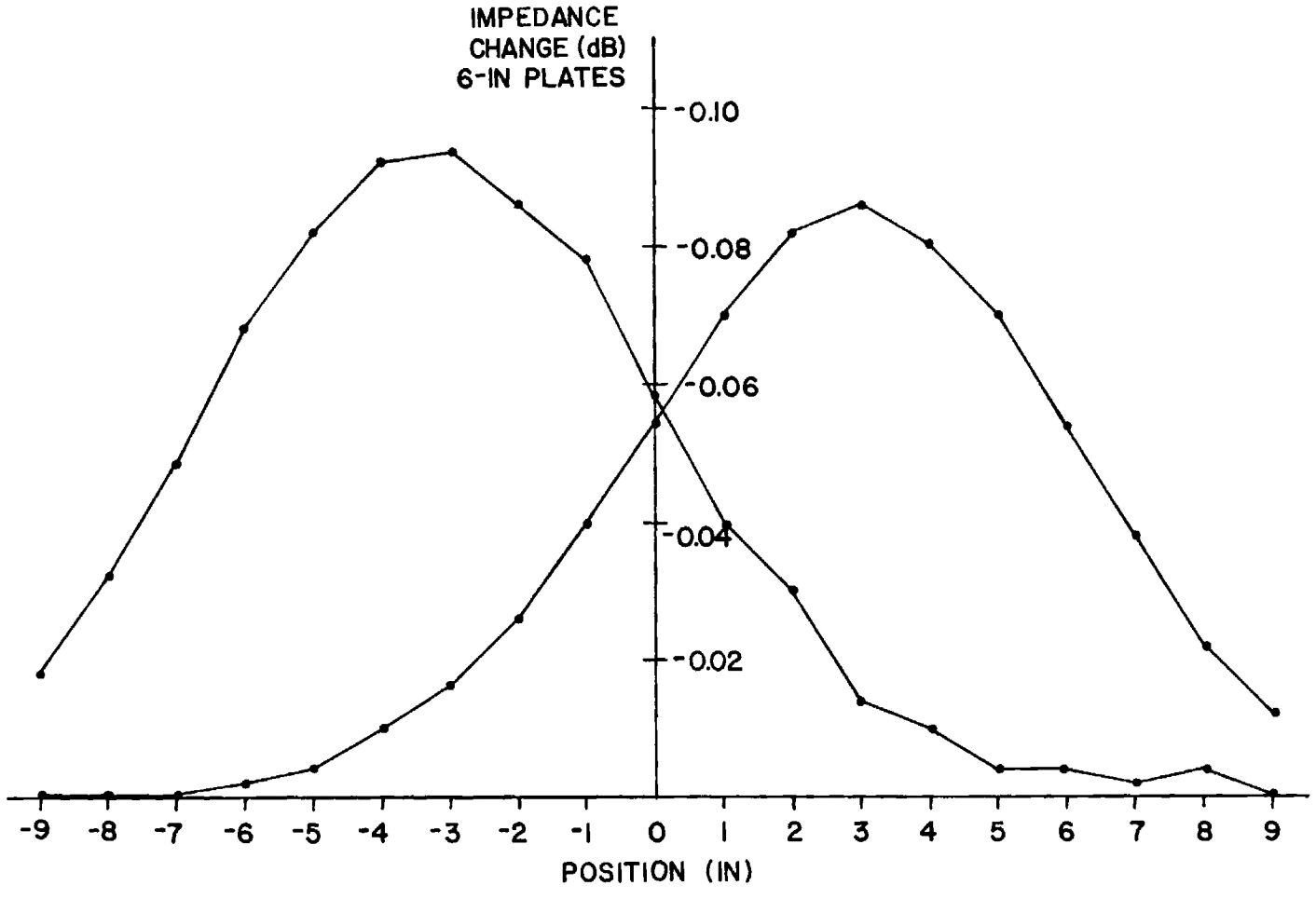

Figure 4. Impedance changes for two pairs of guarded 6-inch plates versus sample position. Plates were between positions -6 and 0 and 0 and 6. Sample was 250 ml of saline. Frequency was 5 MHz.

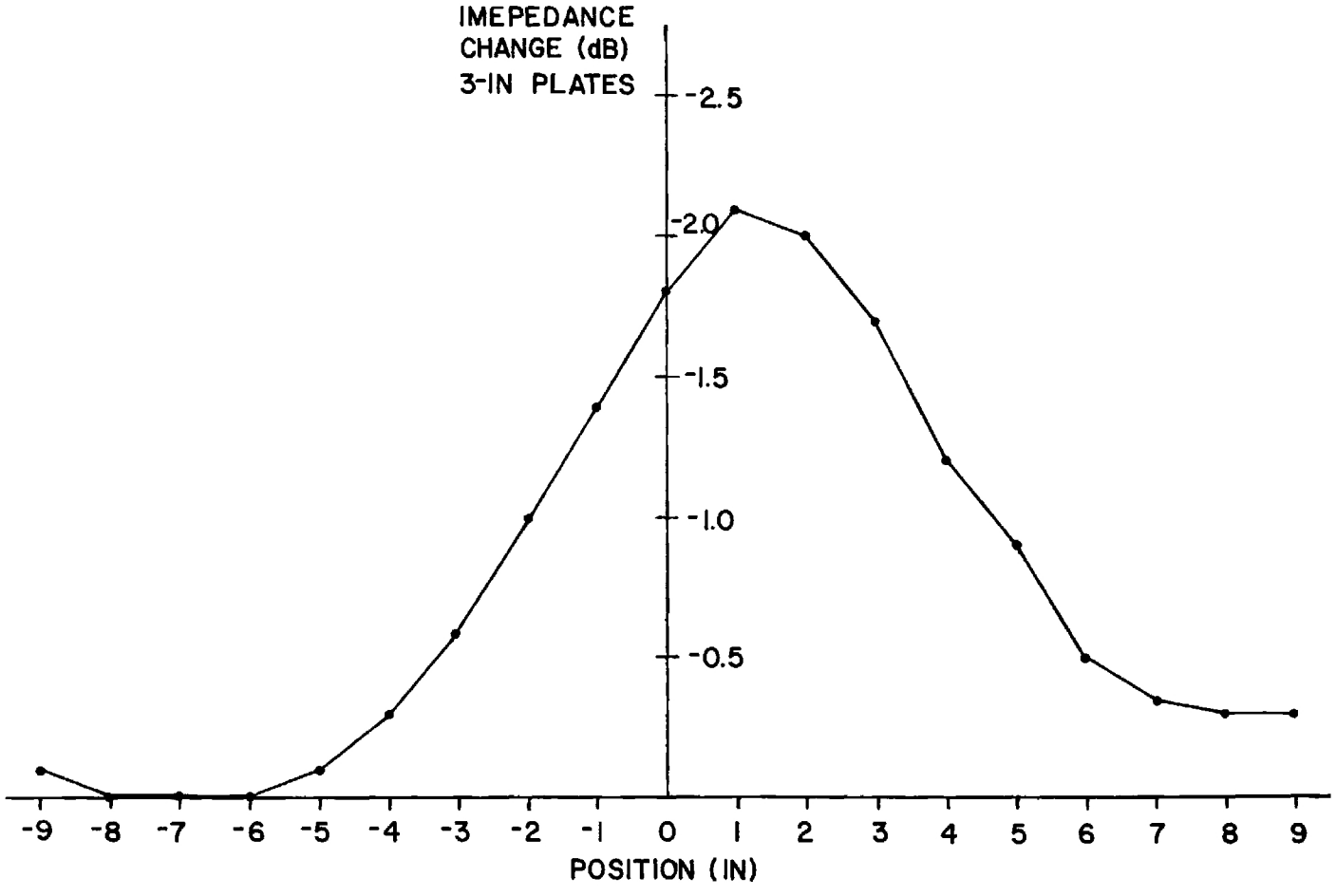

Figure 5. Impedance changes for one of two pairs of guarded 3-inch plates versus sample position. Plates were between positions -3 and 0 and 0 and 3. Sample was 250 ml of saline. Frequency was 10 MHz.

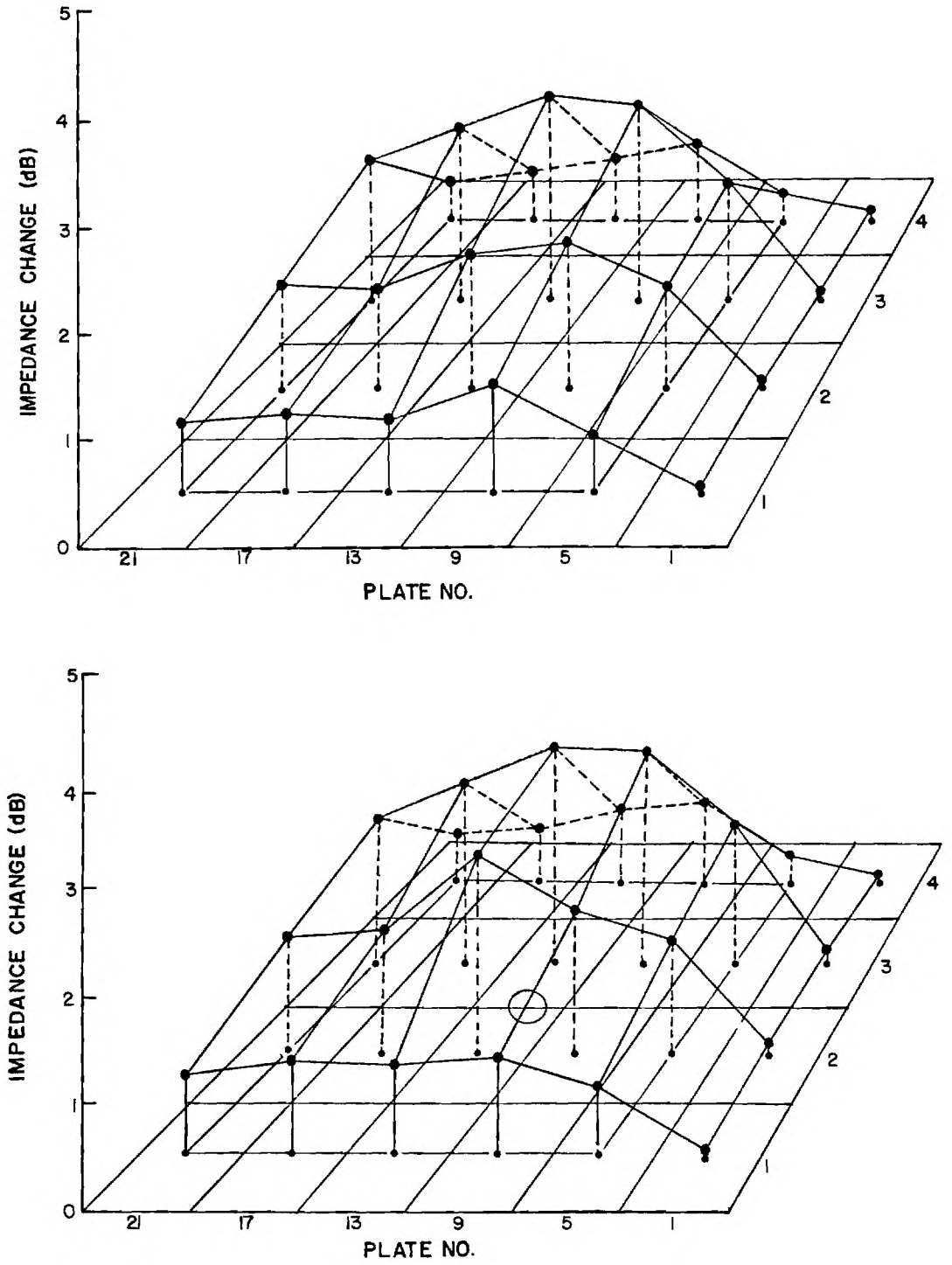

Figure 6. Contours of impedance changes for capacitor plate array: suitcase with clothes and suitcase with clothes and 1 apple. Suitcase corners under plates 5, 8, 21, and 24, as outlined. Apple indicated under plates 14 and 15.

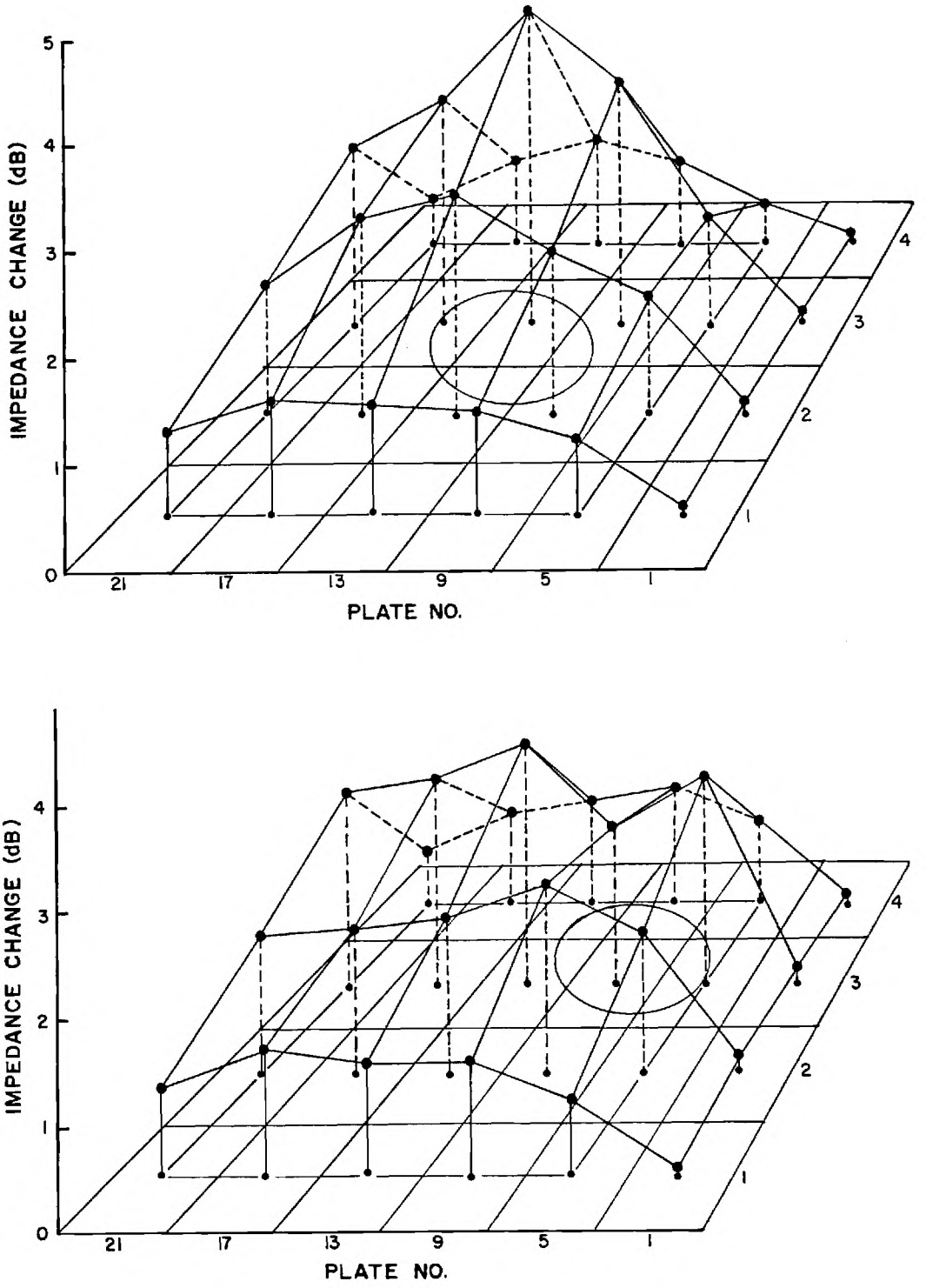

Figure 7. Contours of impedance changes for capacitor plate array: suitcase with clothes and 5 apples. Suitcase corners as in Figure 6, as outlined. Apple locations indicated by ovals at center of suitcase (top) and at corner of suitcase (bottom).

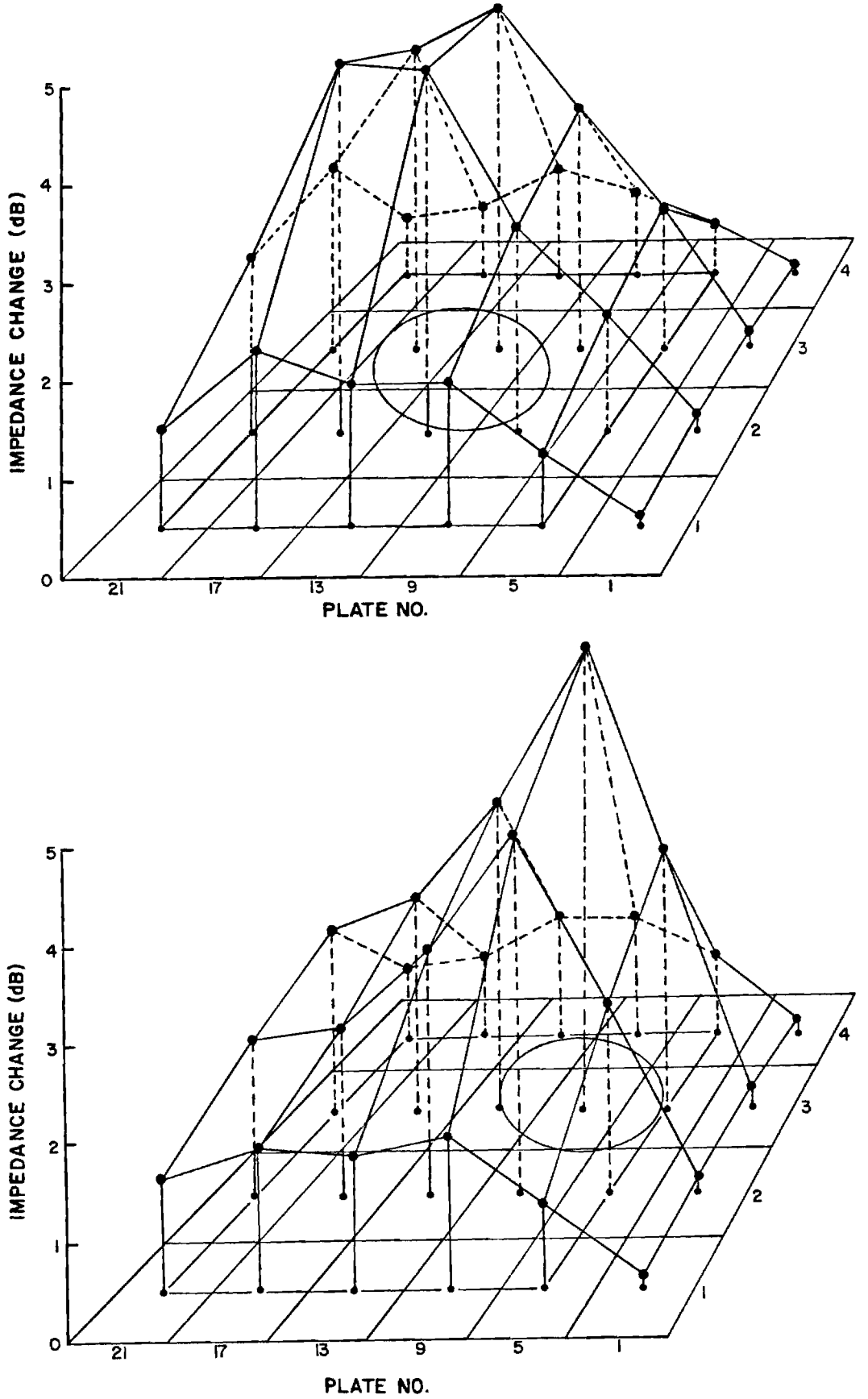

Figure 8. Contours of impedance changes for capacitor plate array: suitcase with clothes and 12 apples. Suitcase corners as in Figure 6, as outlined. Apple locations indicated by ovals at center of suitcase (top) and at corner of suitcase (bottom).

variation in impedance over the array. Since the relative impedance change caused by a single apple in the suitcase with clothes was approximately -0.7 dB and the average difference in relative impedance changes caused by the suitcase with clothes was approximately -1.5 dB, it was difficult to distinguish the presence of the apple without a priori knowledge of its existence (Figure 6). However, by comparing Figures 7 and 8 with the top of Figure 6, the presence of clusters of five and twelve apples can readily be seen. For each size cluster, larger impedance changes occurred when the cluster was placed in the center of the suitcase. The ridge along the center of the reference suitcase (Figure 6) was believed due to field distortion by a combination of the metal frame and the dielectric properties of the sides of the suitcase.

C. Conclusions

The capacitor plate array was shown to be capable of detecting the presence of moderate amounts of fruit in a typical piece of luggage. Its spatial resolution was limited by the size of plates which had to be used. The array has the potential that, with suitable electronic hardware, it could provide a simple yes-no indication signifying the probable presence of agricultural products suitable for unattended operation. The parallel plates also would provide a convenient configuration for feeding luggage through the detector. There may be a limited capability to discriminate between similar volumes of metal and agricultural products.

Further investigations would require the construction of an automated system so that array scanning may be accomplished quickly enough to allow examination of array response to more baggage and agricultural product combinations. The examination of more baggage configurations would be utilized in an attempt to maximize detection efficiency and establish performance characteristics for a prototype surveillance system which would require operator attention only for articles containing agricultural products.

III. RESONANT CAVITY APPROACH

The initial analyses and measurements presented in Quarterly Technical Report No. 3 examined the response of a cavity's resonant frequency and reflection coefficient as a function of the position of an apple target within the cavity. To assess the practicality of this approach further, measurements were performed to examine changes caused by suitcases and their contents and the potential for discriminating agricultural products from suitcase contents. Due to the high degree of mismatch with a suitcase in the cavity, measurements of transmission coefficient proved more practical than reflection coefficient.

A. Measurements

Measurements made during this reporting period produced data on the cavity response to insertion of a suitcase with clothing and on changes in target position. The results demonstrated the advantages of the TE_{101} mode over the TM_{110} mode and of transmission measurements over reflection measurements. Field configurations of these modes were described in Quarterly Technical Report No. 3.

Reflection coefficient measurements described in Quarterly Technical Report No. 3 were continued on the same cavity. All locations in the cavity were specified using the scheme given in Figure 16 of that report. A HP Network Analyzer System was used to display reflection coefficient amplitude and phase on a polar display for different objects in the cavity. It was discovered that insertion of a suitcase or a grapefruit caused a large impedance mismatch at resonance producing a large reflection coefficient at resonance. This was in contrast to the previously reported small reflection coefficient seen with an apple in the cavity. Because the cavity was normally mismatched at frequencies off resonance, a sharp change in reflection coefficient occurred at resonance with the apple, as shown in Figure 9, allowing rather precise determination of the resonant frequency. The resonant frequency of the cavity loaded with the suitcase or grapefruit was more difficult to measure accurately because changes in reflection coefficient were much smaller, as illustrated in Figure 9.

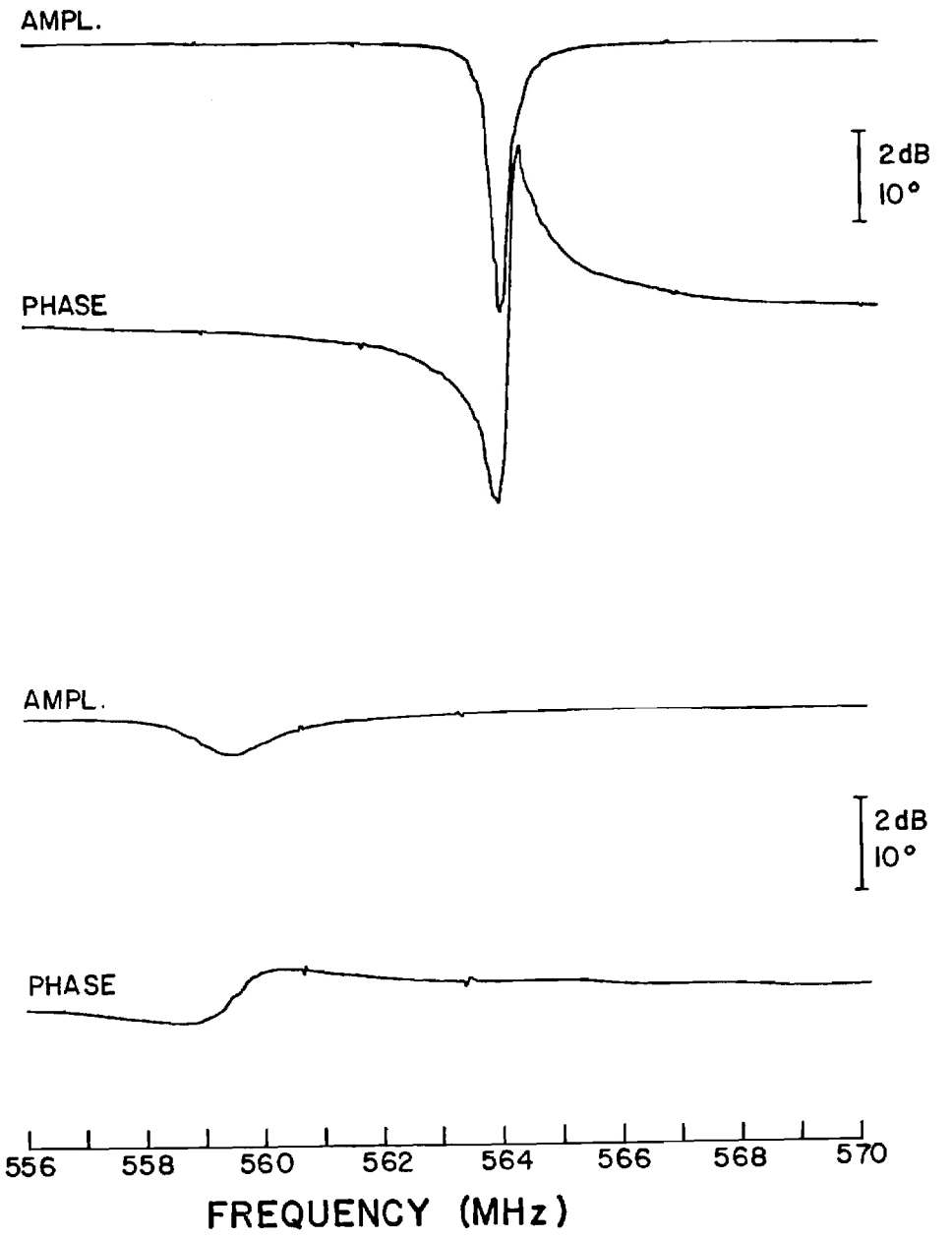

Figure 9. Reflected voltage signals for resonant cavity in TM_{110} mode showing resonance. Top two curves are for apple at (a/2, b/2, a/4); bottom two, for grapefruit at (a/2, b/2, a/4). Curves are representative of those seen for both modes.

Measurements of transmission coefficient were also made using the HP Network Analyzer System for both cavity modes. Instead of measuring the signal reflected from the cavity, the Analyzer measured the signal transmitted through the cavity. This signal was picked up by a receiving electric field probe installed in the cavity in addition to the probe which excited the cavity. Peak transmitted signal amplitude, related to cavity Q, was measured and referenced to transmitted signal amplitude for the empty cavity at resonance (0 dB). In the transmission measurements, it was much easier to measure resonant frequency because there was a large increase in power transmission at resonance compared to very small power transmitted off resonance. It was found in a few spot checks that the resonant frequency determined from a transmission measurement corresponded closely to that from a reflection measurement except for a small decrease in resonant frequency caused by the loading of the cavity by the receiving probe. After these checks for consistent results, only transmission measurements were subsequently utilized to facilitate measurements made with the suitcase.

The suitcase was a typical soft-sided one measuring 22 inches by 13 inches by 6 inches deep with a zipper closure. Three pairs of men's slacks and a T-shirt were used to pack the suitcase and were present for most measurements. To have information for more than one luggage shape, a briefcase was also used for some measurements. Figure 10 shows typical transmitted signal amplitude curves for the empty cavity and for the suitcase with clothes and an apple.

Figure 11 summarizes the results of transmission measurements made for the TE_{101} mode. It can be seen that the resonant frequency shift due to the apple is a small portion of the changes caused by the apple packed in the suitcase or briefcase. The resonant frequency consistently decreased with insertion of clothes and the apple as expected. The shift in resonant frequency due to the luggage with clothes was of the same order of magnitude as the shift due to the luggage with the apple. For the same suitcase location, there was a difference in resonant frequency shift with apple position in the suitcase with the largest shift caused by the apple at the center and the smallest shift by the apple at the corner. This variation

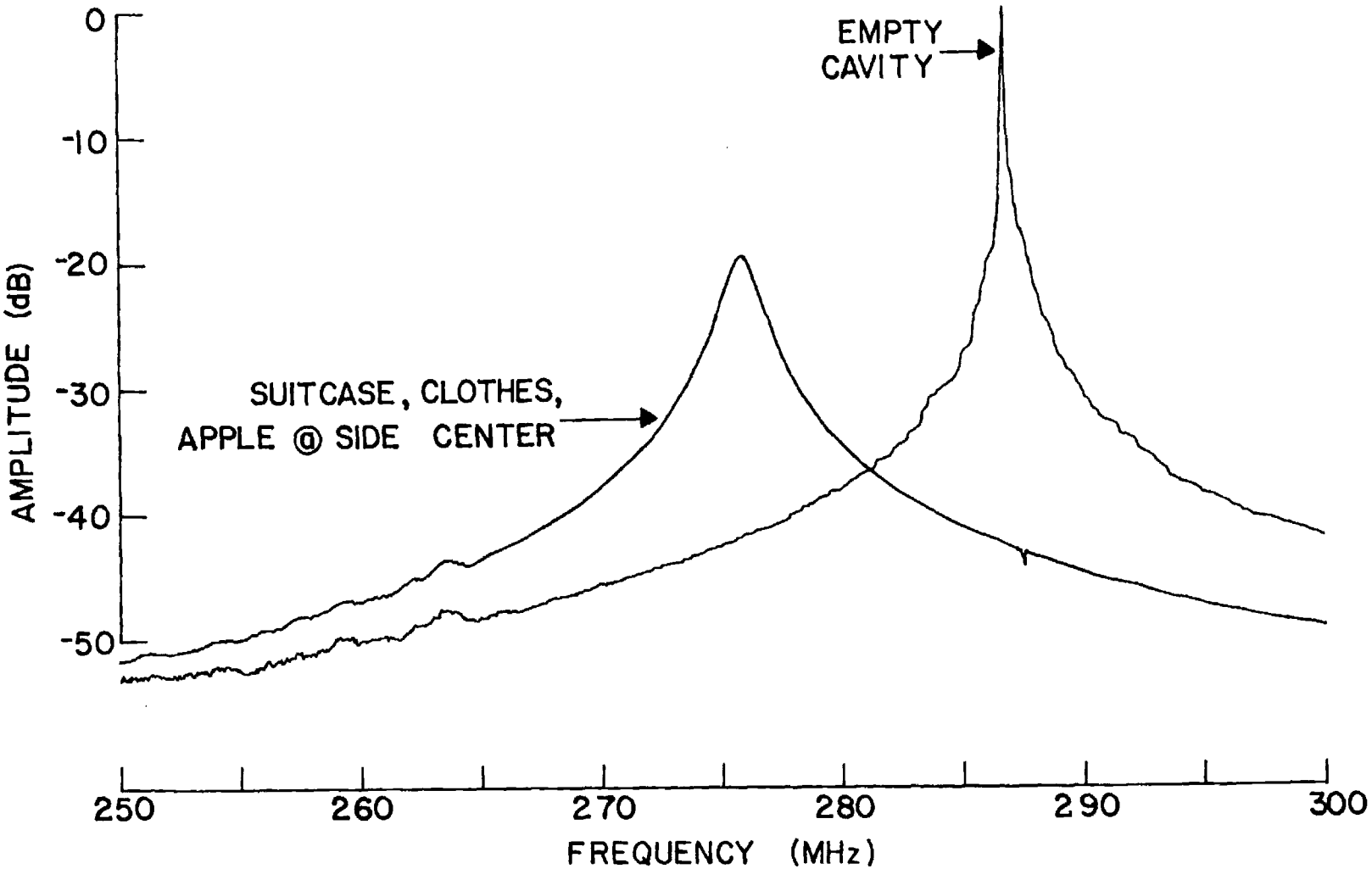

Figure 10. Transmitted signal amplitudes for resonant cavity operating in TE_{101} mode showing resonance.

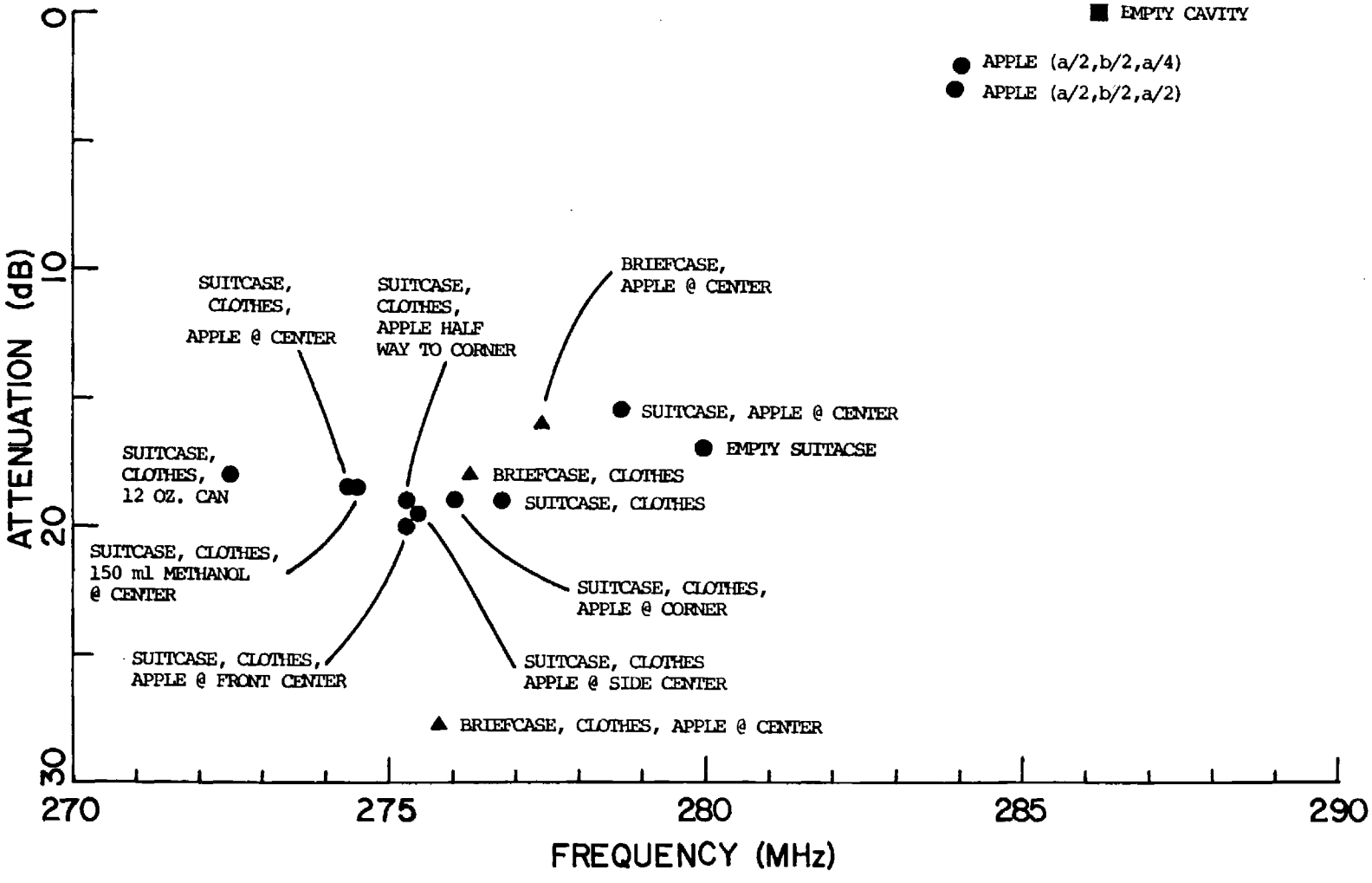

Figure 11. Summary of transmitted signal changes for TE_{101} mode of resonant cavity. Attenuation at resonance (referenced to empty cavity) versus resonant frequency for the indicated conditions.

corresponded to differences seen in measurements of the apple alone shown in Table I of Quarterly Technical Report No. 3. Simulated toiletry articles, a 12-ounce aluminum can, and a bottle containing 150 ml of methanol, caused resonant frequency shifts similar to and, in the case of the can, greater than that caused by the apple. Although the suitcase itself caused a pronounced attenuation in the transmitted peak signal, the addition of contents to the suitcase produced relatively little change in this parameter with no apparent pattern. It seemed, therefore, that the resonant frequency shift was the most useful information to be derived from the TE_{101} configuration.

Figure 12 summarizes transmission measurements made for the TM_{110} mode. Results obtained for the soft-sided suitcase were similar to those for the TE_{101} mode. The suitcase with clothes and apple caused a larger shift than did the suitcase with clothes. The shift for the suitcase with clothes was in turn larger than for the empty suitcase. The shift in resonant frequency for a 12-ounce aluminum can in a suitcase with clothes was very similar to the shifts for alcohol and for an apple in a similarly packed suitcase. Results using the hard-sided briefcase, which had a thick metal frame, are not shown in Figure 12, but alone it increased the resonant frequency to 568.31 MHz, above that of the empty cavity. Also, the briefcase with clothes or apple had a smaller resonant frequency shift than seen for the apple alone. This inconsistency in resonant frequency shift with suitcase construction along with a lack of pattern in transmission peak amplitudes indicated that the TM_{110} configuration would provide little information by itself or in tandem with the TE_{101} configuration.

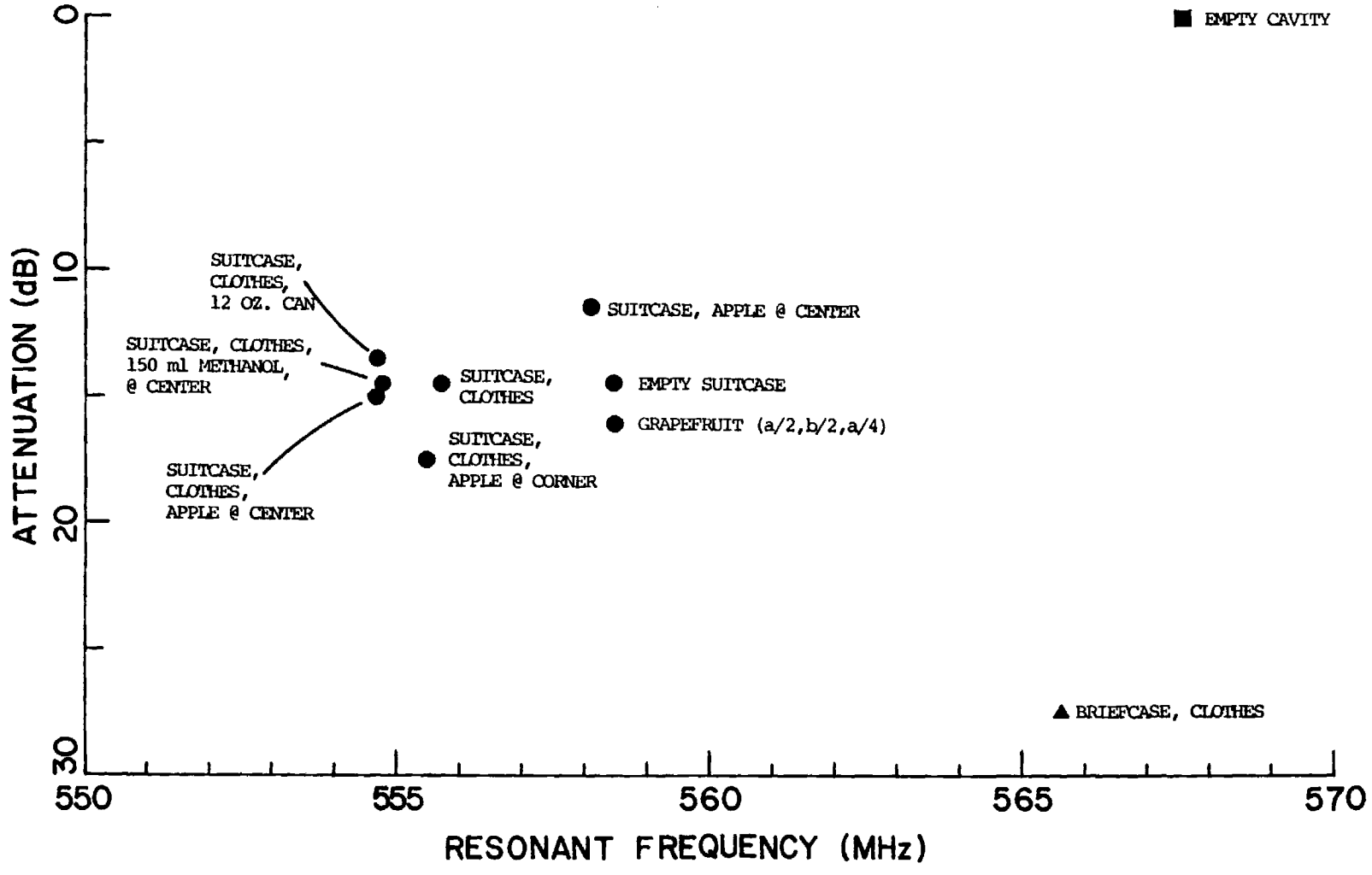

Figure 12. Summary of transmitted signal changes for TM_{110} mode of resonant cavity. Attenuation at resonance (referenced to empty cavity) versus resonant frequency for the indicated positions.

B. Conclusions

Of the two excitation configurations, the TE_{101} mode seemed to be the more promising. It appeared that a metal frame greatly perturbed the cavity's fields in the TM_{110} mode, as seen in the increase of resonant frequency with insertion of the empty briefcase while a decrease was seen with insertion of the suitcase. The frames, being roughly perpendicular to the TE_{101} fields, did not seem to perturb the TE_{101} fields to as great an extent, producing more predictable resonant frequency shifts. Resonant frequency shifts for the TE_{101} mode occurred in a fairly consistent fashion although the shifts due to the addition of a single apple were within the range of those which might normally be expected for typical baggage contents.

Transmission measurements proved more useful than reflection measurements because the change in reflection coefficient became very small when measuring the cavity loaded with a suitcase or a larger volume of agricultural product. Changes in transmission peak signal amplitudes with a suitcase present were small in general and were not correlated with trends in baggage contents. The amplitude variations were most likely due to differences in absorption by the baggage and contents caused by slight differences in the location of the apple. The attenuation due to the suitcase, being much larger than that due to the apple, also tended to mask the absorption by the apple.

These measurement results meant that a fairly simple, and relatively inexpensive, system consisting of a resonant cavity operating in the TE_{101} mode connected to a device for measuring resonant frequency, could be used to detect agricultural products in baggage. The system would have the advantages of speed, simplicity and yes/no output requiring no operator interpretation. The threshold frequency shift to indicate presence of an agricultural product would have to be set high enough to minimize the number of false positive indications for normal suitcases but also low enough to minimize the number of false negative indications, especially for small volumes of agricultural products. Such a system may be unable to discriminate between large metal or fluid-filled articles and agricultural products.

IV. SIGNAL TRANSMISSION/REFLECTION APPROACH

The signal transmission/reflection approach as a means of noninvasively detecting the presence of agricultural products in baggage, like other approaches, is based upon the differences in dielectric properties between agricultural products and other baggage contents. These differences arise primarily from the relatively high moisture content of fresh fruits, vegetables, and meats as compared to materials such as leather and cloth. For a given object, the factors affecting transmitted and reflected signals are its position, shape, size, permittivity, and loss factor. The transmitted and reflected signals, being complex, are completely described by four parameters: two magnitudes and two phases.

In Quarterly Technical Report No. 2, an analysis of the transmitted and reflected signals for a planar multi-layered model was described. Preliminary experimental results obtained from a layered target arrangement with the use of a network analyzer operated in a manual mode were also presented. In Quarterly Technical Report No. 3, further experimental results using the network analyzer under computer control were reported. In this mode, phase and magnitude changes resulting from the insertion and removal of a sample were obtained for two frequency ranges: 1.8 - 2.6 GHz and 2.6 - 3.9 GHz. These measurements have been extended to 8.2 - 9.0 GHz during this reporting period.

A. Measurements

The HP Network Analyzer System used to measure reflection and transmission coefficients under computer control was described in Quarterly Technical Report No. 3. Use of a computer to control the network analyzer had two major advantages over manual use. First, a calibration procedure using known terminations and loads could be used to make error corrections to parameters obtained in the course of an

experiment. The second advantage was that measurements could be reproducibly made for a set of frequencies and compared with a set of stored values. This capability allowed changes in transmission and reflection parameters with the insertion of the sample to be determined. In all experiments, the "device under test" consisted of the transmitting and receiving antenna pair (along with their coaxial to waveguide adaptors) and the object placed between the antennas.

A matched pair of X-band horn antennas was used for the transmitting and receiving antennas. Each horn's aperture was 19.4 cm by 14.4 cm. The longer sides were horizontal so that the transmitted electric field was vertical. These antennas were used for measurements of reflection and transmission coefficients for a sample target alone and for the sample in a suitcase otherwise filled with clothing. Each experimental arrangement was surrounded by anechoic absorber material to reduce the effect of extraneous reflections.

The same grid described in Quarterly Technical Report No. 3 (Figure 19 of that report) was used for measurements of the sample alone. The antennas were placed 50 cm apart at the edges of the grid with their bottom edges at the level of the grid. The sample was a glycerol solution (30% by weight in water) in a plastic bottle, described in Quarterly Technical Report No. 3 to provide an upright cylindrical target with a height of 9.5 cm and diameter of 6 cm.

As in previous experiments, transmission and reflection coefficients were first determined with no sample present at preassigned frequencies in 0.1 GHz increments, this time from 8.2 to 9.0 GHz. The sample was then placed at each position on the grid and transmission and reflection measurements were taken for each frequency. After measurements at all positions were completed, the "no sample" measurements were repeated. Drift between the "no sample" condition before and after sample measurements was less than 1% for all parameters.

Results were put in the form of changes in the reflection and transmission coefficients with insertion of the sample. These were obtained by subtracting the numbers obtained from the "no sample" runs from those of the "sample present" runs. Because changes, rather than absolute transmission and reflection coefficients, were examined, effects arising from extraneous signals were minimized. The reported parameter changes are thus indicative of the effect one can hope to observe if agricultural products (of similar size, shape, and position) are present compared to when they are not present.

For the results plotted in Figures 13 - 18, the data were grouped for positions along axes parallel to the center axis of the horn antennas. Positions 4, 5 and 6 were on the center axis with position 5 midway between antennas. Positions 4 and 6 were 5 cm from this midpoint with position 4 closer to the transmitting antenna. Positions 1, 2, and 3 were 10 cm to the left of the center axis and were 5 cm apart; positions 7, 8 and 9 were 10 cm to the right with 5 cm spacing. In Figures 13 - 18, as in Quarterly Technical Report No. 3, broken lines correspond to positions (1, 4, or 7) nearest the transmitting antenna; solid lines, to center positions (2, 5, or 8); and dashed lines, to positions (3, 6, or 9) nearest the receiving antenna.

Amplitude difference trends with frequency shown in Figures 13 - 15 for reflection and transmission coefficients were similar for sample positions on the same axis. Transmission amplitude showed about a 4 dB reduction for positions on the center axis (Figure 14) while for off-center positions, it showed much smaller changes (Figure 13 and 15). Reflection amplitude exhibited more variation with frequency but had a similar pattern for off-center positions (Figure 13 and 15) which were more regular than the center axis values (Figure 14).

Phase difference trends with frequency shown in Figures 16 - 18 for reflection and transmission coefficients were also similar for sample positions on the same axis. Transmission phase showed a 20 - 35° negative shift for center-axis positions (Figure 17) and a 1 - 15° positive shift for off-center positions (Figure 16 and 18). Patterns

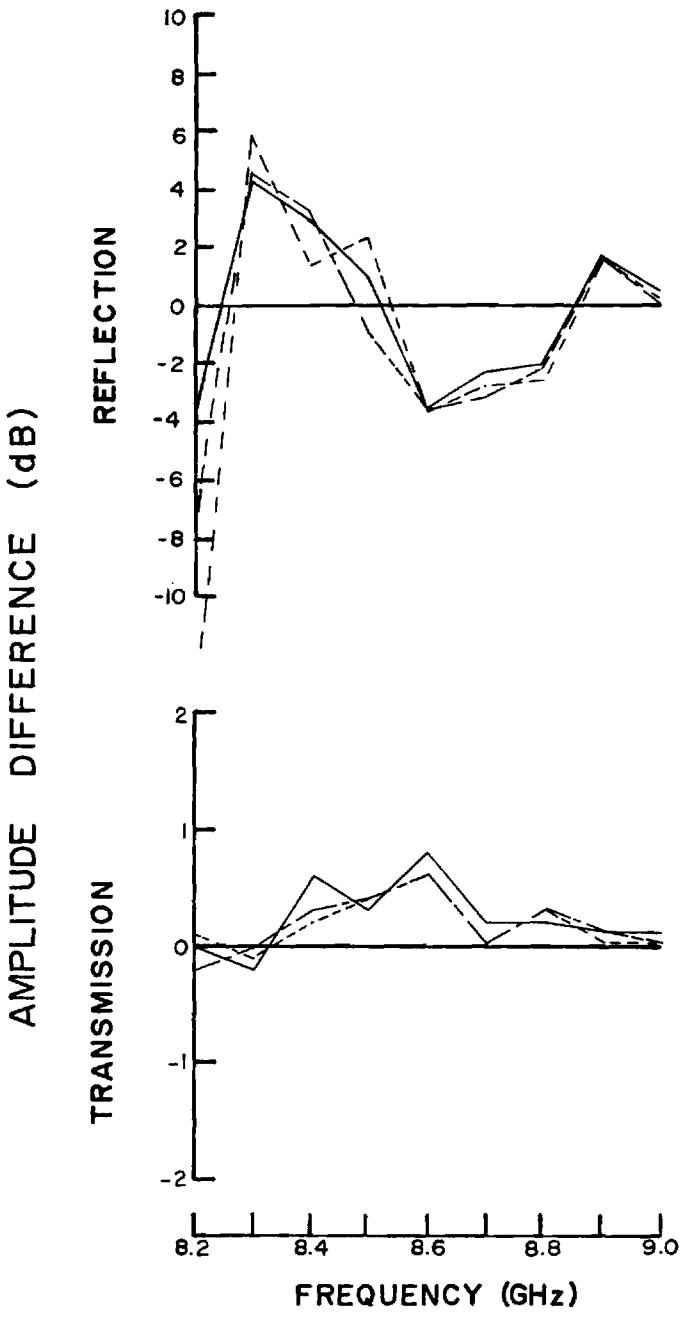

Figure 13. Amplitude differences in reflection and transmission coefficients with insertion of the sample on the left-of-center axis. Broken lines are for position 1; solid lines, position 2; and dashed lines, position 3.

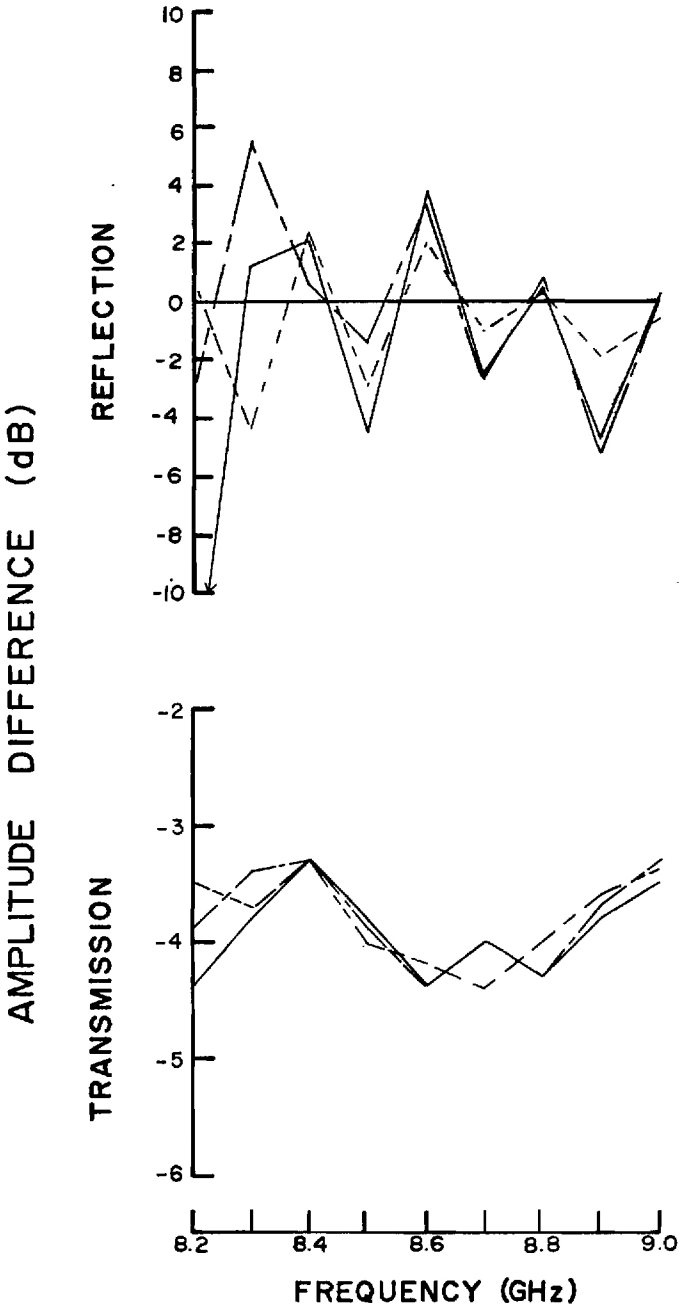

Figure 14. Amplitude differences in reflection and transmission coefficients with insertion of the sample on the center axis. Broken lines are for position 4; solid lines, position 5; and dashed lines, position 6.

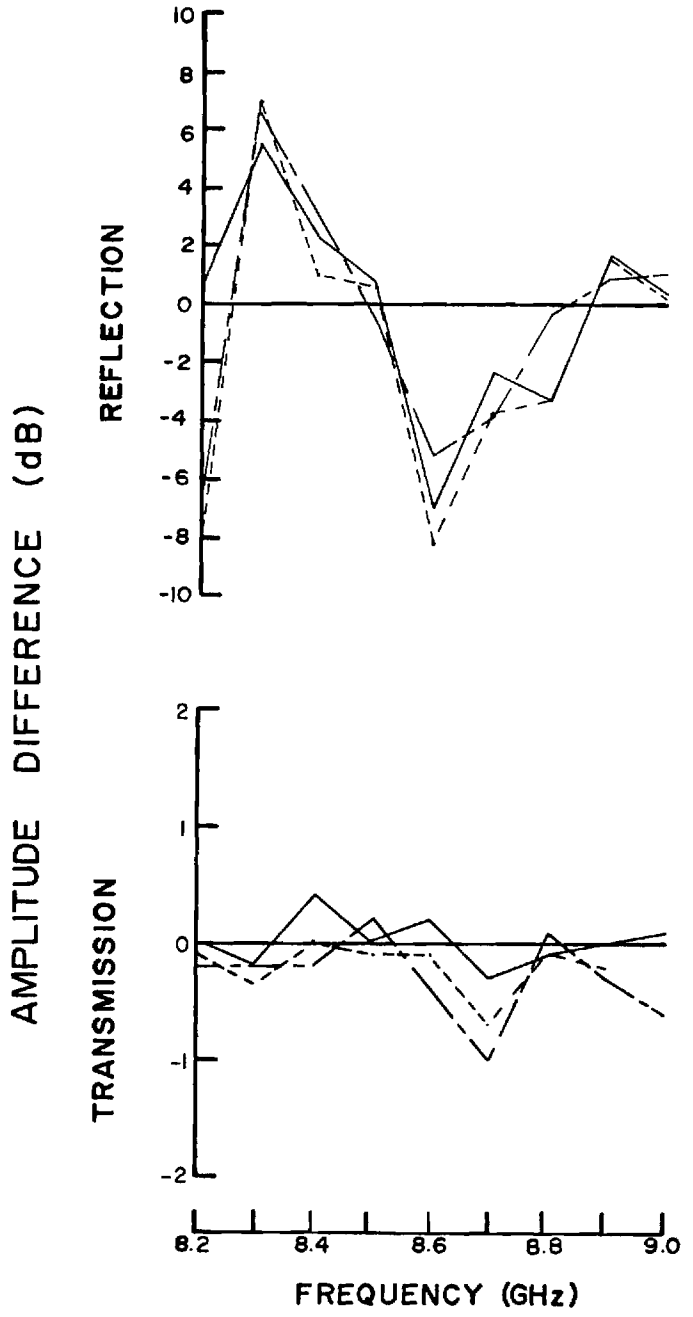

Figure 15. Amplitude differences in reflection and transmission coefficients with insertion of the sample on the right-of-center axis. Broken lines are for position 7; solid lines, position 8; and dashed lines, position 9.

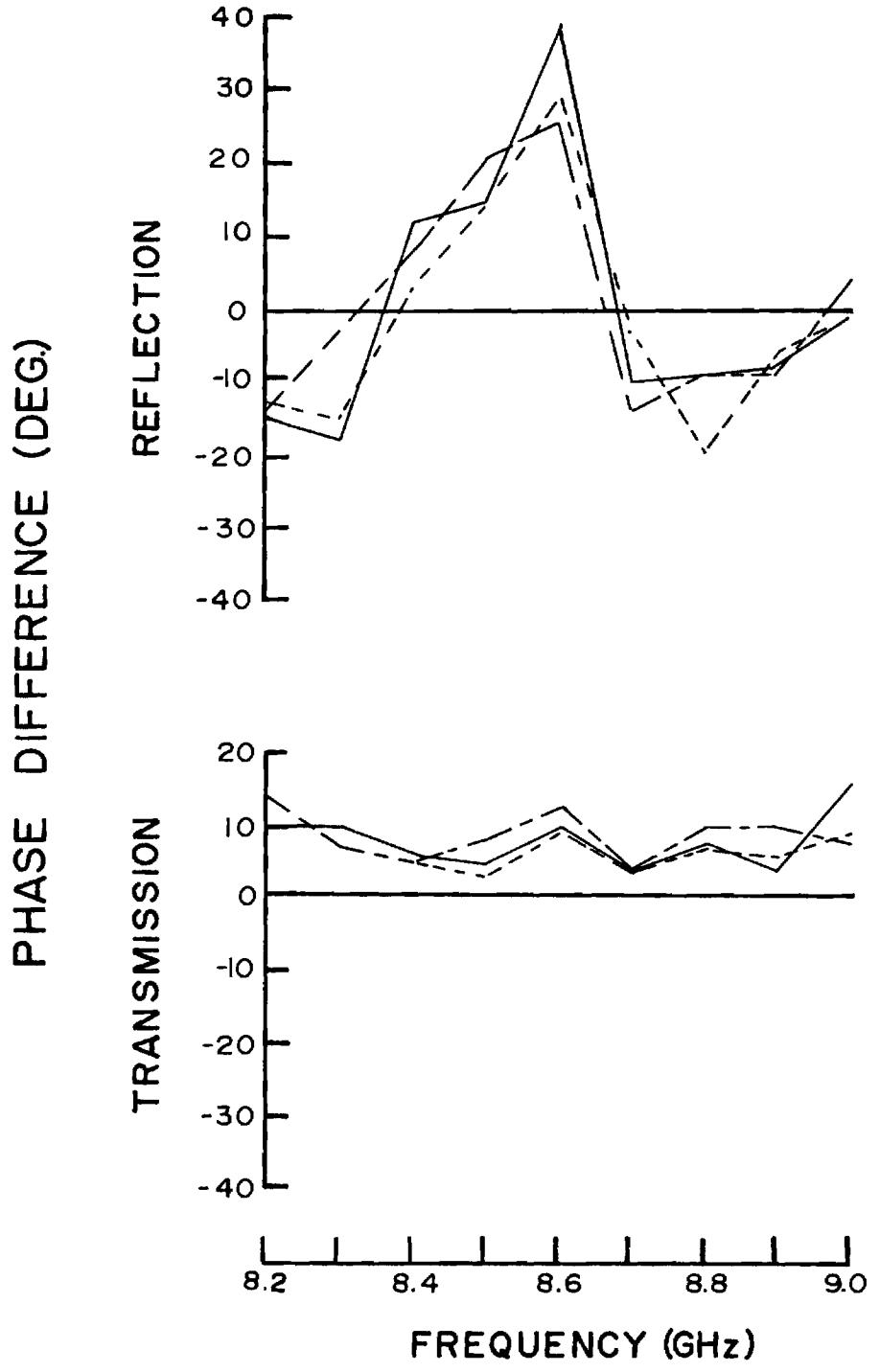

Figure 16. Phase differences in reflection and transmission coefficients with insertion of the sample on the left-of-center axis. Broken lines are for position 1; solid lines, position 2; and dashed lines, position 3.

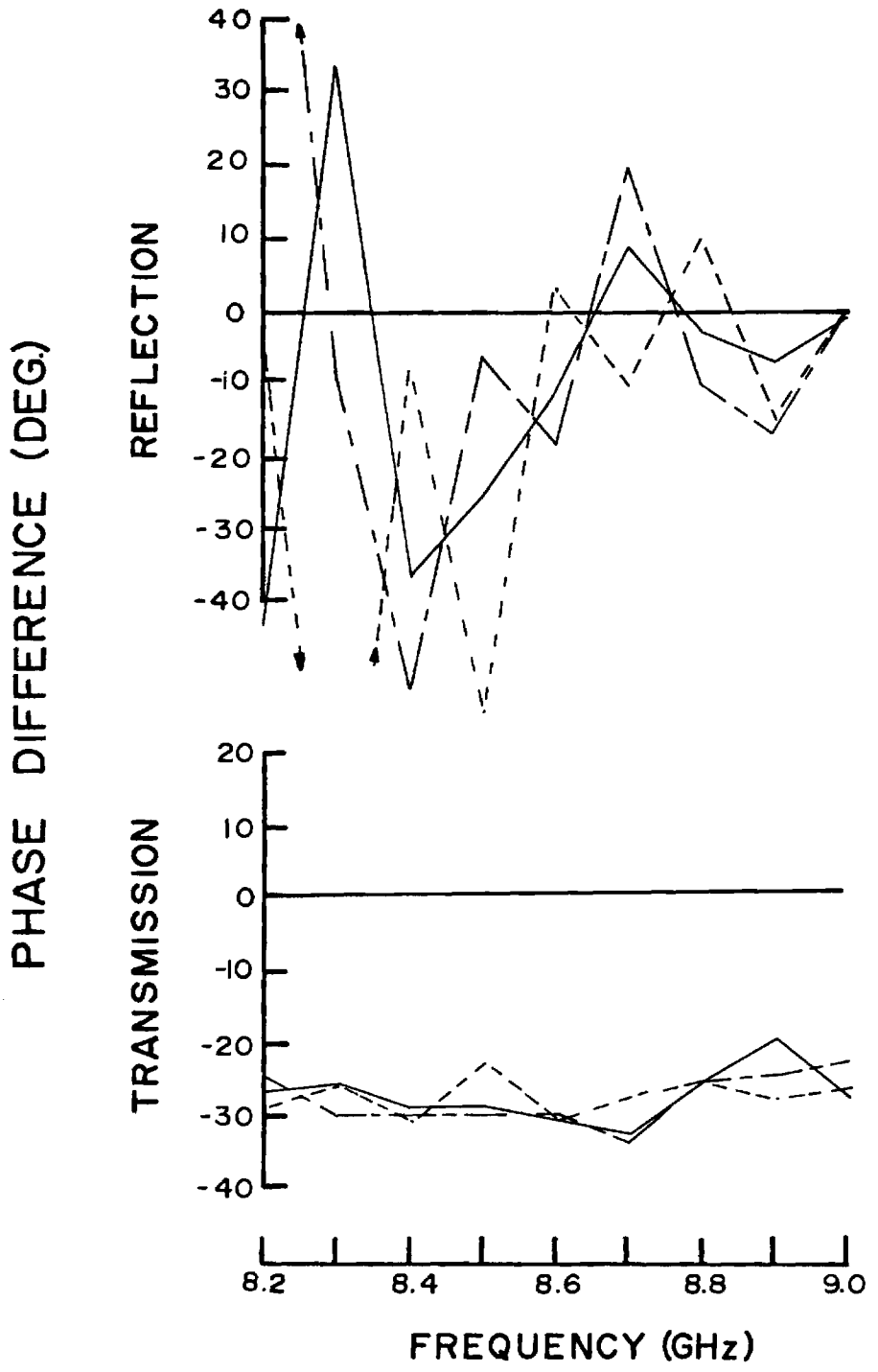

Figure 17. Phase differences in reflection and transmission coefficients with insertion of the sample on the center axis. Broken lines are for position 4; solid lines, position 5; and dashed lines, position 6.

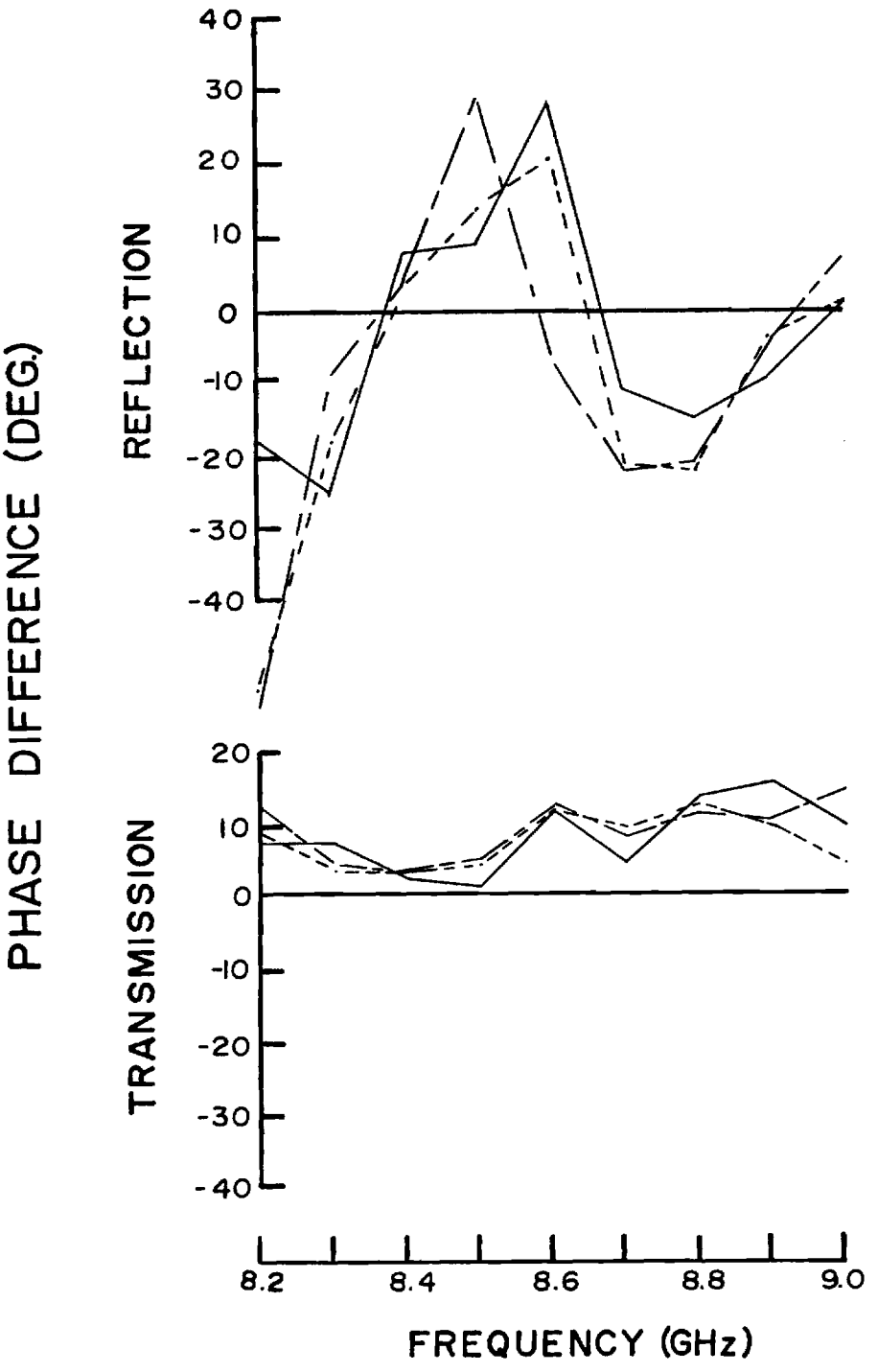

Figure 18. Phase differences in reflection and transmission coefficients with insertion of the sample on the right-of-center axis. Broken lines are for position 7; solid lines, position 8; and dashed lines, position 9.

for off-center reflection phase were similar (Figure 16 and 18) and were different from the center-axis pattern (Figure 17). The center-axis reflection phase was less consistent among positions as was the reflection amplitude (Figure 14).

To have a measurement situation more like actual baggage inspection, reflection and transmission coefficients were also measured for a suitcase with and without the glycerol/water sample enclosed. For measurements involving the suitcase, the horn antennas were spaced 45.7 cm apart with the bottom aperture edges 10.2 cm above the surface on which the suitcase rested. The soft-sided suitcase, 22 inches by 13 inches by 6 inches deep, was positioned midway between the antennas with its largest surfaces perpendicular to the antenna center axis so that transmitted signals passed through 6 inches of suitcase material. The suitcase was stepped through the space in 2-inch increments determined by aligning one end of the suitcase with marks on the surface supporting the suitcase. Reflection and transmission coefficients were recorded for each of these positions numbered 1 through 15. Position 8 corresponded to the center of the suitcase roughly aligned with the antenna center axis. The suitcase was filled with clothing for the "suitcase/clothes" case. The bottle of glycerol solution was placed in the center of the clothing for the "suitcase/glycerol" case. The bottle position in the suitcase was stabilized with foam rubber packing.

Figures 19 - 22 present the reflection and transmission coefficients for the suitcase measurements. Again, data are presented as differences between actual measured values and stored reference values found with the suitcase absent. Results for representative frequencies -- 8.4, 8.6, and 8.8 GHz--are given in each figure. Broken lines correspond to 8.4 GHz; solid lines, to 8.6 GHz; and dashed lines, to 8.8 GHz. Position numbers refer to the 2-inch increments already described.

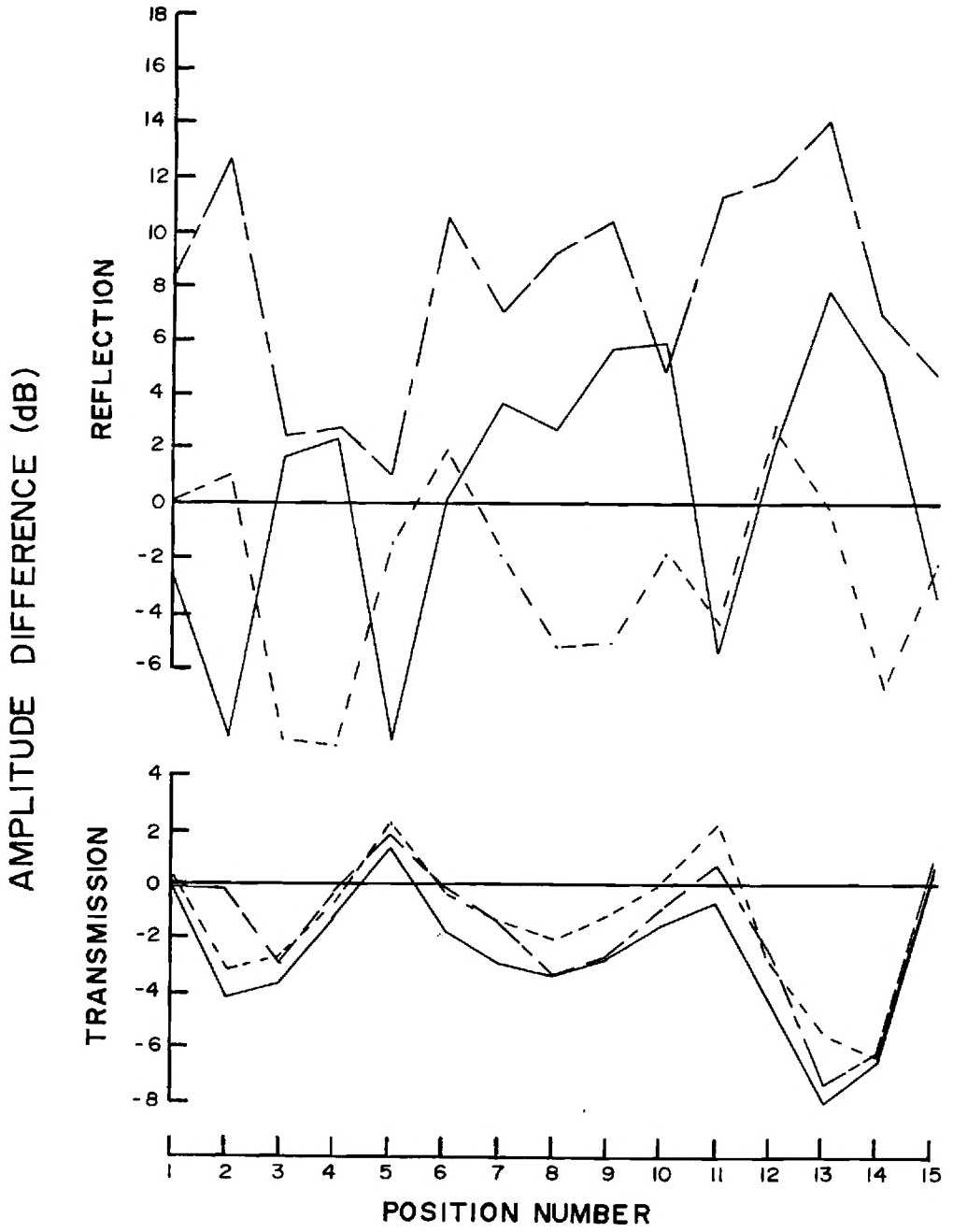

Figure 19. Amplitude differences in reflection and transmission coefficients for different positions of suitcase containing only clothes. Each position number represents a 2-inch increment of suitcase position. Broken lines are for 8.4 GHz; solid lines, 8.6 GHz; and dashed lines, 8.8 GHz.

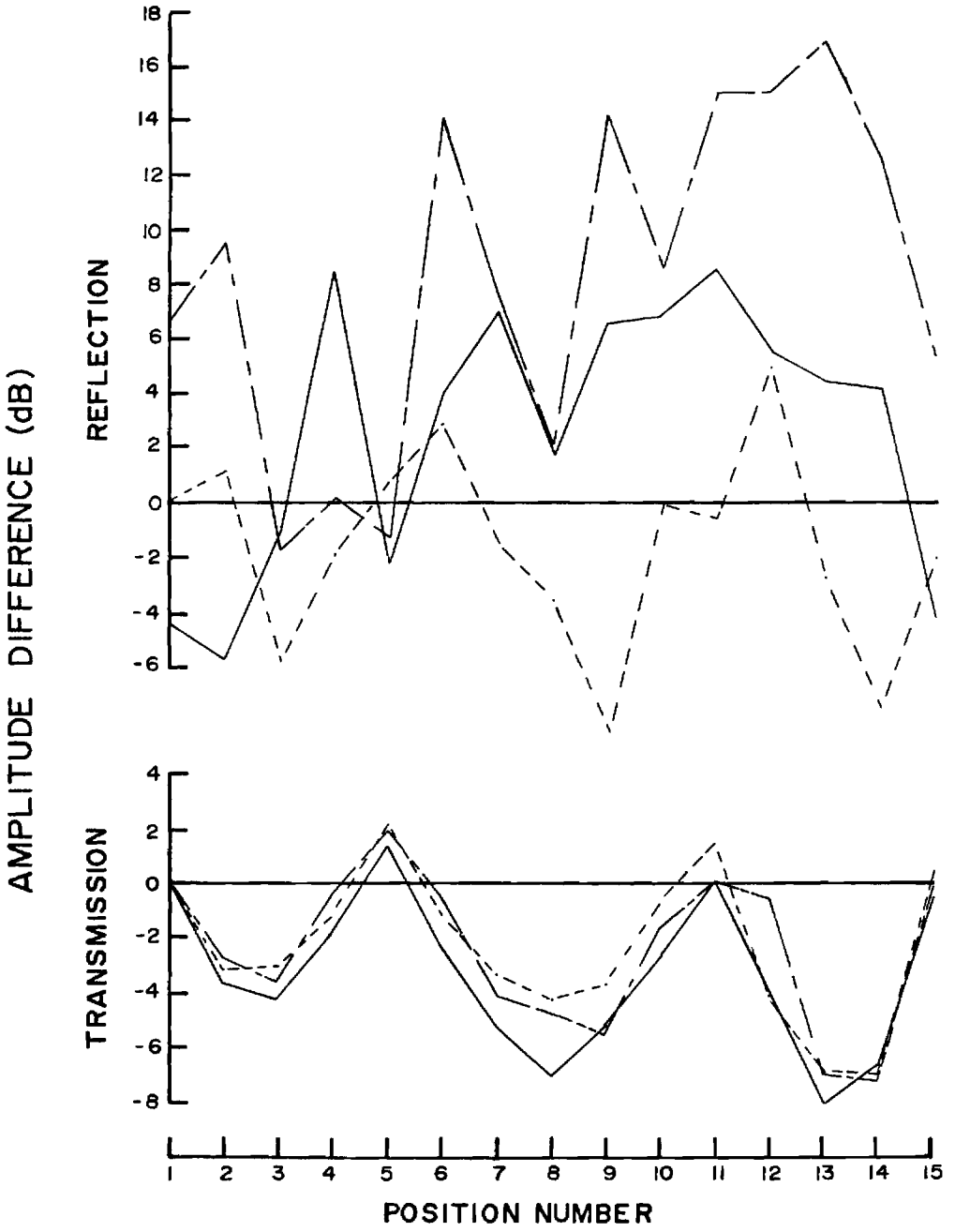

Figure 20. Amplitude differences in reflection and transmission coefficients for different positions of suitcase containing clothes and a bottle of glycerol solution. Each position number represents a 2-inch increment of suitcase position. Broken lines are for 8.4 GHz; solid lines, 8.6 GHz; and dashed lines, 8.8 GHz.

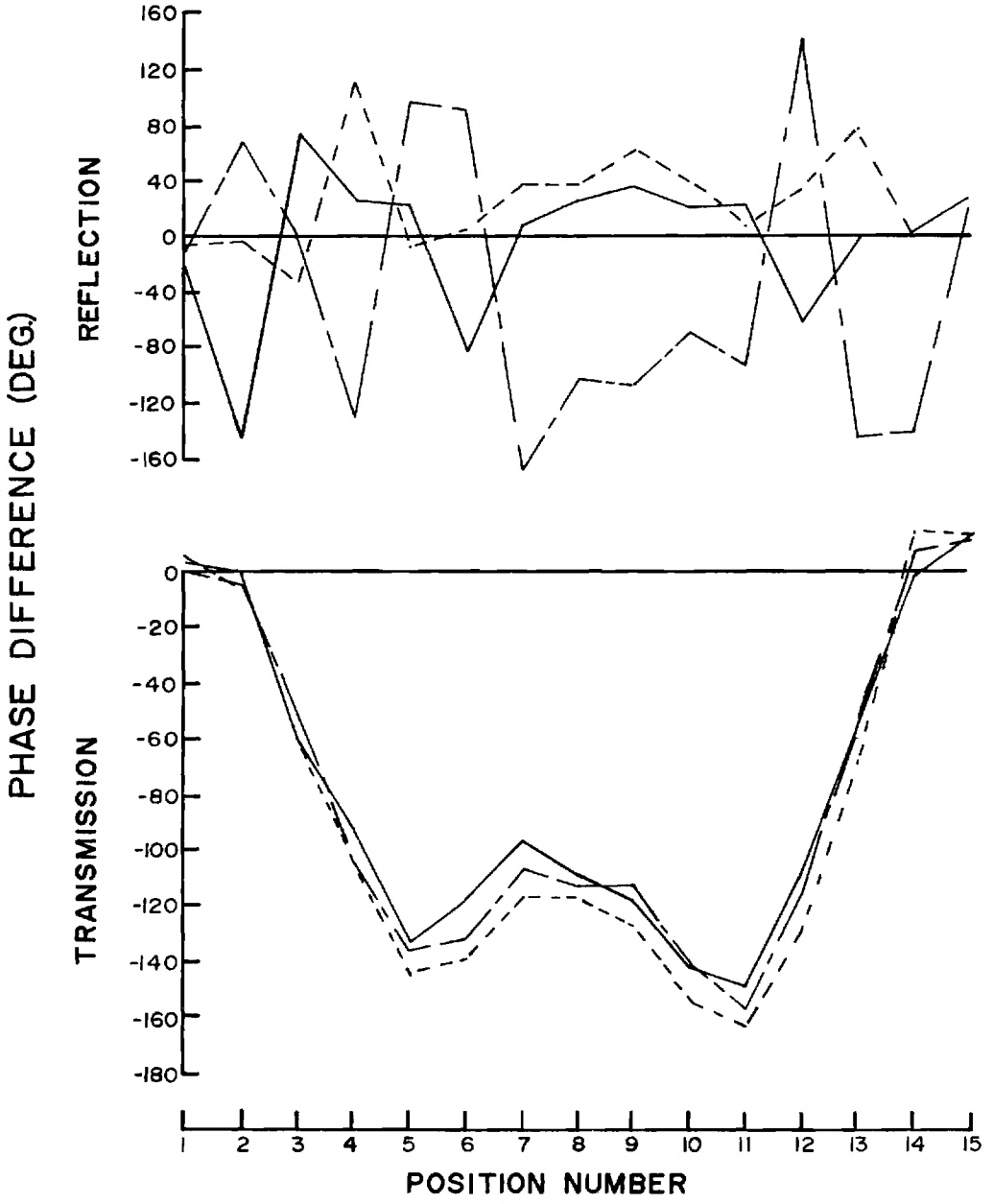

Figure 21. Phase differences in reflection and transmission coefficients for different positions of suitcase containing only clothes. Each position number represents a 2-inch increment of suitcase position. Broken lines are for 8.4 GHz; solid lines, 8.6 GHz; and dashed lines, 8.8 GHz.

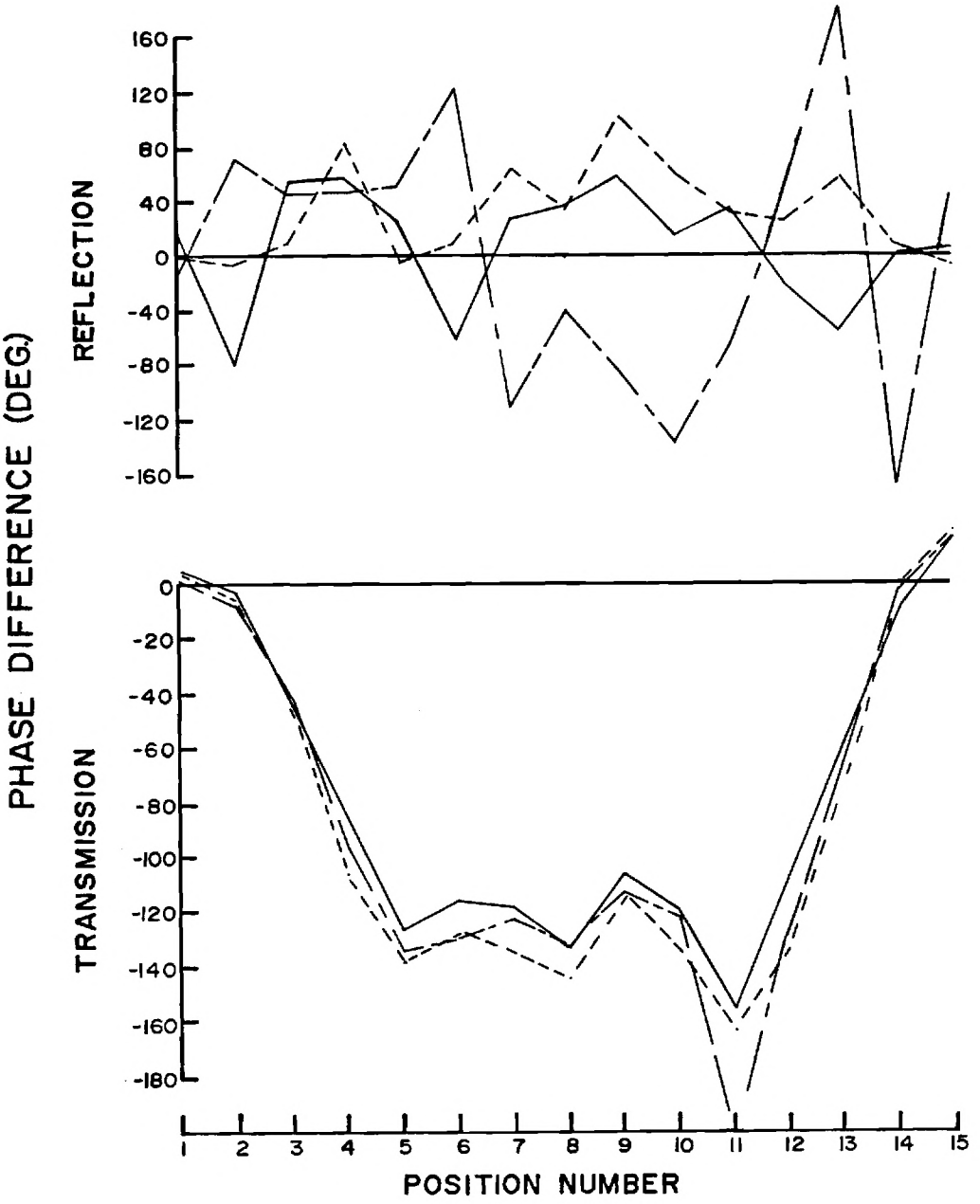

Figure 22. Phase differences in reflection and transmission coefficients for different positions of suitcase containing clothes and a bottle of glycerol solution. Each position number represents a 2-inch increment of suitcase position. Broken lines are for 8.4 GHz; solid lines, 8.6 GHz; and dashed lines, 8.8 GHz.

Amplitude differences for the reflection coefficients, illustrated in Figures 19 and 20, did not show a consistent pattern with suitcase position for the three microwave frequencies. In contrast, amplitude differences for the transmission coefficients, also illustrated in Figures 19 and 20, showed a similar pattern with position for both cases across frequency. This characteristic pattern had three dips in it. The dips at position 2-3 and at position 13-14 corresponded to the ends of the suitcase aligned with the antenna axis and were very similar for suitcase/clothes and suitcase/glycerol cases. The dip at position 8 corresponded to the center of the suitcase aligned with the antenna axis. This dip was larger for suitcase/glycerol (Figure 20) than for suitcase/clothes (Figure 19) by 1.3 to 3.6 dB depending on frequency. This difference was similar to that seen for the centered bottle of glycerol solution by itself (Figure 14).

Phase differences for the reflection coefficients, illustrated in Figures 21 and 22, did not show a consistent pattern among frequencies with suitcase position for either case. However, for each frequency, the pattern with suitcase position was similar for both cases. Phase differences for the transmission coefficients showed similar U-shaped patterns with suitcase position for both cases across frequency. Since positions 2-3 and 13-14 corresponded to the suitcase ends aligned with the antenna axis, phase decreased when more than roughly half of the horn antenna aperture was occluded by the suitcase. For the suitcase/clothes case in Figure 21, the decrease peaked at positions 5 and 11 with a smaller decrease between them at position 7-8, the center of the suitcase. For the suitcase/glycerol case in Figure 22, similar peak decreases were located at positions 5 and 11, but they were separated by an almost constant phase difference. The major difference between these two phase patterns occurred in this central region. The larger transmission phase decrease for suitcase/glycerol was expected since the glycerol solution by itself on center-axis caused a phase decrease of 25-30° (Figure 17) for the frequencies plotted in Figures 21 and 22. The difference between phases at position 8 in these two figures, ranging from 19 to 27°, was comparable to the shift for the glycerol solution alone.

B. Conclusions

Results obtained from the glycerol solution during this reporting period using frequencies from 8.2 to 9.0 GHz showed that transmitted signals were more uniform than reflected signals. This was consistent with results for 1.8 to 3.9 GHz reported in Quarterly Technical Report No. 3 and for the layered model reported in Quarterly Technical report No. 2. Although these measurements were made in three different frequency bands (LS, 1.8-2.6 GHz; S, 2.6-3.9 GHz; and X, 8.2-9.0 GHz) using different sets of antennas, transmission parameters, listed in Table I, were found to show progressive trends across frequency. Center-axis amplitude decreased from -0.5 to -4 dB while side-axis amplitude increased from -1 to 0 dB with values in the intermediate frequency range showing the transition. Center-axis phase decreased from -15 to about -25° while side-axis phase increased from -3 to +7°.

Center-axis transmission coefficient amplitude and phase values for the glycerol solution in the 8.2 to 9.0 GHz range in Table I were very similar to the differences between this solution being present and absent in a suitcase. This meant that, in this frequency range at least, the amplitude and phase changes introduced by a fruit-like object in a suitcase added to the changes caused by the suitcase with clothes. This observation may provide the basis for being able to detect the presence of agricultural products using transmitted signal parameters.

From the cumulative results on the signal transmission/reflection approach, the transmitted signal appeared to be more suitable for detecting agricultural products in baggage for several reasons. First, the transmitted signal was more uniform with frequency and with target position. In practice, this would mean more reliable measurements and fewer required calibration procedures. The additive changes noted above would be more obvious in transmitted signals. The transmitted signal, especially at X-band, was usually changed most for center-axis positions of the target. This characteristic would allow better localization of an agricultural product in baggage.

TABLE I

SUMMARY OF TRANSMISSION
COEFFICIENT CHANGES
FOR
GLYCEROL SOLUTION TARGET

	FREQUENCY (GHz)		
	1.8 - 2.6	2.6 - 3.9	8.2 - 9.0
Amplitude (dB)			
Center axis	- 0.5	-0.3 → -1	-4
Side axis	- 1	-1.5 → 0	0
Phase (°)			
Center axis	- 15	-25	-25 → -20
Side axis	- 3	+ 7	+7

The larger differences between center-axis and side-axis objects in the X-band measurements were attributable to some extent to a smaller beamwidth at these frequencies. A rough comparison of beamwidths was made by recognizing that beamwidth was inversely proportional to frequency and to the antenna dimension in the plane of interest [2].For the transmitting antennas used in this study, the X-band beamwidth was approximately one-half of the LS-band beamwidth and approximately one-seventh of the S-band beamwidth. These comparisons were qualitative since beamwidth actually applies to far-field radiating fields which were not achieved in the experimental measurements. The more narrow relative beamwidth calculated for X-band could also explain the greater stability of X-band signals since less perturbation by surrounding objects would be expected.

Signal transmission coefficients exhibited measurable changes in both phase and amplitude for a target consisting of a 6 cm diameter, 9.5 cm long cylinder. A sphere with a diameter of 8 cm has the same volume and would be representative of a large apple or a small grapefruit. From the magnitude of the changes observed for the glycerol solution target, changes should be detectable for spherical targets with diameters as small as 5 cm. Of course, changes would be larger for volumes larger than that tested.

Based on results obtained on this program, further work on the transmission/reflection approach would be most profitably done with X-band transmitted signals. The larger changes for these higher frequencies were more easily measured. The greater directivity of the signal at X-band will provide a more position sensitive signal as well as reducing interference from nearby objects.

V. SHORT PULSE RADAR APPROACH

As outlined in Quarterly Technical Report No. 2, a Short Pulse radar (SPR) may be useful in detecting fruit within baggage. This type of radar emits a very brief pulse of electromagnetic energy which is directed toward the material to be interrogated. The received signals, or returns, resulting from reflections at material interfaces are displayed as voltage versus time. Delays between the transmitted and received signals are typically on the order of a few nanoseconds and can be translated into distance by using the propagation velocity in the materials interrogated.

The SPR has previously been used to obtain profiles of underground strata and locate buried objects, as reviewed in Quarterly Technical Report No. 2. This situation is similar to that of objects "buried" in a suitcase. To explore more fully the potential of SPR to detect fruit in baggage, discussions were held with personnel of the Radar Applications Division during the third quarter of this program. This division of the Radar and Instrumentation Laboratory of Georgia Tech's Engineering Experiment Station has used SPR to detect buried objects and subsurface voids [3,4]. From these discussions, it was concluded that SPR had enough promise as a detector of agricultural products to warrant some actual measurements to check the feasibility of this approach. The SPR measurements were started at the end of the third quarter of this program and completed during the current reporting period.

A. Measurements

Experimental measurements were made on citrus fruits buried in sand. This arrangement was chosen for two reasons. First, the experimental SPR system used for these measurements was already set up for recording returns from subsurface objects. The antenna pointed downward and its height was adjustable. The antenna along with all

electronic instrumentation and small computer was mounted on a wheeled cart which was moved to change antenna positions. Second, the buried fruits were electrically very similar to agricultural products in a suitcase filled with clothing and other personal items. From the propagation velocity derived from the differential delay between returns from the top and bottom of the dry sand, the dielectric constant of the sand was determined to be approximately 3.6. This value was not much different than the dielectric constant of 2 to 3 expected for clothing and plastics in a suitcase.

A 6-foot by 10-foot box with a height of 2 feet was constructed of plywood. It was filled with dry construction-grade sand to a depth of 18 inches. Figure 23 shows schematically the box with sand and its location with respect to the SPR antenna and instrumentation cart. Before a series of measurements, the surface of the sand was leveled and smoothed to provide a constant distance between antenna and sand as the antenna position was changed. Returns were measured for each condition at several antenna positions spaced 6 inches apart. One antenna position was directly over the fruit.

Three types of citrus fruit were used as targets. Tangerines, oranges, and grapefruits were selected to represent a size range of fruit with very similar dielectric properties. As discussed in Quarterly Technical Report No. 3, these dielectric properties were representative of those for other agricultural products.

The return voltage signal was processed by electronic circuits using sampling oscilloscope techniques. Under the control of an Apple computer, the return signal information was stored in disk memory for later access and processing. The return signal was displayed on an oscilloscope as it was received (and also stored) with one millisecond representing one nanosecond, a factor of 1,000 times slower. The computer sampled and stored 220 values proportional to voltage for each return. Each point represented 0.026 nanosecond in real time so that there was the capability to analyze and plot 5.72 nanoseconds of each return. The velocity of propagation in sand was 6.2×10^9

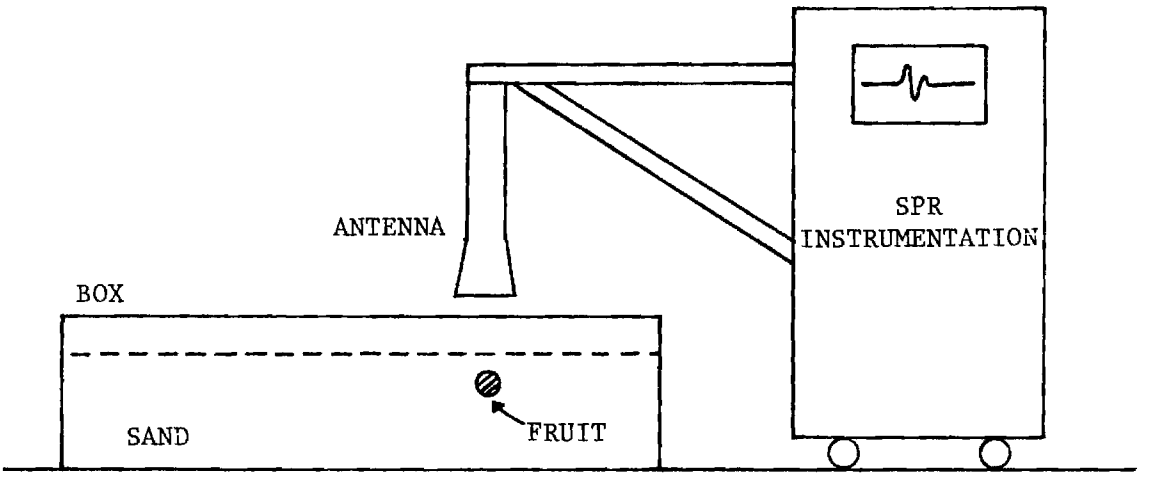

Figure 23. Short pulse radar measurement setup.

inches/second, or 6.2 inches/nanosecond. Thus, each nanosecond of the display represented 3.1 inches of travel in sand since the signal traveled to and from the reflecting surface before reception.

Initial measurements were made with fruit placed on top of the sand. When multiple fruits were tested they were placed side by side on the surface. Figure 24 shows the results obtained for one and three oranges on the surface. Each trace represented 5.72 nanoseconds of return voltage signal and the same arbitrary voltage scale applied to all traces. The set of seven traces for each condition were recorded for antenna positions 6 inches apart. The center trace in each set was the signal recorded with the antenna directly over the fruit. For antenna positions furthest from the fruit--top and bottom traces in each set, there were small returns from the sand. As the antenna was moved closer to the fruit, there was a larger, earlier return due to the fruit. The fruit return was maximum with the antenna directly over the fruit. The maximum return from three oranges was larger and was received earlier than the maximum return from one orange. Returns from two oranges on the surface were intermediate in amplitude and had delays similar to the ones for three oranges.

Returns from other fruits on the sand surface were similar in shape to those from oranges. For both tangerines and grapefruits, fruit returns were larger for more fruit. Tangerine returns were slightly smaller than those for the same number of oranges; grapefruit returns were larger than those for oranges. Tangerine returns occurred with approximately the same delay that orange returns occurred, but grapefruit returns occurred earlier. The delays for one, two and three tangerines were similar as were the delays for one, two and three grapefruits.

Measurements were also made for fruit buried 3 inches below the sand surface for one and for three each of tangerines, oranges, and grapefruits. Amplitudes of these returns were smaller than for fruit placed on the surface. The gain of the receiver electronic circuits

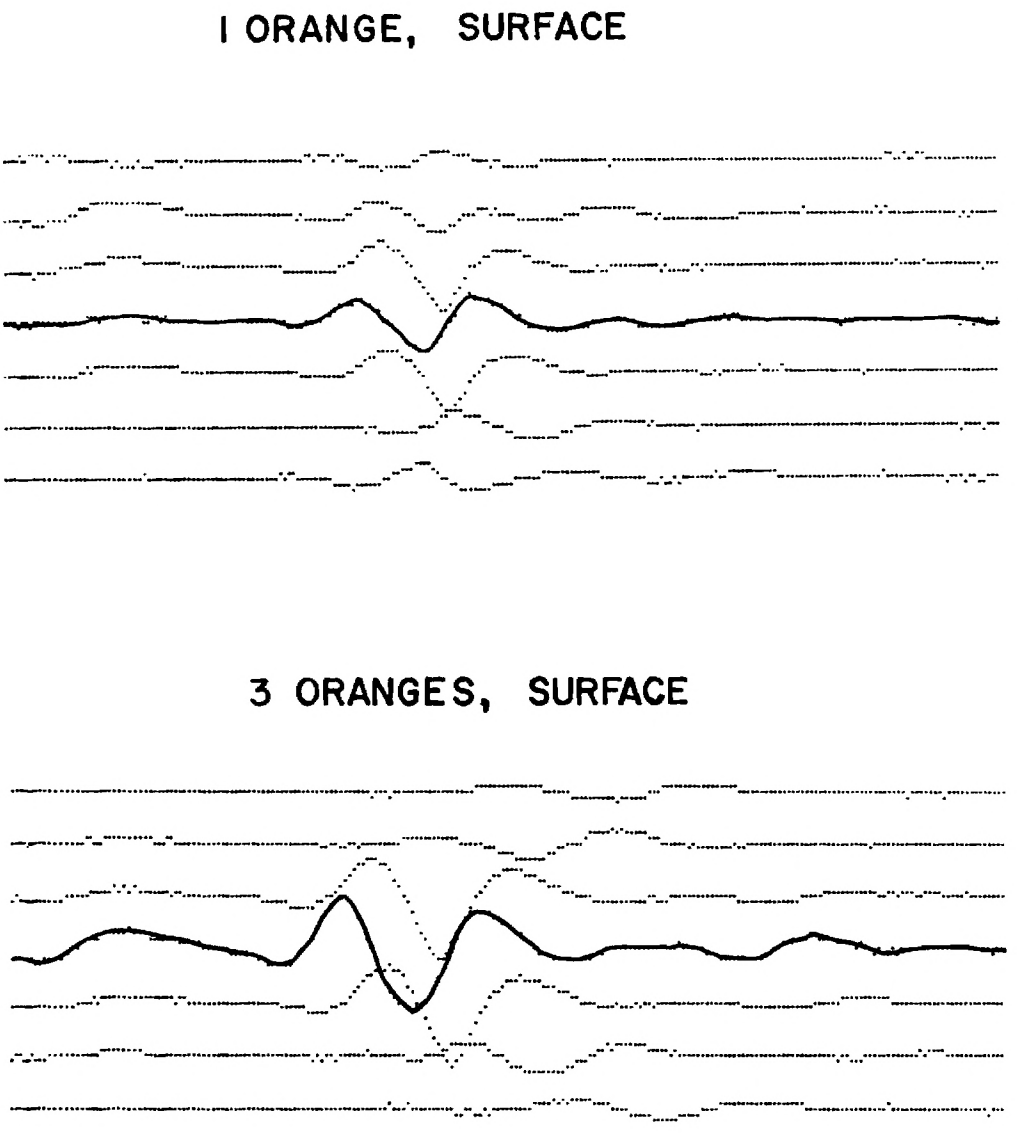

Figure 24. SPR returns for one and three oranges on surface of sand. Solid traces are for antenna position directly over fruit.

was increased to provide a signal large enough to display and to store accurately. Figure 25 shows the results obtained for one and three buried oranges. Traces for each condition were again taken for antenna positions 6 inches apart. Because of the higher gain used for these returns, early returns from the SPR system internal connections, the antenna, and the sand surface were often larger than the later fruit returns. The early returns, seen as small humps on the left-hand portion of the traces in Figure 24, often caused amplifier saturation at the higher gain needed to detect the deeper fruit. For this reason, early returns were deleted to show more clearly the fruit return traces in Figure 25, which had a duration of only 3.58 nanoseconds due to the deletion.

The returns from three buried oranges were larger than those from one buried orange, as seen by comparing the highlighted traces in Figure 25. Fruit returns were discernible in traces for antenna positions eighteen inches away from the position directly over the oranges. These statements also describe the results for tangerines and grapefruits. In general, larger returns were observed for the larger fruit. Comparison of delays of returns from buried fruit was not possible because many of the returns overlapped the earlier large returns.

Measurements were also made for single fruits buried 9 inches below the sand surface. Results for a buried orange are shown in Figure 26 where the traces are again 3.58 nanoseconds long. When amplifier gains were increased still more to obtain reasonable amplitudes for the fruit returns, many other returns of similar amplitudes were also present. Attempts to cancel out these non-fruit returns were made by subtracting stored returns from only the sand. A set of these difference returns is shown in Figure 26 which clearly shows the return from the orange in the central traces. Similar return patterns were also obtained from a tangerine and from a grapefruit buried nine inches deep.

In canceling unwanted returns to reveal small returns from fruit for the 9 inch deep fruit, a problem was encountered. The SPR recording system was designed to trigger on a large, early return from the ground surface. This return was not always reproducible from

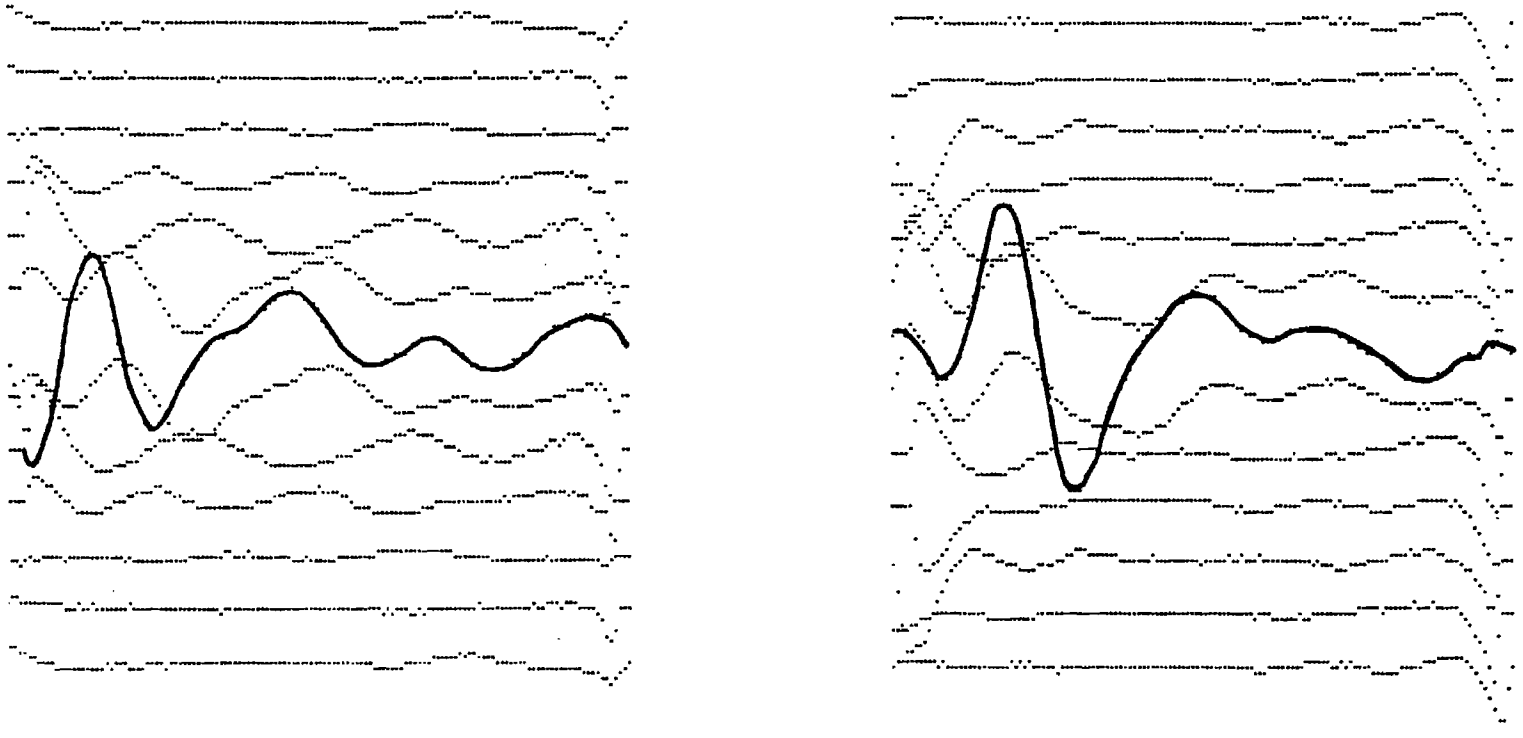

Figure 25. SPR returns for one and three oranges buried 3 inches below surface of sand. Solid traces are for antenna position directly over fruit.

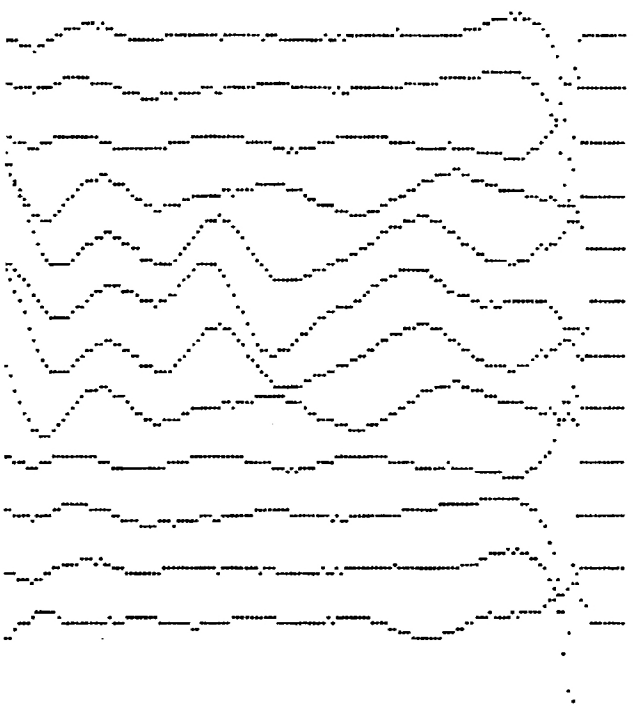

Figure 26. SPR returns for an orange buried 9 inches below surface of sand.

experiment to experiment so that the triggering point varied in time. A single set of no-fruit returns was stored to subtract from subsequent returns obtained with fruit present. When the triggering point differed in time for a pair of returns being subtracted, the resultant difference trace contained amplitude variations not related to the fruit return. From this experience, it was learned that a trigger stationary in time was required. The SPR system used in these studies could not be easily modified to include such a trigger within the time and budget limitations of this program.

B. Conclusions

From the various SPR returns from fruit on, and buried in, sand, it was seen that detection of fruit in a closed suitcase with SPR was feasible. The returns from fruit had several characteristics which would be useful in differentiating returns from fruit and from other suitcase contents such as clothing. The returns from fruit were all similar in shape and their amplitudes were larger with larger volumes of fruit. The delay to a return was shorter for fruit closer to the antenna and, to a lesser degree, for larger fruit.

The presence of fruit was readily detectable from the appearance of the voltage traces representing received signals. These traces gave target location information in two dimensions: laterally as the antenna was moved and depth along each trace. In a few measurements, individual returns from fruits one above another separated by 3 inches were also detectable. Other types of signal encoding, such as line density proportional to amplitude, may make the fruit return even more obvious. One definite requirement for an SPR system in future experiments is a time-synchronized trigger for received signals. This improved trigger would make possible the detection of returns from even smaller fruits than those used in this study.

Based on the reported results of detecting fruit with an existing SPR system, it is felt that such a system could be used successfully to detect fruit in closed luggage. Information on fruit location (lateral position and depth) and size is contained in received signals displayed as voltage versus time. Information on fruit shape and type will require further analysis of fruit returns obtained under a variety of situations. Detection of small fruits will require an improved SPR system.

VI. CONCLUSIONS AND RECOMMENDATIONS

The results obtained on this program indicated that electromagnetic methods can successfully detect agricultural products in baggage. Although there was no previously published work in this area, these results were expected because of the differences between the dielectric properties of agricultural products and the dielectric properties of clothing and other suitcase contents. The following four approaches using different electromagnetic techniques were studied:

1. Capacitor plate, in which impedance of pairs of parallel metal plates was measured;
2. Resonant cavity, in which resonant frequency and losses of a metal box were measured;
3. Signal transmission/reflection, in which transmitted and reflected signals between two antennas were measured; and
4. Short pulse radar, in which the reflected portion of a transient pulse was measured.

For all four approaches, fruit and fruit-like objects were detected alone and in situations simulating inclusion in baggage. Experimental findings have been described in Quarterly Technical Reports Nos. 2 and 3, as well as in this report.

Since a basic ability for detection has been shown, further development to produce an automated system requiring minimal operator attendance and inexpensive enough for wide deployment, will involve refinement of current experimental models. This refinement would include not only instrumentation necessary for automation but enhancement of detection capabilities and definition of performance levels as they relate to baggage inspection requirements. These requirements include rapid, reliable inspection of closed baggage and an appropriate indication for inspectors when an agricultural product is present. It is anticipated that rapid inspection would be best achieved by using a conveyor belt apparatus which would carry each piece of baggage past an electromagnetic detector based on one of the four approaches. This would be similar to systems currently in use for

the X-ray examination of baggage. Three of the four approaches are compatible with this inspection scheme. The resonant cavity approach, which utilizes a closed metallic box, would require extensive modification for this scheme. For this reason, and because of the ambiguities seen in the results obtained with this approach, it is recommended that the resonant cavity approach not be pursued.

With available laboratory instruments, sufficient sensitivity was displayed by the four approaches to detect one or a few medium-sized fruit. Measurements were done passively, i.e., perturbations of electromagnetic fields created by fruit were indicated by the instruments. It is anticipated that active circuits incorporating devices already tested in this program will not only increase sensitivity but will provide output signals to indicate the presence of agricultural products. Such an active circuit could take the form of an amplifier with positive feedback similar to ones which have already been developed for other applications [5,6]. The frequency of oscillation and power output level of such a circuit depend on the terminal properties of a feedback element. If this element consisted of capacitor plates, resonant cavity, or transmission/reflection antenna pair, then changes in these parameters could indicate the presence of an agricultural product. The range of oscillation frequencies would be different for each type of element. The resonant cavity would not be suitable for the practical reasons stated above.

The capacitor plate approach is attractive for several reasons. First, its parallel-plate configuration readily allows the passage of baggage to be interrogated. Secondly, instrumentation of these plates operating at relatively low frequencies of 1 - 5 MHz is fairly straightforward. Lastly, at these frequencies there should be the greatest difference between dielectric properties of agricultural products and dielectric properties of other baggage items with high-water content such as perfumes, lotions, and beverages. This difference may allow for discrimination between these items and fruits and vegetables to reduce false positive indications of agricultural products.

The short pulse radar approach is attractive because of its capability to provide target depth information. This approach has the highest potential for displaying object shape and location information conveniently on a screen. This information would assist an inspector in distinguishing suitcase items as well locating items for follow up visual inspection. Characteristic shapes of different agricultural products would also aid the decision whether to inspect further.

The following recommendations for device development are based on the findings in this program:

1. Pursue the capacitor plate approach by developing instrumentation, possibly active circuits, to provide indications of agricultural product presence;
2. Pursue the short pulse radar approach using a dedicated system with an easily interpreted visual display; and
3. Investigate on a limited basis the applicability of the transmission/reflection antenna pair at X-band to an active circuit to provide indications of agricultural product location in baggage.

VII. REFERENCES

1. U.S. Department of Agriculture, "Travelers' Tips on Bringing Food, Plant, and Animal Products into the United States," USDA, APHIS, Program Aid No. 1083, U.S. Government Printing Office, 725-104, 1981, 17 pp.

2. S. Silver, ed., Microwave Antenna Theory and Design, McGraw-Hill, New York, 1949, 623 pp.

3. J. D. Echard, J. A. Scheer, E. O. Rausch, W. H. Licata, J. R. Moore, and J. A. Nestor, "Radar Detection, Discrimination, and Classification of Buried Non-Metallic Mines," Final Technical Report for U.S. Army Mobility Equipment Research and Development, Contract No. DAAG54-76-C-0112, Georgia Tech Project A-1828, February 1978.

4. J. R. Moore and J. D. Echard, "Radar Detection of Voids Under Concrete Highways," Final Technical Report for Georgia Department of Transportation, Georgia Tech Project A-2107, May 1978.

5. R. C. Ajmera, D.B. Batchelor, D.C. Moody, and H. Lashinsky, "Microwave Measurements with Active Systems," Proc. IEEE 62: 118-127, 1974.

6. R. G. Bosisio, R. Dallaire, and P. Phromothansy, "A Non Contact Temperature Monitor for the Automatic Control of Microwave Ovens," J. Microwave Power 12: 309-317, 1977.

FINAL TECHNICAL REPORT
PROJECT A–2673

ELECTROMAGNETIC DETECTION OF AGRICULTURAL PRODUCTS IN TRAVELERS' BAGGAGE

By

R. L. Seaman, M. L. Studwell, J. Seals and A. R. Moser

Prepared for

U.S. DEPARTMENT OF AGRICULTURE
SCIENCE AND EDUCATION ADMINISTRATION
AGRICULTURAL RESEARCH – SOUTHERN REGION
701 LOYOLA AVENUE
NEW ORLEANS, LOUISIANA 70153

Under

Research Agreement No. 53-7B30-0-247

FEBRUARY 1982

GEORGIA INSTITUTE OF TECHNOLOGY
A Unit of the University System of Georgia
Engineering Experiment Station
Atlanta, Georgia 30332

1982

ELECTROMAGNETIC DETECTION OF AGRICULTURAL PRODUCTS IN TRAVELERS' BAGGAGE

Final Technical Report

Project A-2673

February 1982

Under

Research Agreement No. 53-7B30-0-247

By

R. L. Seaman, M. L. Studwell, J. Seals
and A. R. Moser

Prepared for

U.S. DEPARTMENT OF AGRICULTURE
Science and Education Administration
Agricultural Research - Southern Region
701 Loyola Avenue
New Orleans, Louisiana 70153

By

BIOMEDICAL RESEARCH DIVISION
Electronics and Computer Systems Laboratory
Engineering Experiment Station
Georgia Institute of Technology
Atlanta, Georgia 30332

FOREWORD

Research on this project was performed by personnel of the Biomedical Research Division of the Electronics and Computer Systems Laboratory of the Engineering Experiment Station at the Georgia Institute of Technology, Atlanta, Georgia. This project was sponsored by the Science and Education Administration of the U.S. Department of Agriculture, New Orleans, Louisiana, under Research Agreement 53-7B30-0-247 and was assigned Georgia Tech Project No. A-2673. This report summarizes efforts carried out from 30 May 1980 through 31 December 1981, the technical performance period for this project.

Dr. R. L. Seaman served as Project Director. Mr. M. L. Studwell performed the analysis and the experiments on the resonant cavity approach and the final analysis and experiments on the capacitor plate approach. Mr. J. Seals performed the initial analysis and experiments on the capacitor plate approach as well as the measurements of fruit dielectric properties. Dr. A. R. Moser performed the analysis and the experiments on the signal transmission/reflection approach. Dr. W. J. Steinway of the Radar Applications Division supervised the measurements with the short pulse radar. Mr. P. G. Friederich performed measurements of ethanol dielectric properties and Mr. R. M. Kobert assisted in several aspects of the technical efforts.

Respectfully submitted,

Ronald L. Seaman,
Project Director

Approved:

J. C. Toler, Manager
Biomedical Research Division

TABLE OF CONTENTS

LIST OF FIGURES

LIST OF FIGURES

continued

LIST OF FIGURES

continued

I. INTRODUCTION

The overall goal of this project was to conduct theoretical analyses and experimental investigations to determine the feasibility of using electromagnetic methods for detecting agricultural products (fruits, vegetables, and meats) in closed baggage. Such a method of inspecting baggage would greatly assist the Animal and Plant Health Inspection Service (APHIS) in detecting agricultural products brought into this country by international travelers. A division of the U.S. Department of Agriculture (USDA), APHIS is charged with the interception and destruction of agricultural products which may be diseased or harbor insect pests. Of course, agricultural products must be detected before they are inspected and destroyed. Since not all products are declared by travelers, a noninvasive method of detecting the products in baggage would greatly facilitate the inspection process.

International travelers are questioned about agricultural products which they are bringing into the country and, in some cases, their baggage is searched. Although the regulations and inspection procedures are well publicized [1] and are well known, travelers still attempt to bring illicit agricultural products through ports of entry. About 2% of international travelers declare possession of agricultural products, but it is estimated by APHIS officials that many more than this actually carry agricultural products. Visual inspection of the contents of travelers' baggage obviously offers the most reliable method for revealing agricultural products. However, this procedure is time consuming and often creates delays for travelers. A method of detecting products without opening baggage would minimize the inspection time and provide the additional benefit of an increased intercept rate.

To obtain background information on baggage inspection procedures, a visit was made to the International Concourse of Atlanta's Hartsfield International Airport. The visit was arranged through Atlanta APHIS personnel, who were very interested in this project. During the visit, passengers from several international flights were processed through

customs, immigration, and APHIS. It was observed that all inspections were referred to APHIS by customs officials, who had first contact with passengers. That is, the customs inspectors sent passengers who had declared agricultural products, or who had been discovered to have them, to the APHIS inspector on duty. This inspector then determined whether the product could be admitted or should be intercepted. The decision to intercept was based on several factors including product species, country of origin, and recent plant pathologies and pests in the country of origin. During the airport visit, inspectors related experiences of examining all baggage from international flights when it would not inconvenience passengers. During such complete searches, more than half of the baggage was sometimes found to contain agricultural products. It was clear that noninvasive inspection of baggage could substantially increase the intercept rate of contraband agricultural products.

Electromagnetic detection methods are based on differences between the dielectric properties of agricultural products and those of other baggage contents. Review of the literature revealed significant differences both in dielectric properties and in moisture content. During this project, measurements of dielectric properties were made to complement those found in the literature. Results of the literature review and measurements are given in Section II.

The following four approaches were initially identified to have the greatest potential for electromagnetic detection of agricultural products:

- o capacitor plate,
- o resonant cavity,
- o signal transmission/reflection, and
- o short pulse radar.

These four approaches were investigated using analytical and experimental methods and are described in Sections III, IV, V, and VI, respectively. Except for the short pulse radar in Section VI, the approaches are presented in the order of increasing frequency of operation. Conclusions based on

the results of this research and recommendations for further research are given in Section VII.

Technical efforts have been previously described in three reports to the USDA Science and Education Administration (SEA). These were Quarterly Technical Reports Nos. 2 and 3 and an Interim Technical Report.

II. DIELECTRIC PROPERTIES AND MOISTURE CONTENT OF AGRICULTURAL PRODUCTS

Since the electromagnetic detection of agricultural products depends strongly on the differences between the dielectric properties of the products and those of other baggage items, the dielectric properties and the related moisture content of agricultural products were researched in some detail. After an initial literature survey of moisture content and dielectric properties revealed certain gaps, measurements of dielectric properties of fruits were performed.

A. Values from Literature

Agricultural products considered for detection in this project were initially presumed to have high water, or moisture, content which would strongly influence their dielectric properties. The term "agricultural products" is used here to mean fruits, vegetables, and meats in fresh or near-fresh condition. These products are the most likely ones to harbor disease organisms and insect larvae. Their detection is thus more desirable than detection of dried fruits and meats which are less likely to be infested.

A survey of the literature was carried out to evaluate the moisture content of fruits, vegetables, and meats [2-6]. In Quarterly Technical Report No. 2, data collected for representative fruits and vegetables were listed in Table I; for meats and selected meat products, in Table II. Values were collected without regard to method of determination. Since most values were taken from recent compilations which did not reference original sources, it was possible that the identical values from different references came from the same original source. In all cases, the moisture content of fruits and vegetables was greater than 65% and in most greater than 80%. Moisture content of meats was generally lower than this with most values falling between 40 and 60%. Thus, as expected, moisture content was high in the agricultural products which were to be detected in baggage.

Because of the high moisture content of agricultural products, their dielectric properties are determined to a large extent by the dielectric properties of water, particularly above about 100 MHz. A survey of the literature revealed values for agricultural products over the wide frequency range of 1 kHz to 10 GHz [6-14]. It was found that work had been done over a 30-year span using several different methods. Data were gathered as, or converted to, the real and imaginary parts of the relative complex permittivity, $\varepsilon_r^* = \varepsilon_r' - j\varepsilon_r''$. The relative dielectric constant ε_r' is a measure of the electromagnetic energy storage capability of a material. The relative loss factor ε_r'' is a measure of the capability of a material to dissipate electromagnetic energy as heat. These two parameters are functions of frequency and temperature.

Dielectric property data were collected for temperatures from 20 to 25°C so that values could be validly compared across frequency. This range included common room temperatures and temperatures expected in baggage inspection areas. Data for frequencies from 1 kHz to 100 MHz are presented in Figures 1 and 2 for relative dielectric constant and relative loss factor, respectively. Log-log plots are used, as was done in Quarterly Technical Report No. 2, because of the large ranges of values. Data for frequencies from 100 MHz to 10 GHz are presented in Figure 3 with linear scales for dielectric properties in order that a straightforward comparison could be made with measured values described below. The scatter in the dielectric values found in the literature was probably due to several factors. One factor was, of course, the use of different techniques by different investigators. Another was the difference in moisture content among different fruits, vegetables, and meats by species and variety. Other possible factors included duration of storage and state of maturity.

Despite the scatter, certain trends were evident in the values of dielectric properties taken from previous studies. The decreases in relative dielectric constant and loss factor from 1 kHz to 100 MHz were obvious (Figures 1 and 2). A much smaller decrease seemed to occur in

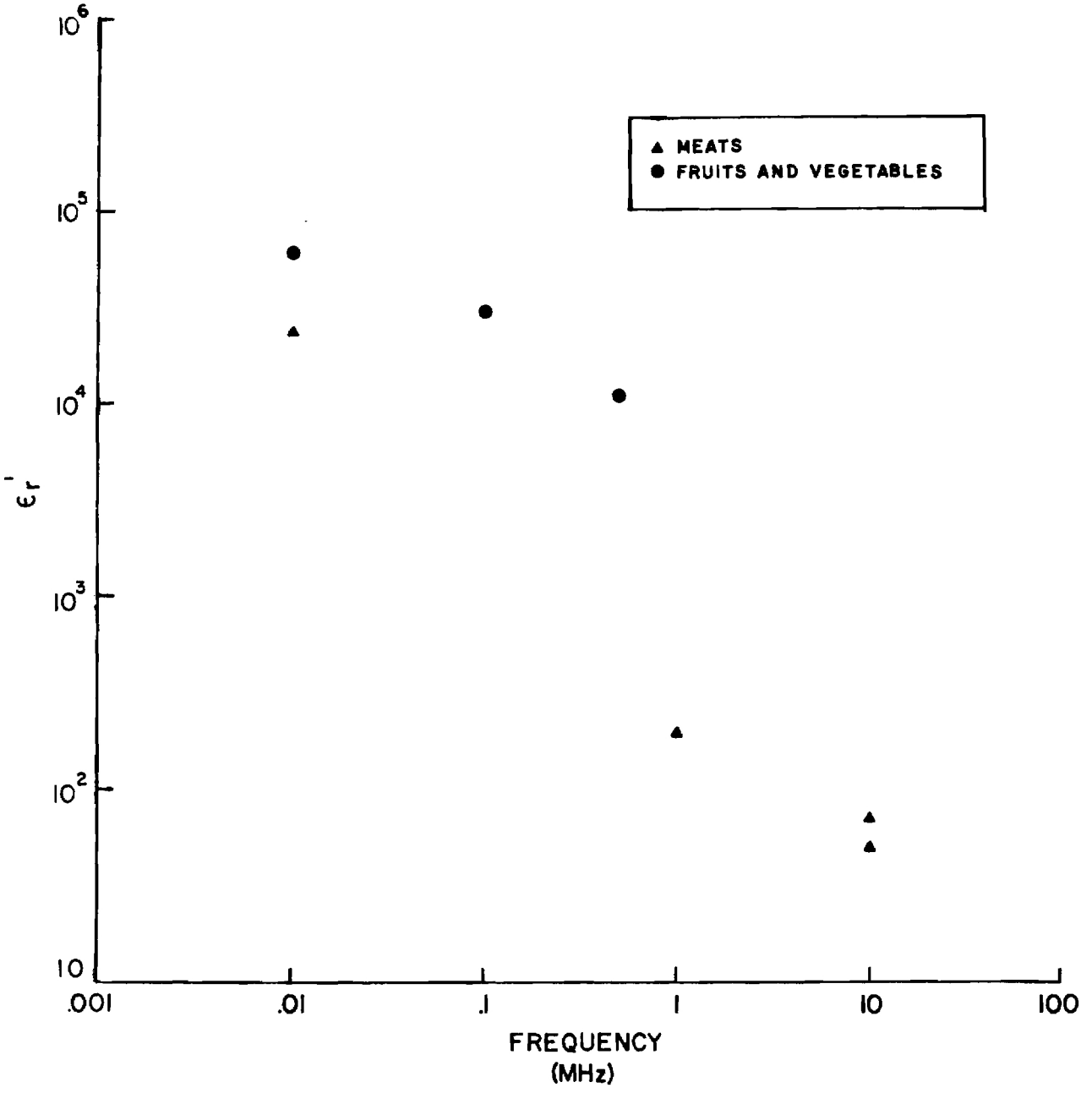

Figure 1. Relative dielectric constant of agricultural products versus frequency, 1 kHz to 100 MHz, 20 to 25°C. Literature values for fruits and vegetables (circles) and for meat (triangles).

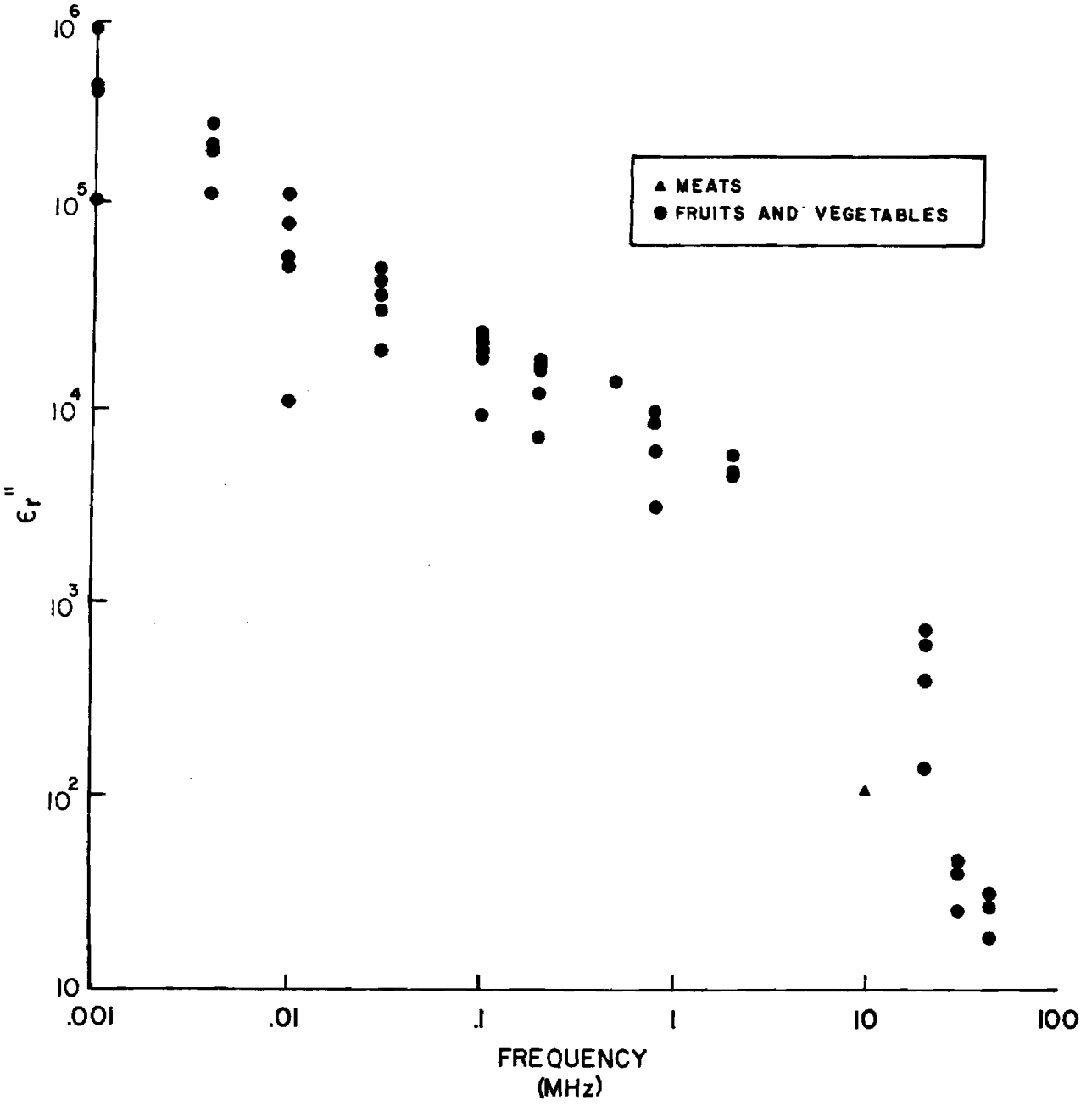

Figure 2. Relative loss tangent of agricultural products versus frequency, 1 kHz to 100 MHz, 20 to 25°C. Literature values for fruits and vegetables (circles) and for meat (triangles).

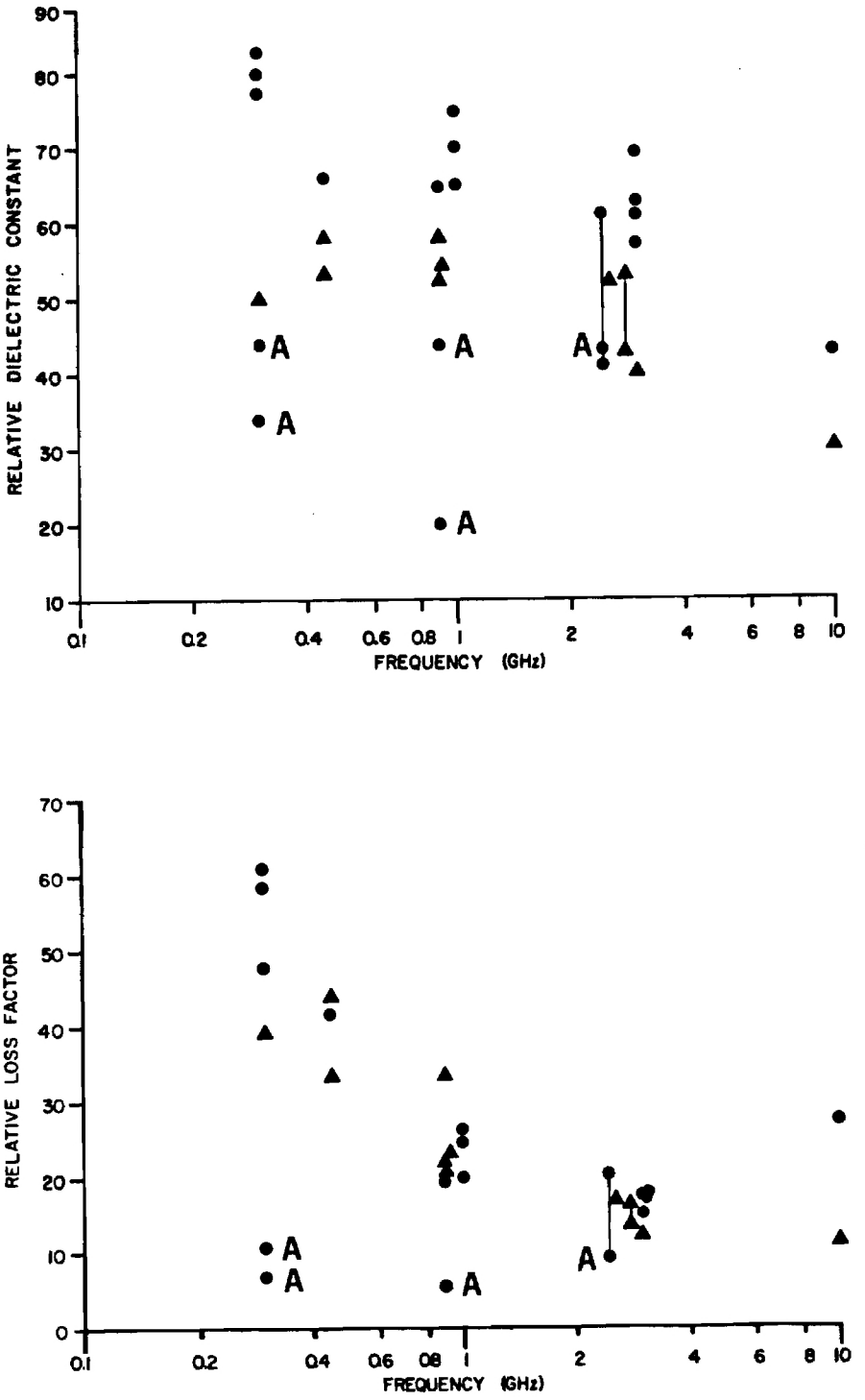

Figure 3. Relative dielectric constant and loss factor of agricultural products versus frequency, 0.1 to 10 GHz, 20 to 25°C. Literature values for fruits and vegetables (circles) and for meat (triangles). Letter A designates data for apples.

the relative dielectric constant for frequencies from 100 MHz to 10 GHz (Figure 3). The relative loss factor from 100 MHz to 10 GHz (also in Figure 3) showed considerable scatter, especially at the lower frequencies in this range. Although there was a general decrease in relative loss factor with frequency, a pattern was difficult to discern.

The dielectric data summarized in Figures 1-3 were used in initial evaluation of electromagnetic approaches investigated. Representative values of dielectric constants and loss factors were initially estimated from these data for all frequencies being considered. For frequencies from about 3 GHz to 10 GHz, relative dielectric constant and loss factor were described by analytic functions. These functions were derived by modifying previous expressions [15] with appropriate constants. The procedure resulted in the following expressions:

$$\varepsilon_r' = 40 + 10/f \qquad (1)$$

and

$$\varepsilon_r'' = \frac{20}{f} + \frac{f}{1 + (f/25)^2} \quad , \qquad (2)$$

where f is the frequency in GHz. These relationships were especially useful in initial studies of the signal transmission/reflection approach described in Section V.

B. Measurements of Fruit and Alcohol Dielectric Properties

Because three of the four proposed approaches for detecting agricultural products utilized frequencies between 0.1 and 10 GHz, more definitive dielectric data were desired in this frequency range in which a trend in relative loss factor could not be readily determined from published data. More exact values were especially desirable for theoretical analyses of the approaches. After discussion with the USDA technical monitor for this project, it was decided that Georgia Tech's Biomedical Research Division would measure the dielectric properties of representative

fruits by using methods already developed within the Division.

The dielectric properties of fruit were measured using an in-vivo probe technique. This technique had been used successfully to measure the dielectric properties of liquids and animal tissues from 0.1 to 10 GHz [16,17]. As reported here and in Quarterly Technical Report No. 3, the technique also worked well for plant tissues.

The in-vivo probe technique for measuring dielectric properties is based on an antenna modeling theorem which relates the complex reflection coefficient of an antenna to the intrinsic impedance of the surrounding medium. A medium's intrinsic impedance is determined by its dielectric and magnetic properties as discussed in Section V. Since the magnetic properties of plant and animal tissues are that of free space, differences in intrinsic impedance of tissue are directly related to differences in dielectric properties. Consequently, changes in an antenna's complex reflection coefficient can also be related to the dielectric properties of the medium into which the antenna is submerged.

The complex reflection coefficient was measured using an HP Network Analyzer System. Results were obtained from 150 MHz (0.15 GHz) to 6.4 GHz using this system. To cover this broad frequency range, several instrument sub-unit substitutions were made. Accuracy and speed were maximized by having the system under the control of a computer which also calculated dielectric properties from the reflection coefficient. The reflection coefficient with the antenna in air had been measured and stored in computer memory as part of calibration procedures before measurements on tissue were made.

The probe antenna consisted of the cut end of a small section of 0.085-inch semi-rigid coaxial cable. The cable's copper center and outer conductors had been gold plated to resist corrosion so that antenna properties would remain constant with use. The center conductor was extended only slightly beyond the cut outer conductor and insulator so that a large majority of the coupling of electromagnetic fields to plant tissue was by a capacitive, fringing electric field (and the magnetic field associated with it). This meant that the measurement was influenced

most strongly by dielectric properties within a few hundred micrometers of the antenna. Thus, the results indicated rather localized values for dielectric properties. This regional nature was taken advantage of to measure values for both the skin and the interior flesh of several fruits.

The measurement procedure started with calibration of the probe and determination of correction factors for use in compensating for various sources of error in the transmission lines used. Correction factors were derived for each frequency investigated. The properties of deionized water (assumed known) were determined to check for correct operation of the measurement setup. The skin of an intact fruit was then placed against the probe antenna by moving up a specimen on a laboratory jack until good contact was made with the downward pointing antenna on a smooth, level section of skin. For measurement of fruit flesh, a surface was exposed by slicing with a sharp scalpel blade and the sliced fruit was moved up with the laboratory jack.

Dielectric properties were computed as relative dielectric constant, relative loss factor, and conductivity. Conductivity is the ratio of induced current density (combined conduction and displacement) to the electric field and is also equal to the product of the relative loss factor and angular frequency ($2\pi f$). Relative dielectric constant and relative loss factor are dimensionless; conductivity values were given in Quarterly Technical Report No. 3 in millisiemens per centimeter (mS/cm). Relative dielectric constant and relative loss factor completely describe the dielectric behavior of a material and are used here for comparative purposes. Temperature, measured by inserting a YSI thermistor probe into the fruit, ranged from 17.5 to 24.0°C, the laboratory room temperature range.

Dielectric properties were determined for the skin and flesh of the following fruits over the entire frequency range of 0.15 to 6.4 GHz:

1. Golden Delicious apples,
2. Red Delicious apples,
3. Ripe (yellow skin) bananas, and
4. Tangelos.

In addition, measurements were made on oranges from 0.15 to 2.0 GHz; on peaches from 0.15 to 0.60 GHz and 3.8 to 6.4 GHz; and on over-ripe bananas with black skins from 1.8 to 6.4 GHz. All fruits were purchased during winter months in Atlanta area supermarkets. Due to technical problems with the 1.8 to 4.2 GHz instrumentation, results were not obtained for oranges and peaches in this frequency range. Also in this range, values of relative dielectric constant and loss factor for other fruits varied considerably more than typically seen in previous experience with this measurement technique. This was attributed to incomplete error correction factors.

Figures 4, 5, and 6 are plots of relative dielectric constant and loss factor for Golden Delicious apple, ripe bananna, and tangelo, respectively. Each figure contains values for the flesh (circles) and the skin (triangles) of the particular fruit. Values were plotted as the mean of 3 to 5 measurements at each frequency. Bars were used to show the standard deviation around each mean when it was greater than 5% of the mean.

Values of relative dielectric constant for the flesh of these three fruits were similar across the frequency range with the values (approximately 80 at low frequencies) for tangelo being about 15 units greater than for apple and banana. Tangelo flesh relative dielectric constant was very similar to that of distilled water (17.6-24.0°C) measured to be 80 at low frequencies and decreasing to 70 at 6.4 GHz (also see Figure 7). Values of relative loss factor for the flesh of bananna and tangelo were similar across the frequency range, forming a U-shaped curve for each fruit. The relative loss factor of apple flesh also had a U shape but was 5 to 20 units less than the values for banana and tangelo, with the larger differences occurring at lower frequencies. As shown in Quarterly Technical Report No. 3, values of conductivity were very similar for all three fruits' flesh across this frequency range.

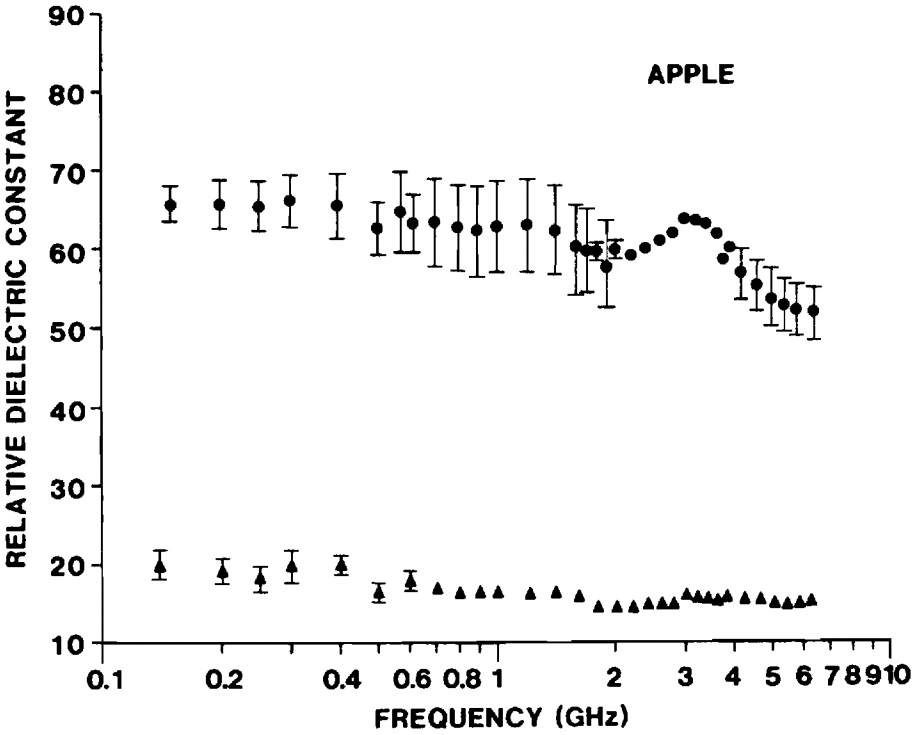

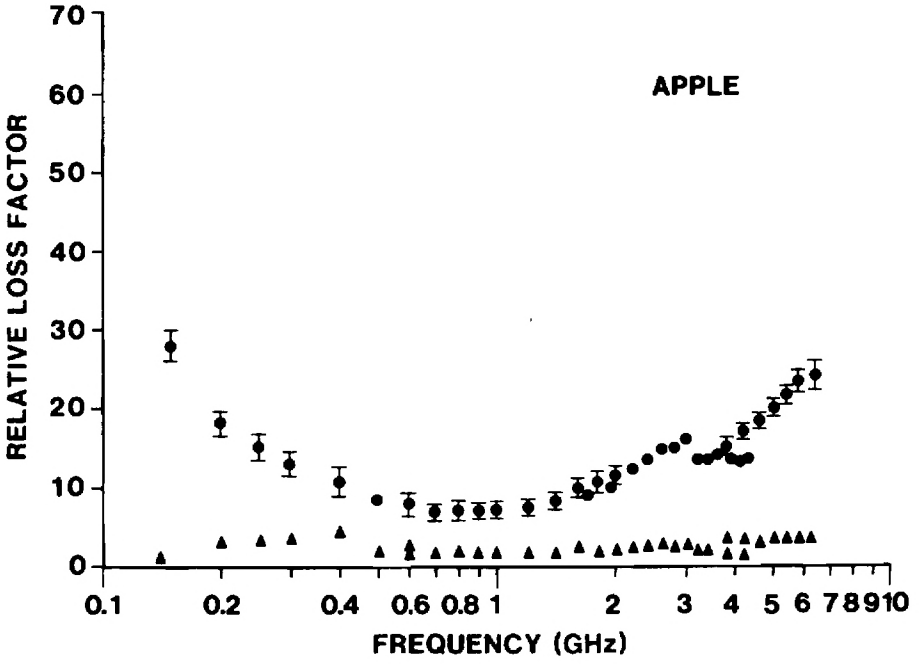

Figure 4. Measured relative dielectric constants and loss factors of Golden Delicious apples. Flesh (circles) and skin (triangles). Temperature 17.5 - 24.0°C.

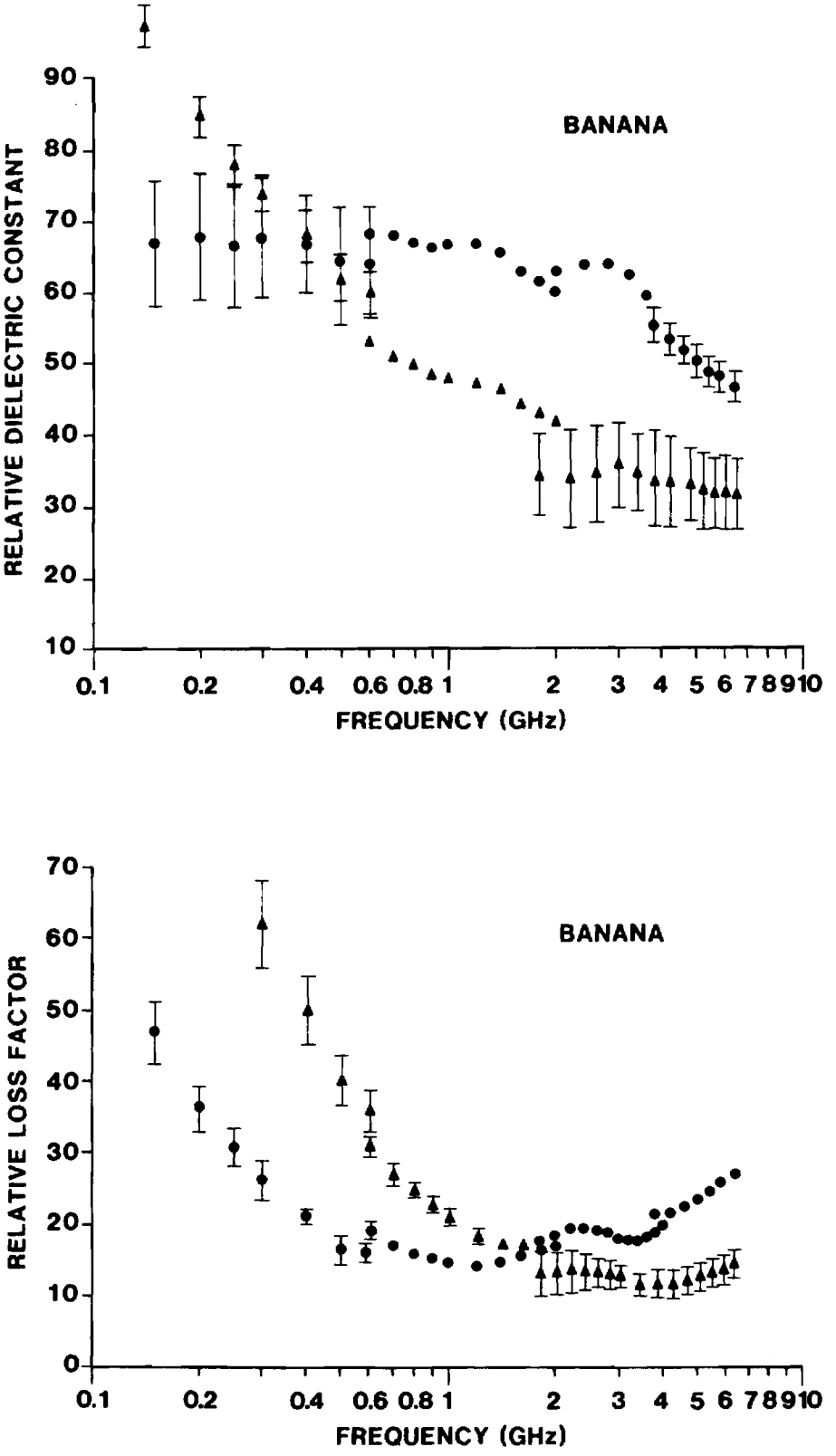

Figure 5. Measured relative dielectric constants and loss factors of bananas. Flesh (circles) and skin (triangles). Temperature 17.5 - 24.0°C.

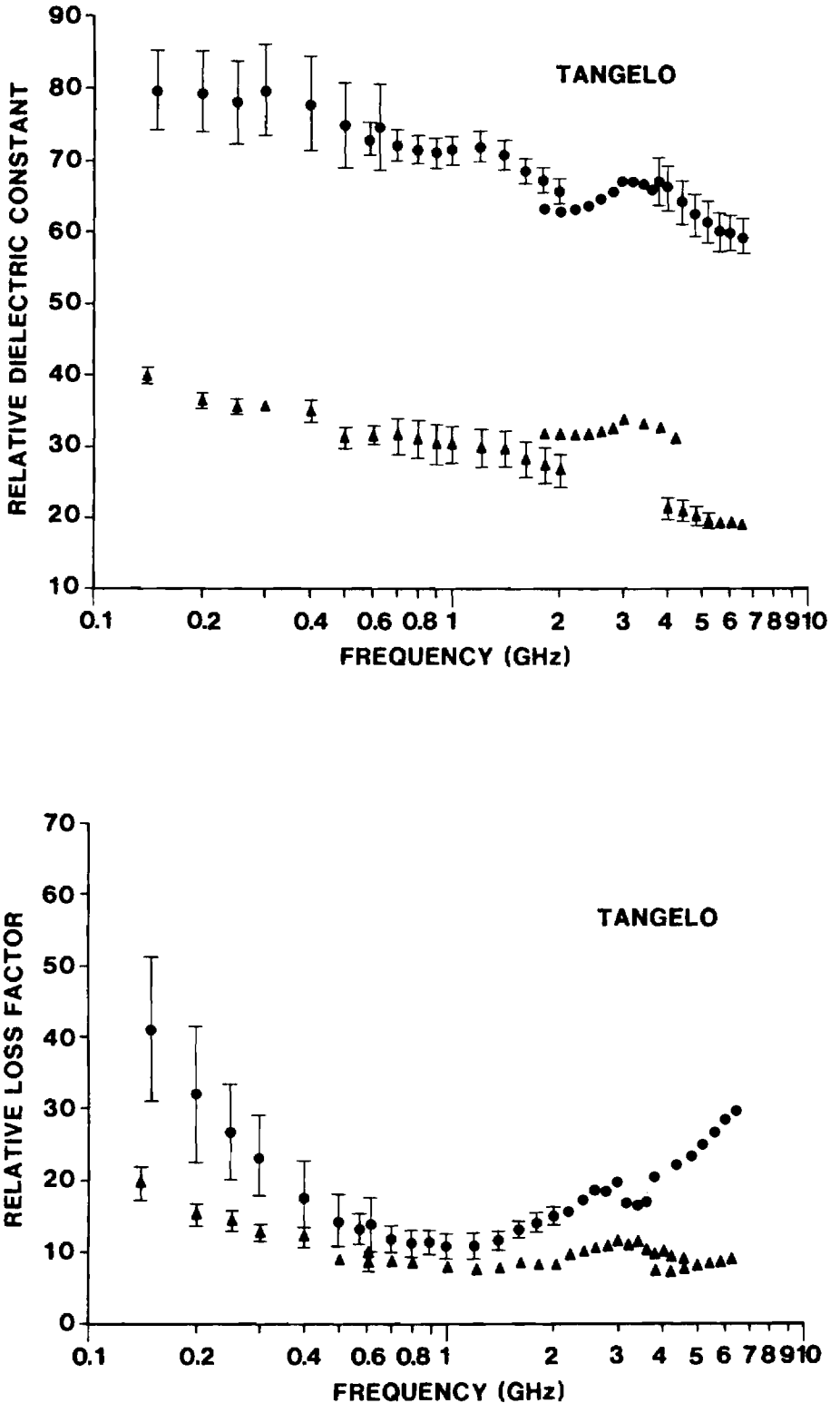

Figure 6. Measured relative dielectric constants and loss factors of tangelos. Flesh (circles) and skin (triangles). Temperature 17.9 - 24.0°C.

The dielectric properties of the flesh of other fruits could be described in terms of those shown in Figures 4, 5, and 6. Within measurement accuracy, dielectric properties of Red Delicious apple flesh were the same as those of Golden Delicious apple flesh. No difference was seen in the dielectric properties of ripe and over-ripe banana flesh from 1.8 to 6.4 GHz. Dielectric properties of orange flesh were the same as those of tangelo flesh from 0.15 to 2.0 GHz. For the two frequency ranges studied, relative dielectric constant of peach flesh was similar to that of tangelo flesh and about 15 units greater than that of banana flesh; peach flesh relative loss factor was similar to that of banana flesh.

Values of the relative dielectric properties of a fruit's skin were generally less than those for the respective fruit's flesh, with banana values at low and middle frequencies being the only exception. Values for apple skin (Figure 4) were the lowest measured: relative dielectric constant was between 15 and 20 and relative loss factor was less than 5 across the frequency range. Values for tangelo skin (Figure 6) were somewhat larger than this: relative dielectric constant was between 20 and 40 and relative loss factor was between 7 and 20. For frequencies higher than about 2 GHz, values for banana skin (Figure 5) were less than those for banana flesh and were only slightly greater than those of respective parameters for tangelo skin. At lower frequencies, both relative dielectric constant and relative loss factor were greater than banana flesh values, increasing to 97.28 ± 3.63 and 98.20 ± 11.79, respectively, at 150 MHz.

The dielectric properties of most other fruit skins could be described in terms of those shown in Figures 4, 5, and 6. Mean relative dielectric constant of Red Delicious apple skin was 2 to 3 units less than that of Golden Delicious apple skin for frequencies less than about 0.5 GHz and may have resulted from the small number of fruits measured. There was no difference at higher frequencies. Relative loss factor of Red Delicious apple skin was between 1 and 4 across frequency as it was for Golden Delicious apple skin. Mean relative dielectric constant of orange skin

was 2 to 7 units greater than that of tangelo skin for 0.15 to 2.0 GHz. Because of scatter in this parameter for both fruits, actual orange and tangelo skin values probably overlapped. A similar difference occurred in relative loss factors of these two fruit skins for frequencies below about 0.6 GHz, but values for orange skin above this frequency were smaller by about 1 unit. Again, these small differences may be attributable to sample size and values in larger samples may actually overlap. The dielectric properties of peach skin over the two frequency ranges studied were different than for other fruits. Relative dielectric constant of peach skin was relatively constant with mean values between 10 and 11 from 0.15 to 0.60 GHz and between 8 and 9 from 3.8 to 6.4 GHz. Relative loss factor of peach skin was less than 2.5 in these two frequency ranges and in some cases was too small to be measured with accuracy.

For each fruit, the dielectric properties of flesh and skin were different over the frequency range of 0.15 to 6.4 GHz. The ability to measure differences in relative dielectric constant and relative loss factor was due to the regional measurement capability of the probe technique. These differences should be taken into account in analysis of electromagnetic field interaction with fruit.

The scatter seen in measured relative dielectric constants and relative loss factors was assigned to three factors. The first is, of course, a combination of experimental error and variation in the measurement method itself. This latter source was probably responsible for the oscillatory nature of the dielectric properties from 1.8 to 4.2 GHz, originating in an incomplete error correction for this band. The second factor was variation in properties from measurement site to measurement site. The third factor was temperature which, from past experience, had been seen to cause as much as 1 unit/°C change in both properties in animal tissues.

The ultimate usefulness of an electromagnetic detection method may depend on its ability to discriminate between agricultural products and other items with high water content. For this reason, it was decided to measure the dielectric properties of ethanol solutions as models of

distilled spirits. Bottles of distilled spirits are frequenctly transported in travelers' baggage and could provide the most interference for electromagnetic detection of agricultural products. In a separate set of experiments, the same techniques described above for fruit were used to measure dielectric properties of aqueous solutions of ethanol from 110 MHz to 4 GHz. Concentrations of 25, 50, 75, and 95% ethanol by weight were used, the last being the purest form readily available.

Figure 7 shows the relative dielectric constant and relative loss factor measured for ethanol solutions along with values measured for distilled water (0% ethanol). Measurement-to-measurement variability in these properties was less than 1% due to the homogeneous nature of the ethanol solutions. Relative dielectric constant decreased for higher concentrations of ethanol. For lower concentrations, these values were not unlike those for fruit flesh. Relative loss factor was very small at lower frequencies and could not be measured accurately with the techniques used and these values were omitted from the plot in Figure 7. This was in contrast to the increasing values seen for fruit at lower frequencies. This difference in loss factor between 0.1 and 1 GHz may form the basis for discriminating between fruit and distilled spirits by electromagnetic methods. At high frequencies, relative loss factor increased by different rates depending on concentration but, in all cases, was smaller than values for fruit (note different scale used for ethanol relative loss factor).

C. Comparison of Measured Dielectric Properties with Previous Values

The measured fruit flesh relative dielectric constant and relative loss factor presented in Figures 4-6 can be compared with values for fruit taken from the literature. The various methods used previously required rather large samples which undoubtedly consisted entirely, or almost entirely, of flesh. To our knowledge, there is no previous report of dielectric properties of fruit skins for comparison with measured data.

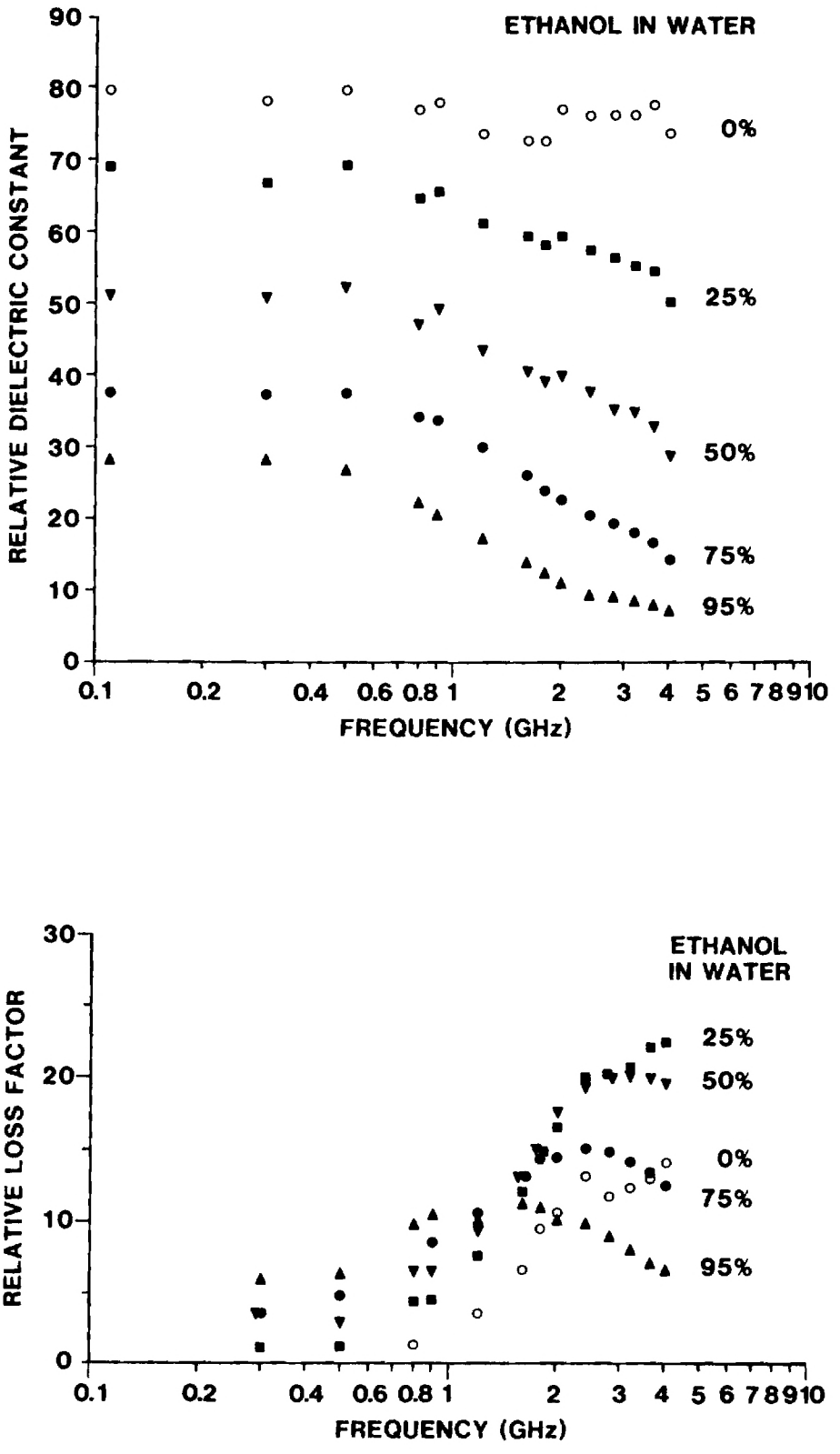

Figure 7. Measured relative dielectric constants and loss factors of ethanol solutions. Temperature 21.8 - 25.0°C.

Measured values of relative dielectric constant for the three fruits' flesh were in the upper part of the reported range (Figure 3). For the fruits in this study, this parameter was found to be relatively constant across the frequency band of 0.15 to 6.4 GHz, showing a decline of less than 20 units at higher frequencies. This shape was not obvious in the composite data of Figure 3. Measured values of relative loss factor showed a dip near 1 GHz which was not evident in reported data although measured values fell among the scatter in those data.

Thus, the measured values displayed definite patterns and were consistent with previous data in many respects. It should be kept in mind that the previous data were taken from several fruits and vegetables and that a better comparison can be had by comparing data by species. With existing data, such a comparison can be made for apples and peaches. In Figure 3, the letter "A" was placed beside data points associated with apples. Data at 0.3 and 0.9 GHz were taken from reference 13; those at 2.45 GHz, from reference 6. All previous values of relative dielectric constant were smaller than those measured here for apple. This was also true when original data for mature and immature apples for 0.3 to 0.9 GHz [18] were compared. Previous values of relative loss factor were similar to those measured for apple, being only slightly less. Previous dielectric property values for peaches [6] were measured at 2.45 GHz. Although peach measurements were not made at this frequency in this project, a comparison can be made by interpolating between the frequency ranges studied. In this way, peach flesh relative dielectric constant was estimated as 72, about 15 units higher than previous values of 55 to 61. An estimated relative loss factor of 15 fell within the previously reported range of 13 to 17 for ripe peaches.

Since it was expected that the dielectric properties of all tissues of high water content would be similar above about 100 MHz, it was not surprising to see similar values for all three fruits studied. Values for fruit relative dielectric constant and relative loss factor were different from those of water which vary approximately from 80 to 70 and 1 to 25, respectively, from 0.1 to 10 GHz [17]. This difference was

expected because of the cell structure and dissolved substances in the plant tissues. Measured values of relative dielectric constant (Figures 4-6) and conductivity (Figures 7-9 of Quarterly Technical Report No. 3) were very similar to those reported for animal tissues of high water content [15-17, 19]. These similarities were predictable from the comparable water content and structure of plant and animal tissues.

Measured relative dielectric constant and relative loss factor of ethanol solutions (Figure 7) can be compared with values in the literature. Measured values of these two parameters at 1 GHz and 3 GHz agree very well with previous measurements made at 25°C [20]. They also match other measurements at 3 GHz at 25°C which were made to show the utility of an interactive model for the dielectric properties of aqueous mixtures [21].

The measurements of dielectric properties in this project confirm the differences between fruit and other suitcase items such as clothes. Data on ethanol solutions showed some similarities and some differences with fruit. This information, along with differences in fruit skins, was valuable in further assessing electromagnetic methods for detection of agricultural products.

III. CAPACITOR PLATE APPROACH

Introduction of an agricultural product into a capacitor will change the electric field between the capacitor's plates. The change will be related to the product's permittivity which differs from that of the low-loss, low-dielectric constant material which usually fills interplate space. Effects of agricultural products on capacitance, and, consequently, capacitor impedance, were investigated.

Parallel plates were used to form capacitors and were studied as individual capacitors and as arrays of capacitors. Both theoretical analyses and experimental studies were performed on these two configurations.

A. Analysis and Array Design

A capacitor is formed by any two conductors separated by a dielectric medium. Voltage applied across the capacitor's conductors (usually plates) will result in (a) a build-up of electrical charge on each conductor and (b) an electric field between the conductors.

Capacitance is equal to the ratio of the magnitude of charge Q on each conductor to voltage V between conductors:

$$C = Q/V. \qquad (3)$$

Capacitance is determined by (a) the size and separation of the plates forming the capacitor and (b) the dielectric properties of material between the plates. Because of this latter factor, measurement of capacitance can be used to detect objects placed between a capacitor's conductors.

An empty capacitor is one in which the electric field is established in a vacuum. The capacitance of an empty capacitor is denoted here by C_o, the vacuum capacitance, which represents the effect of capacitor geometry on capacitance. It was extremely useful in analyzing the effect of an object inserted between the capacitor's conductors. For example, if the region between the conductors was completely filled by a material having a real relative permittivity ε_r, capacitance was given by [14]:

$$C = C_o \varepsilon_r . \qquad (4)$$

Capacitance was experimentally determined by measuring a capacitor's electrical impedance Z:

$$Z = 1/j\omega C = -j/\omega C , \qquad (5)$$

where ω = angular frequency = $2\pi f$ and $j = \sqrt{-1}$. The simple relationships given by equations (4) and (5) were useful in evaluating the parallel-plate capacitor.

A capacitor consisting of a set of parallel metal plates was considered because of several features that make it extremely well-suited for detection applications. These features included the following:

- Restricted electric field to minimize potential problems such as electromagnetic interference and hazards that could result from unconfined, radiated fields;
- Uniform electric field, perturbations of which would be relatively insensitive to object location; and
- Conveniently modeled electrical response.

In an ideal parallel-plate capacitor, vacuum capacitance C_o can be accurately described as

$$C_o = \varepsilon_o A/d, \qquad (6)$$

where ε_o = permittivity of free space,
A = area of each plate, and
d = distance between plates.

This relation made it possible to study the electrical response of an ideal parallel-plate capacitor. Since C_o of most capacitors is extremely small, equation (5) indicated that the impedance of an empty parallel-plate capacitor was a very large negative reactance.

The electric field of a parallel-plate capacitor was assumed to be completely contained within the volume directly between its plates. This meant that if the volume between the plates were filled by a material with a relative complex permittivity ε_r^*, equation (4) held and, from equation (5), impedance of the filled capacitor was

$$Z = -j/\omega\varepsilon_r^* C_o. \qquad (7)$$

Knowledge of C_o from equation (6) and ε_r^* (from measurement or from the literature) made it possible to predict accurately the impedance magnitude and phase of a capacitor. Materials such as plastics, fabrics, air, or other non-conductors that are normally found in baggage typically have a real relative permittivity (relative dielectric constant) that is between 1 and 5. With these materials placed between the plates of a parallel plate capacitor, equation (7) showed that the impedance was a large negative reactance comparable in magnitude to that of the empty capacitor.

Conversely, agricultural products with high moisture content have complex relative permittivities, as discussed in Section II. With these materials placed between the plates of a parallel-plate capacitor, the impedance was no longer purely reactive. Instead, it was of the form

$$Z = [j\omega C_o \varepsilon_r^*]^{-1}$$

$$= [\omega C_o \varepsilon_r'' + j (\omega C_o \varepsilon_r')]^{-1}. \qquad (8)$$

That is, the impedance had both resistive and reactive components and could be modeled as a parallel resistor and capacitor.

Figures 1-6 show large values of relative dielectric constant and relative loss factor for agricultural products. For frequencies between 1 and 10 MHz, the values range between approximately a hundred and several thousand. This meant that, in addition to impedance being a complex quantity, its magnitude was significantly smaller than the impedance when only non-conducting, low-dielectric constant materials were present

between the plates. In fact, for comparative purposes, the complex impedance of equation (8) was approximated as zero, a short-circuit.

In Quarterly Technical Report No. 2, the simple capacitor model was modified by introducing a pair of metallic sheets to represent a block of agricultural product, as shown schematically in Figure 8. This was justified by the approximation that the product's internal impedance was very small. Analysis of this filled capacitor as three simple capacitors in series resulted in the following expression:

$$Z_{total} = \frac{2}{3} (j\omega C_o \varepsilon_{r1}')^{-1} + \frac{1}{3} [\omega C_o \varepsilon_{r2}'' + j(\omega C_o \varepsilon_{r2}')]^{-1} . \qquad (9)$$

As noted above, the impedance magnitude of a capacitor filled with an agricultural product was extremely small relative to the impedance magnitude of the same capacitor filled with a non-conducting, low-dielectric constant material. When this fact was applied to the impedance described by equation (9), it was seen that the total impedance of the capacitor configuration in Figure 8b was approximately two-thirds of the impedance with no agricultural product present. That is, the presence of the agricultural product effectively short-circuited its volume fraction of the impedance. Therefore, plate size as it affected capacitor volume became an important design factor. Since the impedance in equation (9) is a complex quantity, it initially seemed that its amplitude and phase could serve as useful measurement parameters. However, because an object with a large relative complex permittivity essentially acted as a "short-circuit," the net impedance remained almost purely reactive even with an object present. Therefore, the impedance phase was judged not to be very useful for detection purposes since it would not deviate far from -90°.

Impedance magnitude was potentially useful if the capacitor plates were of appropriate size in relation to the object to be detected. The effect of capacitor plate size was examined analytically with a cube of saline d x d x d in size between plates separated by 3d. Figure 9 shows

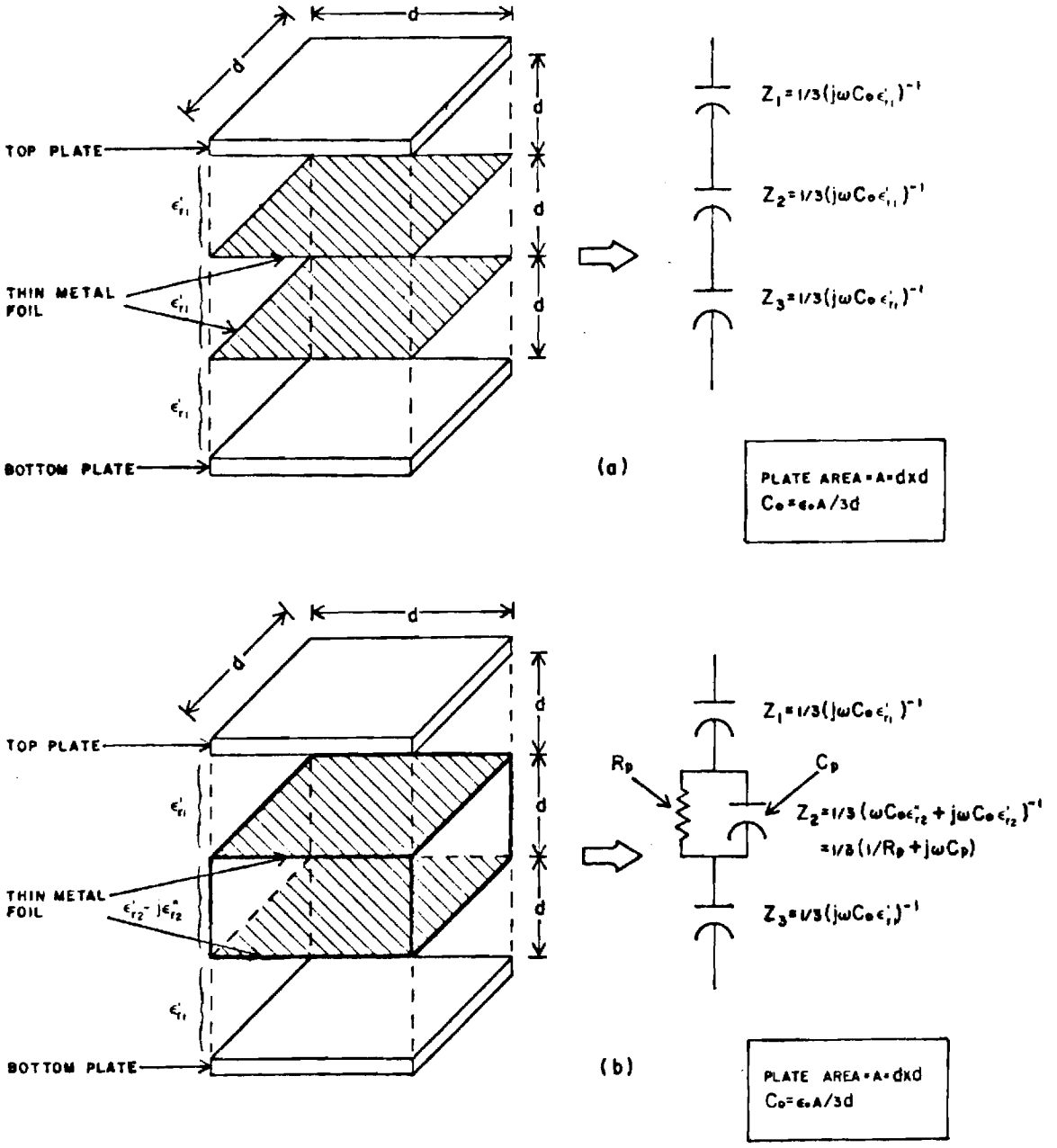

Figure 8. Parallel-plate capacitor with thin metal sheets inserted. In Figure 8a, the volume between the plates is filled with materials that have a real relative permittivity (ε'_{r1}) that is small in magnitude. In Figure 8b, the volume between the two metal sheets is filled by material with a complex relative permittivity ($\varepsilon'_{r2} - j\varepsilon''_{r2}$) that is large in magnitude.

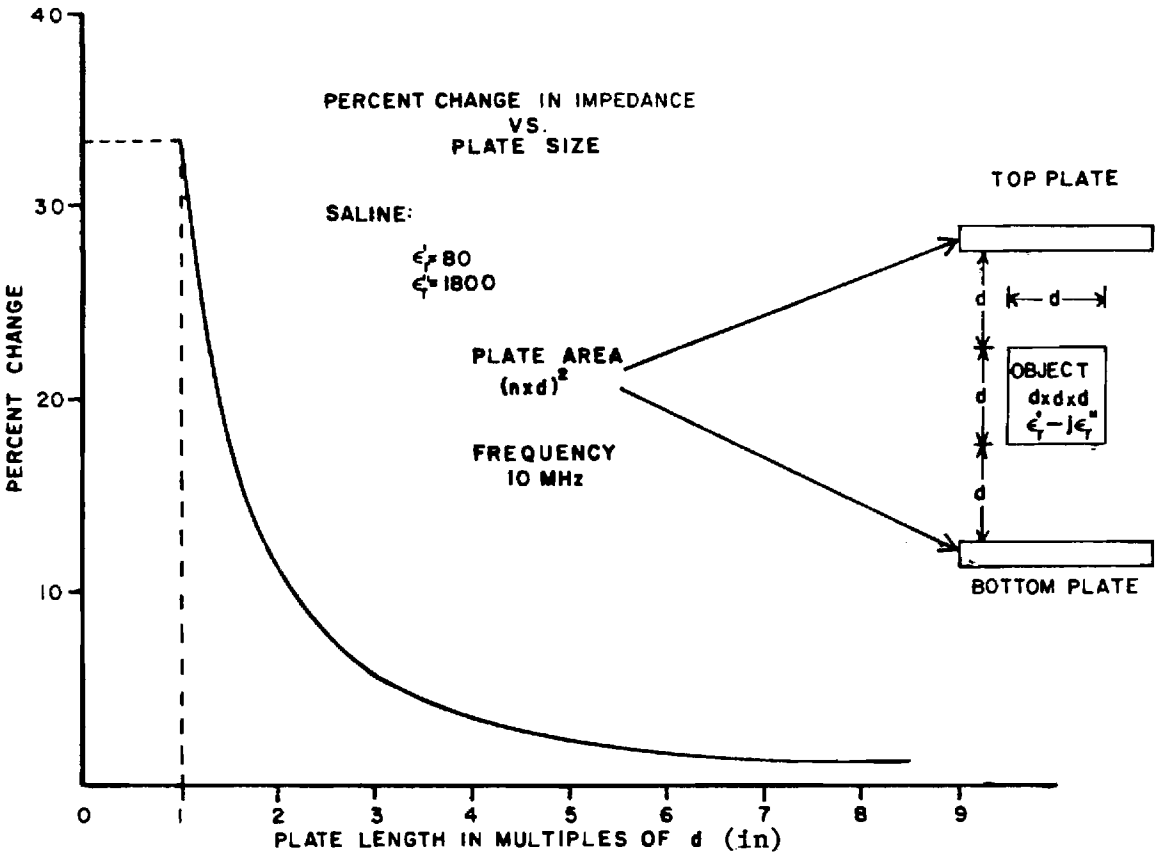

Figure 9. Percent change in impedance of capacitive plate detector as a function of plate size. The target object is modeled as a dxdxd cube centered between the air filled ($\epsilon_r' = 1$) plates. Percent impedance change is determined from the difference in impedance of the plate capacitor when empty and with the target present. Plate size (square) is specified by the length of one side in integral multiples of d.

that the maximum change in impedance occurred when the size of the capacitor plates was equal to or smaller than the cross-sectional area of the target cube. Therefore, for maximum sensitivity, the size of the capacitor plates should be comparable to the dimensions of the agricultural products to be detected.

One way in which capacitor plate detection can be used most efficiently to scan a suitcase for agricultural products is to use an array of capacitors. The design of a multiple-plate array required that array size as well as element size and spacing be specified. Each element of an array consisted of a pair of parallel metal plates forming a capacitor. In some cases, one plate was large enough to act as a second plate for several array elements. Initial studies on guard rings, plates arranged around actual array plates, were made using two array plates and a guard ring. Measurements of plate impedance with a beaker of saline inserted as a target showed that although a guard ring produced a more uniform field in the area under array elements, the electric field lines were distorted by the target so that the impedance change versus target displacement still showed a "fringing" response. Figure 10 illustrates electric field line configurations for empty plates and for plates with a spherical fruit-like object between them. The object tends to "pull in" the field lines and when the plate is small enough or the object is close to a plate edge, field lines from an adjacent pair of plates are affected. This resulted in an effective fringing for the adjacent array element and was measured as a change in impedance. Thus, guard rings produced more uniform fields but did not improve spatial resolution of object detection.

Calculations based on equations describing the fields surrounding a solid dielctric sphere and a metal sphere in a uniform electric field showed that distortion by the target was small beyond two radial distances from the center of the sphere. In addition, it was found that dielectric spheres introduced very nearly the same field distortions as metal spheres when the relative dielectric constant was greater than 5. Even dielectric constants between 2 and 5 exhibited substantial field distortion. However, it was noted that, although the spatial distribution varied little with

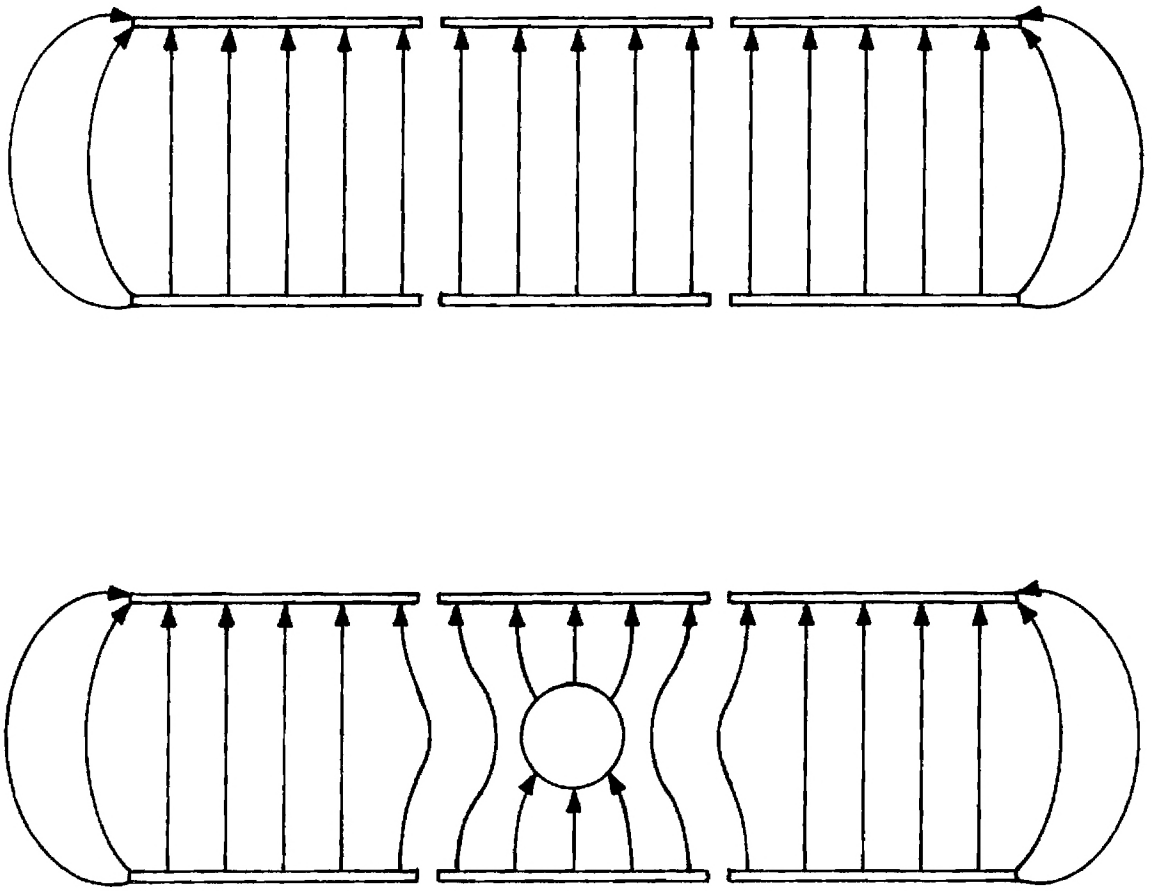

Figure 10. Electric field lines between capacitor plates with and without fruit present. Shows effective "fringing" in adjacent pairs of plates due to fruit.

small dielectric constant, the relative impedance change varied substantially with dielectric constant. Metal objects would cause impedance changes similar to those caused by objects with a high dielectric constant.

Analysis had shown that an array element which was similar in size to a target's cross-sectional area would exhibit a larger relative change in impedance than a larger element. However, impedance magnitude increased proportionally as element area decreased (see equations 6 and 7) creating measurement difficulties. A trade-off between sensitivity and measurement capability resulted in prototype array elements of 6 inches by 6 inches, corresponding to roughly twice the diameter of apples which were selected as trial targets. This size also provided an element large enough to support nearly all electric field lines passing through a centered apple. Air gaps between the plates and target decreased sensitivity by effectively inserting large impedances in series with the small impedance of the target. Therefore, the prototype array was designed so that the plate separation could be adjusted to allow positioning of the plates close to the sides of the baggage.

A guard ring configuration was installed on the prototype array to help make element responses uniform with respect to their distance from the array border. It was also decided to maintain initial field uniformity by driving all array elements and the guard ring at the same voltage. With the elements at the same voltage, stray coupling between elements because of reduced plate-to-plate current flow. Frequencies in the range of 1 to 5 MHz were chosen to drive the array so that element impedances would be low enough to be conveniently measured. Resonance in the cables connected to the array was also avoided at these frequencies.

B. Measurements

Results of the theoretical analysis indicated the potential feasibility of the capacitor plate detection concept. However, since this theoretical analysis was based on idealized models, a series of laboratory tests were performed to provide further evaluation of this approach. Measurements were made on pairs of plates forming a single capacitor, two pairs of

plates, and an array of 24 pairs of plates. It was decided to use relatively high frequencies to reduce the large reactive impedance of the large plate spacing required to accommodate luggage. A frequency range of 1 to 10 MHz was initially selected because of the availability of a network analyzer system which operated over this range. Later, this range was narrowed by considering frequencies of 1 to 5 MHz for the capacitor array.

A diagram of the apparatus used in tests on one and two capacitors is shown in Figure 11. This diagram includes the feed system developed through experience and described in detail in Quarterly Technical Report No. 2. A Hewlett Packard (HP) 8601 Sweeper/Generator provided the 1-10 MHz RF signal. An HP 8407 Network Analyzer mainframe with an HP 8412 Phase-Magnitude Display was used to compute the complex ratio of the two sampled test signals (V_v/V_i). Since V_v and V_i were directly proportional to the capacitor voltage V and current I, respectively, their ratio was directly related to the capacitor impedance ($Z = V/I$). The magnitude of the ratio was displayed in dB units (i.e., 20 log V_v/V_i) while the phase was displayed in degrees. Since initial observations confirmed the analytical prediction of phase insensitivity to objects inserted between plates, only impedance magnitude was studied in detail.

The capacitor plates selected for initial tests were one small plate (6 by 6 inches) and one large plate (22 by 17 inches) with a separation distance of 10 inches. The smaller plate was fed RF energy while the larger plate served as the ground plate. Swept-frequency measurements of the capacitor plate impedance were made with the plates empty and with 750 ml of a saturated sodium chloride solution in a 1000 ml glass beaker present. Since capacitor impedance was inversely proportional to frequency, it was anticipated that, in both cases, the impedance magnitude should decrease by 20 dB as the frequency was increased from 1 to 10 MHz. Further, based on the volume of saline, a constant 2-3 dB decrease in impedance magnitude was expected over this frequency range when the beaker of saline was placed between the plates. As shown in Quarterly Technical Report No. 2, measurement results were in excellent agreement with these analytical predictions, indicating the validity of the derived equivalent circuit models.

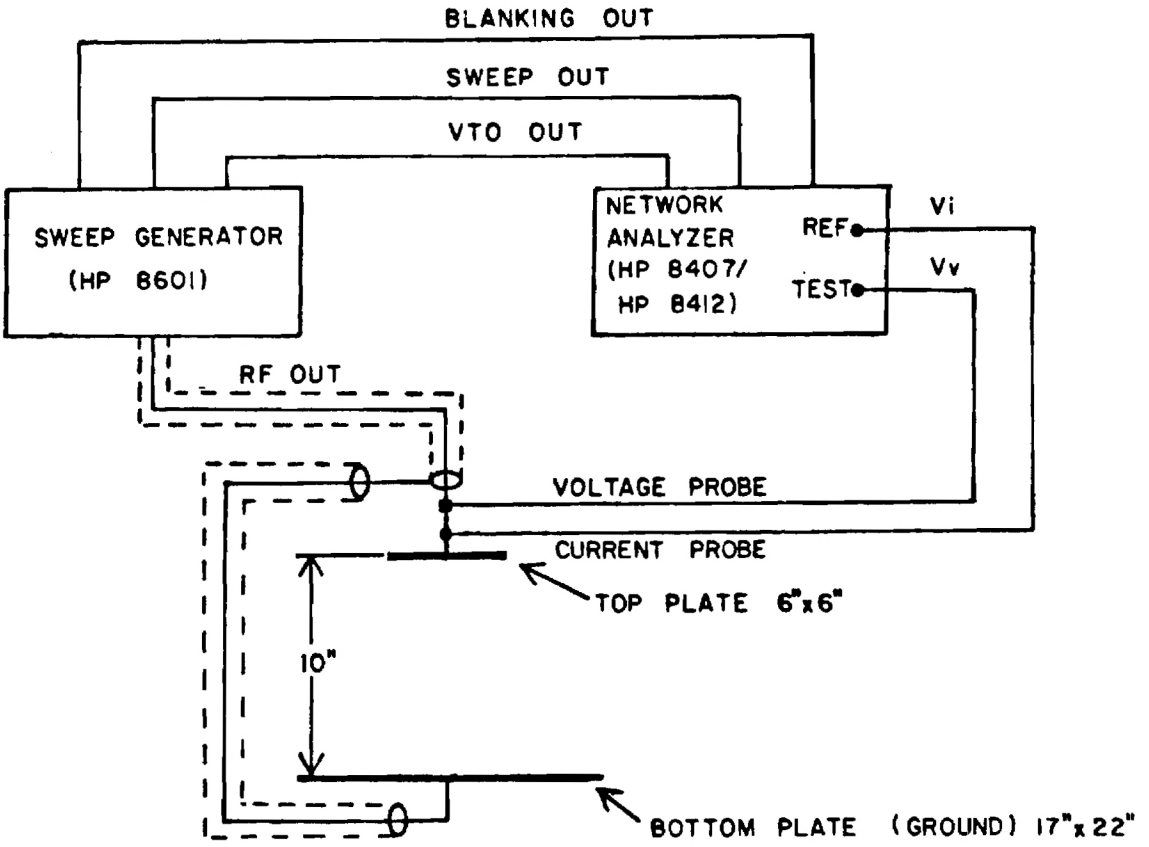

Figure 11. Apparatus used in testing capacitor-plate detection concept. The voltages V_v and V_i sampled by the network analyzer are respectively proportional to the voltage and displacement current across the capacitor formed by the two plates.

For the next sequence of measurements, capacitor impedance magnitude was measured as a function of object position between plates forming a capacitor. Two capacitors were studied: one with the plates described above and one with both plates 6 by 6 inches. For both capacitors, plates were positioned horizontally and a beaker of water was moved horizontally in a straight line through the inter-plate space in 1-inch steps. These measurements were facilitated by using a plywood structure to support the plates and Plexiglas platform to move the beaker. The details of this apparatus were given in Quarterly Technical Report No. 3. A single frequency was used in these tests as object position became the independent variable. The origin of an x-y-z coordinate system was chosen to be half-way between the centers of the two plates.

The relative changes in impedance magnitude (referenced to empty plates) with beaker location in horizontal x and y directions in the capacitor with the small plate are shown in Figure 12. As expected, the electrical response was approximately Gaussian in shape. Also, the changes in impedance magnitude when the target was postioned beneath the smaller capacitor plate are reasonably well-defined. However, the impedance roll-off at positions beyond the edges of the smaller plate was not as sharp as would be expected for an ideal parallel plate capacitor. This non-ideal electrical response was partially due to the finite dimensions of the test object which resulted in an impedance change even though the x-y position of the target center was clear of the smaller plate. The response of the prototype capacitor was also influenced by electric fields fringing beyond the inter-plate space. Fortunately, these effects did not appear to be severe enough to affect significantly the feasibility of the capacitor-based detection approach.

Effects of plate size and frequency on the changes in impedance were studied with test object positions along a center line. Figure 13 shows that the effect of changing plate size was small. Only for distances greater than 3 to 4 inches from plate center were the responses consistently different and then only by a small fraction of the total change caused by the test object. Tests made at 1 and 10 MHz showed very small differences in response with frequency. Thus, it is unlikely that ground-plate size

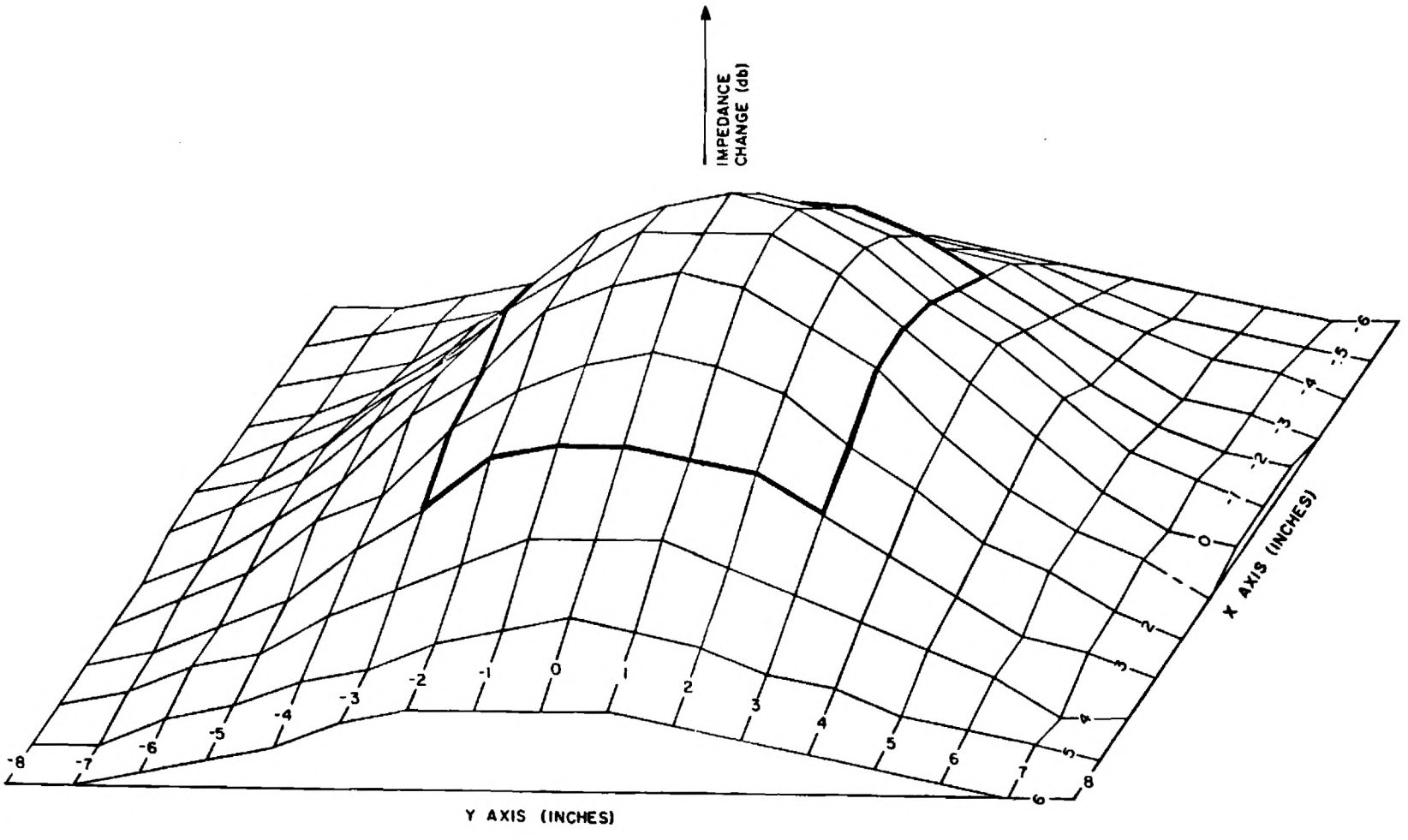

Figure 12. Profile of the electrical behavior of the prototype capacitor. Values taken at positions corresponding to the edges of the top 6 x 6 inch plate are indicated by heavy lines. Measurements performed at 10 MHz.

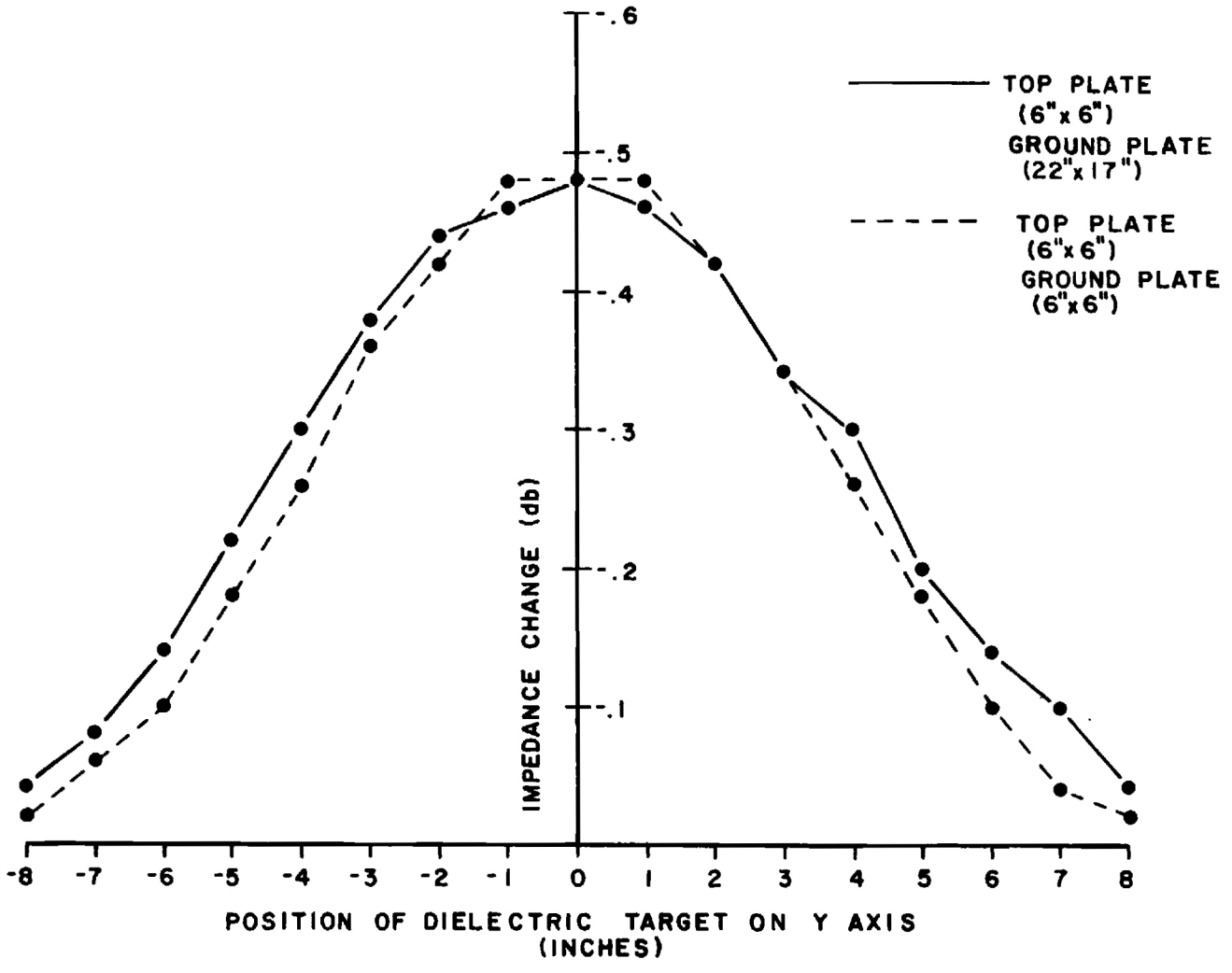

Figure 13. Effect of ground plate size on the electrical response of parallel plate capacitors. Measurements were performed at 10 MHz.

and frequency will be critical factors in the design of capacitor plate detectors.

Measurements on two pairs of capacitor plates were performed using a configuration similar to that used for a single pair with addition of another 6-inch by 6-inch capacitor plate and 6-inch guard ring plates on top of the plywood structure. Measurements taken with this configuration confirmed that the guard ring, although helping eliminate non-uniform field effects at the sensing plate edges, did not significantly reduce the sensing of the target beyond the plate edges. Figure 14 shows typical results which, like all results in this section, are expressed as changes in impedance relative to that of empty plates.

Measurements were also made on a pair of 3-inch by 3-inch plates with a 6-inch guard ring in the same setup as above to give the results shown in Figure 15. The frequency was increased to 10 MHz to provide a lower, more conveniently measured impedance. The relative impedance changes were on the order of twenty times greater with the 3-inch plates than those measured with the 6-inch plates. Ten megahertz was approximately the highest frequency which could be used without resonance problems due to the cabling and measurement configuration.

An array of 24 6-inch by 6-inch metal plates and surrounding 6-inch guard plates was supported on a sheet of 1/2-inch plywood. These plates formed the top of a 6 by 4 element array of capacitors. Each plate was insulated from adjacent plates so that each element's current could be measured individually. A single 36-inch by 48-inch plate was fastened to another 1/2-inch sheet of plywood to which four Plexiglas support rods were attached to serve as the bottom of the prototype array. The support rods had a series of holes so that pins could be inserted to hold the top array at plate separations from 4-1/2 to 14-1/2 inches in 1-inch increments. The top plates were each connected by a separate length of wire to a common tie point to which the guard ring plates were also connected. The connection at each top array plate was made by a tip plug so that a current probe could easily be inserted in series with each array element. Array and guard ring plates were connected to the

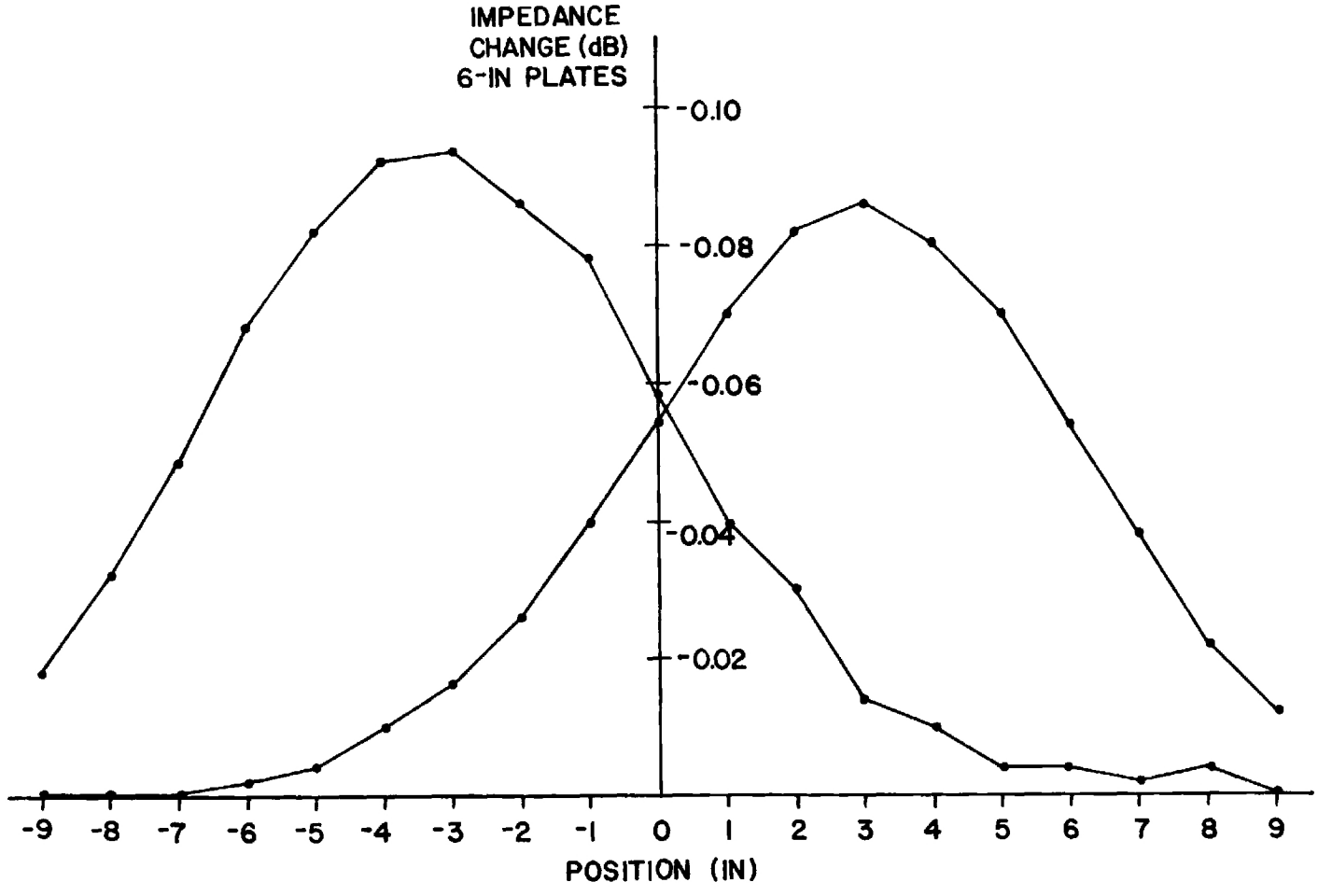

Figure 14. Impedance changes for two pairs of guarded 6-inch plates versus sample position. Plates were between positions -6 and 0 and 0 and 6. Sample was 250 ml of saline. Frequency was 5 MHz.

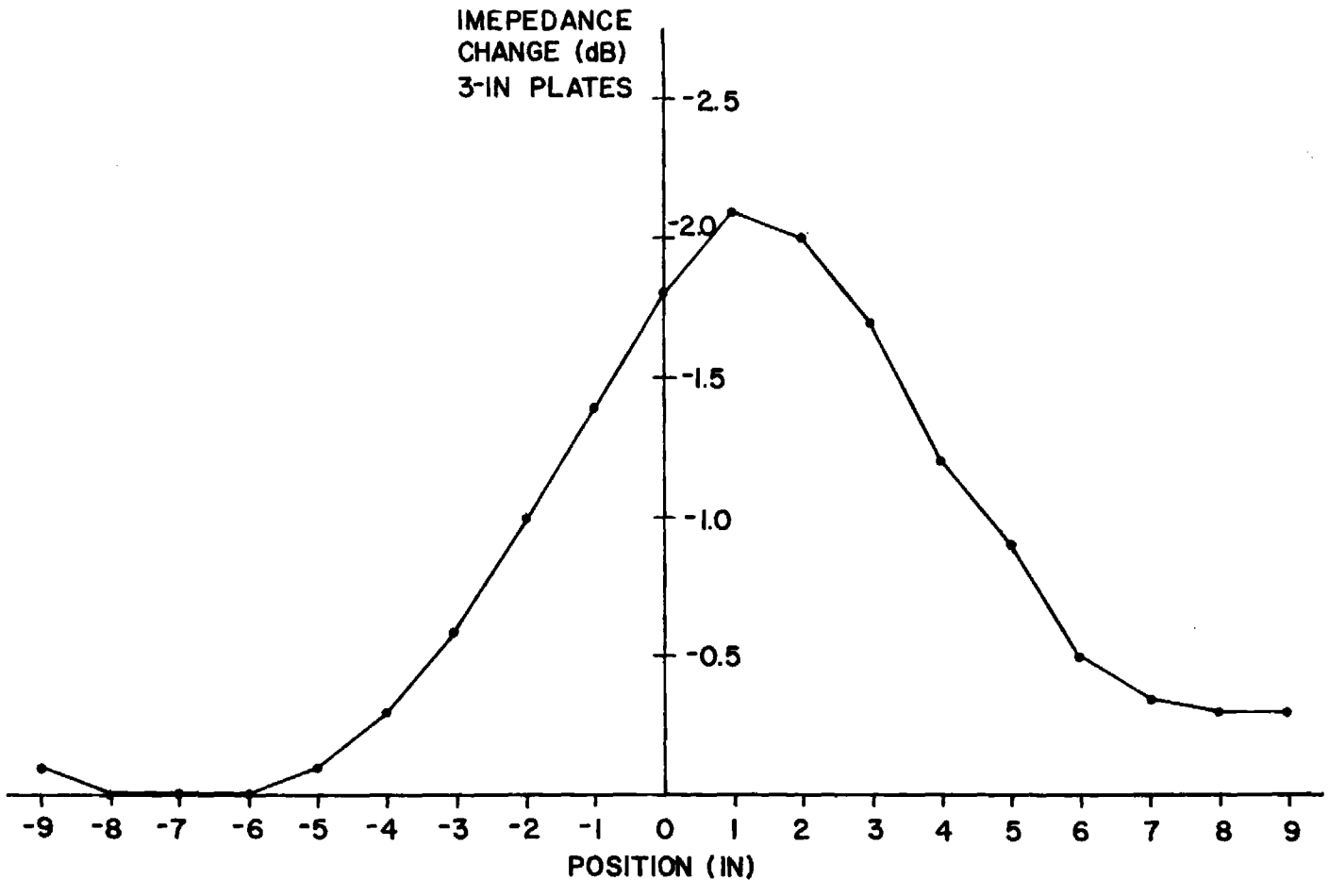

Figure 15. Impedance changes for one of two pairs of guarded 3-inch plates versus sample position. Plates were between positions -3 and 0 and 0 and 3. Sample was 250 ml of saline. Frequency was 10 MHz.

signal generator ground and the large bottom plate was connected to the high side of the generator. The array was grounded to minimize current measurement errors due to stray reactive coupling to shields on current probe leads. The instrumentation and electrical configuration of the array are pictured in Figure 16.

After design and construction of the prototype capacitor array, impedance measurements were performed using a representative hardsided suitcase packed with clothes and with different numbers of apples as a realistic test object. Typical results of these measurements are depicted as impedance-change contours in Figures 17, 18, and 19. Results showed that the suitcase with clothes caused a substantial variation in impedance over the array. Since the relative impedance change caused by a single apple in the suitcase with clothes was approximately -0.7 dB and the average impedance change caused by the suitcase with clothes was approximately -1.5 dB, it was difficult to distinguish the presence of the apple without a priori knowledge of its existence (Figure 17). However, by comparing Figures 18 and 19 with the top of Figure 17, the presence of clusters of five and twelve apples can readily be seen. The ridge along the center of the reference suitcase (Figure 17) was believed to be due to field distortion by the suitcase's metal frame and sides.

C. Conclusions

Results of theoretical analyses and laboratory measurements indicated the potential feasibility of the capacitor plate approach. Future investigations should include both theoretical analysis and laboratory testing. Performance characteristics that should be further investigated include the following:

- Accuracy (ability to detect an agricultural product consistently),
- Resolution (ability to yield an estimate of the size and position of any detected agricultural product), and
- Speed (ability to analyze quickly raw data and indicate whether an agricultural product is present).

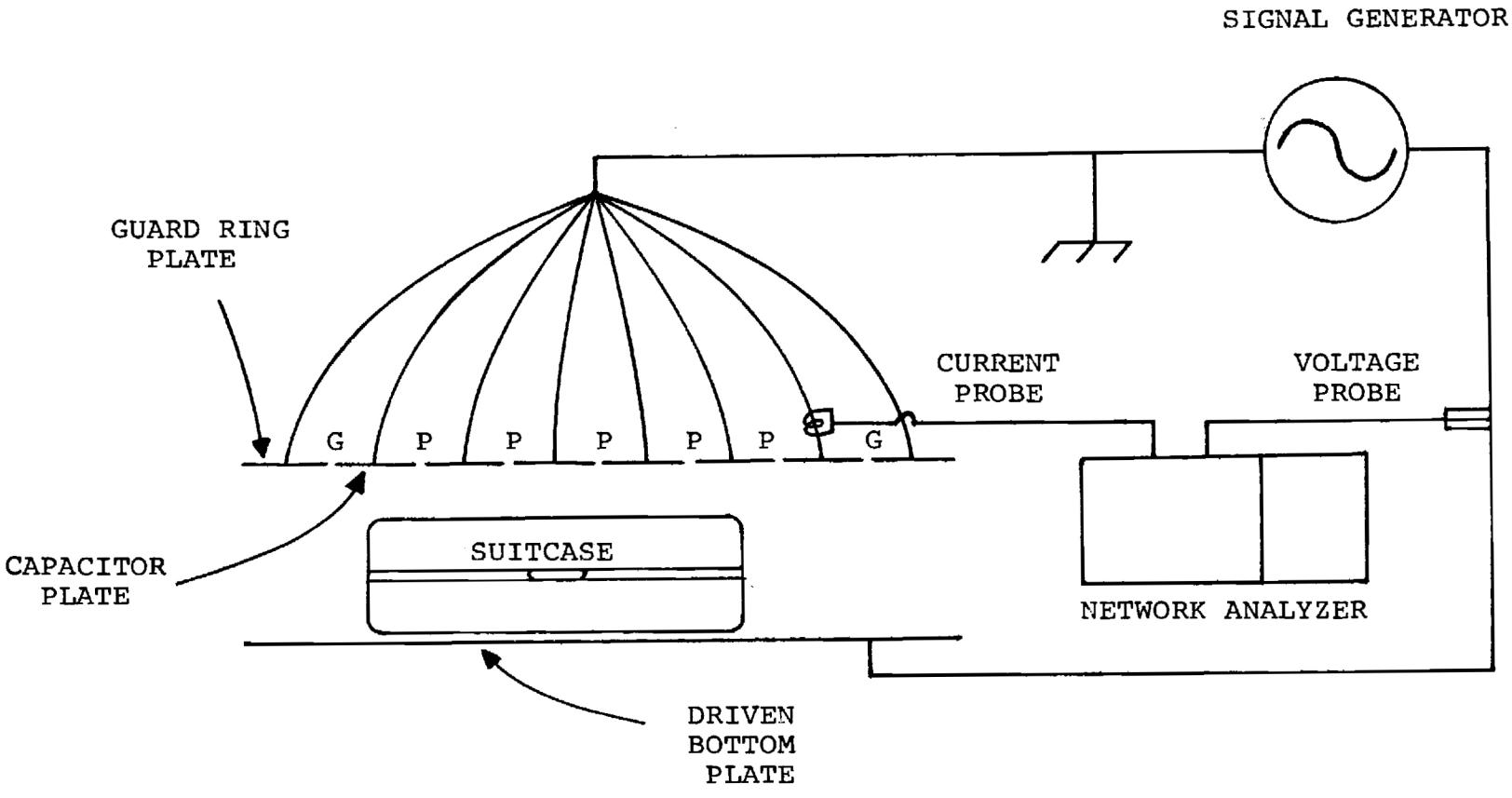

Figure 16. Electrical connections for capacitor plate array.

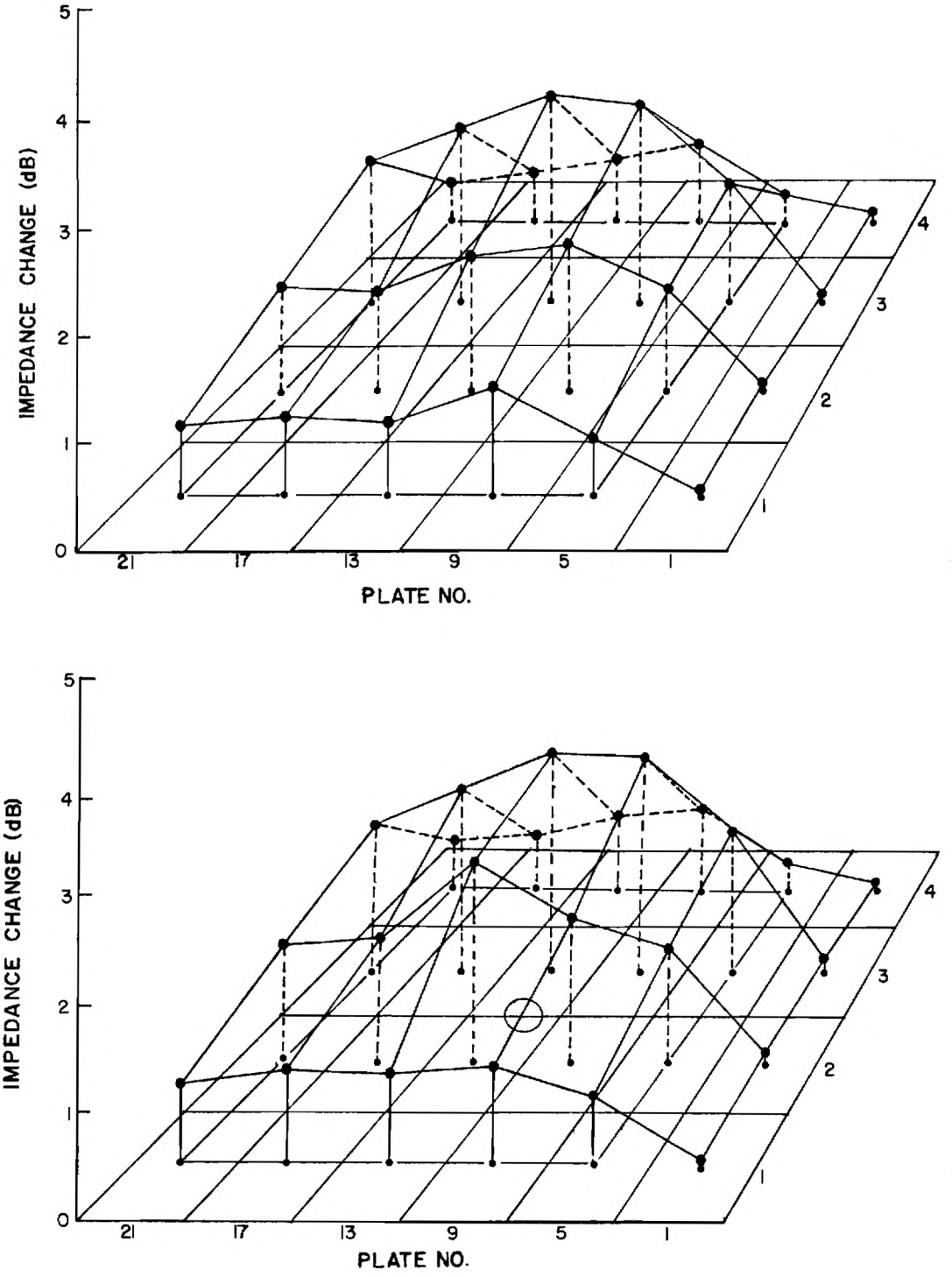

Figure 17. Contours of impedance changes for capacitor plate array: suitcase with clothes and suitcase with clothes and 1 apple. Suitcase corners under plates 5, 8, 21, and 24, as outlined. Apple indicated under plates 14 and 15.

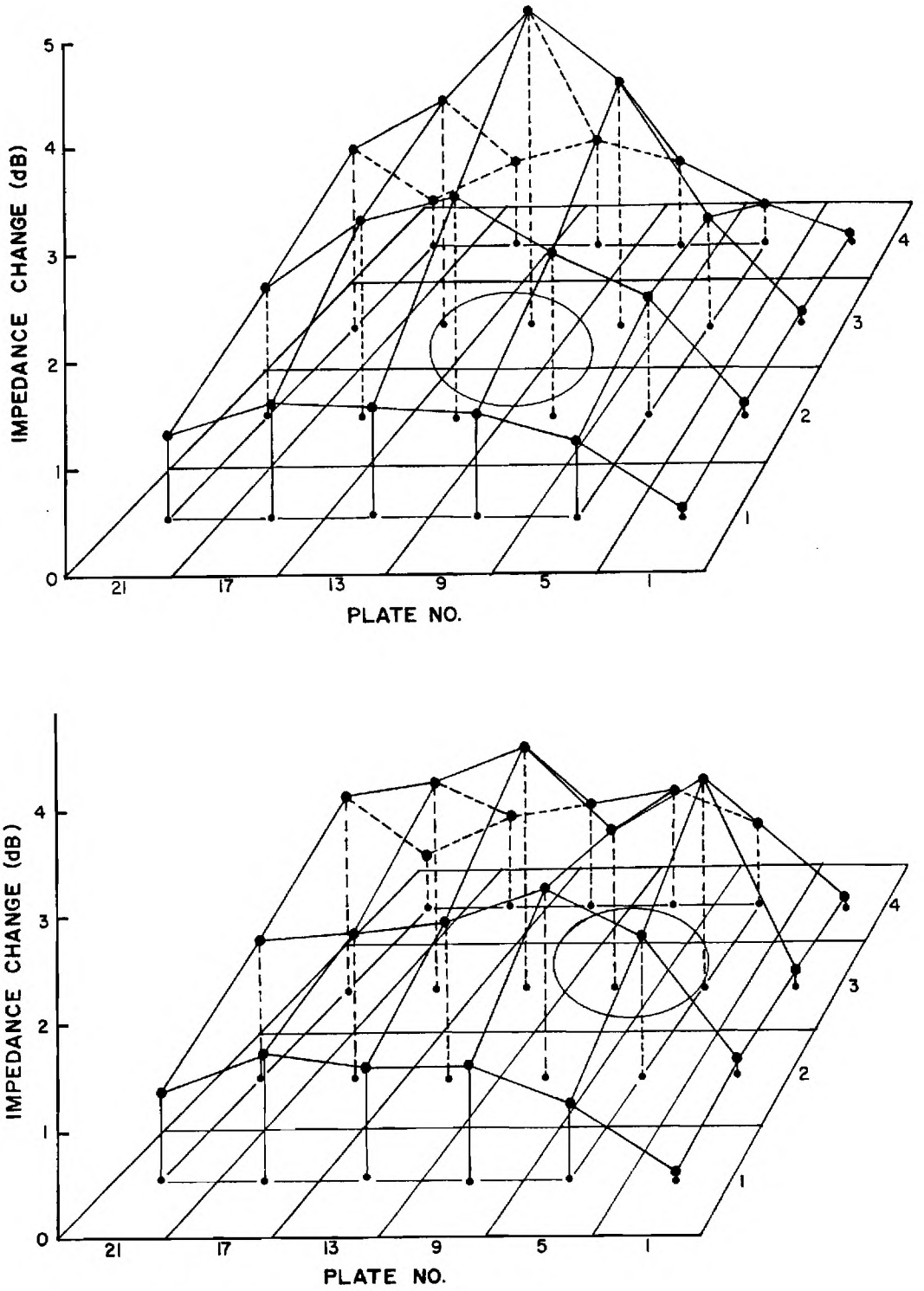

Figure 18. Contours of impedance changes for capacitor plate array: suitcase with clothes and 5 apples. Suitcase corners as in Figure 6, as outlined. Apple locations indicated by ovals at center of suitcase (top) and at corner of suitcase (bottom).

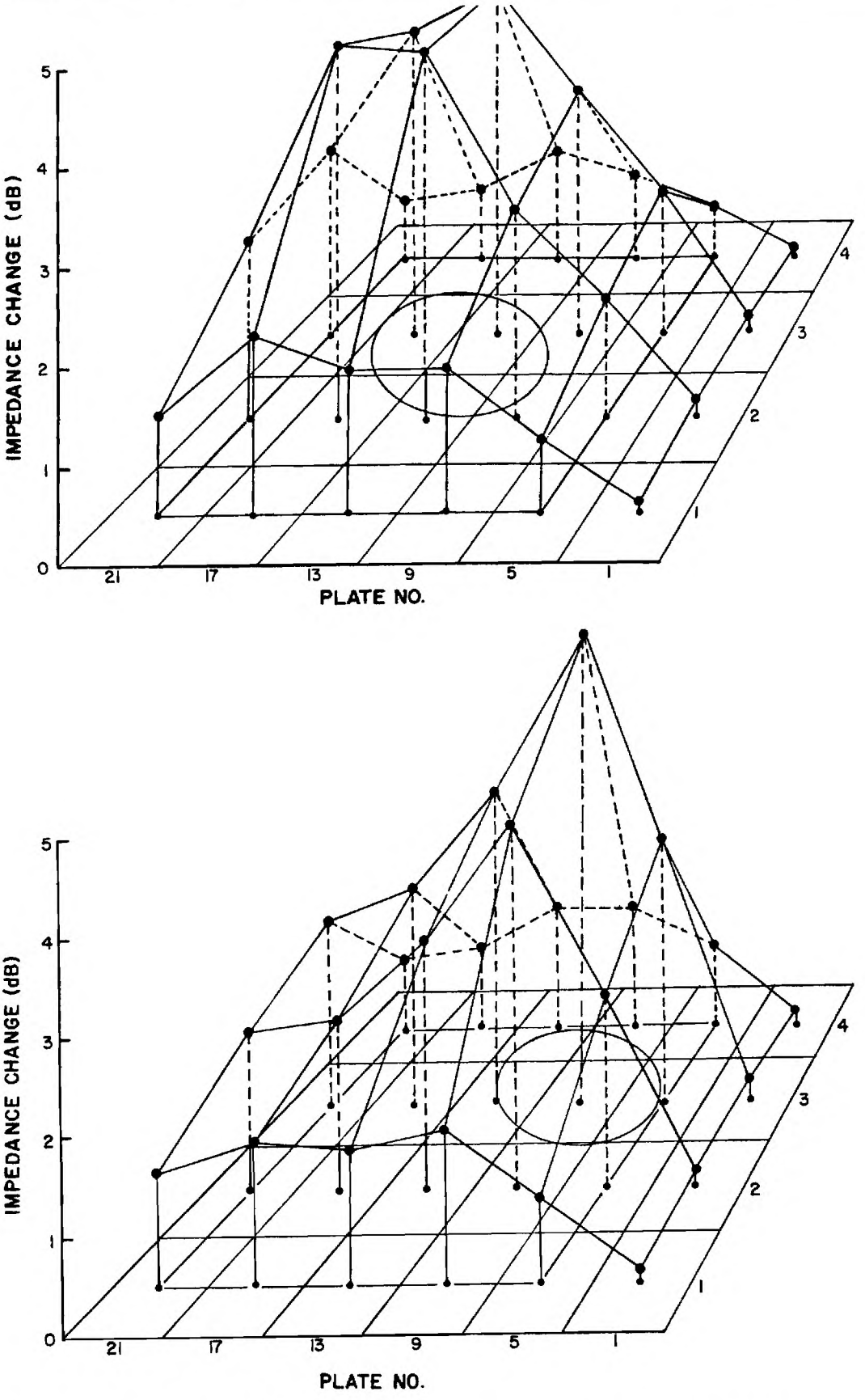

Figure 19. Contours of impedance changes for capacitor plate array: suitcase with clothes and 12 apples. Suitcase corners as in Figure 6, as outlined. Apple locations indicated by ovals at center of suitcase (top) and at corner of suitcase (bottom).

The size of the capacitor plates significantly impact the attainable resolution. An advantage (in terms of resolution) of small plates is that it should be possible to detect small objects. A disadvantage of small plates is that only a small part of the volume of an average suitcase could be interrogated. Using small plates will probably make it necessary to implement either multiple sets of capacitor plates with electronic switching among them or moving capacitor plates in order to interrogate an entire piece of baggage.

The capacitor plate array was shown to be capable of detecting the presence of moderate amounts of fruit in a typical piece of luggage. Its spatial resolution was limited by the size of plates which had to be used. The array has the potential that, with suitable electronic hardware, it could provide a simple yes-no indication signifying the probable presence of agricultural products suitable for unattended operation. The parallel plates also provide a convenient configuration for feeding luggage through the detector. There is a limited capability to discriminate between similar volumes of metal and agricultural products.

IV. RESONANT CAVITY APPROACH

A metal box exhibits cavity resonance characteristics when excited by an electromagnetic probe. At a resonant frequency, a maximum amount of energy is stored in the cavity's electric and magnetic fields. With the introduction of an agricultural product or other material into the cavity, it was anticipated that the resonant frequency would change and power losses within the cavity at resonance would increase. These changes would result from the agricultural product's complex permittivity which, in general, exhibits relatively high loss and high dielectric constant which are potentially capable of producing substantial changes in cavity loss and resonant frequency. To investigate feasibility, analyses of an agricultural product's interaction with cavity fields were performed. Measurements of resonant frequency and loss-related parameters were made using an experimental cavity with and without fruit and suitcase present.

A. Analysis

At resonant frequencies, electromagnetic standing waves are excited within a cavity and satisfy boundary conditions imposed by the walls. At these resonant frequencies, maximum energy storage in the fields is achieved and power is dissipated only by I^2R losses in the cavity walls or losses due to cavity perturbations. In general, the cavity boundary conditions do not require a unique solution and are satisfied by a theoretically infinite number of resonant frequencies above and including a fundamental frequency which is uniquely determined by cavity dimensions and contents.

The field configuration corresponding to each resonant frequency is called a mode of the cavity. Modes of the higher resonant frequencies have a number of null points and repetitions of the standing wave pattern which could result in ambiguity in the interpretation of resonant frequency shifts caused by the introduction of agricultural products and so were not considered. The TE_{101} and TM_{110} modes were used because they each have only one cycle of the standing wave pattern and have resonant frequencies in the range where the complex permittivity of agricultural products is

relatively high. Electric field configurations of these two modes were shown in Figures 14 and 15 of Quarterly Technical Report No. 3. For brevity, the two modes are here referred to as TE and TM modes, respectively.

Electromagnetic waves traveling in a medium with a high complex permittivity, such as in an agricultural product, travel slower and are more highly attenuated with distance than waves traveling in free space or air. When such a medium is introduced into a cavity, it effectively increases the electrical size of the cavity, lowering its resonant frequency, and attenuates the waves passing through it to increase the power loss at resonance.

The relative amounts of resonant frequency shift and power loss at resonance with insertion of a dielectric into a cavity will be related to the magnitude of the electric field within the dielectric sample compared to the average magnitude in the rest of the cavity [23]. Because the electric field magnitude varies with the cavity mode and position of the sample within the cavity, the resonant frequency shift and loss at resonance will vary with sample position.

The Q (quality) factor of a resonant circuit is defined as 6.28 times the energy stored in the reactive components of the circuit divided by the energy dissipated per cycle. Q is therefore a measure of energy dissipated within a cavity and one of the quantities normally used to describe a resonant cavity electrically. The power dissipated within a lossy sample inserted into the cavity also depends on the magnitude of the electric field in the sample and therefore the cavity Q will change not only with the amount of agricultural product but also with the product's position within the cavity.

Q is often approximated by a formula obtained from a lumped circuit cavity model:

$$Q = \frac{f_r}{f_2 - f_1} \quad , \qquad (9)$$

where f_r is the resonant frequency and f_2 and f_1 are frequencies at

which the magnitude of the cavity reactance is equal to the cavity resistance. This formula becomes less accurate with low Q and large amounts of high loss dielectrics, but it was believed that it would show significant changes with the introduction of agricultural products and serve as a relative index of power loss within the cavity.

It was anticipated that the effective impedance at resonance would change with insertion of agricultural products by changing cavity impedance itself along with probe coupling efficiency. The cavity impedance at resonance is indicative of real power losses inside the cavity which would be increased by the loss factor of the agricultural product. The impedance of the cavity/probe system is also dependent upon the coupling coefficient between the probe and cavity. The coupling coefficient, which is analogous to a transformer turns ratio, depends on the electrical length of the probe and its position with respect to the cavity's field configuration. The electrical length of the probe varies with frequency and thus will vary as resonant frequency changes with introduction of an agricultural product. The agricultural product will alter the field configuration to some extent and will therefore alter the probe's relative position with respect to the field pattern. Because impedance at resonance would provide another measurable quantity, it was selected to be examined. It was anticipated that the impedance at resonance would show significant changes with insertion of agricultural products.

B. Measurements

Because the effort involved in complete quantitative prediction of the cavity's behavior with insertion of an agricultural product was prohibitive due to the complexity of the cavity field equations and need to recalculate for each sample position and volume, a cavity system was designed to measure the behavior. Considerations for cavity design, given in detail in Quarterly Technical Report No. 3, included the following:

- Cavity Size. A cavity approximating baggage size was needed to enable measurements to be made at the lower frequencies projected for final use.

- o Low Order Mode Excitation. Low order modes, TE_{101} and TM_{110}, were selected because it was felt that changes in measured parameters would be less ambiguous and more predictable than those made using higher order modes with multiple null points within the cavity.
- o Coupling Probes. Electric field probes were selected for ease of construction and efficiency in size needed for impedance matching.
- o Closed Cavity. A closed cavity design was selected rather than an open ended configuration because of anticipated higher immunity from external interference and increased sensitivity due to the tendency for open ended resonators to radiate.

A closed rectangular cavity with internal dimensions of 29 x 29 x 12 inches was fabricated from 25 guage tin-plated sheet steel and reinforced with plywood. The cavity's seams were all soldered with the exception of those along one removable side which was sealed by a compliant metal braid tube. Electric field probes consisted of a length of wire soldered to the center contact of a "type N" panel mount connector. Further details of the cavity's construction were given in Quarterly Technical Report No. 3.

Impedance measurements were made using an HP Network Analyzer System with a swept frequency source. This system sampled the signal delivered to the cavity and the signal reflected from the cavity and was set up to display voltage reflection coefficient as a function of frequency on a Smith Chart overlay. These measurements were used to determine resonant frequency f_r, impedance at resonance, and the frequencies at which cavity/probe reactance magnitude equalled cavity/probe resistance. Resonant frequency was determined by noting the frequency at which impedance was purely real. The cavity "Q" with the sample introduced, Q_s, was determined by dividing f_r by the difference in the frequencies at which reactance magnitude equalled resistance, i.e., by using equation (9).

Measurements of voltage transmission coefficient were also made using the HP Network Analyzer System. Instead of sampling the signal reflected from the cavity, the Analyzer measured the signal transmitted through the cavity. This signal was picked up by a receiving electric field probe installed in the cavity in addition to the probe which excited the cavity. Peak transmitted signal amplitude, related to cavity Q, was measured and referenced to transmitted signal amplitude for the empty cavity at resonance (0 dB). In the transmission measurements, it was much easier to measure resonant frequency because there was a large increase in power transmission at resonance compared to very small power transmitted off resonance. It was found in a few spot checks that the resonant frequency determined from a transmission measurement corresponded closely to that from a reflection measurement except for a small decrease in resonant frequency caused by loading the cavity with the receiving probe. After these checks for consistent results, only transmission measurements were utilized to facilitate measurements made with a suitcase in the cavity.

Measurements of resonant frequency and Q were first made on the empty cavity and the cavity with a representative agricultural product, a 6.4 cm diameter apple, present using the reflection coefficient. The measured resonant fequencies, 286.13 MHz for the TE mode and 569.01 MHz for the TM mode, were close to calculated values of 288.00 MHz and 570.20 MHz. The frequency differences were attributed to slight cavity dimension variations from the nominal design values. The unloaded Q of the cavity was measured to be 3577 for the TE mode, and 4064 for the TM mode.

With the apple in the cavity at positions shown in Figure 20, measurements were made of f_r, Q_s and impedance at f_r. Frequency was swept from approximately 283 to 287 MHz for the TE_{101} mode and 560 to 570 MHz for the TM_{110} mode. Measurements were made in one quadrant of the cavity only, due to symmetry of the unperturbed fields about the planes $x = a/2$, $y = b/2$, $z = a/2$. Figures 21 and 22 illustrate some of these changes in f_r and Q_s with changes in sample position along with empty-cavity values for comparison.

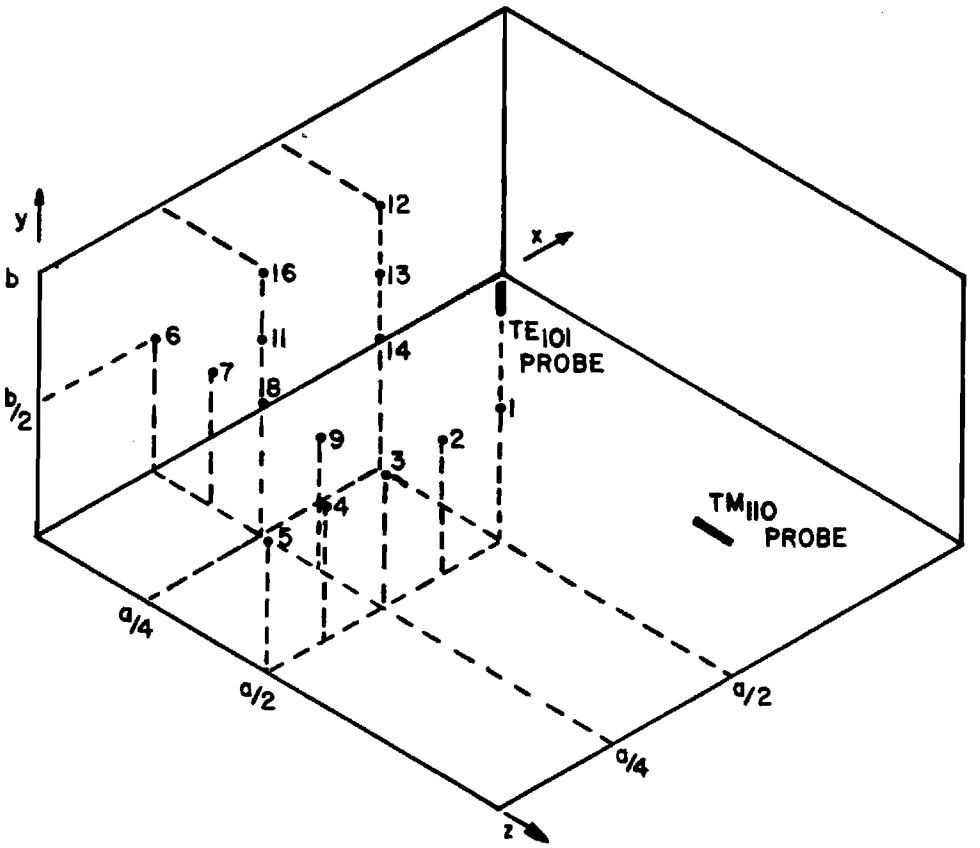

Figure 20. Apple positions for resonant cavity measurements. Positions in one quadrant were selected because of the unperturbed field symmetry about the planes x=a/2, y=b/2, z=a/2 (a=73.7 cm, b=30.5 cm).

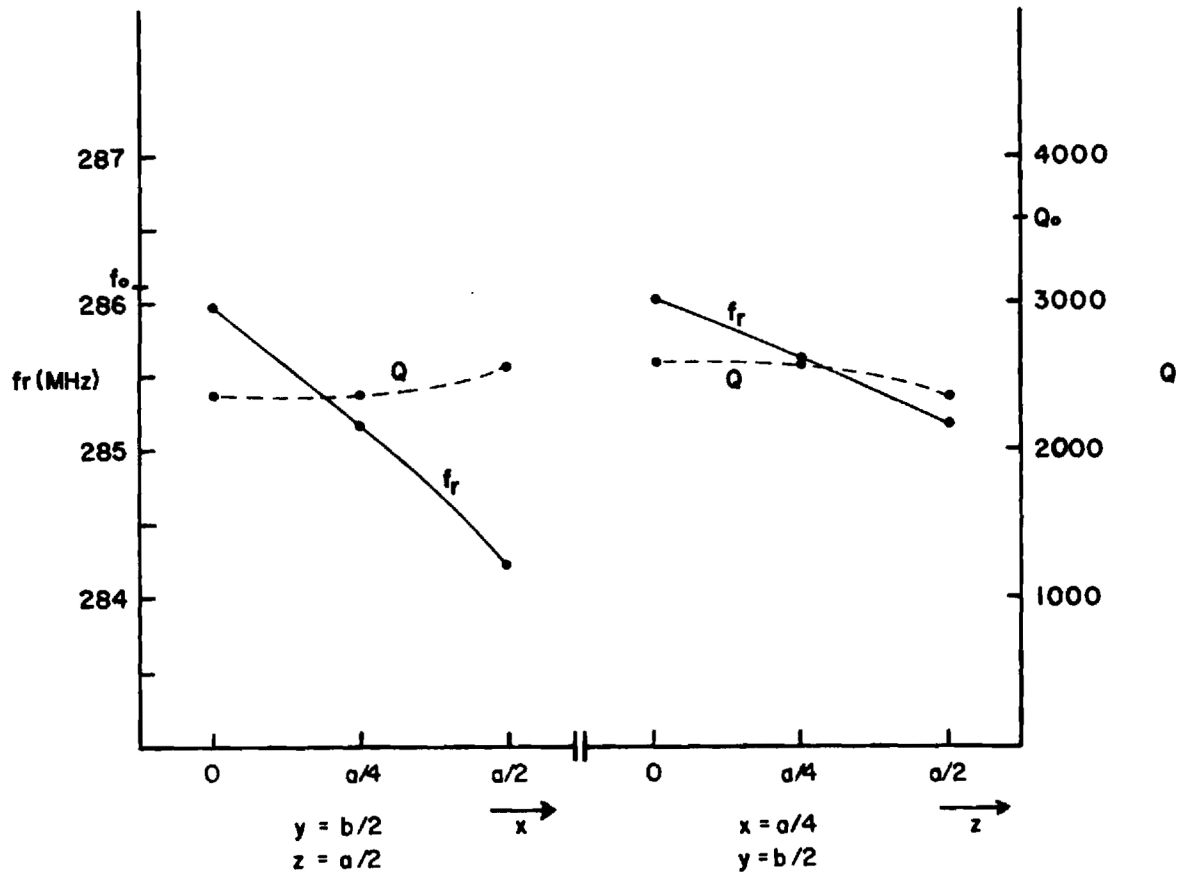

Figure 21. Q and f_r as functions of apple position in the TE_{101} mode. From left to right, the values are for positions 5, 3, 1, 6, 8, and 3 in Figure 20. Q_o and f_o were empty cavity Q and resonant frequency. Q demonstrated little change; f_r showed maximum change in the cavity center (x=a/2).

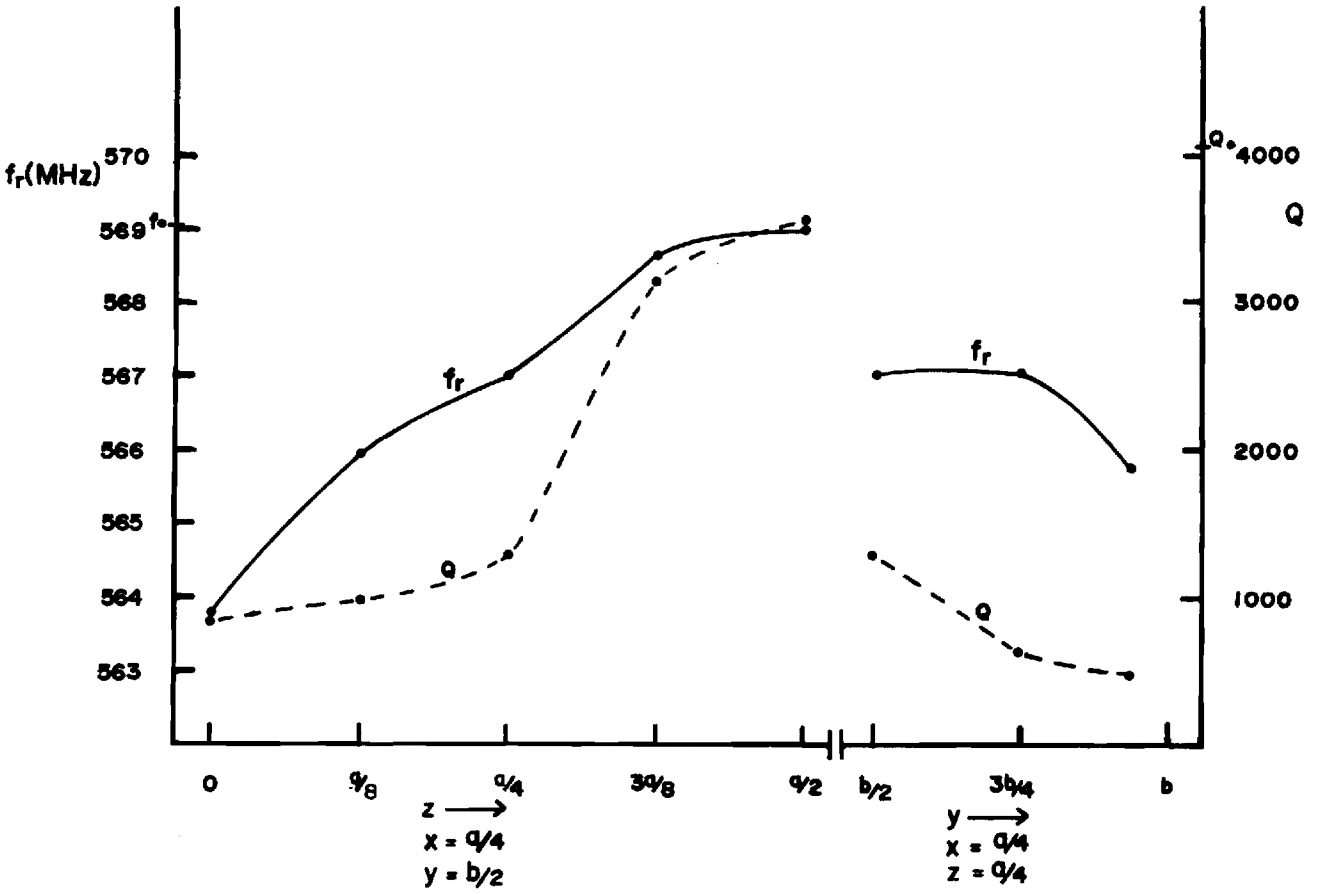

TM_{110} CAVITY RESONANT FREQUENCY AND Q AS A FUNCTION OF APPLE POSITION

Figure 22. Q and f_r as functions of apple position in the TM_{110} mode. From left to right, the values were for positions 6, 7, 8, 9, 3, 8, 11, and 16 in Figure 20. Q_o and f_o were empty cavity Q and resonant frequency. Largest changes occurred for positions around the periphery of the cavity (z=0, y=b); minimal changes, near the center (z=a/2, y=b/2).

From consideration of the field configurations within the cavity for the two modes, it was determined that the largest changes in resonant frequency and Q tended to occur at sample positions where the unperturbed electric field is most intense. Some exceptions to this occurred at z = a/2 in the TM_{110} mode and these were attributed to substantial changes in the field distribution caused by the apple. In general, these comparisons indicated that it may be possible to detect an agricultural product throughout much of the cavity volume by measuring changes in both modes.

The suitcase in these studies was a typical soft-sided one measuring 22 inches by 13 inches by 6 inches deep with a zipper closure. Three pairs of men's slacks and a T-shirt were used to pack the suitcase for most measurements. To have information for more than one luggage shape, a briefcase was also used for some measurements. Insertion of the suitcase or a grapefuit caused a large impedance mismatch at resonance producing a large reflection coefficient. This was in contrast to the small reflection coefficient seen with an apple in the cavity. Because the cavity was normally mismatched at frequencies off resonance, a sharp change in reflection coefficient occurred at resonance with the apple, as shown in Figure 23, allowing rather precise determination of the resonant frequency. The resonant frequency of the cavity loaded with the suitcase or grapefruit was more difficult to measure accurately because changes in reflection coefficient were much smaller, as illustrated in Figure 23.

Figure 24 shows typical transmitted signal amplitude curves for the empty cavity and for the suitcase with clothes and an apple. Curves like these were obtained for a variety of objects in the cavity for both modes. Results are discussed here for both the TE and TM modes (Figures 25 and 26).

For the TE mode in Figure 25, it can be seen that resonant frequency shift due to the apple is a small portion of the changes caused by the apple packed in the suitcase or briefcase. The resonant frequency consistently decreased with insertion of clothes and the apple as expected. The shift in resonant frequency due to the luggage with clothes was of the

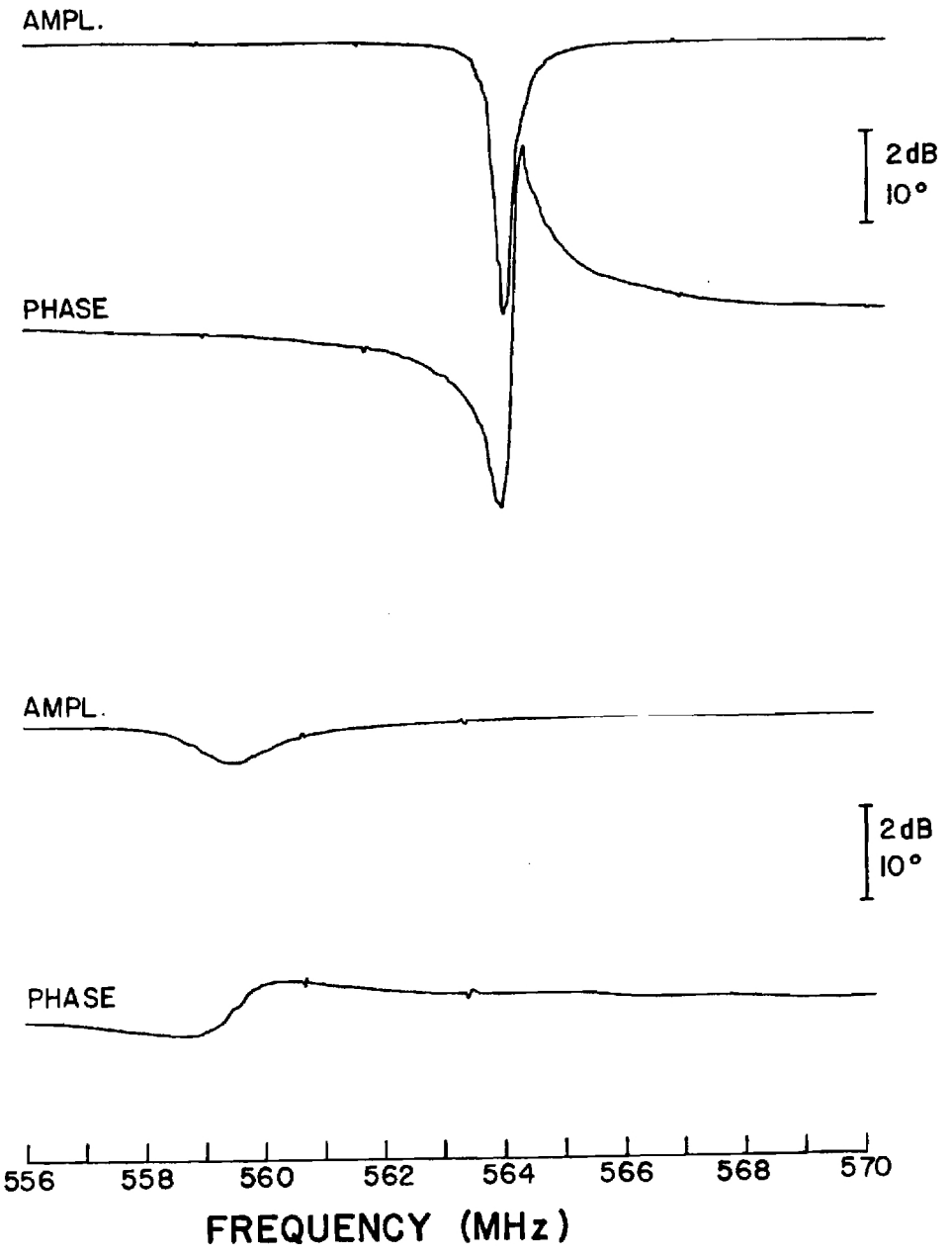

Figure 23. Reflected voltage signals for resonant cavity in TM_{110} mode showing resonance. Top two curves are for apple at (a/2, b/2, a/4); bottom two, for grapefruit at (a/2, b/2, a/4). Curves are representative of those seen for both modes.

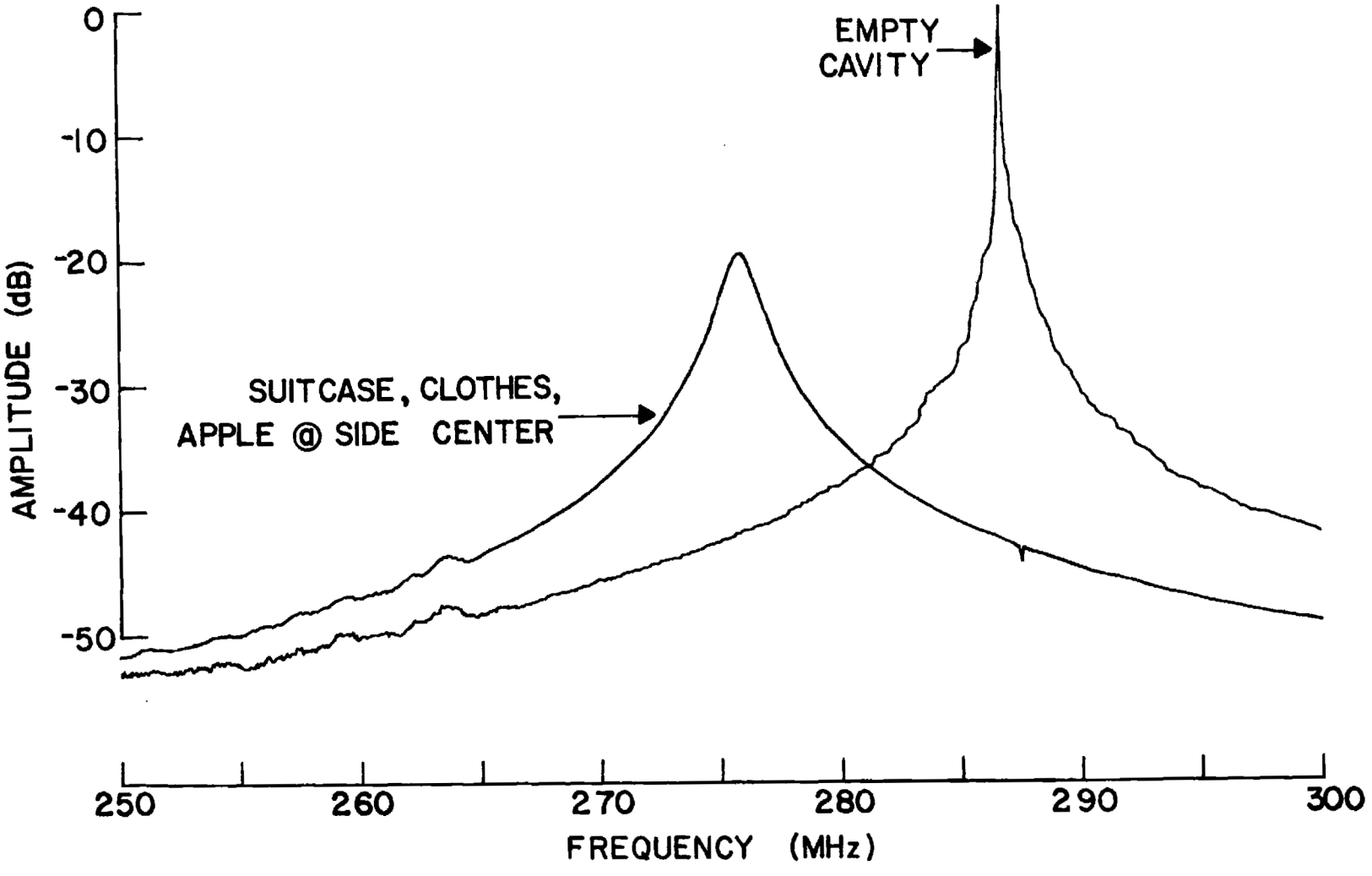

Figure 24. Transmitted signal amplitudes for resonant cavity operating in TE_{101} mode showing resonance.

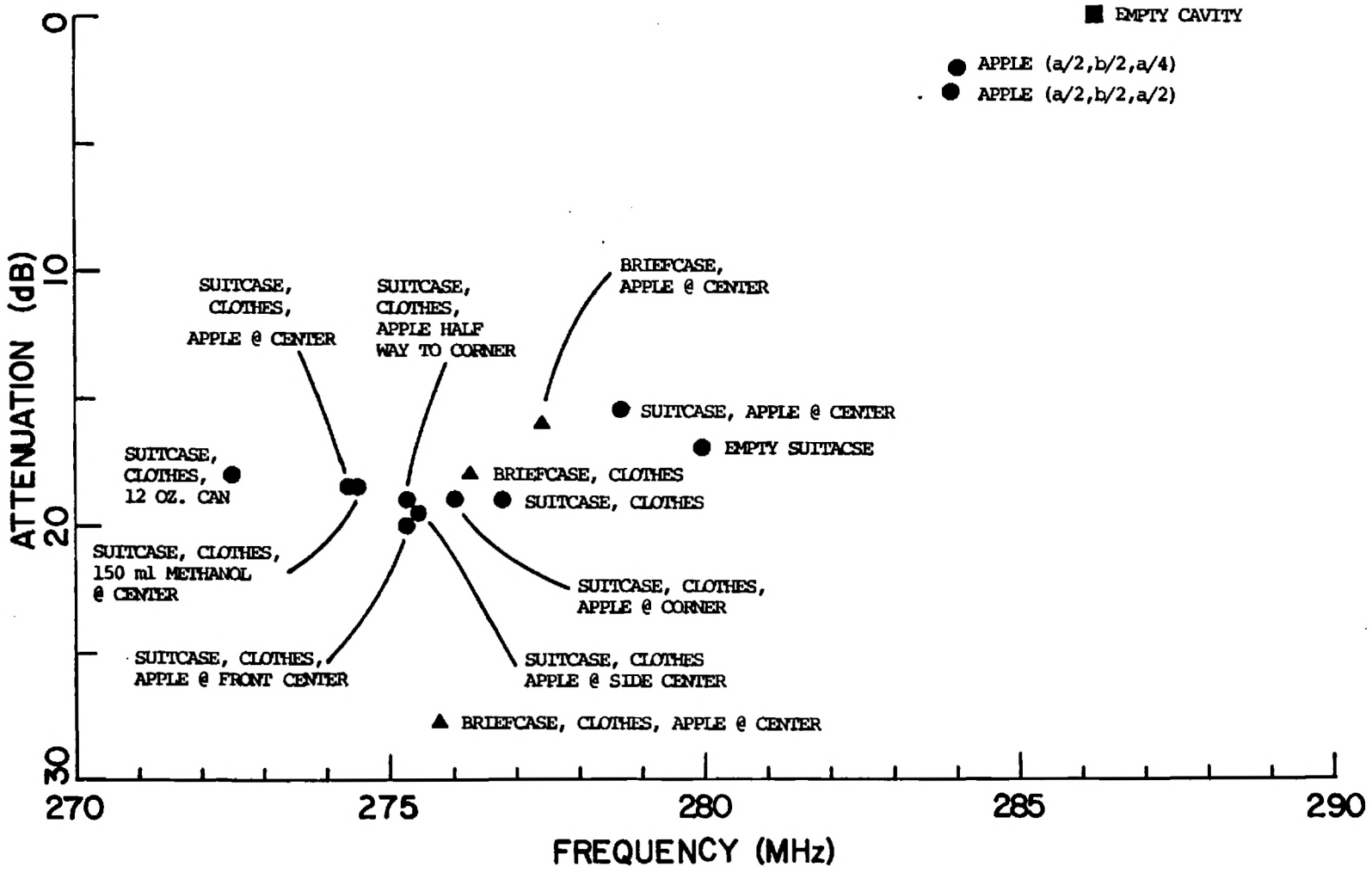

Figure 25. Summary of transmitted signal changes for TE_{101} mode of resonant cavity. Attenuation at resonance (referenced to empty cavity) versus resonant frequency for the indicated conditions.

same order of magnitude as the shift due to the luggage with the apple. For the same suitcase location, there was a difference in resonant frequency shift with apple position in the suitcase with the largest shift caused by the apple at the center and the smallest shift by the apple at the corner. Simulated toiletry articles, a 12-ounce aluminum can, and a bottle containing 150 ml of methanol, caused resonant frequency shifts similar to and, in the case of the can, greater than that caused by the apple. Although the suitcase itself caused a pronounced attenuation in the transmitted peak signal, the addition of contents to the suitcase produced small changes in this parameter with no apparent pattern. It seemed, therefore, that the resonant frequency shift was the most useful information to be derived from the TE configuration.

As seen in Figure 26, results for the TM mode were similar to those for the TE mode. The suitcase with clothes and apple caused a larger shift than did the suitcase with clothes. The shift for the suitcase with clothes was in turn larger than for the empty suitcase. The shift in resonant frequency for a 12-ounce aluminum can in a suitcase with clothes was very similar to the shifts for alcohol and for an apple in a similarly packed suitcase. Results using the hard-sided briefcase, which had a thick metal frame, are not shown in Figure 26, but alone it increased the resonant frequency to 568.31 MHz, above that of the empty cavity. Also, the briefcase with clothes or apple had a smaller resonant frequency shift than seen for the apple alone. This inconsistency in resonant frequency shift with suitcase construction along with a lack of pattern in transmission peak amplitudes indicated that the TM configuration would provide little information by itself or in tandem with the TE configuration.

C. Conclusions

Of the two excitation configurations for the resonant cavity, the TE mode seemed to be the more promising based on measurements with a suitcase present. It appeared that a suitcase metal frame greatly perturbed the cavity's fields in the TM mode. The frames, being roughly perpendicular

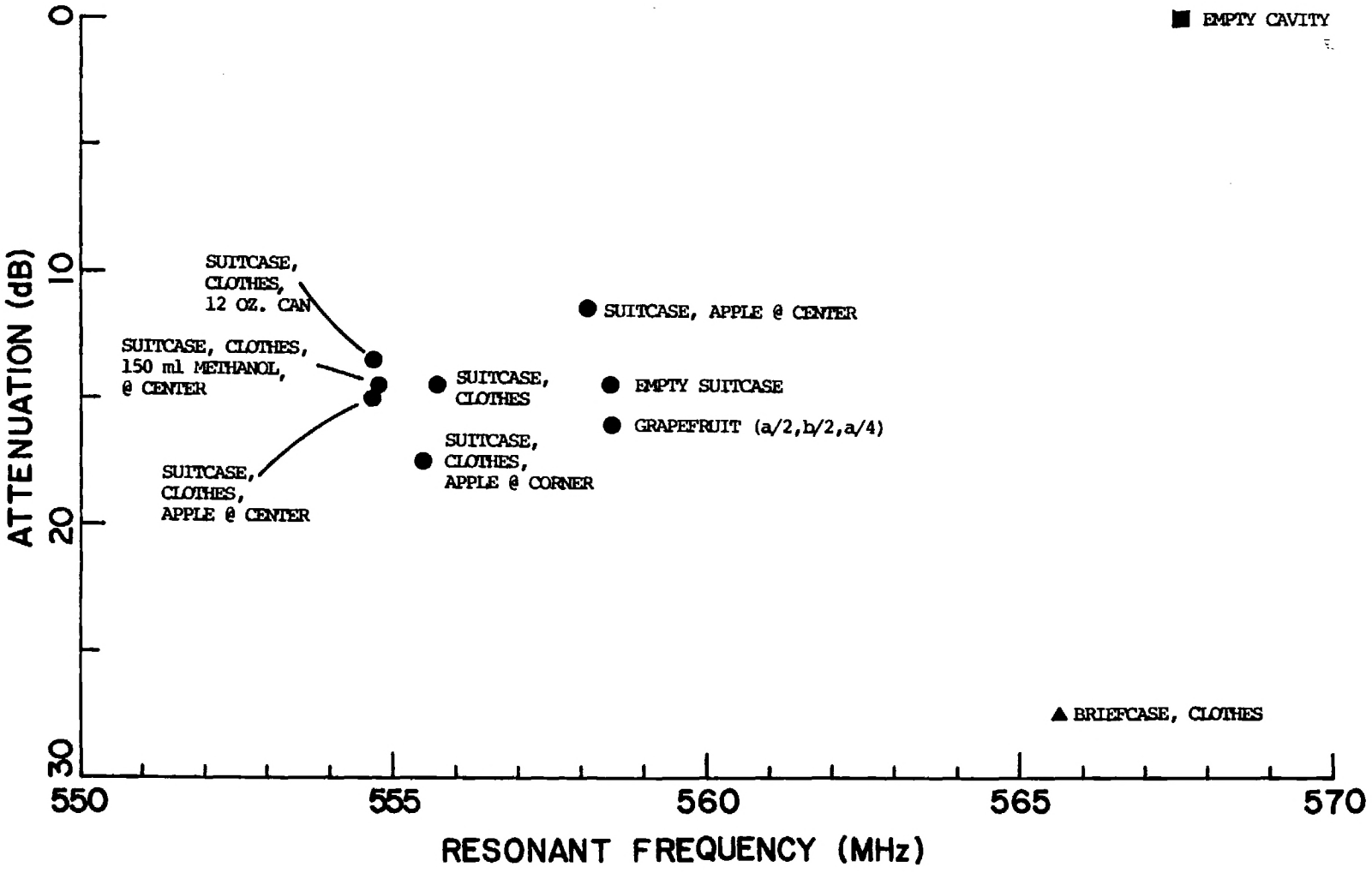

Figure 26. Summary of transmitted signal changes for TM_{110} mode of resonant cavity. Attenuation at resonance (referenced to empty cavity) versus resonant frequency for the indicated positions.

to the TE fields, did not seem to perturb the TE fields to as great an extent, producing more predictable resonant frequency shifts. Resonant frequency shifts for the TE mode occurred in a fairly consistent fashion although the shifts due to the addition of a single apple were within the range of those which might normally be expected for typical baggage contents.

Transmission measurements proved more useful than reflection measurements because the change in reflection coefficient became very small when measuring the cavity loaded with a suitcase or a larger volume of agricultural product. However, changes in transmission peak signal amplitudes with a suitcase present were small in general and were not correlated with trends in baggage contents. The attenuation due to the suitcase, being much larger than that due to the apple, also tended to mask absorption by the apple.

These measurement results meant that a fairly simple, and relatively inexpensive, system consisting of a resonant cavity operating in the TE_{101} mode connected to a device for measuring resonant frequency, could be used to detect single agricultural products in baggage in the absence of metallic and toiletry objects. The threshold frequency shift to indicate presence of an agricultural product would have to be set high enough to minimize the number of false positive indications for normal suitcases but also low enough to minimize the number of false negative indications, especially for small volumes of agriultural products. Such a system will be unable to discriminate between large metal or fluid-filled articles and agricultural products.

V. SIGNAL TRANSMISSION/REFLECTION APPROACH

The possibility of detecting the presence of agriucltural products in baggage utilizing the transmission and reflection of electromagnetic waves depends upon the differences between dielectric properties of these items and those of other common objects found in travelers' baggage. Because of the different properties, electromagnetic waves in air are more strongly reflected and more greatly attenuated in encounters with agricultural products than they are when striking materials such as cloth, leather, and plastic. For the transmitted signal, a phase shift results from the slower velocity of the wave through the material. Similarly, a phase shift in the reflected signal comes from the discontinuity at the dielectric interface. These differences in transmitted and reflected signals were investigated using theoretical analyses and experimental measurements.

For a given object, the factors affecting the transmitted and reflected signals are its position, shape, size, and permittivity. The transmitted and reflected signals, being complex, are completely described by four parameters: two magnitudes and two phases. Theoretical work was done for frequencies from 1 to 5 GHz. Experimental work was done for three frequency ranges: 1.8 - 2.6 GHz (LS-band), 2.6 - 3.9 GHz (S-band), and 8.2 - 9.0 GHz (X-band).

A. Analysis

One of the simplest cases involving the transmission and reflection of electromagnetic waves is that of a uniform plane wave passing through two dielectric materials occupying regions of semi-infinite extent. These regions adjoin at a single planar interface as illustrated in Figure 27. The reflected and transmitted electric fields, E_R and E_T, at the interface are given in terms of the incident field E_F, by:

$$\rho \equiv \frac{E_R}{E_F} = \frac{\eta_2 - \eta_1}{\eta_1 + \eta_2} \qquad (10)$$

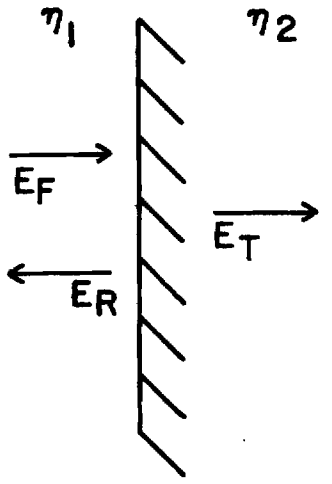

Figure 27. Forward, reflected, and transmitted signals at a planar interface between two dielectric media.

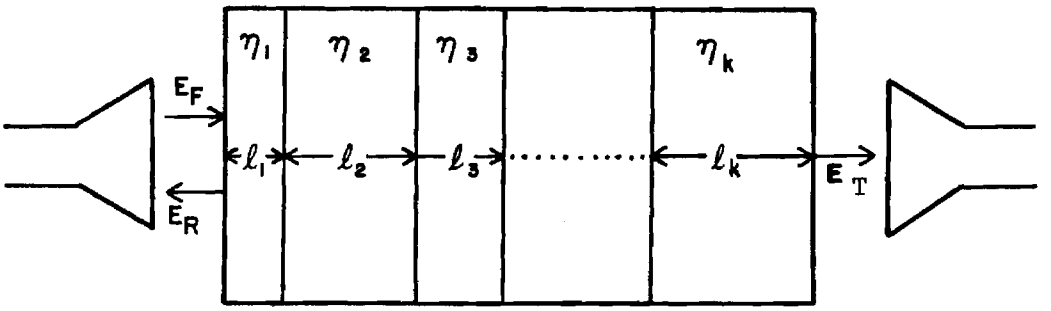

Figure 28. Forward, reflected, and transmitted signals for layers of dielectric materials.

and

$$\tau \equiv \frac{E_T}{E_F} = \frac{2\,\eta_2}{\eta_1 + \eta_2}, \qquad (11)$$

where η_1 and η_2 are the intrinsic impedances of materials 1 and 2, and ρ and τ are defined as the voltage reflection and transmission coefficients, respectively. The intrinsic impedance is given by

$$\eta = \sqrt{\mu/\varepsilon^*} \qquad (12)$$

where μ is the magnetic permeability of the material (assumed to be that of free space for all materials discussed in this report) and ε^* is the complex permittivity discussed in Section II. This example illustrates the basic phenomena, namely, that part of the wave is reflected while part is transmitted and that phase shifts occur because of the complex nature of the impedances. However, this case is much too simple to give an accurate indication of the signals which might be observed reflecting from or traveling through baggage containing many items. For the transmitted signal, one is interested in describing the wave after it has passed through the suitcase, possibly having met several interfaces, and arrived at the detector. Similarly, the reflected signal is influenced by the baggage thickness and its contents.

A slab model, illustrated in Figure 28, was chosen for modeling the next level of complexity approaching that of an agricultural product in a suitcase. This model consisted of a plane wave impinging upon successive planar layers, or slabs, of material characterized by their intrinsic impedances and thicknesses. Although this was still a highly idealized geometry, it better represented a suitcase with inhomogeneous contents. It was adequate for an investigation of the behavior of reflected and transmitted signals as functions of the characteristics of a lossy layer and of frequency.

Even with this simple geometry, a complex situation existed because reflections occur at each interface. This problem was analyzed by utilizing the analogy of plane waves propagating through dielectrics to signals traveling through transmission lines. As presented in detail in Quarterly Technical Report No. 2, the powerful tools of network theory for cascaded two-port devices were employed [24]. Each interface and section of dielectric was treated as a two-port device characterized by a transmission matrix T. Signals in each layer were represented by complex numbers and related to each other through the T-matrix. A scattering matrix, or S-matrix, was derived from the T-matrices for the various layers and interfaces and was used to relate voltage reflection and transmission coefficients to model parameters. Representative dielectric properties were assigned to the different layers. Values for wood and cloth were taken from the literature [10]; for the agricultural product layer, from the equations described in Section II.

Results of the computer calculations based on this slab model were presented in Quarterly Technical Report No. 2. The magnitude and phase of reflected and transmitted signals relative to those with no agricultural layer present were shown as a function of frequency from 1 to 5 GHz. Reflection magnitude was generally greater with the insertion of the high dielectric, lossy layer and showed sharp peaks which arose from a half-wavelength window effect. Attenuation of the transmitted wave was about 30 dB with the lossy layer and generally increased with frequency. There were smooth bumps due to the attenuation of the transmitted wave and the window effect. Phase shifts of both signals generally increased with frequency. For the reflected signal, the detailed phase structure was roughly periodic with deviations corresponding to peaks in reflection magnitude. For the transmitted signal, the increase was quite regular and was thought to be a potentially good indicator of the nature of the intervening dielectric.

Results were also obtained for changes in reflected and transmitted signals with thickness of the agricultural product layer for a frequency of 2 GHz. The reflected magnitude ratio had some fine structure at small thicknesses caused by half-wavelength window phenomena in the air

layers of the model, while for larger thicknesses, the ratio curve was fairly smooth. As expected, the transmitted wave magnitude diminished with thickness. For a thickness of 30 cm, the transmitted signal was about 90 dB below the signal with no agricultural product present. Reflected signal phase shift had a weak dependence on thickness. In contrast, the transmitted phase shift showed a rapid period with thickness because of the increasing electrical length through which the wave propagated.

B. Measurements

Experiments were performed in order to determine the feasibility of observing changes in the reflected and transmitted signals when fruit-like material was placed in a radiofrequency (RF) field. The equipment employed included an HP 8410B network analyzer, an HP 8743A transmission/reflection unit, and an HP 8620C/86222A sweep oscillator. This network analyzer system indicated magnitude and phase of the voltage reflection coefficient and voltage transmission coefficient. Since the forward signal was a constant, the magnitude and phase changes for a particular coefficient were the same as for the signal referenced to the forward signal. This can be seen in equations (10) and (11) which show the direct proportionalities between coefficients and signals. The changes described here can be thought of in terms of either the coefficient or the signal. As a first step, a wooden box was constructed with the approximate dimensions of a suitcase, 10 x 18 x 30 inches, with a slot into which a plastic (Plexiglas) tray containing a liquid with fruit-like dielectric properties could be inserted. This test apparatus was designed to correspond, roughly, to the analytic case examined in the preceding section.

Tests were made with the Plexiglas tray empty and with it filled with a 30% by weight glycerol solution. The properties of this solution [25] mimic those of agricultural products. The thickness of this layer was 3 inches. The box was placed 2-1/2 feet from the LS-band transmitting horn antenna, outside the near field but not actually in the far field region. This horn also functioned as the receiving antenna for the

reflected signal. The receiving horn for the transmitted signal was placed 2 feet from the opposite side of the box. The RF generator was swept from 1.8 to 2.4 GHz to correspond to the frequency range of the waveguide and horn antennas.

As shown in Quarterly Technical Report No. 2, reflection coefficient magnitude as a function of frequency showed a great deal of structure not related to the box or its contents. These variations were probably caused by the match of the transmitting system to air and signals reflected from nearby objects. When the lossy layer was inserted, this structure did not change appreciably; however, the overall magnitude of the reflected signal increased by about 2 dB. The transmission coefficient magnitude had less structure and measurements taken with and without the inserted layer showed a 14 dB reduction in transmission caused by the layer.

Oranges were then substituted for the lossy layer at the center of the box. Because of the large variation of the reflected signal with frequency due to factors unrelated to the "suitcase" and oranges, a sensitivity of 5 dB/division had to be used to display the entire frequency range. Changes on the order of 1 dB were seen at some frequencies; however, the largest change, occuring at 1870 MHz, involved a -1 dB change for one orange and a +1 dB change for two oranges. The more uniform transmitted signal, displayed with a greater sensitivity of 0.5 dB/division, was attenuated approximately 0.3 dB for one orange and 0.9 dB for two oranges. Thus, the changes in transmitted signal magnitude were more consistent over the frequency range and with the number of oranges than was reflected signal magnitude.

Large variations in phase precluded any attempt to see details of phase shift due to oranges over the entire frequency range. A narrow frequency band from 1799.5 MHz to 1800.5 MHz was examined to see the order of magnitude of the phase shift. For the reflected signal, the phase shift was about 4° for one or two oranges and appeared to decrease with frequency. The transmitted phase shift was fairly constant around 5° for one orange and 10° for two oranges. Transmitted phase thus seemed to be more sensitive than reflected phase to the number of oranges over this narrow frequency range.

As a result of the initial experiences with measuring reflection and transmission coefficients with a dielectric layer, computer control of the HP Network Analyzer System was instituted for subsequent measurements to provide two major advantages. First, a calibration procedure using known terminations and loads could be used to make error corrections to parameters obtained in the course of an experiment. This calibration also allowed losses and phase shifts occurring in the connecting cables to be taken into account. The second advantage was that measurements could be reproducibly made for a set of frequencies on different runs. This capability allowed changes in transmission and reflection parameters with the insertion of the sample to be determined. In all experiments, the "device under test" consisted of the transmitting and receiving antenna pair (along with their coaxial to waveguide adaptors) and the sample placed between the antennas.

Different sets of horn antennas were required to cover the three frequency ranges. For LS-band measurements, the transmitting horn had an aperture of 27.3 cm by 37.5 cm; the receiving horn, 11.4 cm by 11.4 cm. The dimensions of the transmitting horn were such that the near field extended to about 38 cm and the transition field to about 188 cm. For S-band, the apertures of both horns were 7.5 cm by 7.5 cm. In this case, the near field extended to about 3 cm and the transition field to about 15 cm. For X-band, a matched pair of horn antennas with apertures of 19.4 cm by 14.4 cm were used. Antennas were placed 50 cm apart in each set of measurements. This separation was chosen to be compatible with the spacing required for the insertion of a suitcase. The bottom edge of the transmitting horn was placed 15 cm above the surface of the support upon which the sample was placed and each receiving horn was aligned so that its aperture was centered with respect to the transmitting horn.

The sample in these later experiments consisted of a plastic bottle containing glycerol solution (30% by weight) having dielectric properties described in Quarterly Technical Report No. 2 to be $\varepsilon_r' = 48$ and $\varepsilon_r'' = 14$ at 2.45 GHz [also reference 25] which were comparable to then-available

literature values for agricultural products. These values are also similar to those measured, except that measured values of relative dielectric constant were somewhat larger. However, these differences should have little net effect on measured transmission and reflection coefficients. The bottle was filled to the neck and thus, ignoring the thin plastic shell, the sample could be considered a cylinder of glycerol solution of diameter 6 cm and height 9.5 cm. This sample target was chosen in lieu of fruit to allow reproducible results to be obtained over a period of several weeks.

The sample was placed on a 50 x 40 cm grid so that its position relative to the horn antennas could be accurately reproduced. Figure 29 shows a schematic top view of the horns and grid with the different sample positions ennumerated. The complete assembly of horn antennas and sample was surrounded by anechoic material to reduce the influence of extraneous reflections and noise upon the measurements.

During experiments for all three bands, the transmission and reflection coefficients were first determined with no sample present at preassigned frequencies in 0.1 GHz increments. The sample was then placed at each position shown in Figure 29 and transmission and reflection measurements were taken for each frequency. After measurements at all positions were completed, the "no sample" measurements were repeated to check for drift in the system. Over the three frequency bands covered, the drift for "no sample" conditions was less than 1% in all parameters except for measurements at 2.1 GHz. At this one frequency, the phase shift for the transmitted signal was near 180° and with little variation in frequency could change quadrants making the measurement somewhat unstable. Accordingly, some data obtained at this frequency were too unreliable to be reported. The normally small instability in the measurements was most likely due to the accuracy with which frequency could be controlled and slight movements of the horn antennas.

Results were expressed as changes in the reflection and transmission coefficients with insertion of the sample. These were obtained by subtracting the numbers obtained in the "no sample" runs from those of the "sample present" runs. Because changes rather than absolute transmission and reflection coefficients were examined, effects arising from imperfect

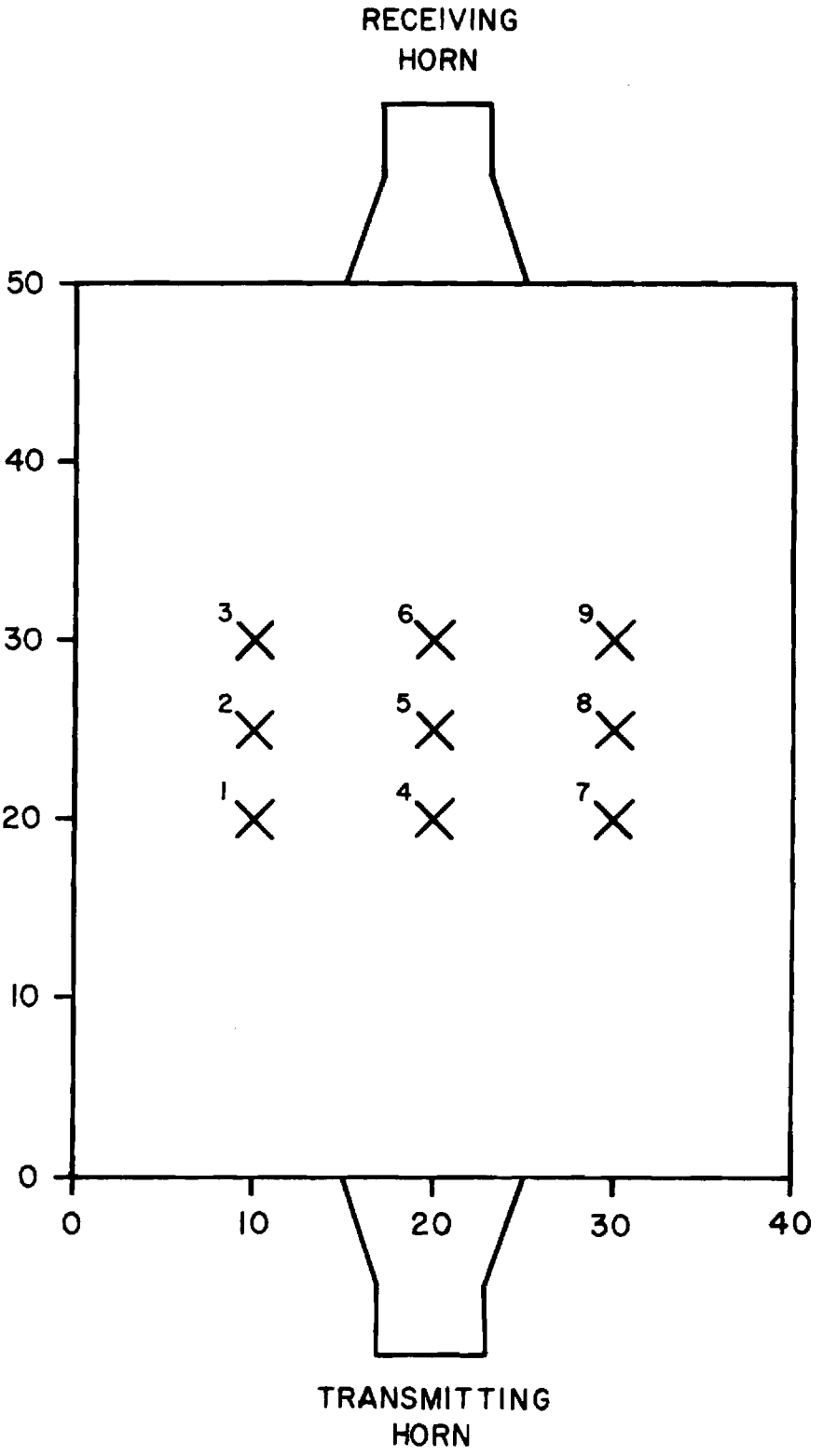

Figure 29. Top view of the horn antenna and sample positions (X) 1 through 9 used in transmission/reflection measurements. The axes show distances from the lower left-hand corner of the grid in centimeters.

shielding of the apparatus were minimized. These parameter changes were thus indicative of those one can hope to observe with agricultural products (of similar size, shape, and position) present relative to their absence.

Results of these measurements were reported fully in Quarterly Technical Report No. 3 and a subsequent Interim Technical Report. Magnitude and phase of reflected and transmitted signals were given for each frequency band. For each band, it was concluded that reflection magnitude and phase were less reliable because of their variability with signal frequency and among positions along a line between antennas. Here, the better-behaved transmission magnitude and phase are presented (Figures 30 through 35) to illustrate the potential for detecting agricultural products. In each figure, either relative signal magnitude or phase for the respective band is shown for all 9 positions defined in Figure 29. Three frames in each figure contain the results for positions on the left-of-center axis, for positions on the center axis, and for positions on the right-of-center axis. Along each axis, the positions are coded as broken line, position closest to transmitting horn (1, 4, or 7); solid line, center position (2, 5, or 8); dashed line, position closest to receiving horn (3, 6, or 9). Since transmission results were very similar for target positions along an axis, this latter distinction was almost unnecessary.

The LS-band signal magnitude and phase results are shown in Figures 30 and 31, respectively. Magnitudes of the voltage transmission coefficient changes were consistently negative, ranging from 0 to -1.5 dB. They were fairly uniform and exhibited little variation with frequency. There was also a similarity between signals in the left and right groupings. The largest transmission phase shift occurred for center-axis positions. As with magnitudes, there was left-right symmetry with very small phase difference among left and right groupings. The average phase shift for the central positions was about -15° and was roughly independent of frequency.

The S-band signal magnitude and phase results are shown in Figures 32 and 33, respectively. For both parameters, there was a high degree of similarity within the three axis groupings -- left, center, and right -- demonstrating translation invariance along the direction between the two

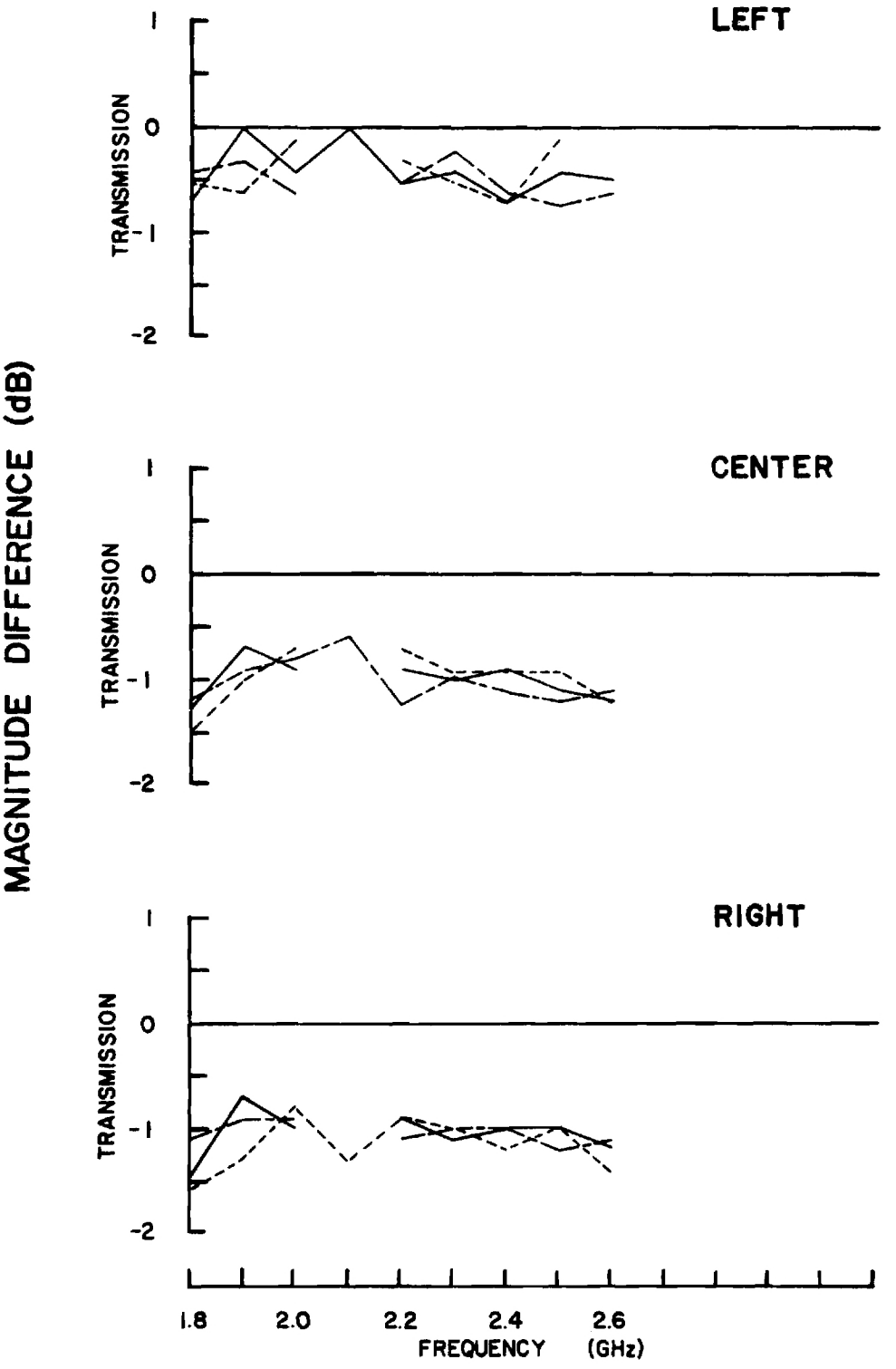

Figure 30. Magnitude differences in LS-band transmission coefficient with sample target present. Data for three target positions along each indicated axis.

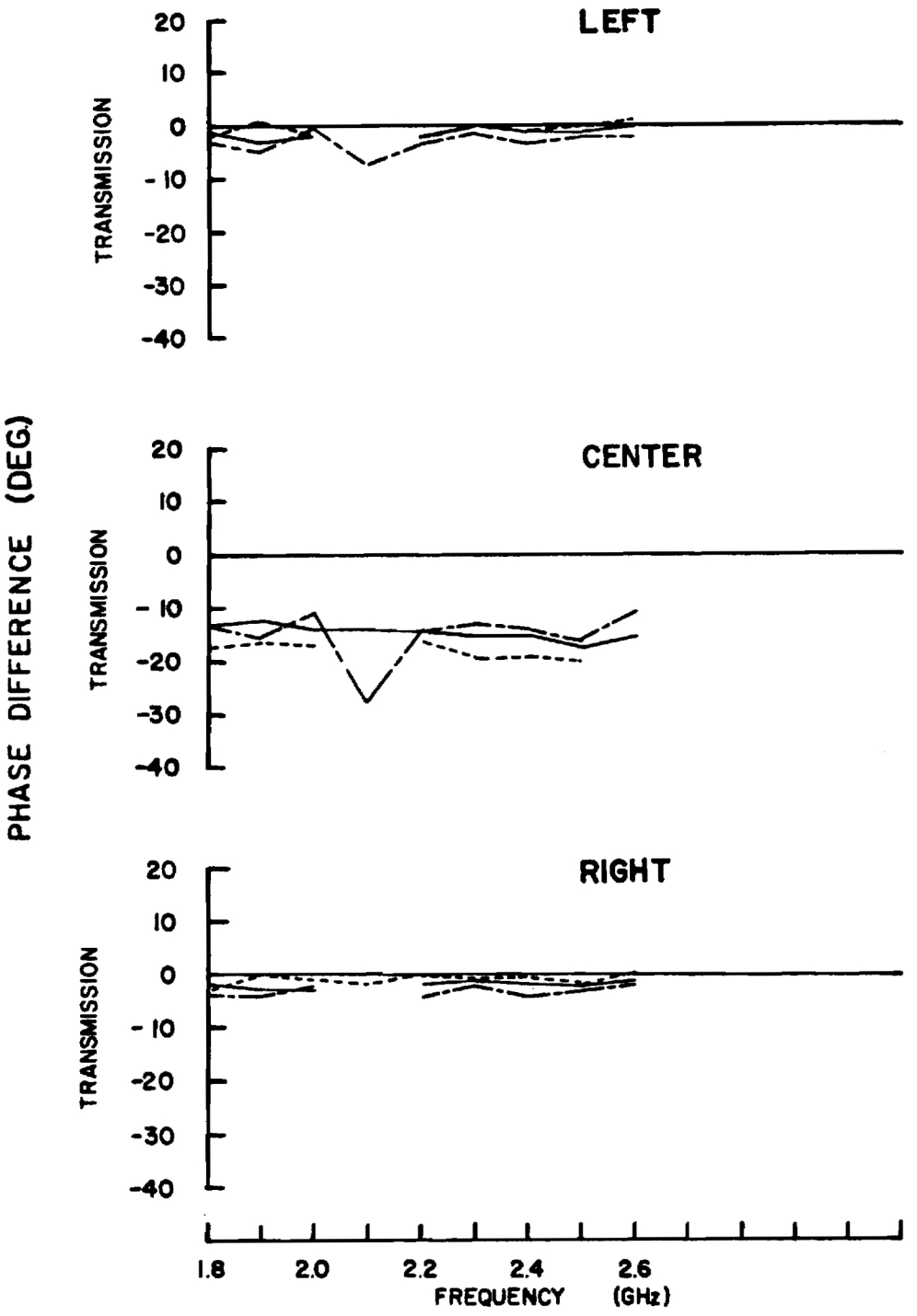

Figure 31. Phase differences in LS-band transmission coefficient with sample target present. Data for three target positions along each indicated axis.

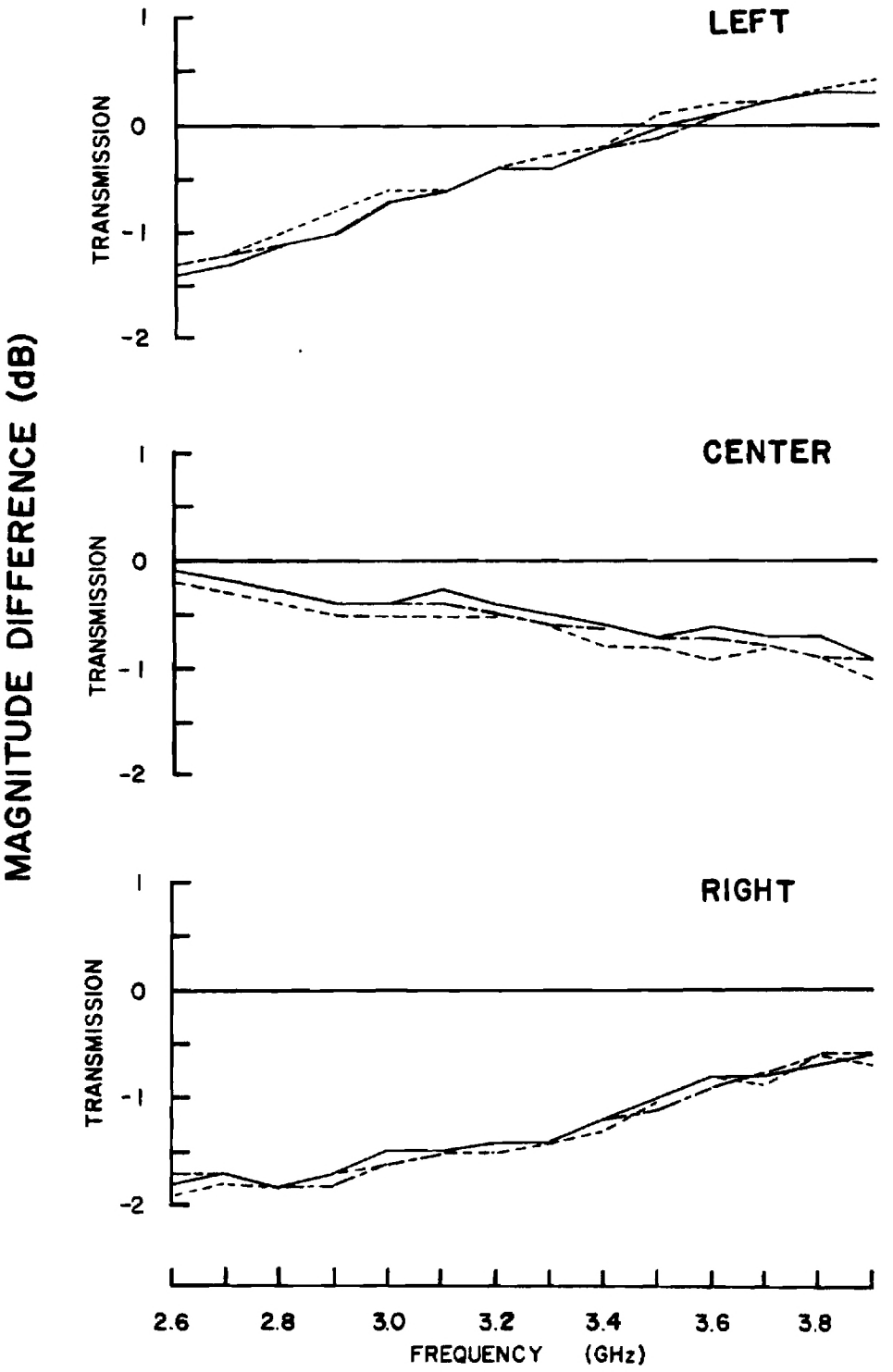

Figure 32. Magnitude differences in S-band transmission coefficient with sample target present. Data for three target positions along each indicated axis.

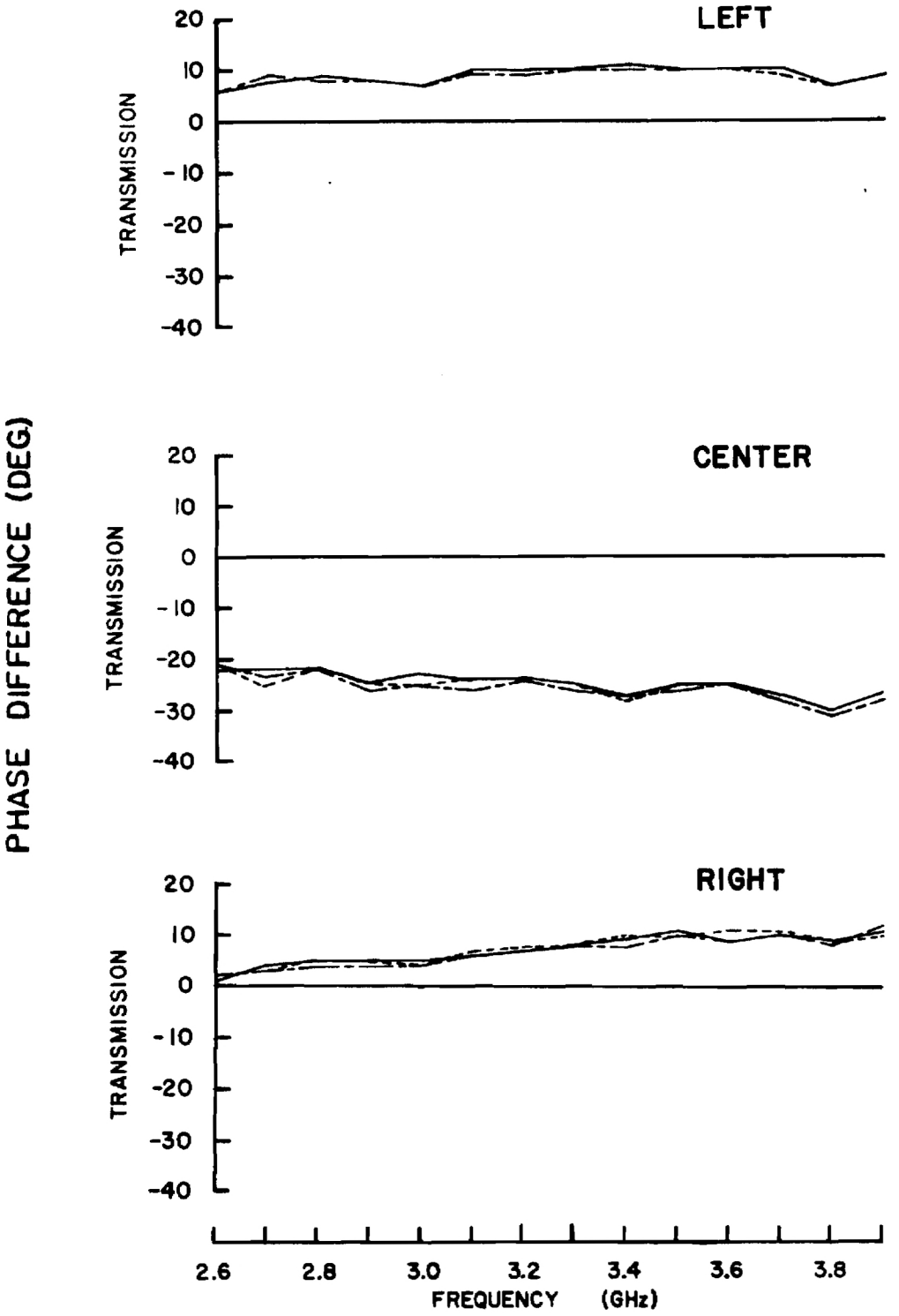

Figure 33. Phase differences in S-band transmission coefficient with sample target present. Data for three target positions along each indicated axis.

antennas. There was also a strong left-right symmetry about the center line as evidenced by the similarity of the data in left and right groupings. Magnitudes of the transmission coefficient change exhibited a marked frequency dependence. Additionally, the slope of this frequency dependence was different for the center positions as compared to the side positions. These magnitude changes ranged from -2 dB to + 0.3 dB. Phase shifts were fairly independent of frequency, with an average value of about +6° for the side positions and about -25° for the central positions.

The X-band signal magnitude and phase results are shown in Figures 34 and 35, respectively. Transmission magnitude showed about a 4 dB reduction for target positions on the center axis while for off-center positions it showed much smaller changes. Magnitude did not show as much left-right symmetry as it did for the lower-frequency bands. Transmission phase showed a 20-35° negative shift for center-axis positions and a 1-15° positive shift for off-center positions. There was more left-right symmetry in phase than in magnitude in this frequency band.

To have a measurement situation more like actual baggage inspection, reflection and transmission coefficients were also measured for a suitcase with and without the glycerol/water sample enclosed. For measurements involving the suitcase, the X-band horn antennas were spaced 45.7 cm apart with the bottom aperture edges 10.2 cm above the surface on which the suitcase rested. X-band was chosen for investigation because of the large changes seen with the glycerol target.

The soft-sided suitcase, 22 inches by 13 inches by 6 inches deep, was positioned midway between the antennas with its largest surfaces perpendicular to the antenna center axis so that transmitted signals passed through 6 inches of suitcase material. The suitcase was stepped through the space in 2-inch increments determined by aligning one end of the suitcase with marks on the surface supporting the suitcase. Reflection and transmission coefficients were recorded for each of these positions numbered 1 through 15. Position 8 corresponded to the center of the suitcase roughly aligned with the antenna center axis. The suitcase was filled with clothing for the "clothes only" case. The bottle of glycerol solution was placed in the center of the clothing for the "clothes and glycerol solution" case. Bottle position in the suitcase was stabilized with foam rubber packing.

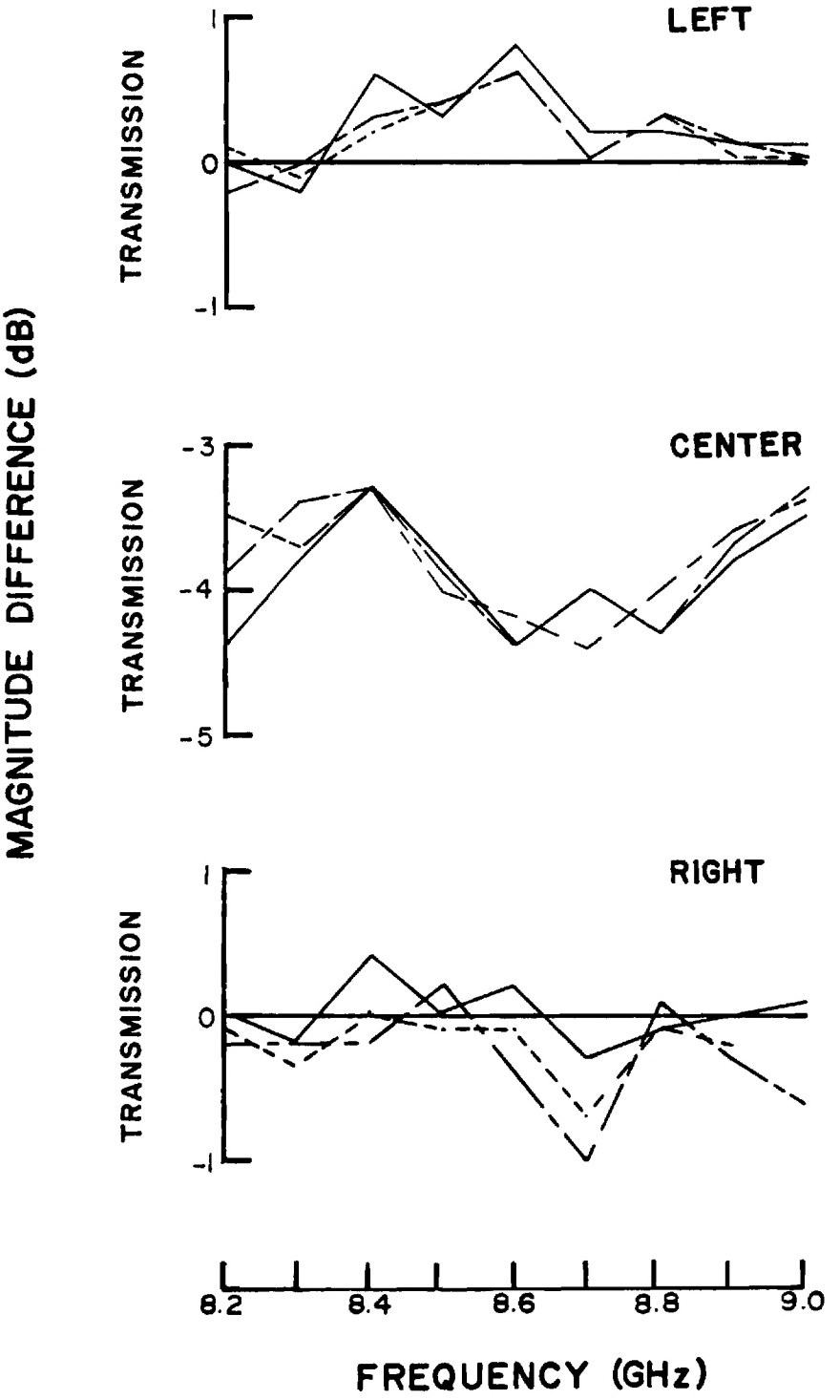

Figure 34. Magnitude differences in X-band transmission coefficient with sample target present. Data for three target positions along each indicated axis.

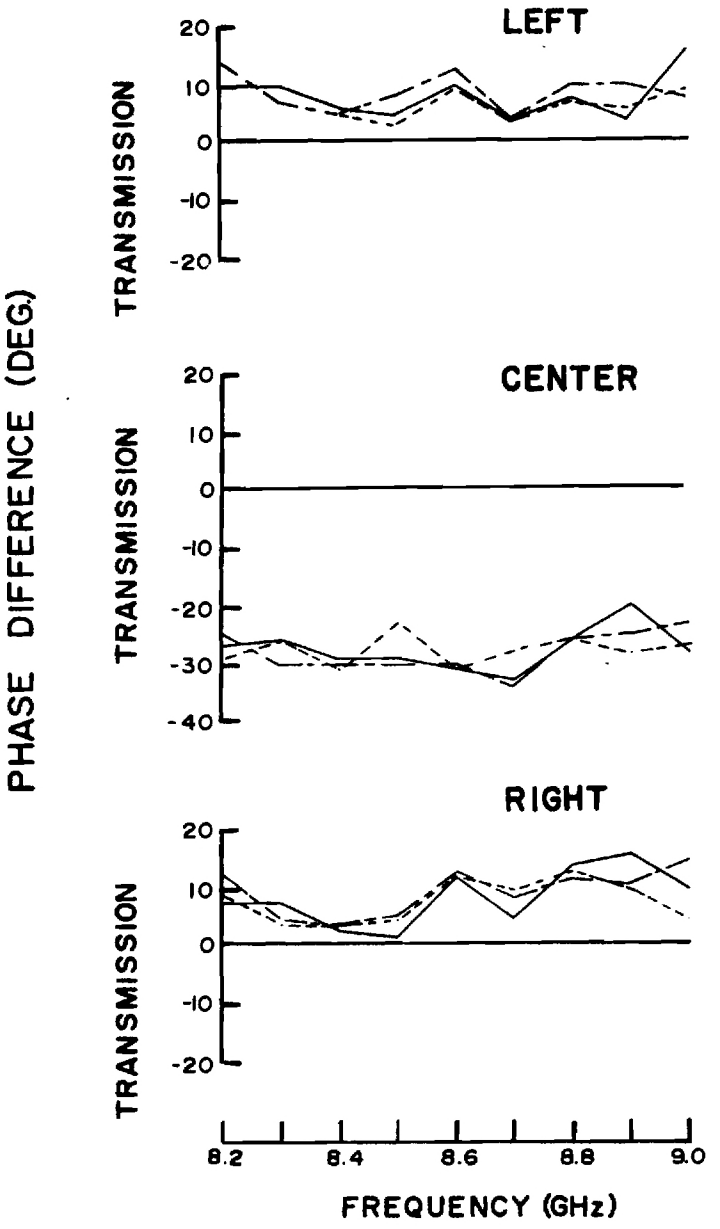

Figure 35. Phase differences in X-band transmission coefficient with sample target present. Data for three target positions along each indicated axis.

Figures 36 and 37 present the signal magnitude and phase, respectively, for the suitcase with and without the glycerol solution. Again, data are presented as differences between actual measured values and stored reference values found with the suitcase absent. Results for representative frequencies -- 8.4, 8.6, and 8.8 GHz -- are given in each figure. Broken lines correspond to 8.4 GHz; solid lines, to 8.6 GHz; and dashed lines, to 8.8 GHz. Position numbers refer to the 2-inch increments already described.

Magnitude differences for the transmission coefficients (Figure 36) showed a similar pattern with position for both cases across frequency. This characteristic pattern had three dips in it. The dips at position 2-3 and at position 13-14 corresponded to the ends of the suitcase aligned with the antenna axis and were very similar with and without the glycerol solution. The dip at position 8 corresponded to the center of the suitcase aligned with the antenna axis and was larger with glycerol present by 1.3 to 3.6 dB. This difference was similar to that seen for the centered bottle of glycerol solution by itself at these frequencies (Figure 34). Phase differences for the transmission coefficients (Figure 37) showed similar U-shaped patterns with suitcase position for both cases across frequency. Phase decreased when more than roughly half of the horn antenna aperture was occluded by the suitcase. For the clothes only case, the decrease peaked at positions 5 and 11 with a smaller decrease between them at position 7-8, the center of the suitcase. For the clothes and glycerol case, similar peak decreases were located at positions 5 and 11, but they were separated by an almost constant phase difference. The major difference between these two phase patterns occurred in this central region. The larger transmission phase decrease with glycerol present was expected since the glycerol solution by itself on center-axis caused a phase decrease of 25-30° (Figure 35) at these frequencies. The difference between phases at position 8, ranging from 19 to 27°, was comparable to the shift for the glycerol solution alone.

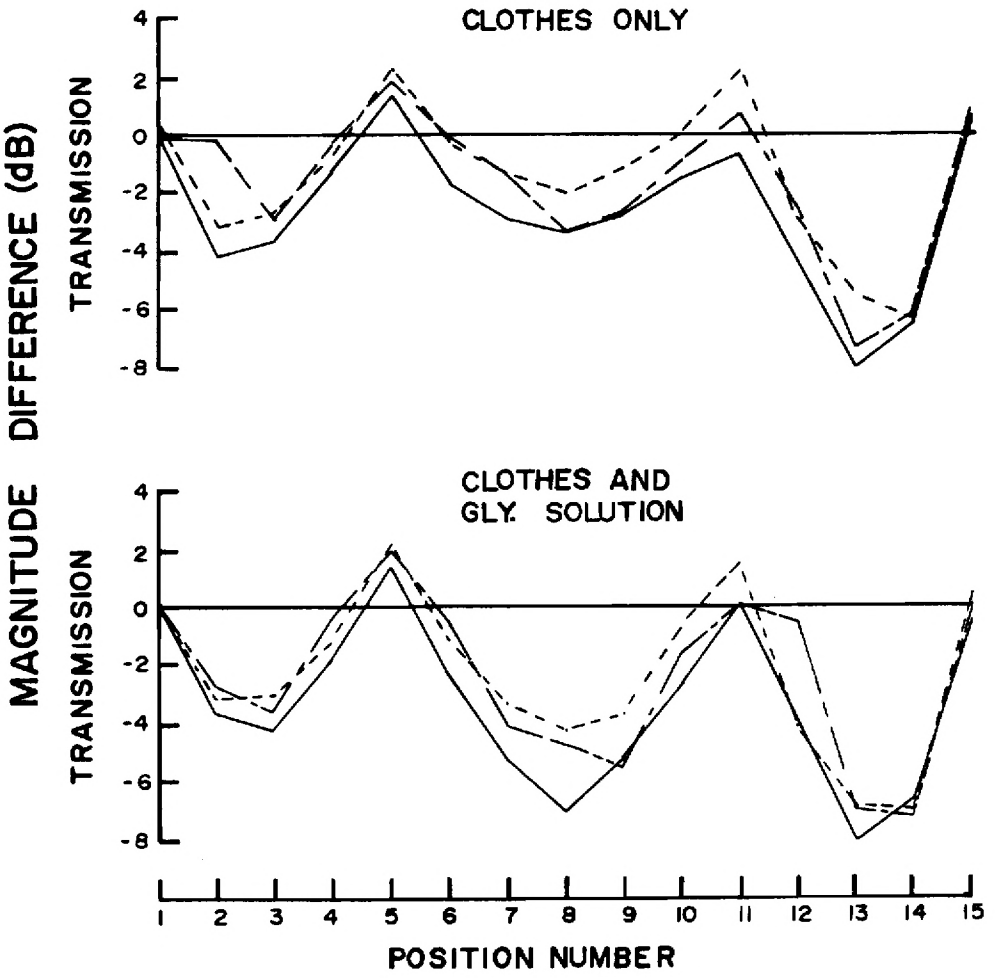

Figure 36. Magnitude differences in X-band transmission coefficient with and without sample target in center of suitcase. Suitcase position given by number of 2-inch increments. Separate curves represent the three signal frequencies tested.

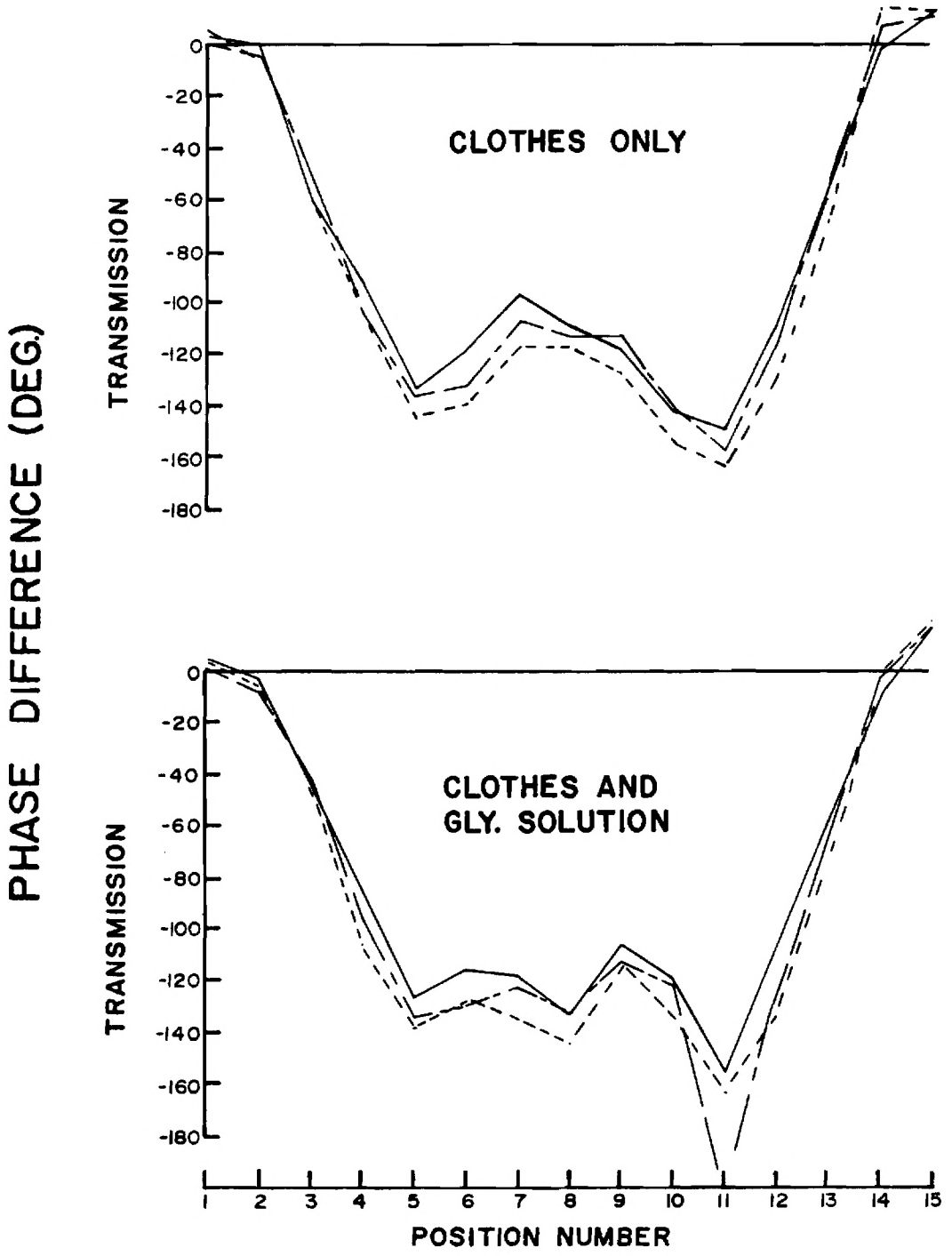

Figure 37. Phase differences in X-band transmission coefficient with and without sample target in center of suitcase. Suitcase position given by number of 2-inch increments. Separate curves represent the three signal frequencies tested.

C. Conclusions

Results obtained from the glycerol solution showed that transmitted signals were more uniform than reflected signals. This finding was consistent with results from the slab model. Although these measurements were made in three different frequency bands (LS, 1.8-2.6 GHz; S, 2.6-3.9 GHz; and X, 8.2-9.0 GHz) using different sets of antennas, transmission parameters were found to show progressive trends across frequency. Center-axis magnitude decreased from -0.5 to -4 dB while side-axis amplitude increased from -1 to 0 dB with values in the intermediate frequency range showing a transition. Center-axis phase decreased from -15 to about -25° while side-axis phase increased from -3 to +7°.

One surprising aspect of the data was the almost flat frequency response for the transmission phase shift in a given frequency band. This was in contrast to the multi-layered model which had a periodic frequency response. This difference in behavior may be explained by the smaller relative cross section of the scattering object causing only a minor perturbation in the received signal. The difference in two ranges, -15°for 1.8 - 2.6 GHz and -25° for 2.6 - 3.9 GHz, indicated that antenna geometry may have influenced this signal.

Center-axis transmission coefficient magnitude and phase changes for the glycerol solution in the 8.2 to 9.0 GHz range were very similar to the differences between this solution being present and absent in a suitcase. This meant that, in this frequency range at least, the magnitude and phase changes introduced by a fruit-like object in a suitcase added to the changes caused by the suitcase and clothes. This observation may provide the basis for being able to detect the presence of agricultural products using transmitted signal parameters.

From the cumulative results of the signal transmission/reflection approach, the transmitted signal appeared to be more suitable for detecting agricultural products in baggage for several reasons. First, the transmitted signal was more uniform with frequency and with target position. In practice, this would mean more reliable measurements and fewer required calibration procedures. Secondly, the additive changes noted above were more obvious in transmitted signals. Thirdly, the transmitted signal,

especially at X-band, was changed most for center-axis positions of the target which would allow better localization of an agricultural product in baggage.

The larger differences between center-axis and side-axis objects in the X-band measurements were attributable to some extent to a smaller beamwidth at these frequencies. A rough comparison of beamwidths was made by recognizing that beamwidth was inversely proportional to frequency and to the antenna dimension in the plane of interest [26]. For the transmitting antennas used in this study, the X-band beamwidth was approximately one-half of the LS-band beamwidth and approximately one-seventh of the S-band beamwidth. These comparisons were qualitative since beamwidth actually applies to far-field radiating fields which were not fully achieved in the experimental measurements. The more narrow relative beamwidth calculated for X-band could also explain the greater stability of X-band signals since less perturbation by surrounding objects would be expected.

Signal transmission coefficients exhibited measurable changes in both phase and amplitude for a target consisting of a 6 cm diameter, 9.5 cm long cylinder. A sphere with a diameter of 8 cm has the same volume and would be dielectrically representative of a large apple or a small grapefruit. From the magnitude of the changes observed for the glycerol solution target, changes should be detectable for spherical targets with diameters as small as 5 cm. Of course, changes would be larger for volumes larger than that tested.

Another facet of the data was the dependence of the transmitted signal upon the lateral position of the target. This indicated that there may be some ability to scan the contents of a suitcase in order to detect the location of agricultural products. Development of this approach could then lead to a microwave imaging device. This type of imaging is already being developed for biomedical applications [27]. Because of high attenuation in the water and immersed sample, necessary for impedance matching, that study was limited to frequencies below 3.5 GHz. For the case of an agricultural product in a suitcase, however, reflections

at the suitcase-air interface should not be too large and attenuation not as much a problem because of the small thickness of typical scattering objects. Since detailed resolution is not a necessity (5 cm should be sufficient), a frequency of 6 to 10 GHz would seem appropriate for this kind of imaging.

VI. SHORT PULSE RADAR APPROACH

Short Pulse Radars (SPRs), also known as "impulse" and "baseband" radars, use very brief, transient pulses in their operation. The narrow pulse, typically 1-to-10 nanosecond width, provides a transmitted signal with broad frequency content. Typical pulse amplitude is on the order of 1000 V to provide sufficient energy across the frequency spectrum. The SPR works by emitting a pulse from an appropriate antenna and then receiving the energy reflected by objects in front of the antenna. Received signals (also called reflections, or returns) tend to be pulsatile but their shape is determined by the nature of the object causing the reflection, as well as by the shape of the transmitted pulse. Distance to the object, or target, can be derived from the delay between transmitted and reflected pulses and is easily extracted from SPR returns when dielectric properties of the propagation medium are known. Additional information about the target can be gained from an analysis of reflected pulse shape.

The SPR has already been used successfully in several applications. Identification of underground objects such as utility pipes [28], tunnels and voids [29], metallic and dielectric explosive mines [30-31], and pieces of wood and plastic [31] is possible. Voids under concrete highways have also been detected [32]. In another type of application, SPR has been used to determine subsurface structure of icebergs [33] and geophysical strata [29,34]. All of these applications utilize returned pulse delays to determine distances. Returned pulse frequency content is usually required to identify and classify buried objects.

In the SPR approach, detection of a buried object is very similar to detection of an agricultural product in a suitcase. In both cases, an object a few centimeters in size is surrounded by a larger volume with dielectric properties different from the object's. Also, in both cases, the larger volume's surface facing the antenna is flat. Thus, a description of SPR detection of buried objects is useful in considering SPR detection of agricultural products in baggage.

A. Analysis

For the idealized situation of a single buried object, SPR operation can be simply explained. A pulse of electromagnetic energy is emitted from the SPR antenna and propagates in air to the ground surface. At this interface, part of the energy is reflected to the antenna now acting in a receive mode. The remainder of the energy propagates through the soil to the target where part of it is reflected through soil and air to the antenna. The part of the energy not reflected by the target proceeds on through the soil and is dissipated. This situation is shown in Figure 38 in which forward energy propagates to the right.

Shape and amplitude of the reflected pulse waveform depend on the differences in dielectric properties at the respective interfaces. A feel for the approximate shapes can be had from consideration of the voltage reflection coefficient ρ, which is the complex ratio of reflected to forward electric fields of the propagated waves as given by equation (10) in Section V. The reflected electric field can be expressed as

$$E_R = \rho E_F . \qquad (13)$$

Since all materials considered here have the magnetic permeability of free space, ρ is a function only of the complex permittivities involved. Using equations (10) and (12),

$$\rho = \frac{\sqrt{\varepsilon_1^*} - \sqrt{\varepsilon_2^*}}{\sqrt{\varepsilon_1^*} + \sqrt{\varepsilon_2^*}} . \qquad (14)$$

Forward energy propagates through region 1 into region 2. For $\varepsilon_2^* > \varepsilon_1^*$, as it is for the air/soil interface, $\rho < 0$ and $E_R < 0$ with $E_F > 0$ assumed. Thus, the pulse reflection will be mostly negative, as shown in the sample reflected waveform in Figure 38. The pulse return is an inversion of the transmitted pulse. By following a similar procedure for the buried target with $\varepsilon_{ob}^* < \varepsilon_2^*$, $\rho > 0$ at the soil/target interface. The result is illustrated in Figure 38 as a mostly positive waveform.

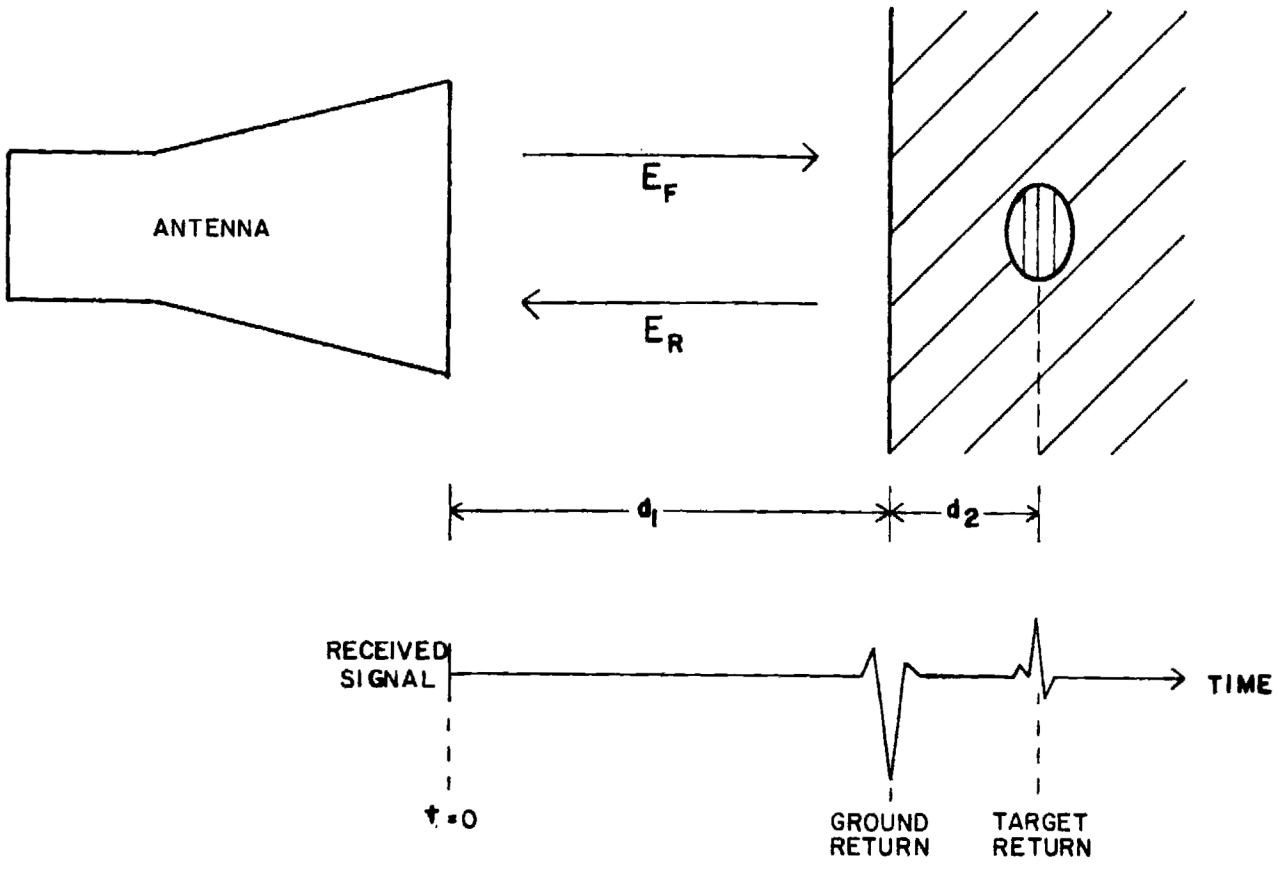

Figure 38. Diagram of typical SPR arrangement and response for subsurface targets.

Delay to reception of the reflected pulse from the air/soil interface is twice the product of propagation velocity in air and antenna distance above ground, d_1. Similarly, the additional delay to the target return is twice the product of propagation velocity in soil and burial depth, d_2. These delays are thus longer for larger distances.

Relative amplitudes of the returns can be estimated from equation (14). It is seen that a larger difference in permittivities causes a larger reflected pulse. Attenuation of propagating signals must also be considered since it is not accounted for in this equation. Dissipation of energy in soil would also reduce the amplitude of the target return estimated from equation (14).

To consider baggage interrogated by SPR, a dielectric slab is taken to represent the suitcase and its contents. For simplicity, the slab extends infinitely in directions orthogonal to the direction of energy propagation. A suitcase and its normal contents of clothing has a relative permittivity of approximately 2.5 and is essentially lossless (nondissipative). The target fruit has relative complex permittivity of approximately 50 - j 20, corresponding to frequencies in the gigahertz range (Section II). Propagation velocity in air is 30×10^9 cm/s (11.8×10^9 in/s); in the suitcase, 19.9×10^9 cm/s (7.5×10^9 in/s). Propagation delays in the two media are then 0.033 ns/cm (0.085 ns/in) in air and 0.053 ns/cm (0.134 ns/in) in the suitcase.

For the suitcase alone, there will be two returns: one from the front surface and one from the rear surface. Substituting the dielectric constants for air (free space) and slab into equation (14) gives $\rho = -0.225$ for the front surface and $\rho = 0.225$ for the rear surface. The first return will thus be similar to the ground return in Figure 38; the second, an inverted form of the ground return. The two returns will be separated by a delay of twice the product of propagation delay per unit length and suitcase thickness. For a thickness of 10 inches, the delay is 2.68 ns; for 5 inches, 1.34 ns. The range of 5-to-10 inches includes most baggage thicknesses. Typical time courses for target returns are 1-to-2 ns [29-31]. For the suitcase alone, there would be two signals of this duration only 1.3-to-2.7 ns apart, onset to onset. In other words,

the suitcase returns would be very close to one another and may even overlap.

For a suitcase with fruit inside, there will be three returns: two for the suitcase surfaces and one for the fruit. The fruit return will occur between the two surface returns discussed above. This fact alone may prevent its observation because it may be obscured by the surface returns which will be very close to one another. But, if the fruit return is much larger than the surface returns, it may be discernible. Based on equation (14), the reflection coefficient for the fruit return will be nearly -1 since the magnitude of the fruit's permittivity is much larger than that of the suitcase. This reflection is 4 times that predicted for the suitcase surface. The return to the antenna will actually be only about 3 times larger since only a fraction of the incident energy reaches the fruit. However, since the fruit will present a smaller cross section to the propagating wave, its return may instead actually be smaller than the surface returns.

Various strategies may improve the detectability of fruit with SPR. The rear surface return could be effectively eliminated by placing an appropriate absorbing material next to this surface. Returns from the front surface and the fruit could then be better discriminated. However, fruit near the front surface would produce a return nearly simultaneous with the front-surface return. Detection of a fruit return would be reliable for all possible fruit locations only if the fruit return is larger than the surface return. Hence, the absorbing material would provide no overall advantage since this was also the case with both surface returns.

B. Measurements

To explore more fully the potential of SPR to detect fruit in baggage, discussions were held with personnel of the Radar Applications Division. This division of the Radar and Instrumentation Laboratory of Georgia Tech's Engineering Experiment Station had already used SPR to detect buried objects and subsurface voids [30,32]. From these discussions, it was learned that an appropriate mathematical model for representing

agricultural products in baggage did not exist. However, it was decided that SPR had enough promise as a detector of agricultural products to warrant performing some measurements to check the feasibility of this approach. An SPR system with a transmitted signal consisting of a single cycle of 1-GHz energy was used.

Experimental measurements were made on citrus fruits buried in sand. This arrangement was chosen for two reasons. First, the experimental SPR system used for these measurements was already set up for recording returns from subsurface objects. The antenna pointed downward and its height was adjustable. The antenna along with all electronic instrumentation and small computer was mounted on a wheeled cart which was moved to change antenna positions. Secondly, the buried fruits were electrically very similar to agricultural products in a suitcase filled with clothing. From the propagation velocity derived from the differential delay between returns from top and bottom surfaces of the dry sand used, the relative dielectric constant of the sand was determined to be approximately 3.6. This value fell into the relative dielectric constant range of 1 to 5 expected for clothing and plastics in a suitcase.

A 6-foot by 10-foot box with a height of 2 feet was constructed of plywood. It was filled with dry construction-grade sand to a depth of 18 inches. Figure 39 shows schematically the box with sand and its location with respect to the SPR antenna and instrumentation cart. Before a series of measurements, the surface of the sand was leveled and smoothed to provide a constant distance between antenna and sand as the antenna position was changed. Returns were measured for each condition at several antenna positions spaced 6 inches apart with one antenna position directly over the fruit. Tangerines, oranges, and grapefruits were selected as targets to represent a size range of fruit with similar dielectric properties.

The return voltage signal was processed by electronic circuits using sampling oscilloscope techniques. Under the control of an Apple computer, the return signal information was stored in disk memory for later access and processing. The return signal was displayed on an oscilloscope as it was received (and also stored) with one millisecond representing one nanosecond, a factor of 1,000,000 times slower. The

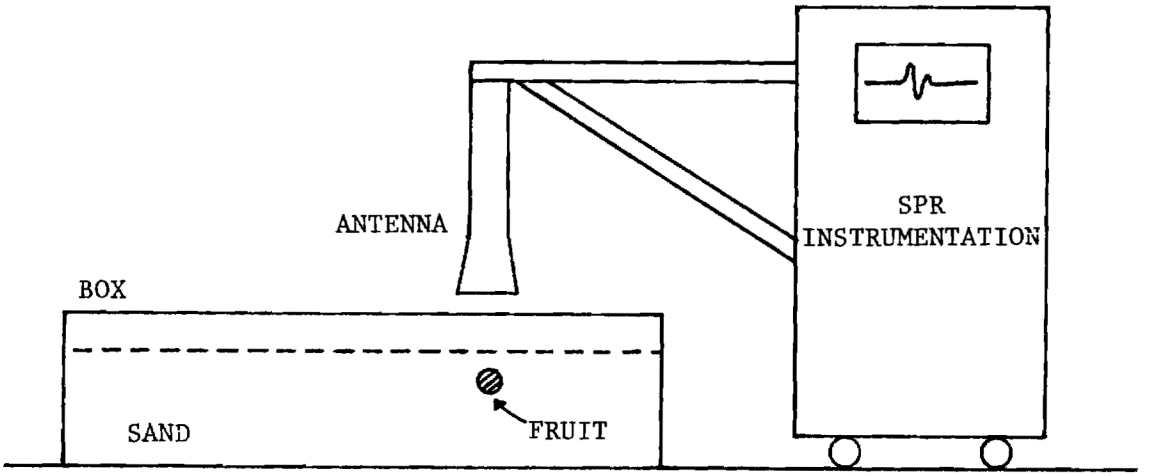

Figure 39. Short pulse radar measurement setup.

computer sampled and stored 220 values proportional to voltage for each return. Each point represented 0.026 nanosecond in real time so that there was the capability to analyze and plot 5.72 nanoseconds of each return. The velocity of propagation in sand was measured to be 6.2 x 10^9 inches/second, or 6.2 inches/nanosecond. Thus, each nanosecond of the display represented 3.1 inches of travel in sand since the signal traveled to and from the reflecting surface before reception.

Initial measurements were made with fruit placed on top of the sand. Both single fruits and multiple fruits placed side by side were tested. Figure 40 shows the results obtained for one and three oranges on the surface. Each trace represented 5.72 nanoseconds of return voltage signal with the same arbitrary voltage scale applied to all traces. The set of seven traces for each condition were recorded for antenna positions 6 inches apart. The center trace in each set was the signal recorded with the antenna directly over the fruit. For antenna positions furthest from the fruit--top and bottom traces in each set--there were only small returns from the sand. As the antenna was moved closer to the fruit, there was a larger, earlier return due to the fruit. The fruit return amplitude was maximum with the antenna directly over the fruit. The maximum return from three oranges was larger and was received earlier than the maximum return from one orange. Returns from two oranges on the surface were intermediate in amplitude and had delays similar to the ones for three oranges.

Returns from other fruits on the sand surface were similar in shape to those from oranges. For both tangerines and grapefruits, fruit returns were larger for more fruit. Tangerine returns were slightly smaller than those for the same number of oranges; grapefruit returns were larger than those for oranges. Tangerine returns occurred with approximately the same delay that orange returns occured, but grapefruit returns occurred earlier. The delays for one, two and three tangerines were similar as were the delays for one, two and three grapefruits.

Measurements were also made for fruit buried 3 inches below the sand surface for one and for three each of tangerines, oranges, and grapefruits. Amplitudes of these returns were smaller than for fruit

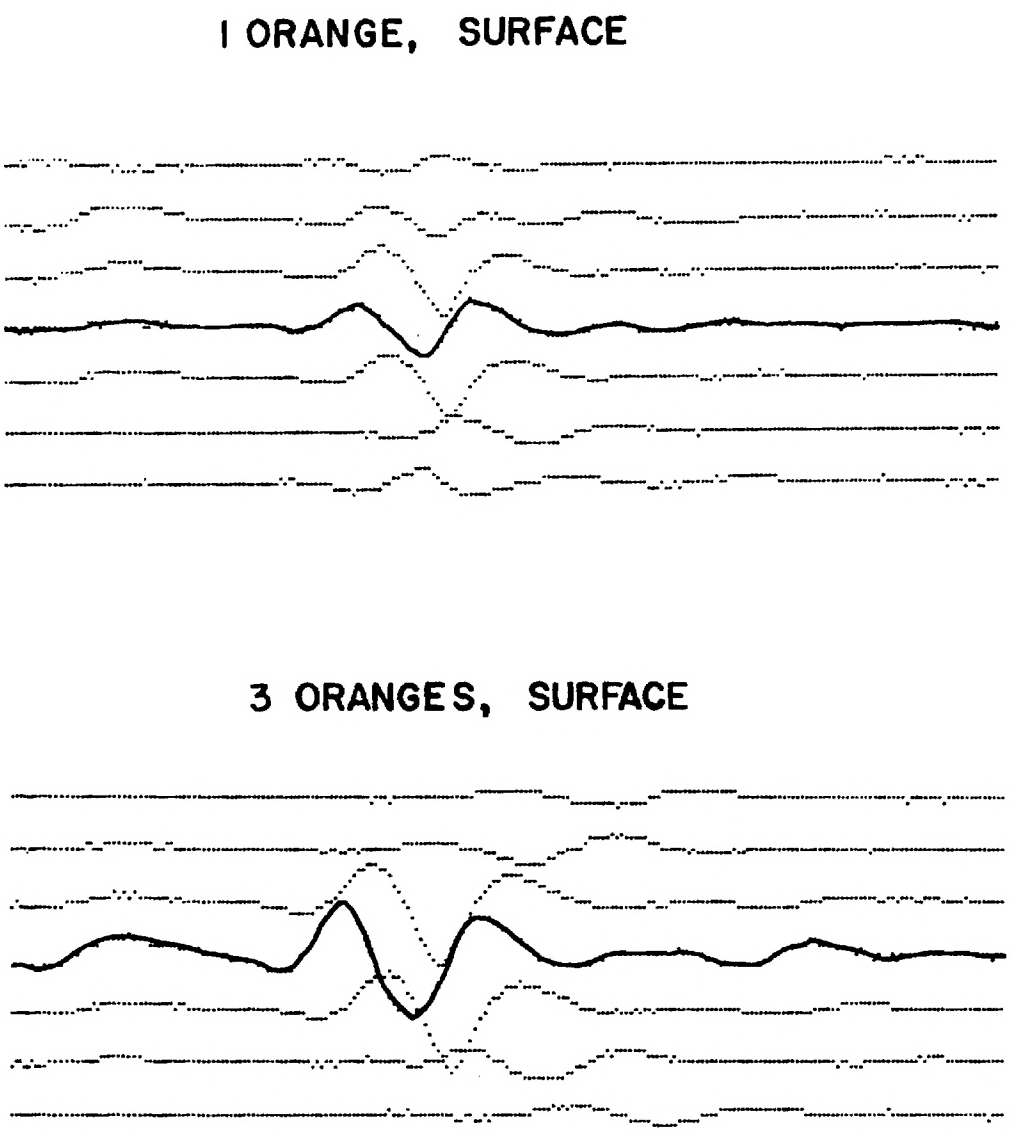

Figure 40. SPR returns for one and three oranges on surface of sand. Solid traces are for antenna position directly over fruit. 5.72 nanosecond signals.

placed on the surface because of signal attenuation in the sand, spreading of the transmitted signal over a larger area, and the slightly better impedance match in sand. The gain of the receiver electronic circuits was increased to provide a signal large enough to display and to store accuractely. Figure 41 shows the results obtained for one and three buried oranges. Traces for each condition were again taken for antenna positions 6 inches apart. Because of the higher gain used for these returns, early returns from the SPR system internal connections, the antenna, and the sand surface were often larger than the later fruit returns. The early returns, seen as small humps on the left-hand portion of the low-gain traces in Figure 40, often caused amplifier saturation at the higher gain needed to detect the deeper fruit. For this reason, early returns were deleted from Figure 41 to show more clearly the fruit return traces, which had a duration of only 3.58 nanoseconds due to the deletion.

Returns from three buried oranges were larger than those from one buried orange, as seen by comparing the highlighted traces in Figure 41. Fruit returns were discernible in traces for antenna postions eighteen inches away from the position directly over the oranges. These statements also describe the results for tangerines and grapefruits and, in general, larger returns were observed for larger fruit. Comparison of delays of returns from buried fruit was not possible because many of the returns overlapped the earlier large returns.

Measurements were also made for single fruits buried 9 inches below the sand surface. Results for a buried orange are shown in Figure 42 where the traces are again 3.58 nanoseconds long. When amplifier gains were increased still more to obtain reasonable amplitudes for the fruit returns, many other returns of similar amplitudes were also present. Attempts to cancel these non-fruit returns were made by subtracting stored returns from only the sand. A set of these difference returns is shown in Figure 42 which clearly shows the return from the orange in the central traces. Similar return patterns were also obtained from a tangerine and from a grapefruit buried 9 inches deep.

In subtracting returns to reveal small returns from the 9-inch deep fruit, a problem with triggering was encountered. The SPR recording

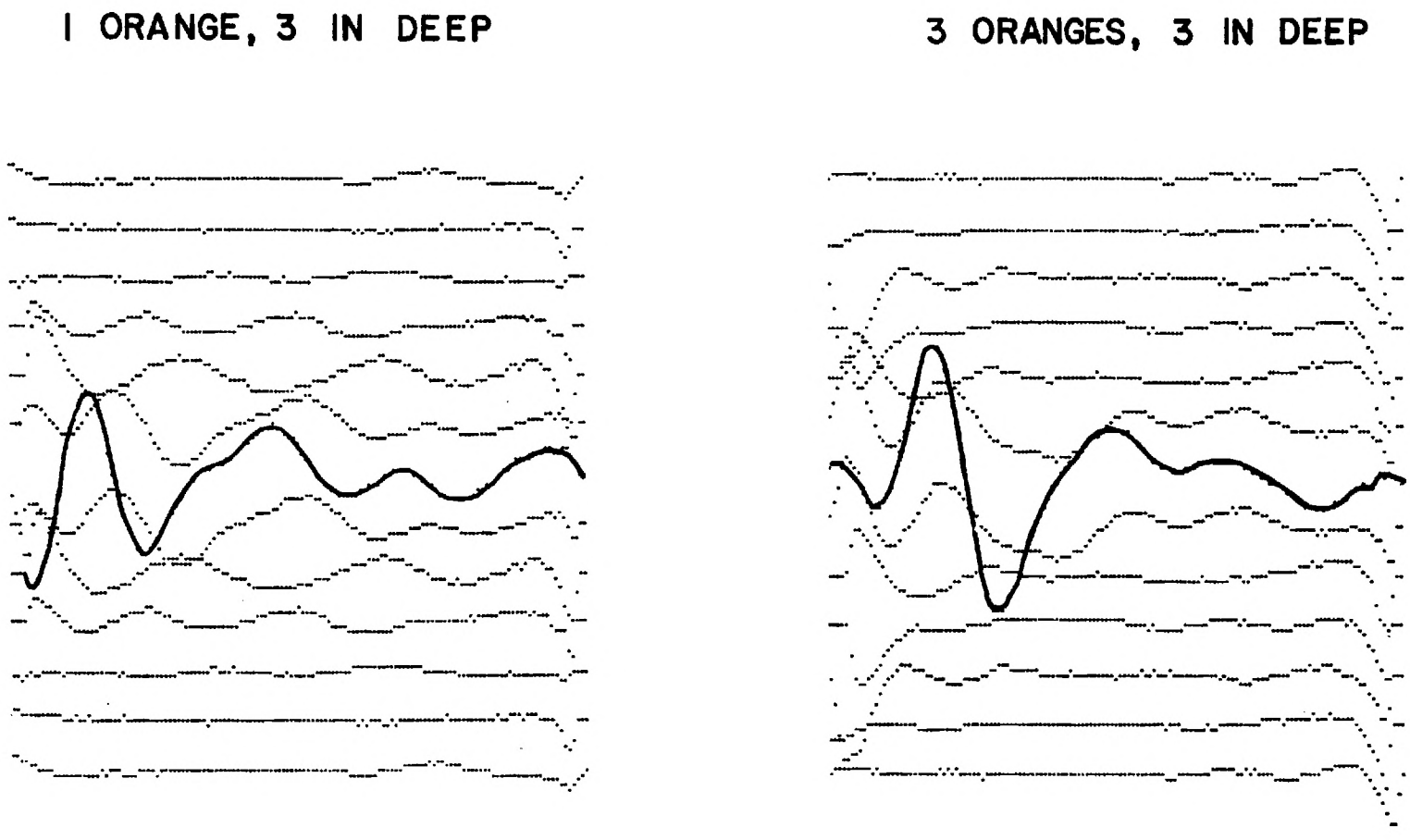

Figure 41. SPR returns for one and three oranges buried 3 inches below surface of sand. Solid traces are for antenna position directly over fruit. 3.58 nanosecond signals.

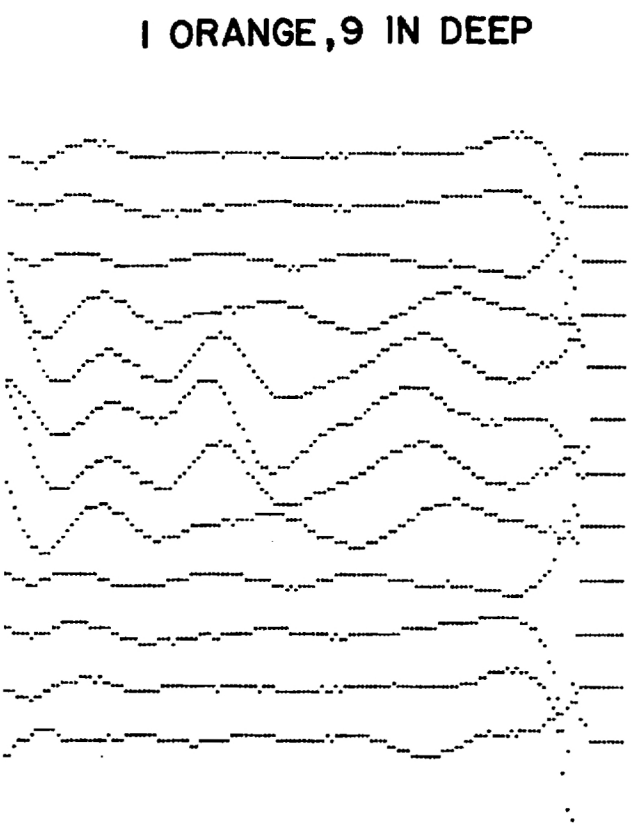

Figure 42. SPR returns for an orange buried 9 inches below surface of sand. 3.58 nanosecond signals.

system had been designed to trigger on a large, early return from the ground surface. This return was not always reproducible from experiment to experiment so that the triggering point varied in time. A single set of no-fruit returns was stored to subtract from subsequent returns obtained with fruit present. When the triggering point differed in time for a pair of returns being subtracted, the resultant difference trace contained amplitude variations not related to the fruit return. From this experience, it was determined that a trigger stationary in time was required. The SPR system used in these studies could not be easily modified to include such a trigger within the time and budget limitations of this project.

C. Conclusions

From the various SPR returns from fruit on, and buried in, sand, it was seen that detection of fruit in a closed suitcase with SPR was feasible. The returns from fruit had several characteristics which would be useful in differentiating returns from fruit and from other suitcase contents such as clothing. The returns from fruit were all similar in shape and their amplitudes were larger with larger volumes of fruit. The delay to a return was shorter for fruit closer to the antenna and, to a lesser degree, for larger fruit.

The presence of fruit was readily detectable from the appearance of the voltage traces representing received signals. These traces gave target location information in two dimensions: laterally as the antenna was moved and depth along each trace. In a few trial measurements, individual returns from fruits one above another separated by 3 inches were also detectable. Other types of signal encoding, such as line density proportional to amplitude, may make the fruit return even more obvious. One definite requirement for an SPR system in future experiments is a time-synchronized trigger for received signals. This improved trigger would make possible the detection of returns from even smaller fruits than those used in this study.

VII. CONCLUSIONS AND RECOMMENDATIONS

The results obtained during this project indicated that electromagnetic methods can successfully detect agricultural products in baggage. Although there was no previously published work in this area, these results were expected because of the differences between dielectric properties of agricultural products and dielectric properties of clothing and other suitcase contents. The following four approaches using different electromagnetic techniques were studied:

1. Capacitor plate, in which impedance of pairs of parallel metal plates was measured;
2. Resonant cavity, in which resonant frequency and losses of a metal box were measured;
3. Signal transmission/reflection, in which transmitted and reflected signals between two antennas were measured; and
4. Short pulse radar, in which the reflected portion of a transient pulse was measured.

In all four approaches, fruit or fruit-like objects were detected alone and in situations simulating inclusion in baggage.

Since a basic ability for detection was demonstrated, further development to produce an automated system requiring minimal operator attendance and inexpensive enough for wide deployment will involve refinement of current experimental models. This refinement would include not only instrumentation necessary for automation but enhancement of detection capabilities and definition of performance levels as they relate to baggage inspection requirements. These requirements include rapid, reliable inspection of closed baggage and an appropriate indication for inspectors when an agricultural product is present. It is anticipated that rapid inspection would be best achieved by using a conveyor belt apparatus which would carry each piece of baggage past an electromagnetic detector based on one of the four approaches. This would be similar to systems currently in use for the X-ray examination of baggage. Three of

the four approaches are compatible with this inspection scheme. The resonant cavity approach, which utilizes a closed metallic box, would require extensive modification for this scheme. For this reason, and because of the ambiguities seen in the results obtained with this approach, it is recommended that the resonant cavity approach not be pursued.

With available laboratory instruments, sufficient sensitivity was displayed by the four approaches to detect one or a few medium-sized fruit. Measurements were done passively, i.e., perturbations of electromagnetic fields created by fruit were indicated by the instruments. It is anticipated that incorporating devices tested in this program into active circuits will not only increase sensitivity but will provide appropriate output signals to indicate the presence of agricultural products. Such an active circuit could take the form of an amplifier with positive feedback similar to ones which have been developed for other applications [35,36]. The frequency of oscillation and power output level of such a circuit depend on the terminal properties of a feedback element. If this element consisted of capacitor plates or transmission/reflection antennas, then changes in these parameters could indicate the presence of an agricultural product. Of course, the range of oscillation frequencies would be different for each type of element.

The capacitor plate approach is attractive for several reasons. First, its parallel-plate configuration would readily allow the passage of baggage to be interrogated. Secondly, instrumentation of plates operating at relatively low frequencies of 1-5 MHz is fairly straightforward. Lastly, at these frequencies there should be the greatest difference between dielectric properties of agricultural products and dielectric properties of other baggage items with high-water content such as perfumes, lotions, and beverages. This difference may allow for discrimination between these items and fruits and vegetables to reduce false positive indications of agricultural product presence.

The short pulse radar approach is attractive because of its capability to provide target depth information. This approach has the highest potential for displaying object shape and location information conveniently on a screen. This information would assist an inspector in distinguishing suitcase items as well locating items for follow up visual inspection. Characteristic shapes of different agricultural products would also aid the decision whether to inspect further.

The following recommendations for device development are based on the findings in this project:

1. Pursue the capacitor plate approach by developing instrumentation, possibly active circuits, to provide indications of agricultural product presence using an array of plates;
2. Pursue the short pulse radar approach using a dedicated system with an easily interpreted visual display; and
3. Investigate on a limited basis the applicability of the transmission/reflection antenna pair at X-band to an active circuit to provide indications of agricultural product location in baggage.

VIII. REFERENCES

1. U.S. Department of Agriculture, "Travelers' Tips on Bringing Food, Plant, and Animal Products into the United States," USDA, APHIS, Program Aid No. 1083, U.S. Government Printing Office, 725-104, 1981, 17 pp.

2. N.N. Mohsenin, Physical Properties of Plant and Animal Materials Volume I, Gordon and Breach Science Publishers, New York, 1970, 734 pp.

3. F. L. Hart and H. J. Fisher, Modern Food Analysis, Springer-Verlag, New York, 1971, 519 pp.

4. McGraw-Hill, Encyclopedia of Food, Agriculture, and Nutrition, D. N. Lapedes, ed., McGraw-Hill, New York, 1977, 732 pp.

5. H. W. Ockerman, Source Book for Food Scientists, The AVI Publishing Company, Westport, Connecticut, 1978, 926 pp.

6. S. O. Nelson, "Microwave Dielectric Properties of Fresh Fruits and Vegetables," American Society of Agricultural Engineers, Winter Meeting, Dec. 11-14, 1979, paper 79-3546.

7. T. M. Shaw and J. A. Galvin, "High-Frequency-Heating Characteristics of Vegetable Tissues Determined from Electrical-Conductivity Measurements," Proc. IRE 37: 83-86, 1949.

8. W. E. Pace, W. B. Westphal, S. A. Goldblith, and D. Van Dyke, "Dielectric Properties of Potatoes and Potato Chips," J. Food Sci. 33: 37-42, 1968.

9. N. E. Bengtsson and P. O. Risman, "Dielectric Properties of Foods at 3 GHz as Determined by a Cavity Perturbation Technique. II. Measurements on Food Materials," J. Microwave Power 6: 107-123.

10. W. R. Tinga and S. O. Nelson, "Dielectric Properties of Materials for Microwave Processing-Tabulated," J. Microwave Power 8: 23-65, 1973.

11. T. Ohlsson, N. E. Bengtsson, and P. O. Risman, "The Frequency and Temperature Dependence of Dielectric Food Data as Determined by a Cavity Perturbation Technique," J. Microwave Power 9: 129-145, 1974.

12. E. C. To, R. E. Mudgett, D.I.C. Wang, S. A. Goldblith, and R. V. Decareau, "Dielectric Properties for Food Materials," J. Microwave Power 9: 303-315, 1974.

13. S. O. Nelson, "Electrical Properties of Agricultural Products - A Critical Review," in Quality Detection in Foods, J. J. Gaffney, ed., American Society of Agricultural Engineers, St. Joseph, Michigan, 1976, pp. 86-97, 101.

14. A. R. Von Hippel (ed.), Dielectric Materials and Applications, The M.I.T. Press, 1954, p. 3.

15. K. R. Foster, J. L. Schepps, D. D. Stoy, and H. P. Schwan, "Dielectric Properties of Brain Tissue Between 0.01 and 10 GHz," Phys. Med. Biol. 24: 1177-1187, 1979.

16. E. C. Burdette, F. L. Cain, and J. Seals, "In-Vivo Determination of Energy Absorption in Biological Tissue," Final Technical Report, Project A-1755, U.S. Army Research Office, Grant No. DAAG29-75-G-0182, January, 1979.

17. E. C. Burdette, F. L. Cain, and J. Seals, "In-Vivo Probe Measurement Technique for Determining Dielectric Properties at VHF Through Microwave Frequencies," IEEE Trans. Microwave Theory Tech. MTT-28: 414-427, 1980.

18. D. R. Thompson and G. L. Zachariah, "Dielectric Theory and Bioelectrical Measurements (Part II. Experimental)," Trans. ASAE 14: 214-215, 1971.

19. A. W. J. Dawkins, C. Gabriel, R. J. Sheppard, and E. H. Grant, "Electrical Properties of Lens Material at Microwave Frequencies," Phys. Med. Biol. 26: 1-9, 1981.

20. B. D. Roebuck and S. A. Goldblith, "Dielectric Properties of Carbohydrate-Water Mixtures at Microwave Frequencies," J. Food Sci. 37: 199-204, 1972.

21. R. E. Mudgett, D.I.C. Wang, and S.A. Goldblith, "Prediction of Dielectric Properties in Oil-Water and Alcohol-Water Mixtures at 3,000 MHz, 25°C Based on Pure Component Properties," J. Food Sci. 39: 632-635, 1974.

22. J. D. Kraus and K. R. Carver, Electromagnetics, McGraw-Hill, New York, 1973, pp. 71-73.

23. C. G. Montgomery, R. H. Dicke, and E. M. Purcell, Principles of Microwave Circuits, Dover Publications, New York, 1965, pp. 387, 391.

24. S. Ramo, J. R. Whinnery, and T. Van Duzer, Fields and Waves in Communication Electronics, John Wiley & Sons, New York, 1965, p. 603 ff.

25. M. A. Stuchly, S. S. Stuchly, and G. Kantor, "Diathermy Applicators with Circular Aperture and Corrugated Flange," IEEE Trans, Microwave Theory Tech. MTT-23: 267-271, 1980.

26. S. Silver, ed., Microwave Antenna Theory and Design, McGraw-Hill, New York, 1949, 623 pp.

27. J. H. Jacobi and L. E. Larsen, "Microwave Time Delay Spectroscopic Imagery of Isolated Canine Kidney," Med. Phys. 7: 1-7, 1980.

28. A. C. Eberle and J. D. Young, "The Development and Field Testing of a New Locator for Buried Plastic and Metallic Utility Lines," Transportation Research Record 631: 47-52, 1977.

29. D. L. Moffatt and R. J. Puskar, "A Subsurface Electromagnetic Pulse Radar," Geophysics 41: 506-518, 1976.

30. J. D. Echard, J. A. Scheer, E. O. Rausch, W. H. Licata, J. R. Moore, and J. A. Nestor, "Radar Detection, Discrimination, and Classification of Buried Non-Metallic Mines," Final Technical Report for U.S. Army Mobility Equipment Research & Development, Contract No. DAAG54-76-C-0112, Georgia Tech Project A-1828, February 1978.

31. L. C. Chan, D. L. Moffatt, and L. Peters, Jr., "A Characterization of Subsurface Radar Targets," Proc. IEEE 67: 991-1000, 1979.

32. J. R. Moore and J. D. Echard, "Radar Detection of Voids Under Concrete Highways," Final Technical Report, Georgia Department of Transportation, Georgia Tech Project A-2107, May 1978.

33. J. R. Rossiter and K. A. Gustajtis, "Determination of Iceberg Underwater Shape with Impulse Radar," Desalination 29: 99-107, 1979.

34. A. P. Annan and J. L. Davis, "Impulse Radar Sounding in Permafrost," Radio Sci. 11: 383-394, 1976.

35. R. C. Ajmera, D. B. Batchelor, D. C. Moody, and H. Lashinsky, "Microwave Measurements with Active Systems," Proc. IEEE 62: 118-127, 1974.

36. R. G. Bosisio, R. Dallaire, and P. Phromothansy, "A Non Contact Temperature Monitor for the Automatic Control of Microwave Ovens," J. Microwave Power 12: 309-317, 1977.